The author of this work was supported by FCT through the PhD grant SFRH/BD/69068/2010. This work was supported by FEDER through POFC –COMPETE and by national funds from FCT through the projects PEst-OE/BIA/UI4050/2014, PEst-C/FIS/UI0607/2013 (CFUM) and PTDC/QUI/69795/2006.

Cationic Liposomes as antigenic delivery systems: development of an immunoprotective strategy against *Candida albicans*
Maria Catarina Santos Carneiro
UMinho | 2015

Universidade do Minho
Escola de Ciências

Maria Catarina Santos Carneiro

Cationic Liposomes as antigenic delivery systems: development of an immunoprotective strategy against *Candida albicans*

abril de 2015

Universidade do Minho
Escola de Ciências

Maria Catarina Santos Carneiro

Cationic Liposomes as antigenic delivery systems: development of an immunoprotective strategy against *Candida albicans*

Tese de Doutoramento Biologia Molecular e Ambiental
Especialidade em Biologia Celular e Saúde

Trabalho realizado sob a orientação de:
Professora Doutora Paula Sampaio,
Professora Doutora Maria Elisabete C.D. Real Oliveira
Professora Doutora Andreia C. Gomes

abril de 2015

DECLARAÇÃO DE INTEGRIDADE

Declaro ter atuado com integridade na elaboração da presente tese. Confirmo que em todo o trabalho conducente à sua elaboração não recorri à prática de plágio ou a qualquer forma de falsificação de resultados.

Mais declaro que tomei conhecimento integral do Código de Conduta Ética da Universidade do Minho.

Universidade do Minho, ____de _____de _____

Nome completo:_____

Assinatura:_____

"I am among those who think that science has great beauty. A scientist in his laboratory is not only a technician: he is also a child placed before natural phenomena, which impress him like a fairy tale. We should not allow it to be believed that all scientific progress can be reduced to mechanisms, machines, gearings, even though such machinery also has its beauty.

Neither do I believe that the spirit of adventure runs any risk of disappearing in our world. If I see anything vital around me, it is precisely that spirit of adventure, which seems indestructible and is akin to curiosity."

Marie Curie

During a debate in Madrid, "The Future of Culture" (1933).
In Eve Curie Labouisse, Eve Curie and Vincent Sheean, *Madame Curie* (1937), 341

ACKNOWLEDGMENTS

To Fundação para a Ciência e Tecnologia for funding through the PhD grant SFRH/BD/69068/2010

To NanoDelivery-I&D em Bionanothecnologia, Lda. for access to their equipment.

Agradecimentos

Gostaria de agradecer a todos aqueles que me encorajaram e me proporcionaram as condições necessárias para que este projeto de investigação fosse desenvolvido. De uma maneira especial gostaria de salientar e agradecer:

À Professora Paula Sampaio por me ter aceite no seu grupo de investigação, e me ter proporcionado a oportunidade de trabalhar neste projeto. Acima de tudo agradeço a valiosa e indispensável orientação e dedicação ao longo deste trabalho, a sua constante disponibilidade, amizade, contínuo otimismo, o seu empenho na transmissão de conhecimentos que não só me fizeram crescer como investigadora mas também como pessoa.

À Professora Elisabete Oliveira, por me ter recebido no seu grupo de investigação e pela orientação ao longo destes anos, por me ter iniciado no mundo da biofísica, pelos conhecimentos transmitidos, e pela sua contribuição e dedicação fundamentais ao longo deste trabalho.

À Professora Andreia Gomes, por me ter recebido no seu grupo de investigação e pela orientação ao longo destes anos, pelos conhecimentos transmitidos e pela sua valiosa contribuição e dedicação na realização deste trabalho.

À Professora Célia Pais, por me ter recebido no seu laboratório, por ser a nossa mentora, pelos conhecimentos transmitidos e pela valiosa ajuda ao longo deste trabalho. Acima de tudo pelo carinho e amizade com que sempre me recebeu.

Ao Professor Manuel Vilanova, por ter aceite colaborar neste trabalho, por me ter recebido no seu laboratório e me ter proporcionado todas as condições para o desenvolvimento desta tese. Pela valiosa contribuição para o meu conhecimento teórico e prático na área da imunologia e por todo contributo científico que deu para a realização deste trabalho. A todos os membros do laboratório de imunologia pela amabilidade que sempre demonstraram, em particular ao Pedro Ferreirinha pelos conselhos valiosos e por toda a disponibilidade.

À Alexandra Correia por ter aceite colaborar neste trabalho, pela orientação, por todos os conhecimentos teóricos e práticos que me transmitiu, pela amizade, carinho e constante disponibilidade. Penso que é impossível recorrer a palavras para explicar o quão imprescindível foste no meu crescimento como investigadora.

Ao Tony Collins pela sua colaboração neste trabalho e valiosa transmissão de conhecimentos.

A todos os membros da Micro II, por terem tornado o meu trabalho de bancada muito mais fácil e por sempre me terem incentivado e ajudado. Em particular, à Joana Pereira, à Catarina Vaz, ao João Pacheco, à Filipa Vale e ao Manoel Oliveira. Em especial, à Tânia Lima pela disponibilidade e ajuda laboratorial nesta última fase, pela amizade e carinho tão fundamentais para a conclusão desta tese.

Aos colegas que partilham o meu entusiasmo pelo sistema DODAX:MO, em particular à Ana Oliveira, Odete Gonçalves e ao Ivo Lopes pela amizade e disponibilidade. Ana, obrigada por todo o apoio e compreensão!

Ao CBMA e a todos os seus membros por me terem proporcionado as condições necessárias para a realização desta tese.

A todos os meus colegas do Departamento de Biologia pelo bom ambiente vivido e toda a disponibilidade demonstrada.

À minha família de Braga que me adotaram no momento em que fui viver para Braga, ao Zè, à Letinha, ao Rui e às minhas princesas, Catarina e Margarida, um muito obrigada!!!

Ao Ricardo por todo o carinho.

Ao Paulo por ter estado sempre ao meu lado, ter acreditado sempre em mim e ter tornado esta minha jornada muito mais fácil.

À minha mãe, ao meu pai e às minha irmãs, por todos os dias serem a minha fonte de inspiração e porque cada um deles é, à sua maneira, o meu ídolo. Pelo amor e carinho sem os quais nada na minha vida seria possível.

RESUMO

Os lipossomas catiónicos constituídos pelo lípido catiónico Brometo de Dioctadecil Dimetilamónio (DODAB) são sistemas de entrega eficazes com poder adjuvante, possibilitando a proteção/veiculação do antigénio, tendo sido anteriormente descritos como imuno-estimuladores. Assim, o principal objectivo deste trabalho foi o desenvolvimento e caracterização de lipossomas, constituídos pelo DODAB e pelo lípido não-iónico Monooleína (MO), com poder adjuvante para o estabelecimento de uma estratégia imunomoduladora contra infecções sistémicas causadas pelo fungo *Candida albicans.*

Inicialmente, demonstrámos que o aumento na concentração de MO melhora a estabilidade coloidal, a viabilidade e a internalização celular quer dos lipossomas vazios, quer carregados com BSA (BSA nanoparticulas liposomais (LNPs). Estes lipossomas foram internalizados via endocitose, sendo que a internalização da BSA foi aumentada quando veiculada pelos lipossomas. Selecionámos a razão molar DODAB:MO (1:2) como a mais adequada e demonstrámos que este sistema para além de funcionar como um nanotransportador também aumenta a ativação de células apresentadoras de antigénio (APC). Esta mesma razão molar foi selecionada para preparar sistemas de entrega de antigénios (ADSs LNPs) carregados com proteínas da superfície da parede celular de *C. albicans* (CWSP). Foram avaliadas as propriedade físico-químicas destas ADSs LNPs a diferentes razões de massa entre as proteínas e os lípidos (p/l) para selecionar duas formulações ADS1 (p/l 0.056) e ADS2 (p/l 0.376). Ambas as formulações apresentaram estabilidade coloidal, carga superficial negativa, tamanho médio de cerca de 200 nm e não provocaram efeitos citotóxicos. Estudos *in vitro* possibilitaram verificar que os ADSs induzem uma libertação lenta das CWSP e, como tal, prolongam a estimulação das APCs, tendo sido confirmado o seu potencial imunogénico em estudos *in vivo*, usando ratinhos BALB/c imunizados com os ADSs. Neste sentido, usando um modelo murino (BALB/c) de candidíase disseminada, mostrámos que a imunização com ADS1 prolonga a sobrevida dos ratinhos, comparando com ratinhos imunizados com as CWSP livres. A resposta humoral observada distingue-se pela existência de anticorpos específicos capazes de aumentar a fagocitose de *C. albicans*, e a resposta celular específica desenvolvida apresenta o fenótipo Th1/Th17, conhecido como protetor neste tipo de infeções.

Em resumo, os resultados apresentados nesta tese, revelam o potencial dos lipossomas DODAB:MO como sistemas de entrega de antigénios com poder adjuvante.

ABSTRACT

Cationic liposomes, composed by the cationic synthetic lipid dioctadecyldimethylammonium bromide (DODAB) are effective adjuvant delivery systems that offer antigen protection and have been shown to be immunostimulatory. Thus, the main objective of this thesis was the design and characterization of a novel adjuvant delivery system composed by DODAB and the neutral lipid monoolein (MO) for use as an imunomodulatory strategy against *Candida albicans* systemic infections.

Initially, we demonstrated that DODAB:MO liposomes, empty or loaded with BSA (BSA Liposomal Nanoparticles, LNPs), benefit in terms of colloidal stability, cellular viability and uptake with the increase in MO molar fraction. Both empty liposomes and BSA LNPs were internalized by endocytosis, with increasing BSA uptake upon loading in DODAB:MO liposomes. The most suitable molar ratio of DODAB:MO (1:2) was selected and we demonstrated that this formulation not only acts as antigen nanocarrier, but also enhances activation of bone marrow derived dendritic cells (BMDCs). Following, we used these liposomes to prepare antigen delivery systems liposomal nanoparticles (ADS LNPs) with *C. albicans* cell wall surface proteins (CWSP) as antigens. The physicochemical properties of these LNPs were assessed at different protein/lipid weight ratio (p/l) and selected two formulations ADS1 (p/l of 0.056) and ADS2 (p/l of 0.376). Both ADSs exhibited negatively charged surfaces with mean sizes of approximately 200 nm, good colloidal stability and no associated cytotoxicity. ADSs LNPs not only enhanced but also prolonged BMDCs activation, indicating that entrapped antigen is released in a slow and sustained manner. ADSs immunized mice provided evidence that the LNPs could have potential to be use in an immunoprotective strategy against disseminated candidiasis. Finally, in a murine (BALB/c) model of systemic candidiasis, we showed that mice immunized with ADS1 LNPs significantly extended mice survival in comparison with mice immunized with free CWSP. Mice vaccinated with ADS1 LNPs developed a strong humoral response with specific antibodies able to enhance phagocytosis of *C. albicans* cells and boost a protective and specific Th1/Th17 response.

In summary, in this thesis we show that DODAB:MO-based liposomes can act as adjuvant delivery systems and confer immunoprotection against *C. albicans* systemic infections.

TABLE OF CONTENTS

ABBREVIATIONS LIST

ADS	Antigen delivery systems
ANOVA	Analysis of variance
APC	Antigen presenting cell
ATCC	American Type Culture Collection
BCA	Bicinchoninic acid protein assay
BCIP	5-bromo-4-chloro-3-indolylphosphate
BCR	B cell receptor
BSA	Bovine serum albumin
CD	Cluster of differentiation
CFU	Colony forming unit
CFW	Calcofluor White
Cryo-SEM	Cryogenic scanning electron microscopy
Cryo-TEM	Cryogenic-Transmission Electron Microscopy
CWP	Cell wall proteins
CWSPs	Cell Wall surface proteins
DAMP	Damage associated molecular patterns
DC	Dendritic cell
DC-Chol	Dimethylaminoethane Carbamoyl Cholesterol
DEMEM	Dulbecco’s Modified Eagle’s Medium
DLS	Dynamic Light Scattering
DMEM	Dulbecco's Modified Eagle Medium
DMSO	Dimethyl sulfoxide
DNA	Deoxyribonucleic acid
DODAB	Dioctadecyldimethylammonium Bromide
DODAC	Dimethyl Dioctadecylammonium Chloride
DODAP	Dioleoyl Dimethylammonium Propane
DODAP	Dioleoyl Dimethylammonium Propane
DOPA	Dioleoylphosphatidic Acid
DOPE	Dioleoylphosphatidyl Ethanolamine
DOPG	Dioleoylphosphatidyl Glycerol
DOPS	Dioleoylphosphatidyl Serine
DOTAP	Dioleoyloxypropyl Trimethylammonium Methylsulfate

DOTMA	Dioleoyloxypropyl Trimethylammonium Chloride
DPPC	Dipalmitoylphosphatidyl Choline
DSC	Differential Scanning Calorimetry
DSPC	Distearoyl-glycero-phosphatidylcholine
DTS	Dispersion Technology Software
DTS	Dispersion Technology Software
DTT	Dithiothreitol
EDTA	Ethylenediaminetetraacetic acid
ELISA	Enzyme-linked immunosorbent assay
ELISA	Enzyme linked immunosorbent assay
ELS	Electrophoretic Light Scattering
ER	Endoplasmic reticulum
FCM	Flow cytometry
FBS	Fetal bovine serum
FBS	Fetal bovine serum
FDA	Food and Drug Administration
FITC	Fluorescein isothiocyanate
GM-CSF	Granulocyte-macrophage colony stimulating factor
GPI-	Glycosylphosphatidylinositol-anchored
H	Hexagonal Phase
HBSS	Hanks' balanced salt solution
HBSS	Hank's balanced salt solution
HEPES	4-(2-hydroxyethyl)-1-piperazineethanesulfonic acid
HIV	Human immunodeficiency virus
IFA	Incomplete Freunds's adjuvant
IFN	Interferon
Ig	Immunoglobulin
IL	Interleukin
ISCOMS-	Immune stimulating complexes
kDa	Kilodalton
L	Lamellar Phase
LDH	Lactate Dehydrogenase
LNPs	Liposomal nanoparticles

LPS	Lipopolysaccharide
LUV	Large Unilamellar Vesicle
M	Micellar Phase
MFI	Mean fluorescence intensity
MHC	Major histocompatibility complex
MLV	Multilamellar Vesicle
MO	Monoolein (monooleoyl-rac-glycerol)
MPL	Monophosphoryl lipid A
MR	Mannose receptor
mRNA	Messenger ribonucleic acid
MTT	3-(4,5-dimethyl- thiazol-2-yl)-2,5-diphenyltetrazolium bromide
MVV	Multivesicular Vesicle
MW	Molecular weight
M_{YA}	Macrophages with attached yeast particles
M_{YAI}	Macrophages with ingested and attached yeast particles
MyD88	Myeloid differentiation factor
M_{YF}	Macrophages with ingested yeast particles
M_{YI}	Macrophages with only ingested yeast particles (MYI)
NBT	Nitroblue tetrazolium
NBT	Nitro-blue tetrazolium
NF-kB	NF-kB Nuclear factor kappa-light-chain-enhancer of activated B cells
PBS	Phosphate buffer saline
PBS	Phosphate buffered saline
PC	Phosphatidyl Choline
PCR	Polymerase chain reaction
PDI	Polydispersivity
PI	Propidium iodide
PPR	Pattern recognition receptor
Rho-DHPE	1,2-dipalmitoyl-sn-glycero-3-phosphoethanolamine-N-(lissamine Rhodamine B sulfonyl) (ammonium salt)
RNA	Ribonucleic acid
RPMI	Roswell Park Memorial Institute medium
RT	Room temperature

s.c.	Subcutaneous
SAP	Secreted aspartyl protease
SD	Standard deviation
SDS	Sodium dodecyl sulphate
SDS-PAGE	Sodium dodecyl sulphate polyacrylamid gel electrophoresis
SUV	Small Unilamellar Vesicle
TB	Trypan Blue
TCR T	T cell receptor
TDB	Trehalose 6,6'-dibehenate
Th	T helper
TLR	Toll-like receptor
T_M	Phase transition temperature
TNF	Tumour necrosis factor
Treg	Regulatory T cell
USA	United States of America
WT	Wild-type
YEPD	Yeast extract, Peptone and Dextrose
β -ME	β-mercaptoethanol
ζ-Potential	Zeta Potential
χDODAB	Molar fraction of DODAB
χMO	Molar fraction of Monoolein

CHAPTER I:

Motivation, objectives and thesis outline

1. MOTIVATION

The work developed in our research group has led to a novel and efficient liposomal system composed by dioctadecyldimethylammonium bromide (DODAB) and monooleoyl-rac-glycerol (monoolein, MO) used for DNA transfection. These studies have demonstrated that this liposomal system can be used as a competent molecular nanocarrier for cell transfection, which led to the legal protection of this technology. Since liposomes are versatile tools that can act not only as nanocarries of genes or different types of drugs but also as vaccine adjuvants. In this thesis we exploited the ability of this particular lipidic combination to serve as both nanocarries for antigen delivery and as adjuvants in the development of vaccine.

Currently, systemic infections caused by Candida species represent the fourth leading cause of nosocomial bloodstream infection in modern hospitals with a mortality rate associated of 30-40% due to failures in the current treatment and prevention measures. Thus, new immunomodulatory strategies are needed to decrease this high mortality rates. Subunit vaccines represent safer, less toxic and a more immunological defined approach for vaccine design. Due to the poor immunogenicity of pathogen subunits when used alone, in this thesis we decided to develop a vaccine strategy against systemic candidiasis using the nanodelivery system developed by our team.

2. OBJECTIVE

The overall objective of the present thesis is to design and characterize a novel antigen delivery system taking advantage of cationic liposomes, composed by DODAB and MO lipids and finally use this system for the design of novel immunomodulatory strategy against systemic *C. albicans* infection.

For this purpose, experimental work was divided in the following detailed objectives:

- Biophysical characterization of empty DODAB:MO liposomes and protein loaded DODAB:MO liposomal nanoparticles (LNPs).
- *In vitro* characterization of the DODAB:MO liposomes ability to improved antigen immunogenicity.
- *In vivo* evaluation of DODAB:MO LNPs potential in increase cellular and humoral responses towards *C. albicans* antigens.
- *In vivo* evaluation of DODAB:MO LNPs potential in protecting against a lethal *C. albicans* systemic infection.

3. THESIS OUTLINE

The present thesis is organized in 7 different chapters. The chapters regarding the experimental work (chapters 3 to 6) are presented in form of articles. The manuscripts presented in chapter 3 and 5 are published in the Journal Microbiology Methods and in the European Journal of Pharmaceutics and Biopharmaceutics, respectively, while the manuscripts presented in chapters 4 and 6 are being prepared for publication.

Chapter 1 presents the context, motivation and objectives of this thesis, as well as its global structure.

In **Chapter 2** an overview of the literature related with the theme of the thesis is presented. This chapter starts with an introductory review of the immune system and types of vaccines followed by a review on immunological adjuvants with a focus on cationic liposomes. In addition the immunology of *Candida albicans* infections together with strategies that used delivery systems for vaccination against this pathogen are briefly discussed.

In **Chapter 3,** the work **"A new method for yeast phagocytosis analysis by flow cytometry"** is presented, describing a novel, fast and simple method to study the interaction between phagocytes and *Candida* yeast cells.

In **Chapter 4,** the work "**DODAB:monoolein as protein delivery systems: the role of monoolein"** is presented, showing the effect of monoolein in the liposomal BSA loaded nanoparticles (BSA LNPs). Furthermore, in this chapter DODAB:MO (1:2 molar ratio) liposomes were selected and explored as nanocarriers with the ability to enhance the activation of antigen presenting cells (APCs) promoted by the free antigen.

In **Chapter 5,** the work "**DODAB:monoolein liposomes containing *Candida albicans* cell wall surface proteins: A novel adjuvant and delivery system"** is presented. In this chapter, DODAB:MO (1:2 molar ratio) liposomes loaded with *Candida albicans* proteins are characterized and explored "in vitro" and in "vivo", as protein delivery vehicles and immunoadjuvants.

In **Chapter 6,** the work **"*Candida albicans* cell wall surface proteins incorporated in DODAB:monoolein liposomes confer protection against the fungal infection in BALB/c mice "** is presented, showing that an immunization protocol based on the DODAB:MO (1:2 molar ratio) liposomes loaded with *Candida albicans* proteins effectively protect against a lethal *C. albicans* systemic infection, being considered a promising vaccination approach.

In **Chapter 7,** the overall conclusions and significance of the work is presented. Suggestions for future work are also exposed.

CHAPTER II:

General introduction

1. TYPES OF VACCINES

A vaccine can be defined as a biological preparation that enhances immunity against disease and either prevent (prophylactic vaccines) or treat disease (therapeutic vaccines). The word 'vaccine' originates from the Latin Variolae vaccinae (*vacca* meaning cow) known by the name of cowpox, a virus affecting cows, with which Edward Jenner demonstrated in 1798 could prevent smallpox in humans [1].

An advantageous vaccine produces a long-term adaptive immune response that prevents invasion or multiplication of its target pathogen and essentially produces no significant adverse effects on the host. The effectiveness of the immunoprotection induced by the vaccine depends on various factors including the nature of the pathogen and on the immunocompetence of the host [2].

Vaccines can be grouped into three main types: live-attenuated, inactivated (killed) pathogens or pathogen subunits (protein-based, polysaccharide-based or conjugates). Live-attenuated vaccines are based on a viable pathogen with reduced virulence or ability to cause disease that has been weakened under laboratory conditions, normally attenuated by in vitro passages, chemically, genetically, or by other means. These vaccines are extremely potent because the pathogen will grow in the vaccinated host. However, obvious disadvantages such as reversion to virulent, unwanted host reactions like induction of exacerbated inflammation or autoimmune responses, and perseverance and production issues (like the need to be refrigerated to stay potent) can be spawned with this kind of vaccines [3]. Nevertheless, live-attenuated vaccines are still in clinical use for protection against tuberculosis (BCG), polio (OPV), and yellow fever, among others. Inactivation of pathogens, using chemicals, heat, or radiation, benefit from a safer administration since inactivation reduces danger to the host. However, several disadvantages are associated, as they are less potent and the immune response is largely limited to a humoral response. In many cases for this type of vaccine an adjuvant is needed, since without it vaccination requires additional dosages that may incur undesirable host reactions [4]. For these reasons, there has been a shift towards developing subunit vaccines composed by one or several specific units of the pathogen. Lacking any potential to replicate in the host they represent safer, less toxic and a more immunological defined approach for vaccine design [5]. Although they are promising candidates as the next generation of immunotherapeutics, pathogen subunits are also poorly immunogenic when used alone as vaccines [6]. In this sense subunit vaccines have to be delivered with potent immunostimulatory adjuvants to effectively activate the innate and adaptive arms of the

immune system [7]. In some cases the vaccines are multivalent, targeting diverse organisms combining inactivated pathogens and pathogen subunits (as shown in Table 1). As we move toward the era of modern vaccines novel adjuvants and novel delivery systems that boost immunogenicity are increasingly needed.

In Table 1 a summary of the current licensed vaccines manufactured in Europe that take advantage of licensed adjuvants, are represented and grouped according to the type of vaccine used.

Table 1: Licensed vaccines manufactured in Europe grouped according to the vaccine type. Only vaccines that take advantage of licensed adjuvants are represented.

Type o vaccine	Target Disease	Vaccine Name	Country	Adjuvant
Inactivated pathogen	Influenza	Arepanrix (H1N1)	Belgium	ASO3
		Humenza (H1N1)	France	AFO3
		Pandemrix (H1N1)	Germany	ASO3
		Avaxim	Netherlands	
	Hepatitis A	Epaxal		$Al(OH)_3$ Virosome
Pathogen subunits	Pneumococcal	Synflorix	Belgium	$Al(PO)_4$
	Hepatitis B	Engerix B	Belgium	$Al(OH)_3$
		Fendrix	Belgium	AS04C
		HBvaxPRO	France	$Al(OH)_3$
	Influenza	Celtura (H1N1)	Germany	MF59
		Focetria (H1N1)	Italy	
	Papillomavirus		Belgium	VLP and ASO4
		Cervarix		
	Tetanus toxoid	Tetatox TT vaccine	Bulgaria	
		TETAVAX	France	$Al(OH)_3$
	Diphteria, tetanus	DifTet	Bulgaria	$Al(OH)_3$
		diTe booster	Denmark	
		DT VAX	France	
		IMOVAX dT adult	France	
		Teta-dif	Bulgaria	
	DTaP	Boostrix DtaP	Belgium	$Al(OH)_3$ and $Al(PO)_4$
		Infanri	Belgium	$Al(OH)_3$
Inactivated Pathogen + subunit	DTaP	D.T.COQ/D.T.P	France	$Al(OH)_3$
	DTaP, IPV	Infanrix IPV	Belgium	$Al(OH)_3$
		Repevax	France	$Al(PO)_4$
	DTaP, HepB	Tritanrix HB	Belgium	$Al(OH)_3$ and $Al(PO)_4$
	DTaP, Hib	Quattvaxem	Italy	$Al(PO)_4$
		TETRAct-HIB	France	$Al(OH)_3$
		TriHIBit	France	$KAl(SO_4)_2$
	DTaP, IPV, Hib-IPV	Pentaxim	France	$Al(OH)_3$
		Pediacel	France	$Al(PO)_4$
	DTaP-HepB-Hib-IPV	Hexavac	France	$Al(OH)_3$
		Infanrix hexa	Belgium	$Al(OH)_3$ and $Al(PO)_4$
	DTaP-HepB-IPV	Pediarix	Belgium	$Al(OH)_3$ and $Al(PO)_4$
	HepA and HepB	Vivaxim	Belgium	$Al(OH)_3$ and $Al(PO)_4$

DTaP: Diphtheria, Tetanus, Pertussis; Hep: Hepatite; IPV: Inactivated polio; Hib: Haemophilus influenzae type B. AS03: emulsion with squalene, α-tocopherol and polysorbate 80; AS04: emulsion with monophosphoryl lipid A (MPL) preparation and aluminum salt; MF59: emulsion with squalene, polysorbate 80 and sorbitan trioleate; VLP: virus like particles.

2. STIMULATING THE IMMUNE SYSTEM

Vaccine formulations should be designed rationally to induce specific protective responses. After the first encounter with a specific antigen the immune response is usually slow since the immune system hasn´t yet acquired the necessary knowledge to deal with the pathogen, which makes the human body vulnerable to infection. Throughout this initial encounter the body can develop an acquired immunity. Consequently, a number of T- and B-cells can survive and differentiate into highly reactive memory and effector cells. So, upon re-infection, in a second encounter, these memory cells react to the previously encountered antigen in a stronger and faster manner in comparison to naive cells, reflecting the pre-existence of clonally expanded antigen-specific memory cells [8, 9]. In fact, the conceptual basis for preventative vaccination and possibly the most significant consequence of adaptive immunity is the induction of immunological memory [4].

2.1. The Immune system

The organs of the immune system, the lymphoid organs, are distributed throughout the body. They can be divided mainly into primary and secondary lymphoid organs. Primary lymphoid organs are constituted by the bone marrow and the thymus, where leucocytes are generated and maturate. Adaptive immune responses are initiated at secondary lymphoid organs (also called the peripheral lymphoid organs) constituted by the lymph nodes, spleen and the skin-, mucosal- and gut-associated lymphoid tissues, SALT, MALT and GALT, respectively [10].

Immunity can be provided by the innate and adaptive immune system [11]. The innate arm of the immune system is characterized by limited specificity and the absence of immunological memory. However, the innate responses play a decisive role in the magnitude, quality and duration of adaptive responses [10]. The adaptive arm of the immune system is characterized by long lasting and specific recognition of pathogens [9].

In order to obtain an effective immune response both systems continually interact with each other in a process that involves recognition, uptake and presentation of antigen with subsequent establishment of a memory population composed by T and B cells [12].

2.2. Innate immunity

The innate immune system, which can be activated within a few minutes of the initial invasion through nonspecific recognition of a pathogen [13], relies on the combined action of humoral and cellular components, that fight pathogens in a non- specific manner [11].

2.2.1 Innate humoral immune responses

A crucial factor to the stimulation of innate immune responses is the detection of molecular components commonly belonging to the pathogen that Charlie Janeway dubbed pathogen associated molecular patterns (PAMPs) [14]. Innate humoral response relies on multitude of soluble pattern recognition molecules belonging to several protein families that detect conserved PAMPs on microorganisms. Some mechanism of humoral defense are based on the protease cascades of the complement system as well as naturally occurring antibodies (NAb) and pentraxins [15].

The complement system can be activated through three activation pathways, the classical, the alternative and the lectin pathway. The classical pathway is triggered when immunoglobulin M (IgM) or certain IgG subclass antibodies bind to the surface markers/antigens on a pathogen. The alternative pathway is triggered by the deposition of the complement protein, C3b, onto microbial surfaces and does not require antibodies for activation. The lectin pathway, is triggered by the attachment of plasma mannose-binding lectin (MBL) to pathogens and is also independent of antibodies for activation [11]. Ultimately, complement activation results in the binding of complement component fragments to the pathogen cell surface (opsonization), which enhances phagocytosis. Continuous deposition of other complement components will lyse the pathogen due to the formation of the membrane attack complex (MAC) that perforates microorganisms [16]. Complement activation also results in the formation of other complement fragments with anafilatoxin effects that attracts phagocytic cells to the activation site, enhancing the inflammatory response [16].

NAb are germ line encoded Ab with restricted epitope specificities and are produced in the absence of external antigen stimulations. Natural IgM Abs opsonize a wide range of pathogens, promoting the recognition of pathogens by professional antigen-presenting cells (APCs), and may guide the ensuing functional polarization of T-cell responses, as well the

isotype class-switch recombination of the induced B-cell response and induction of long-term immune memory [17].

Pentraxins are acute phase proteins and therefore markers of infection and inflammation. Pentraxins recognize and bind multiple pathogens which facilitates clearance of pathogens and cell debris, by complement activation and phagocytosis enhancement [15].

2.2.2 **Cell based innate immunity**

Cells of the innate immune system represent a very diverse set of cells that derive from a common myeloid progenitor on the bone marrow. This set is constituted by tissue-residing cells (such as macrophages and dendritic cells) and "moving" cells (such as neutrophils, eosinophils and monocytes). These cells express pattern recognition receptors (PRRs) - such as Toll-like receptors (TLRs), C-type lectin receptors (CLRs) and the galectin family protein that recognized PAMPS [18-20].

Neutrophils and macrophages contribute to the cellular innate immune response mostly through phagocytosis, either directly through PRRs or indirectly through recognition of pathogen coating by complement or antibodies. Phagocytosis represents an important effector mechanism of the innate immune response that takes place upon contact between phagocyte and pathogen. After engulfment, the pathogen is trapped within an intracellular vesicle and targeted for destruction by a complex set of digestive enzymes or toxic reactive oxygen species (ROS) produced within the host cell [21]. For that reason, the phagocyte response to microbes is often referred to as "oxidative burst" [22]. Furthermore, PRRs binding to PAMPs activate a signaling transduction cascade that culminates in NFκB activation [23]. NFκB is a transcription factor that controls the expression of numerous immunologically important cytokines and chemokines as well as membrane receptors [24]. Upon binding of a PAMP to its cognate PRR, NFκB is liberated to translocate to the nucleus, seek out its target genes and initiate transcription [25]. In consequence, diverse groups of chemokines, with the ability to activate and guide other cells of the immune system to the site of infection, as well as cytokines, that induce differentiation, are produced, resulting in the amplification of immune responses. Other transcription factor cascades, involving most notably the interferon-regulated factors (IRFs), are also activated downstream the PRRs. Some of the most important inflammatory mediators synthesized and released in response to PRR engagement include the antiviral interferons, the small protein cytokines interleukin-1β (IL-1β), IL-6, IL-12, and tumor necrosis factor α (TNFα), which activate other cells through

binding to specific receptors [23, 25]. The elevated secretion of cytokines and chemokines leads to the recruitment of cells and soluble mediators, with anti-microbial activity, to the site of infection through increased vessel permeability, leading to the classical signs of inflammation (increased swelling, redness, pain and heat) [10, 26].

Like macrophages, dendritic cells (DCs) are considered professional phagocytes however DCs are not directly involved in immediate pathogen clearance. After efficiently phagocyte pathogens, DCs process antigens derived from these pathogens into peptides and load these peptides on major histocompatibility complex (MHC) class I or MHC class II molecules and therefore are considered potent antigen-presenting cells (APC), capable of activating resting T cells and of initiating primary and memory immune responses. Although macrophages are also capable of presenting antigens on MHC class I and II molecules, they do so less inefficiently.

2.3. Adaptive immunity

The adaptive immune system takes advantage of the innate system's ability to discriminate between dangerous pathogens and innocuous or even beneficial microbes and environmental factors [27].

In order to achieve a successful activation of antigen-specific adaptive immune responses, it is first necessary to activate the pathogen-detection mechanisms of the innate immune system. However, innate responses do not improve upon frequent encounter with the same antigen, thus unlike the adaptive immune system, they do not confer long-lasting immunity on the host. For that adaptive immunity follows the innate immune response [20, 28]. Cell mediated and humoral immunity represent the two major types of adaptive immunity and culminate in the proliferation of pathogen-specific T or B lymphocytes together with T and B memory cells, providing long-term protection against disease [28].

2.3.1 T and B cells

T and B-lymphocytes develop from a common lymphoid progenitor in the bone marrow. During B cell development in the bone marrow, each B lymphocyte expresses numerous copies of a unique antibody as a cell surface receptor (B cell receptor, BCR) and emerges in the bone marrow periphery when the immature B cells express immunoglobulin IgM. Here, B cells further differentiate into naive B cells, which also express IgD, leave the

bone marrow and circulate in secondary lymphoid tissues, where they may encounter specific antigen [29].

The development/maturation of T cells starts in the thymus after T lymphocytes migration from the bone marrow. In the thymus, progenitor T cells undergo stringent positive or negative selection resulting in naive T cells populations that leave the thymus with a unique collection of T cell receptors (TCRs) on the cell surface and either CD4 or CD8 co-receptor [30]. Intact TCRs and BCRs formed the antigen-specific receptors of the adaptive response. The assembly of antigen receptors from a collection of a few hundred germline-encoded gene elements permits the formation of millions of different antigen receptors, each with potentially unique specificity for a different antigen [27]. In a marked contrast, B cell receptors (BCRs) can react to a wide spectrum of antigens while T cells can only be activated in response to protein antigens [10].

2.3.2 **T cell activation**

In order to be effectively activated T-cells require APC cells function. APCs uptake antigen by endocytosis or phagocytosis, broken it down in the lysosomes and migrate from the site of infection to the regional lymph nodes. At this site, antigen presentation occurs via presentation of antigenic material in the major histocompatibility complex (MHC) class I and class II receptor molecules [31]. In essence, MHC molecules function as serving platforms for dismembered proteins since T-cells can only recognize antigen when presented within the cleft of an MHC molecule. T-cells examine antigen presented on DCs using TCR specificity and successful recognition (signal 1 - the antigen specificity) results in activation and the acquisition of various immune-related functions by the T-cell (Figure 1). However, for the activation of protective T cells, signal 1 is not sufficient. Indeed, the presentation of antigen alone is insufficient to cause naive T cells to mature into effector T cells. That is why an ideal vaccine should contain an immunopotentiator agent besides the antigen in order to enhance DCs co-stimulatory signals. In fact, the membrane ligands, B7-1 and B7-2 (also called CD80/ CD86) engagement with CD28 on the surface of the T-cell (signal 2 - the co-stimulation) and cytokine secretion (signal 3 - the polarization) are required for strategic T cell responses (Figure 1) [32-34].

Primed T cells undergo a pattern of clonal expansion and acquisition of effector cell functions, followed by formation of memory cell populations that are long-lived [6, 35, 36]. T cells can be grouped into two main subsets the $CD4^+$ T-cells, often referred as T helper cells,

that express the CD4 co-receptor and, and the $CD8^+$ T-cells, also known as cytotoxic T cells that express CD8 co-receptor.

Three separate T helper (Th) cell lineages can be regulated depending on the cytokine milieu: Th1, Th2, and Th17. IL-12 and IL-4 have previously being shown to regulate Th1 and Th2 differentiation respectively, with Th17 cells differentiation from naive $CD4^+$ T-cells have been shown to be due to IL-6, IL-23 and tumour growth factor-beta (TGF-β) [37].

Two further subsets of $CD4^+$ T-cells have also been identified, the regulatory T-cells and follicular helper T cells. Regulatory T-cells or Tregs are critical for homeostasis and tolerance and are activated by IL-10 producing dendritic cells. Follicular helper T cells (Tfh), appear to be important for guiding B-cell development, class switching and survival within germinal centers [10]. T helper subclasses have distinctive cytokine secretion patterns and functions [38, 39] that are strongly related to the type of microorganism or antigen that first interacts with the host and also depends on antigen dose and vaccine administration route.

$CD8^+$ T cells form the main subset that mediates cytotoxicity being capable of induce the death of infected or otherwise damaged host cells (like tumor cells) [40].

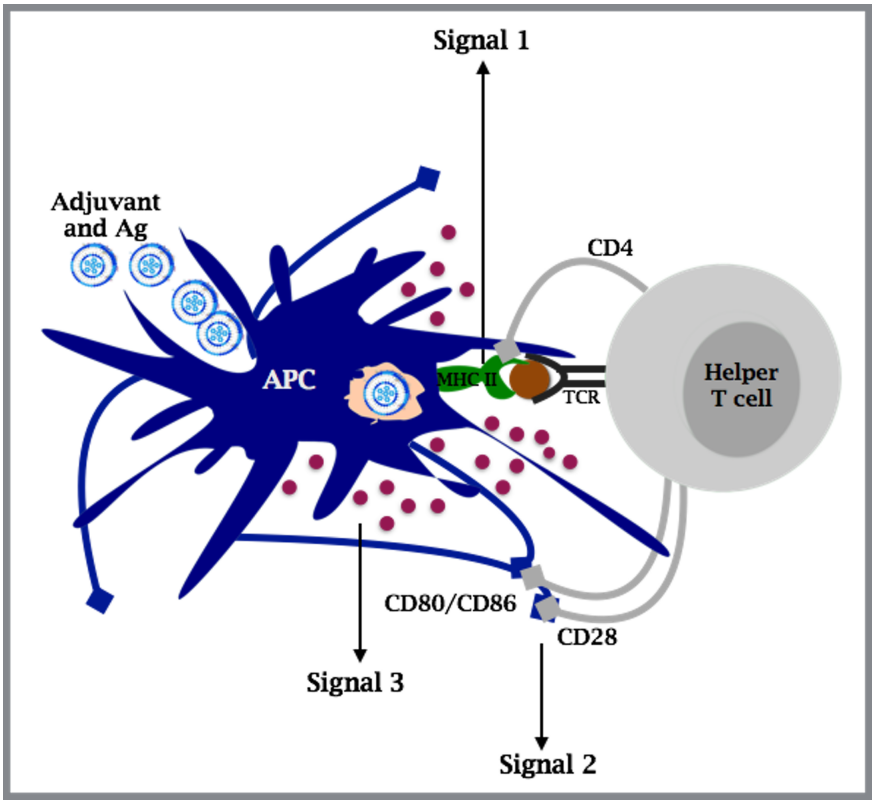

Figure 1: Mechanisms of T cell activation upon uptake and presentation of a liposomal encapsulated antigen (Ag) by APCs. Liposomal encapsulated antigens are uptaken by APCs and processed for display on MHC II molecules. CD4+ T cells recognize antigen via their T cell receptor (TCR) and with co- stimulation, intracellular signaling pathways leads to CD4+ T cell activation.

2.3.3 B cell activation

B cells are responsible for the recognition of pathogen-derived antigen in its native form and circulate in secondary lymphoid tissues. The BCR play two roles in B-cell activation. First, it transmits signals directly to the cell's interior upon binding antigen (Signal 1). Second, they deliver the antigen to intracellular sites where it is digested and returned to the B-cell surface as peptides bound to MHC class II molecules. The peptide-MHC class-II complex can be recognized by antigen-specific $CD4^+$ cells, enhancing co-stimulatory molecules such as CD40 ligand (Signal 2), which in turn causes B cells to divide and differentiate into plasma cells and memory B cells [41, 42].

Plasma cells represent the terminal stage of differentiation for all antigen activated B cells and release high-affinity antibodies that attach to antigens forming antibody-bound complexes that are phagocytized more avidly [26, 43]. Two types of genetic changes occur during B cells differentiation: somatic mutations and class switching. The first changes the antigen binding properties so that binding affinity of B-cell receptor to its cognate ligand increases and the last results from a change in the heavy chain constant region within the Ig, giving rise to the expression of antibodies with the same antigen specificity but of differing isotypes, and therefore of differing effector functions [29]. Roughly Y-shaped, antibodies are flexible molecules made up of two heavy chains and two light chains linked together [44]. The type of heavy chain determines the class, or isotype, of the antibody molecule, i.e. IgA, IgG, IgD, IgE and IgM antibodies. The capacity of a given antibody to reach the site of infection and recruit the adequate effector mechanisms is determined by the type immunoglobulin class. In fact, the binding of an antibody to its target is often sufficient to render the antigen harmless [10].

Antibodies can be considered as bifunctional molecules, that can both recognize and enhance the elimination of a given antigen or pathogen by opsonization rendering the pathogen more susceptible to phagocytosis, by cells of the innate immune system. Depending on their isotype, antibodies can also activate the complement family of proteins, leading to cell lysis and destruction of the target pathogen [10]. The response elicited following an antigen primary injection is slow and is characterized by low affinity IgM antibodies. If the same antigen is encountered again, the secondary response develops more rapidly and is mostly composed of IgG antibodies of higher affinity. The secondary response is characterized by both quantitative (higher and more sustained antibody titers) and qualitative (class switch and affinity maturation) traits that are under the control of T helper cells. [64].

3. IMMUNOLOGICAL ADJUVANTS

Adjuvants (from the latin word *adjuvare*, meaning to "help" or "to enhance" aid) were originally identified in the 1920s by Gaston Ramon a French veterinarian working at the Pasteur Institute. Ramon described it as "substances used in combination with a specific antigen that produced a more robust immune response than the antigen alone" [45].

3.1. The requirement of vaccine adjuvants

In general, vaccine antigens themself are very weakly immunogenic, therefore an adjuvant is needed to intensify the immune response. Additionally, an adjuvant can also be included in vaccine formulation in order to guide and accelerate the type of protective immune response generated [46, 47]. Moreover, a potent adjuvant has the ability to improve the effectiveness of vaccines by preventing competition between antigens when combination vaccines are administered, increase antibody titers, invigorate cellular immunity, increase extent of response to overcome pathogen diversity, induce sustained responses for a longer duration and enhance vaccine efficacy in infants, elderly or immunocompromised individuals. Adjuvants can also be applied to increase cost-effectiveness by minimizing antigen required per vaccine dose [48-50].

3.2. How do adjuvants enhance the immune response?

Currently in widespread use, either in man or in animals, adjuvants have for the most part been developed empirically, without a clear understanding of their cellular and molecular mechanisms of action. This is well captured in a famous quote by Janeway (1989) who observed that adjuvants are "the immunologists' dirty little secret" [14]. In fact, that lack of knowledge delayed the progress and approval of novel adjuvants [51].

Some authors suggested that adjuvants may exert their effects employing one or more of the following mechanisms to elicit immune responses: (1) formation of a depot-effect, (2) cellular recruitment, (3) up-regulation of cytokines and chemokines at the site of injection, (4) increase antigen uptake, (5) activation and maturation of APC, and (6) activation of inflammasomes [52-54]. The details of the various mechanisms of action are crucial for the

rational vaccine design and essential for the approval of new adjuvants for use in vaccine formulations.

3.2.1 The depot-effect

The formation of a depot at the injection site is perhaps the oldest and most widely recognized mechanism of adjuvant action. The depot-effect refers to the antigen trapping (with or without adjuvant) at the injection site. The adjuvant can act by prolonging the release of the antigen at injection site, which results in lengthy presentation of antigen ensuring a constant stimulation of the innate immune cells. The depot-effect is therefore dependent on numerous factors such as the route of injection, the tissue found at the injection site and characteristics associated with the formulation itself such as viscosity and particulate size [54, 55]. A recent example is the use of the cationic adjuvant formulation (CAF), a combination of dimethyldioctadeclammonium/trehalose-6,6-dibehenate (DDA/TDB), currently in phase I clinical trial, which is thought to induce long lasting depot effect [56].

3.2.2 Cellular recruitment and up-regulation of cytokines and chemokines

Particulate adjuvants have been shown to create a local pro-inflammatory environment with the recruitment of immune cells to the site of infection, some of which then transfer the antigen to the draining lymph nodes to induce specific immune responses [57, 58]. In fact, recent studies on the mechanisms of adjuvants have focused on recruitment of innate immune cells at the site of injection involving the increase production of several cytokines, chemokines, up-regulation of innate immune receptors and interferon-induced genes [59-61], and intensification of antigen transportation to the draining lymph nodes [58, 62, 63]. A previous study demonstrated that both Aluminum and an oil-in-water adjuvant named MF59 induce secretion of chemokines involved in cell recruitment from blood into peripheral tissue. Alum appears to act mainly on macrophages and monocytes, whereas MF59 additionally targets granulocytes. However, further studies are required to elucidate the detailed relationship between recruited immune cells and adjuvant activity.

3.2.3 Antigen presentation and APC maturation

A crucial step in the induction of adaptive immune response is the antigen presentation by MHCs on APCs. In this regard, many adjuvants including alum, oil-based

emulsions, and microparticles act by "targeting" antigens to APCs resulting in enhanced antigen presentation by MHC [64-66]. Therefore the antigen trafficking from the site of injection towards the nearest draining lymph nodes is enhanced [67]. Maturation of DCs is essential for T lymphocyte activation and differentiation [54]. Several adjuvants, such as Freund's complete adjuvant, lipopolysaccharide (LPS), liposomes, CpG-ODN, MF59, AS04, or a-galactosylceramide (a-GAL), stimulate DC maturation and enhance the expression of MHC and co-stimulatory molecules [63, 68-72].

3.2.4 **Activation of inflammasomes**

The physical insertion of the needle and vaccine components into the tissue milieu leads to tissue damage. In fact, particulate adjuvants cause local tissue damage and cell death at the injection site [73]. Cells will inevitably be ruptured and molecules associated with tissue damage such as uric acid, nucleotides, adenosine triphosphate (ATP), reactive oxygen intermediates, and cytokines are release [58, 63, 74].

These non-infectious damage signals have been named damage-associated molecular patterns (DAMPs) to distinguish them from pathogen-associated molecular patterns (PAMPs). PRRs can also be activated by DAMPs initiating specific signaling that trigger non-specific activation of the innate immune system, resulting in the production of pro-inflammatory cytokines, chemokines and co-stimulatory molecules required for the productive activation of the T cell upon antigen presentation [75]. The nucleotide-binding oligomerization domain receptors (NLR) family, which includes various other receptors, such as the NODs (NOD1-5), NLRPs (NLRP1-14), NLRP1 (NAIP), NLRC4 (IPAF), and the major histocompatibility complex II transactivator (CIITA), play a critical role in the assembly and activation of inflammasomes, which are large cytosolic multi-protein innate immune signaling complexes that activate caspase-1 [76]. This enzyme is crucial for the maturation and release of proinflammatory cytokines that in turn play crucial roles in directing host responses to infection and injury [77, 78].

Consequently, inflammasomes have been one of the most widely investigated topics due to their potential role in adjuvant activity. Several studies reported the role of inflammasomes in the adjuvant activity of Alum [79, 80], MF59 [81], and monophosphoryl lipid A (MLP) [82].

3.3. Different types of adjuvants

Various classifications have been proposed for adjuvants in an attempt to better understand them. In general, adjuvants can be broadly grouped as antigen delivery systems, immunomodulatory molecules and adjuvants formed by both delivery and immunostimulatory components [49, 54]. Despite this classification, it is currently accepted that some antigen delivery systems may have inherent immunomodulatory properties [49]. Table 1 includes some examples of clinical approved adjuvants.

Immunomodulatory molecules may activate the immune system directly or through PRRs. Cytokines, pathogen derived components, as wells as other ligands of innate immune receptors, (TLRs, NOD-like receptors, C-type lectins and RIG-I–like receptors), directly or indirectly induce the expression of cytokines and chemokines, thereby modulating the local microenvironment to activate and stimulate the immune cells [46]. Among the most advanced compounds are monophosphoryl Lipid A (MLP) and CpG oligodeoxynucleotide (ODN). The first comprises part of the adjuvant system in the Cervarix HPV vaccine against human papillomavirus and the second is the adjuvant in the Hepislav vaccine candidate for hepatitis B [83, 84].

In contrast, particulate delivery system, such as alum, liposomes, emulsions and other particulates, generally work by promoting the uptake of co-administered antigens into APCs [50]. The combination of imunomodulatory molecules coupled to a delivery system provides a great opportunity since generally antigens are not adequately immunogenic and co-administration of successful adjuvant is crucial for the establishment of precise immune responses [48, 85]. In fact, an essential point in the investigation of modern adjuvants is not only the initiation of a potent immune response but mainly targeting APCs receptors to achieve such response, avoiding as much as possible the toxicity associated. Moreover, the ideal adjuvant should be able to promote an antigen-specific immune response, and should be nontoxic, biocompatible, readily biodegraded and eliminated, inexpensive to produce, stable before administration, and physicochemically well defined to facilitate quality control important to ensure reproducible manufacturing and activity [86].

3.4. Delivery systems for use in vaccine formulations

A description of the most well-known delivery systems used in vaccination strategies, aluminium-based adjuvants, polymeric nano and microparticles, emulsions,

immunostimulating complexes (ISCOMs), virosomes, virus like particles (VLP) and liposomes follows below.

3.4.1 **Aluminium-based adjuvants**

Aluminium based mineral salts, normally known as alum, were originally identified as adjuvants in the twenties [87] and remain the most widely used vaccine adjuvants with granted approval for human administration. Aluminium hydroxide ($Al(OH)_3$), aluminium phosphate ($Al(PO)_4$) and aluminium potassium sulphate ($KAl(SO_4)_2$) constitute the general range of salts included in this group [88]. In addition to their inherent adjuvant activity, aluminium salts function as delivery systems and consist in general of crystalline nanoparticles that aggregate to form a heterogeneous dispersion of particles of several microns. They are highly charged and conducive to the adsorption of antigens or immunomodulatory molecules [49, 66, 89, 90]. Indeed, it is widely accepted that physical association between aluminium and the antigen is required for the vaccine adjuvanticity to be retain [91].

Aluminium adjuvants elicit strong humoral immune responses, which are mediated primarily by secreted antigen-specific antibodies, particularly IgG. However they are relatively poor inducers of cell-mediated immune responses, being predominant activators of Th2 biased immunity, and therefore unsuitable for use in vaccines where strong cellular immunity is essential [92, 93].

Albeit the substantial progress in understanding aluminium salts mode of action their mechanism are still poorly understood. In general, it is accepted that alum absorption prevents the rapid removal and degradation of antigen and enhances cell uptake [62, 94]. In addition, a wide range of literature strongly suggests that injection of alum leads to tissue damage and cell death with release of endogenous danger signals and inflamassome activation [73, 76, 88, 95].

Currently, aluminium adjuvants are in clinical used in several vaccines alone or in combination with immunomodulatory molecules, such as Cervarix vaccine that contains MPL and aluminum salt (combination known as AS04) (Table 1) [6, 90, 96].

3.4.2 **Polymeric nano and microparticles**

Particles prepared from biodegradable and biocompatible polymers have been evaluated for drug delivery since the early 1980s [97]. Polymeric nanoparticles are colloidal

carriers and can be divided into two categories: nanocapsules and nanospheres depending on the preparation method used [98]. Nanocapsules are vesicular systems in which the antigen is confined to a cavity surrounded by a polymer membrane, whereas nanospheres are polymeric matrix in which the antigen is physically and uniformly dispersed [99].

Polymers including poly (α-hydroxy acids), poly (amino acids), or polysaccharides can be used for preparation of this nanoparticles. Poly (lactic-*co*- glycolic acid) (PLGA) or poly (lactic acid) (PLA) are the most commonly used poly (α-hydroxy acids), which are often synthesized using a double emulsion-solvent evaporation technique [100-102]. Among others, Poly(γ-glutamic acid) (γ-PGA) is the most well known poly (amino acids) with unique characteristics of enzymatic degradation and reduced immunogenicity [103]. In addition, hydrophilic polysaccharide polymers such dextran and chitosan are also good candidates for vaccine delivery [104-107].

Despite the numerous efforts, polymeric nanoparticles have not yet been approved as vaccine adjuvants despite extensive efforts over the past years. However, scale up, processing and manufacturing are already in place for this technology [108]. Their adjuvant effect is associated with their rapid phagocytosis by macrophages and dendritic cells and prolonged antigen presentation in vitro [109, 110]. The surface of these nanoparticles can be conjugated with antibodies or other specific ligands to improve tissue, cellular, or subcellular targeting specificity [86]. Moreover, these nanoparticles have the potential to co-delivery adsorbed antigens and entrapped immunomodulatory molecules that activate APCs and induce subsequent T-cell immunity and can act as depot from which the encapsulated antigen is gradually release [111-113].

3.4.3 **Emulsions**

An emulsion is a mixture of two non-miscible liquids. One liquid is dispersed, as the internal phase, in another liquid, the continuous outer phase. An emulsifier is required as a substance that stabilizes the emulsion by increasing its kinetic stability. Depending on the water-to-oil ratio, the type of emulsifier, and the mixing procedure, a water-in-oil (W/O) or an oil-in-water (O/W) emulsion may be produced [114]. Emulsion adjuvants have been use since 1940s in vaccine formulation, dating back to the initial studies with Freunds's adjuvants [115].

Freund's complete adjuvant (FCA) is a mixture of mineral oil (Marco 52) and emulsifier (Arlacel A, mannide monooleate) prepared as an emulsion of 85% mineral oil and

15% emulsifier with 500 µg of heat-killed and dried *Mycobacterium tuberculosis* per milliliter of emulsifier mixture. FCA is effective in stimulating cellular immune response and may lead to the potentiation of the production of IgG and IgA however undesirable side effects are associated, such as increased pain and suffering [115]. The incomplete form IFA induces predominantly a Th2-biased response through the formation of a depot at the injection site and the stimulation of antibody producing plasma cells [116-118]. Both Freund's adjuvants are only use for research proposes.

The MF59 is the first oil-in-water adjuvant to be developed and approved for use in human vaccines in 1997 in combination with a seasonal influenza vaccine. It has the property of rapid recruitment and activation of helper CD4+ cells [119]. This successful adjuvant is composed by squalene, polyoxyethylene sorbitan monooleate (TweenTM 80), and sorbitan trioleate [120]. In response to MF59 injection APCs are recruited and up-regulation of multiple inflammatory cytokines, chemokines, receptors and genes responsible for antigen processing and presentation occurs [60]. However like alum, MF59 is predominantly a Th2 inducer [5]. Moreover, despite their excellent adjuvant effect, there have been reports that post-immunization reactions associated with emulsion adjuvants are becoming more frequent [46, 121].

Despite this, completely biodegradable squalene oil is currently a component in 5 approved o/w adjuvanted vaccines, Fluad® (MF59 adjuvanted seasonal influenza), Aflunov® (MF59 adjuvanted prepandemic influenza), Focetrea® (MF59 adjuvanted pandemic influenza), Prepandrix® (AS03 adjuvanted prepandemic influenza), and Pandremix® (AS03 adjuvanted pandemic influenza) [50].

Furthermore, several emulsions have been investigated using different families of natural oils in order to find a more stable, potent and less toxic formulation, such as Montanide [122] and W805EC a soybean based emulsion [123].

3.4.4 **ISCOMs**

ISCOMs are particulate antigen delivery systems composed by cholesterol, phospholipid and saponin forming cage-like structures [124]. Generally, the immunological potency of ISCOMs is linked with the marked adjuvancy of Quillaja saponins [125]. Loading of protein antigens to ISCOM matrices results in more potent immune responses, presumably because antigen and immunostimulatory Quillaja saponins are taken up by the same APC [126, 127].

ISCOM vaccines have been extensively studied with regard to their immunogenicity and it has been demonstrated that such vaccines are able to retained the adjuvant activity of the Quillaja, while increasing its stability, reducing its hemolytic activity, and producing less toxicity [128]. Furthermore, less antigen and adjuvant are required in ISCOMs vaccines for induction of protective immunity in the host when compared with vaccination with a simple mixture of free antigen and saponins/antigen. Indeed, both Th1 and Th2 responses are induced to a wide range of antigens in different animal models using this type of delivery systems [129-131]. As limitation, ISCOM technology is challenging because most soluble proteins do not usually contain exposed hydrophobic regions and are therefore difficult to incorporate into ISCOM structure [132].

3.4.5 **Virosomes**

Virosomes are prepared with solubilized viral spike glycoproteins reconstituted with phospholipids, forming unilamellar structures with a typical mean diameter of 150 nm.

The antigen is incorporated in these empty enveloped particles, which results in enhanced immunogenicity. The greatest advantage of these delivery systems is the exposure of viral proteins on their surface, which may help antigen uptake and immune cell activation [133]. Even though the basic principle is applicable to any enveloped virus, influenza virosomes remain the only virosome type applied in clinical stage vaccine candidates and in licensed products. The first of these was EpaxalTM, a hepatitis A vaccine registered in 1994 in several European, Asian and South American countries [134].

3.4.6 **Virus like particles (VLPs)**

Noninfectious and non-replicating VLP constitute another delivery system for antigens. VLP are self-assembling nanoparticles of approximately 20-100nm made from recombinant viral envelop and/or capsid proteins capable of displaying multiple antigen peptides on their surface [135]. While virosomes use the envelope phospholipid bilayers as a platform to which additional viral components or antigens are attached, VLPs are self-assembled viral capsid proteins [4]. The morphology and cell penetrating ability is similar to infective viral particles.

VLPs promoted uptake by APCs via endocytosis and stimulate both cellular and humoral immunity [136, 137]. The success of VLPs is well exemplified by the vaccine already approved for human papillomavirus (HPV) (Gardozil^{TM}) (USA) [138, 139].

4. LIPOSOMES

Liposomes are, without any doubt, the most studied vesicular systems for drug delivery. The hematologist Alec Bangham described liposomes essentially as bilayer vesicles composed of lipids, with or without additional lipophilic components, that in aqueous systems could form closed bilayer structures [140]. Since their discover liposomes moved a long way from being just another exotic object of biophysical research to becoming a pharmaceutical carrier of choice for numerous practical applications [141].

Table 2: Liposome-based drugs currently in clinical use.

Liposome formulation	Target disease	Drug name	Lipids used	Company
Liposomal Amphotericin B	Fungal Infection	Abelcet	DMPC DMPG	Enzon Pharmaceutical (USA)
Liposomal Amphotericin B	Fungal/Protozoal infection	AmBisome	PC Cholesterol DSPG	Gilead Sciences (USA)
Liposomal Amphotericin B	Fungal Infection	Amphotec	Cholesterol	Sequus Pharmaceuticals (USA)
Liposomal Cytorabine	Malignant lymphomatous meningitis	DepoCyt	DPPG DCPC Cholesterol	Skye Pharma (UK)/Enzon Pharmaceutical (USA)
Liposomal Daunorubicin	HIV-related Kaposi's Sarcoma	DaunoXome	DCPC Cholesterol	Galen (Ireland)
Liposomal Doxorubicin	Metastatic breast cancer	Myocet	DCPC Cholesterol	Zeneus Pharma (USA)
Liposomal Morphine	Post-surgical analgesia	DepoDur	DPPG DOPC	Pacira Pharmaceuticals (USA)/Skye Pharma (UK)
Liposomal Vertepofin	Macular degeneration	Visudyne	Egg PG DMPC	Novartis (Switzerland)
Liposome PEG-Doxorubicin	HIV-related Kaposi's Sarcoma, Breast & Ovarian cancers.	Doxil	DSPE HSPC Cholesterol	Merck (USA)

DMPC:dimyristoylphosphatidylcholine ; DMPG: 1,2-dimyristoyl-sn-glycero-3-phosphoglycerol

DCPC: distearoylphosphatidylcholine; Egg PG: egg phosphatidylglycerol;

DSPG: 1,2-Distearoyl-sn-glycero-3-phosphoglycerol, sodium salt

DPPG: 1,2-dipalmitoyl-sn-glycero-3-phosphoglycerol; DOPC: 1,2-Dioleoyl-sn-glycero-3-phosphocholine

DSPE: 1,2-distearoyl-*sn*-glycero-3-phosphoethanolamine; HSPC: hydrogenated soy phosphatidylcho

Gregoriadis was the pioneer on the subject and highlighted the ability of liposomes to entrap drugs [142], revealed the ability of liposomes to induce immune responses to incorporated or associated antigens [143-145], described methods to improve liposomal stability [146] and discussed the difficulties associated with liposomal clearance in vivo [147, 148]. Since then, liposomes have become important carrier systems and the interest for liposome-based vaccines has markedly increased. Moreover, liposomes are known to be safe and well tolerated as shown by the extensive use of approved liposomal-based drugs (Table 2).

4.1. Self- assembling of lipids

Molecular self-assembly can be defined as the process of spontaneous and reversible association of molecular species to form larger, more complex supramolecular entities according to the intrinsic characteristics contained in their components [149].

Liposomes, are colloidal micro- or nano-structures formed by self-assembly of lipid amphiphiles in water resulting in a bilayer of lipid surrounding an aqueous core [150]. The amphiphilic nature of lipids, a nonpolar hydrophobic tail covalently linked to a polar hydrophilic moiety, defines the way in which liposomes assemble. In most lipids the hydrophobic part consists of hydrocarbon chains, while the hydrophilic part consists of what is called a polar headgroup, that depending on the lipid composition can either have a net negative (anionic), neutral or positive (cationic) surface charge [151]. Above a critical lipid concentration, known as critical vesicle concentration (CVC), and in order to minimize the exposure of the hydrophobic tails to water, the polar heads form a single layer of lipid, with the nonpolar tails in touch with each in the central zone of the layer, which ideally results in bilayer formation. Intermolecular polar interactions, such as electrostatics and hydrogen bonding, can also occur and help define the structural specificity [152-154].

As delivery systems, the liposomes most important feature is the ability to encapsulate hydrophilic drugs inside the water compartment and to incorporate hydrophobic drugs into the liposome bilayer [155].

4.2. Lipid polymorphism

The actual form assumed by an aggregate depends on the molecular constitution of the amphiphilic and is highly dependent on its geometry. The fact that lipids assemble in closed structures or phases, for minimization of exposure of the hydrophobic tails to water, leads to an increase in membrane curvature. The phase behavior can be predicted by comparing the area of the polar group relative to the length of the nonpolar tail of the lipid. Generally, a simple geometric property of the lipid molecule, the so-called Israelachvili–Mitchell–Ninham packing parameter, $p = v / a \times l$, can be applied for determination of the self-assembled morphology. In the equation, **v** is the molecular volume, **a** is the cross-sectional area of the head group, and **l** is the length of the molecule [156-158]. Consequently, for p values close to 1, lipids exhibit cylindrical shape, having nearly equal headgroup to hydrocarbon proportions and are perfect for bilayer forming (Figure 2). Lipids with cone-like geometry with a large headgroup area and a small hydrocarbon tails, presents a $p<1/3$ and self-assemble into spherical micelles with a positive membrane curvature. For $1/3 < p < 1/2$ cylindrical micelles are formed and for $1/2<p<1$ perfect bilayers vesicles assemble. When $p >1$, the hydrophobic body is much larger than the polar head of lipid, resulting in inverted micelle formation such as the inverted hexagonal (H_{II}) phase or cubic phases that are said to exhibit negative membrane curvatures [159]**.** Furthermore, the effective molecular shape and consequently lipid phase behavior can also be modulated by changes in hydration, state of ionization, presence of divalent cations and temperature [160].

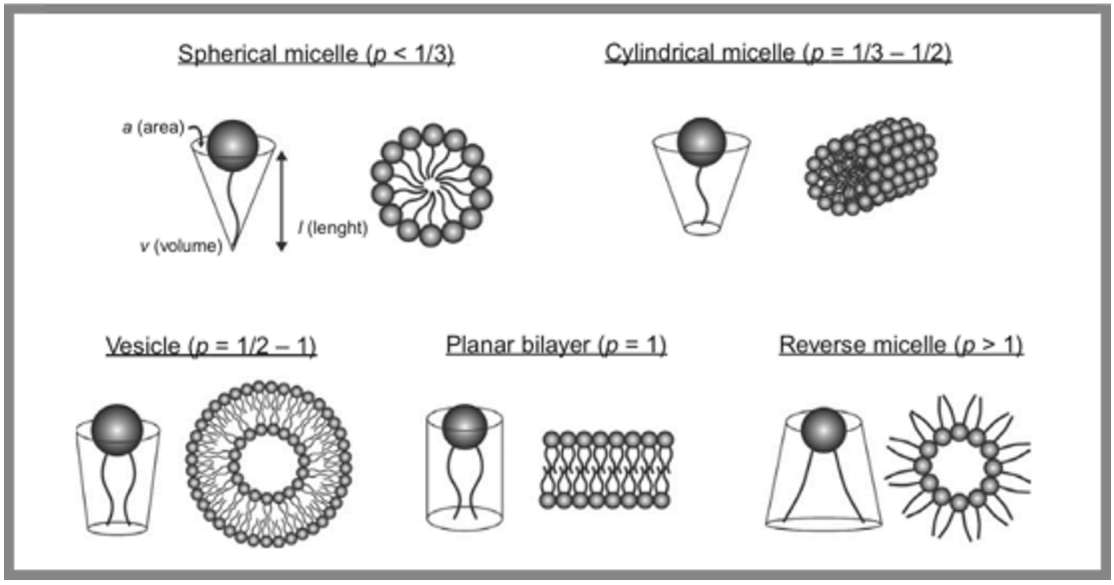

Figure 2: Relationship between the packing parameter (p) and the self-assembled morphology of amphiphilic molecules under aqueous conditions (adapted from Elizondo et al. 2011 [161]).

4.3. Lamellar phase transitions

A lipid bilayer is not static but is a dynamic surface. Consequently, lipids can diffuse over the lipid plane and the faster they do this, the more fluid the membrane is [162, 163]. Effectively, lipid physical state can change from gel phase to liquid phase, at a particular phase transition temperature (T_m), that is mainly dependent on chemical composition of the bilayer, in particular on the length and saturation of the lipid tail, number and saturation of the acyl chain and the size and ion strength of the headgroup. The gel phase, solid-ordered state, is characterized by tightly packed tails neatly ordered where only little diffusion is possible, making the membrane more rigid. When the temperature is raised the tails are more fluid but still ordered (intermediate phase) till T_m is reached and the membrane passes into the fluid phase (disordered state) where the tails are less organized and the membrane is more fluid and has a higher permeability (Figure 3). Therefore, lipids with a high T_m are more tightly packed because the phase equilibrium shifts to the gel phase [162-164]. Thus, liposomal formulations should be prepared above the transition temperature of lipid mixture in order to allow the lipid to hydrate in its fluid permeable phase.

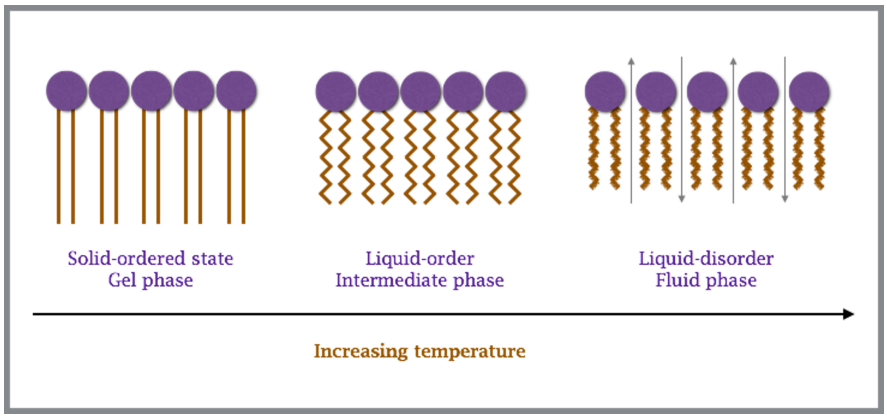

Figure 3: Illustration of the lipid bilayer structure as the temperature is increased above the lipid bilayer transition temperature.

4.4. Liposome preparation methods

A varied range of lipids with well-characterized biophysical behavior can be used for liposome formation. In fact, a key advantage of liposomes is their versatility and plasticity. Thus, selecting the appropriate combination of lipids and the method of assembly provides control over liposome macrostructures, biophysical characteristics, and subsequent in vivo behavior [165].

The correct choice of liposome preparation method should depend on the following parameters: the physicochemical characteristics of the drug to be entrapped and of the lipid mixture, the nature of the solvent in which the liposomes will be dispersed, the effective concentration of the entrapped drug, its potential toxicity and ultimately the application purpose. In addition, the method should proportionate optimum size, polydispersity and shelf--life of the liposomes according to the intended application and batch-to-batch reproducibility and possibility of large-scale production of safe and efficient liposomal products [166, 167].

The more representative liposome preparation methods used are thin film hydration method, the reverse-phase methods and the detergent depletion method. In the different methods, the drug can be loaded simply by adding it to lipid mixture in the organic solvent, dissolving it in the aqueous solution or added to the liposome dispersion. After formation of liposomes other techniques can be applied to improve loading, normally the freeze/thaw cycle method or the dehydration–rehydration procedure. Moreover, in order to further control the size, lamellarity, and homogeneity other methods can be performed post-formation of liposomes, such as sonication and extrusion [161].

Actuality, liposomes can be classified according to their size and lamellarity, which are important structural parameters that need to be controlled, since they are crucial factors affecting the performance of liposomes [168]. These structural properties can be fully explored depending on the preparation method applied. In this manner, according to their diameter (d) liposomes can be classified as small unilamellar vesicles (SUVs, $d \leq 200$ nm), large unilamellar vesicles (LUVs, $d \geq 200$ nm), multilamellar vesicles (MLVs $500 \leq d \leq 1000$ nm) composed of concentric layers of bilayers, or multivesicular vesicles (MVVs. $500 \leq d \leq 1000$ nm) composed of eccentric layers of bilayers (Figure 4) [161, 169].

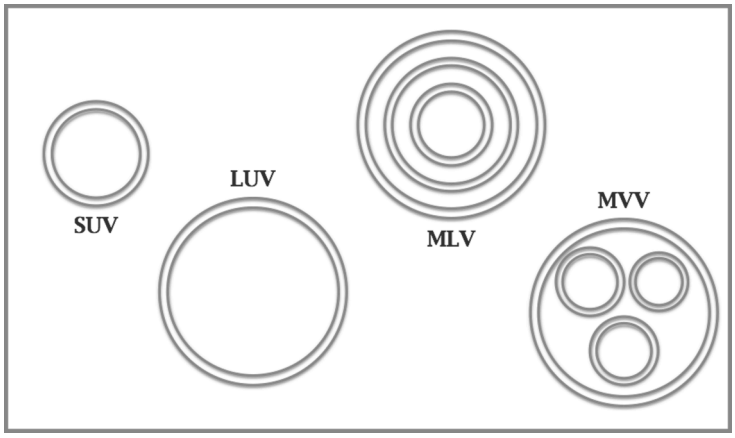

Figure 4: The different types of liposomes according to their size and lamellarity. SUV, small unilamellar vesicle; LUV, large unilamellar vesicle; MLV, multilamellar vesicle; MVV, multivesicular vesicle.

4.4.1 Thin film hydration or Bangham method

This method is the most widely used technique for liposome formation. A mixture of lipids is dissolve in an organic solvent such as ethanol or chloroform. The solvent is removed by rotatory evaporation, at reduced pressure, and the formed dried lipid film is hydrated with a pre-heated, above Tm of the lipid mixture, aqueous solution. This technique provides large and nonhomogeneous multilamellar vesicles (MLVs) with low encapsulation efficiencies [140, 170].

4.4.2 Reverse-phase methods

The reverse-phase methods include the reverse-phase evaporation (REV) method and the solvent injection method. The REV method consists of adding a small volume of aqueous phase to an organic solution of the lipids and results on the formation of inverted micelles. Removal of the organic solvent by rotatory evaporation generates a viscous gel that collapses, yielding an aqueous suspension of MLVs [171]. The solvent injection method starts by slowly injecting a solution of lipids in ethanol or ether into an aqueous phase with continuous vortexing, which forces the organic solvent to evaporate or disperse and lipid molecules to self-assemble in the aqueous phase [172]. Reverse-phase techniques present higher encapsulation efficiencies than thin film hydration, however they are limited by the solubility of the lipids in the organic phase, the subsequent removal of the solvent from the final preparation and the impossibility to control the morphology of formed liposomes, that can range from SUVs to MLVs [161].

4.4.3 Detergent depletion method

This method involves the formation of detergent–lipid micelles by the hydration of a lipid film with a detergent solution and results in the production of LUVs. The micelles coalesce and the lipids adopt a bilayer configuration forming sealed vesicles after detergent removal. The most common methods for detergent depletion are dialyses, dilution and gel filtration. However, a major problem associated with of this technique is the difficulty in removing the detergent. In addition, low trapping efficiency and length of preparation limit their use [173, 174].

4.4.4 **Freeze/thaw cycle**

This method is based on repeated cycles of rapid freezing of liposome dispersion, normally using liquid nitrogen, followed by thawing in warm water. It is often used for improving the loading when liposomes are formed using hydration method, resulting in MLVs. As a result, other techniques are need for the production of homogeneous SUVs. Industrial production is not easily viable since its reproducibility and yield are low, requiring multiple time- and energy-consuming steps to reach the final product [175].

4.4.5 **Dehydration–rehydration procedure**

Described by Kirby and Gregoriadis, this method involves the freeze-drying or the lyophilization of preformed vesicles dispersed in an aqueous medium with the drug followed controlled rehydration. During the drying process, lipid vesicles are concentrated concomitantly with solute, and at some point, fuse into large aggregates containing the drug to be trapped. Since the drug is already present in many of the interbilayer spaces when rehydrating, efficient trapping occurs. The method results in the production of MLVs with high trapping efficiency, however heterogeneous systems with low sample reproducibility are formed [176].

4.4.6 **Sonication**

Sonication is applied to the aqueous lipid dispersion by bath sonication or probe sonication. The ultrasounds disrupt the lipid bilayers of the large vesicles and leads to the formation of relatively homogenous population of SUVs. As the SUV form the lipid suspension begins to clarify yielding a slightly hazy transparent solution. The haze is due to light scattering caused by residual large particles remaining in the suspension. As main drawbacks of this technique are the use of probe tip sonicators which deliver high-energy input to the lipid suspension often causing oxidation and degradation [177, 178].

4.4.7 **Extrusion**

Lipid extrusion is a technique in which a lipid suspension is repeatedly forced through a polycarbonate filter with a defined pore size to yield particles with diameters near the pore size of the filter. It is primarily used to homogenize the dispersion followed by downsized the dispersion according to the size of the filter used. The main disadvantages of the extrusion

method are loss of material in the filters, the difficulty in maintain a high temperature (above lipid phase transition temperature), the extended time needed and the low working volumes of liposome dispersions [179, 180].

5. CATIONIC LIPOSOMES

The emphasis during the course of this thesis is the use of cationic liposomes, so they will be further analyzed. Cationic liposomes can be prepared using cationic lipids (mainly of synthetic nature) alone or in combination with a helper lipid, typically used for improvement of the membrane liposome stability and decrease the toxicity that is generally associated with cationic lipids.

5.1. Cationic lipids

Cationic lipids are amphiphilic molecules that structurally consist of a hydrophobic domain, a cationic polar head-group, and a linker group connecting the polar head-group with the non-polar tail [181].

In general, the different types of headgroups fall into the following categories: primary, secondary, tertiary amines or quaternary ammonium salts and guanidinium salts, amidine, as well as heterocyclic ring. The hydrophobic domains are mainly derived from either simple aliphatic hydrocarbon chains or steroid [182].

Cationic lipids with double-chain hydrocarbons in the hydrophobic domain represent the majority of cationic lipids synthesized so far because they are capable of forming liposomes by themselves or with a helper lipid. Therefore, most of the aliphatic chains in the cationic lipids are double-tailed. In addition, the hydrophobic domain of cationic lipids determines the phase transition temperature and the fluidity of the bilayer, and influences the stability and toxicity of liposomes [183].

The linker group that bridges the cationic lipid headgroup with the hydrocarbon moiety controls the biodegradability of a cationic amphiphile. Most of the linker bonds are ether, ester, or amide bonds [184].

The chemical structure of the most common cationic lipids used for liposomes production with immunostimulatory abilities are represented in the Figure 5.

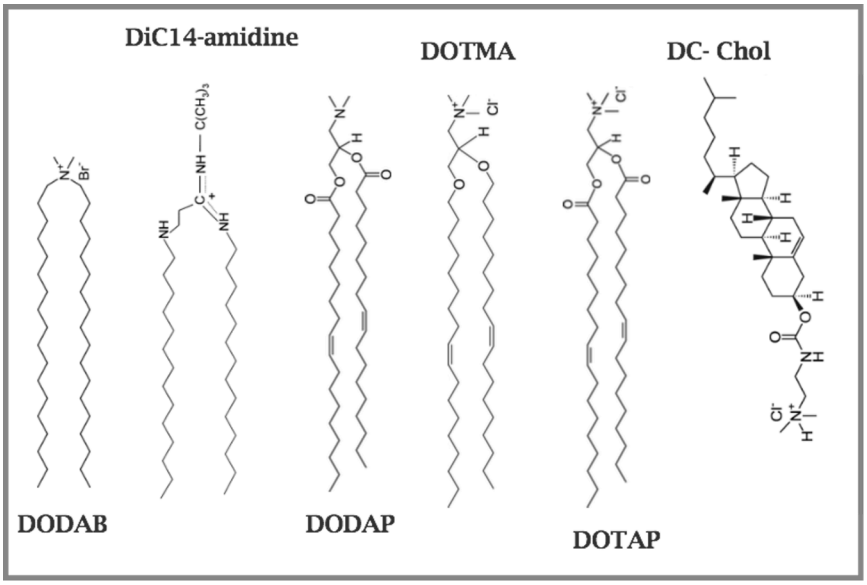

Figure 5: Cationic lipids already described as potential vaccine adjuvants. Diagrams were obtained from *www.avantilipids.com.*
DODAB: N,N-dioleyl-N,N dimethylammonium bromide;
DODAP: 1,2-dioleoyl-3-dimethylammonium-propane;
DOTMA: 1,2-di-O-octadecenyl-3-trimethylammonium propane;
DOTAP: 1,2-dioleoyl-3-trimethylammonium-propane;
DC-Chol: 3β-[N-(N',N'- dimethylaminoethane)-carbamoyl] cholesterol hydrochloride.

5.2. Cationic liposomes as antigen delivery systems

Liposomes were first described as being able to act as immunological adjuvants by Allison et al in the mid-1970s [143]. Since them, several advantages were found in the use of liposomes as adjuvant delivery systems. It is widely accepted that physical association between the liposomes and the antigen is a general prerequisite for adjuvanticity to occur [185]. The antigens can be entrapped within the liposomal aqueous compartment, electrostatically adsorbed onto the bilayer surface or hydrophobically inserted into the lipid structure, which allows a wide range of antigens (including peptides, proteins, carbohydrates, nucleic acids and haptens) to be incorporated in the liposome formulations. Either way liposomes offer antigen protection against host enzymatic degradation. The most important feature of liposomes, as vaccine delivery systems, is their natural ability to be avidly taken up by APCs, which promotes not only the antigen ingestion but also their processing and presentation on MHC molecules [181, 186-188]. Furthermore, due to liposomes flexibility and versatility, formulations can be tailored in terms of lipid composition, liposomal charge, size/lamellarity, and/or membrane fluidity in order to obtain optimal retention and

presentation of the vaccines antigens, leading to the desire vaccine-specific immune responses.

In particular, the surface charge of liposomes has a major importance in the immune response, with cationic liposomes having an advantage over their neutral and anionic counterparts. Indeed, the high surface density of positive charges offers an important platform for antigen adsorption due to electrostatic interactions. Moreover, the interaction between the positively charge liposomes and the negatively charged membranes of APCs enhances liposome uptake increasing the vaccine potency without the need to increase the concentration of antigen [189-192].

A wide range of cationic liposomes has been shown to mediate immunostimulatory effects. For example, DOTIM (octadecenoyloxy[ethyl-2-heptadecenyl- 3-hydroxyethyl] chloride) is the cationic lipid used for preparation of the cationic liposome complex CLDC, which is prepare by mixing liposomes with DNA. Several CLDC vaccines have been tested [193-196], and in particular, CLDC combined with cholesterol shows promise results as an adjuvant for human pre-pandemic inactivated H5N1 virus [193]. DOTAP (1,2-dioleoyl-3-trimethylammonium-propane) nanoliposomes containing soluble *Leishmania* antigens not only induced a Th1 type of immune response but also mediated protection against *L. major*, in BALB/c mice [197]. DC-Chol [N-(N',N'-Dimethylaminoethane)carbomyl] cholesterol) liposomes were also used in several strategies alone or mixtured with other lipids, proving their potential as immunomodulators by forming an antigen depot at the site of injection (SOI) and inducing immunological recall responses against coadministered tuberculosis vaccine antigen Ag85B-ESAT-6 [190] or by inducing protection in mice against Helicobacter pylori [198]. Several other cationic lipid adjuvant complexes were evaluated in various vaccine models and recent reviews report their effects [181, 192, 199-201].

5.2.1 **DODAB liposomes as adjuvants**

The focus throughout this thesis, is on N,N-dioleyl-N,N dimethylammonium bromide (DODAB). DODAB is a cationic surfactant that was first synthesized by Kunitake and Okahata, who prepared and characterized small unilamellar DODAB vesicles [202].

DODAB exhibits a hydrophobic group consisting of two 18-carbon-long acyl chain (C18:0) linked to a stable quaternary ammonium headgroup carrying the positively charged monovalent counterion bromide [203, 204]. The phase behavior of this lipid has been extensively studied [205, 206] thus its physicochemical characteristics can be easily

controlled, making it straightforward to design DODAB-based formulations with specific molecular structures. Due to its amphiphilic character, DODAB can form liposomal structures when dispersed in aqueous media above its relatively high T_m (T_m = 44 °C) [207] with an enthalpy of 47.4 kJ/mol [208]. In addition, DODAB presents a pretransition temperature (Tp) due to the tilting of the DODAB chains prior to the melting temperature [208].

Over the years, DODAB has been used for different applications in drug [208-213] and vaccine delivery [214-217]. The DODAB immunological properties were first observed by Gall in the mid-1960s [218]. The author tested a wide range of compounds for their ability to adjuvant diphtheria or tetanus toxoids in guinea pigs. In the surfactants compound group, Gall observed increased adjuvanticity for those expressing cationic quaternary ammonium head groups and long alkyl chains. Since then, DODAB liposomes have been tested in combination with a wide range of other molecules and their immunological proprieties explored. DODAB is known to enhance antigen uptake [219], induce cell-mediated immunity and delayed-type hypersensitivity [220] and capable of promoting a depot effect at the injection site (both after subcutaneous or intramuscular injection) longer than neutral liposomes [56, 190]. In the mouse model, the depot effect was accompanied by a stronger Th1 response characterized by IFN-γ production and IgG2 antibody titers and a general bias towards humoral immunity [56, 189, 190, 221-223]. In fact, the particular case of DODAB plus trehalose dibehenate (TDB) cationic liposomes, known as CAF01, have been extensively characterized and their potential as strong adjuvant system for vaccines against a wide range of diseases evaluated, showing particular promising results as a vaccine against tuberculosis [217, 224-227]. In another strategy also in a formulation for tuberculosis-unit vaccines DODAB was used in combination with monophosphoryl lipid A (MPL) promoting elevated immune responses [228, 229]. A formulation containing DODAB liposomes with monophosphoryl lipid A (MPL) or with trehalose 6,6'-dibehenate (TDB) were used as adjuvants and Chlamydia T cell antigens as molecular subunits and elicited protective immune responses when used in a vaccine strategy against Chlamydia [230]. In another study, the combination of DODAB with a major antigen of *Paracoccidioides brasiliensis* resulted in the lowest numbers of viable yeast cells in comparison with the use of other adjuvants such as aluminum hydroxide, CFA or flagellin in previously infected mice with *P. brasiliensis* [231]. Quil A cholesterol in combination with DODAB were used for the enhancement of Bovine viral diarrhea virus killed vaccines and elicited higher viral neutralizing antibodies levels and reduced injection site inflammation [232]. In other study, DODAB was used to enhance the efficacy of a DNA vaccine against pseudorabies virus and the authors demonstrated that only

DODAB, but not other adjuvants (such as CpG immunostimulatory motifs), induced significantly stronger immune responses than plasmid vaccination alone [233].

5.2.2 The use o monoolein as a helper lipid in DODAB liposomes

Monooleoyl-rac-glycerol (monoolein, MO) was first proposed as helper lipid in a DODAB liposomal formulation as non-viral transfection system [234]. MO is a natural-occurring neutral surfactant featuring a glycerol polar headgroup attached to a non- polar unsaturated acyl chain (C18:1) by an ester bond (Figure 6).

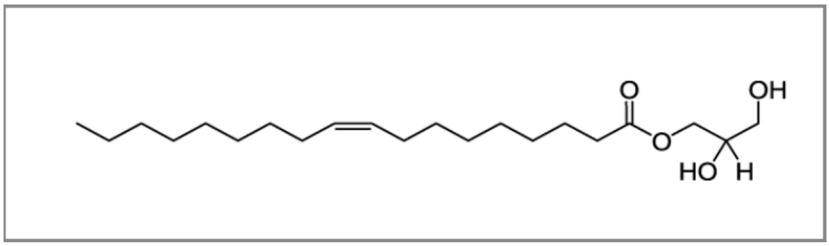

Figure 6: Chemical structure of Monoolein (MO).

MO has the ability to exist in several different phases, with one-, two-, and three-dimensional periodicity, such as lamellar phases (L_α), inverted micelles (L_2), hexagonal (H_2) and bicontinuous cubic phases, under rather easily accessible temperatures and pressure conditions. In particular MO has the peculiarity of forming two inverted bicontinuous cubic phases (Q_{II}^D and Q_{II}^G) in excess water (Figure 7) [60, 61]. The cubic phase is said to be *bicontinuous* since it consists of a curved bilayer extending in three dimensions, separating two congruent water channel net- works (Figure 7) [235].

This polymorphism has been explored in the past in different industrial, scientific and technological areas ranging from pharmaceuticals, food, cosmetics and agriculture to protein crystallization so serve as a emulsifier, solubilizer, absorption enhancer, ora/parental/vagina or periodontal drug delivery system, colloidal carrier system, storage system for protection of macromolecules susceptible to degradation and bioadhesive among others (revised by Ganem-Quintanar et al) [235].

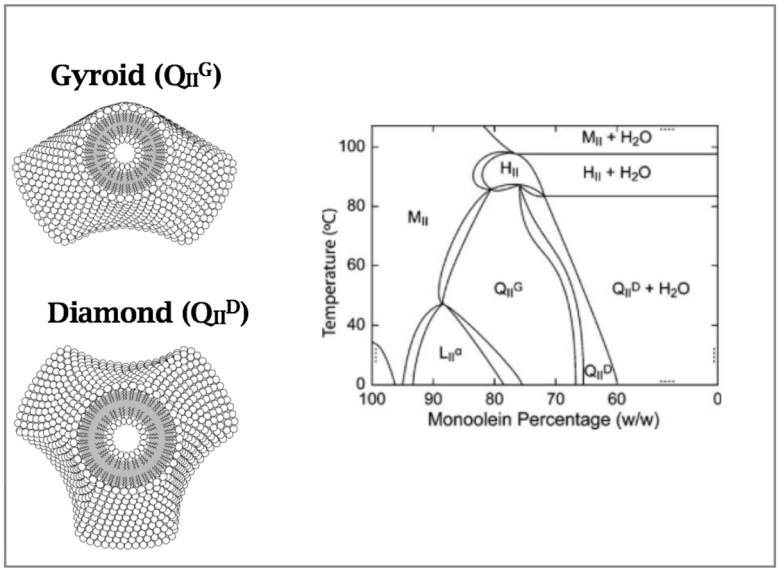

Figure 7: Monoolein phase diagram (right) presenting two inverse bicontinuous cubic phases (illustrated on the left) on the high water side of the lamellar L_α phase (adapted from Neves Silva et al. 2008 [234]).Micellar (M), hexagonal (H), lamellar (L), cubic (Q).

Phase scan imaging shows that DODAB liposomal formulations benefit from the structural richness of MO content, revealing that, at MO higher proportion, DODAB/MO liposomes are dominated by densely packed cubic-oriented particles [236]. This improvement in the structural complexity of DODAB liposomes can be used for the design of novel vaccine delivery systems. However, this is not the only advantage of MO incorporation, the introduction of a helper lipid to formulate drugs or vaccines, at reduced doses of the cationic lipid, is essential for minimization the cytotoxic effect associated with the charged lipid. Effectively, as cationic amphiphilic DODAB exhibits a dose-dependent cytotoxicity, requiring dose minimization for administration in vivo [211, 237, 238]. The incorporation of a helper lipid with a lower T_m value, such as cholesterol or DOPE, into DODAB liposomal membranes has been shown to improved membrane fluidity [236], which in turn leads to an improvement in liposome stability both *in vitro* and *in vivo* [146]. The transition phase temperature of DODAB is relatively high, in fact it is superior to the human physiological temperature, which confers to DODAB bilayers a strong rigidity, rendering DODAB liposomes an in vivo poor stability. The incorporation of MO in DODAB formulation at a higher percentage (MO > 50%) tends to abolish the pretransition temperature (T_p) of DODAB. Despite that, a slight increase in T_m is observed upon MO incorporation, which can be related to the asymmetric distribution of MO in the bilayer, leading to the formation of lipid domains rich in MO (more fluid) and rich in DODAB (more rigid) [208]. However, the energy required for the transition phase occur decreases suggesting that fewer molecules

contribute to the gel-to-liquid crystalline transition when the MO content is higher than DODAB content. In these sense, MO can be incorporated in DODAB liposomal systems for membrane stabilization without altering their T_m. This property can be an advantage since liposomes using high transition temperature lipids are known to retained a higher percentage of antigen at the injection site, thus leading to significantly higher Th1 responses, in comparison with liposomes made by low transition temperature lipids [239].

6. IS A VACCINATION NEEDED FOR PROTECTION AGAINST *CANDIDA ALBICANS?*

In the design of vaccines against fungal pathogens a good understanding of fungal–host interactions, including the possible antigen targets as well as innate and specific immune responses, is essential for the development of a protective immunity. Undoubtedly, other important factor for success in the endeavor to develop future vaccines is the refined selection of adjuvants that can direct the immune response toward the desired protective response.

6.1. *C. albicans* and candidiasis

The genus *Candida* is ubiquitous and composed of more than 150 yeast species, yet only a few are recognized as opportunistic fungal pathogens [240]. *C. albicans* and other *Candida* species are part of the normal flora of the skin, mucous membranes and gastrointestinal tract thus the risk of an endogenous *Candida* infection is always present. Consequently, under certain risk factors, *C. albicans* is capable of cause severe infections [241, 242]. These infections can range from 'superficial candidiasis', mainly in the skin, nail, oral and vaginal surfaces to 'systemic or invasive candidiasis', generally located in the respiratory, urinary tract or other internal organs that can disseminate via the blood stream (candidemia) and virtually infect any other organ.

Currently, systemic infections caused by *Candida* species, mainly caused by *Candida albicans*, represent the fourth leading cause of nosocomial bloodstream infection in modern hospitals, despite the administration of antifungal agents that have potent activity *in vitro* and *in vivo* in preclinical studies. The mortality of affected patients exceeds 30%–40%, and thus this type of infection is considered a significant public health problem, indicating that disease treatment and prevention measures are failing [243, 244].

Several studies have defined the risk factors that predispose patients to developing invasive *Candida* infections. Most of these factors are easily identifiable and precede the infection, which open a window of opportunities to vaccinate acutely at-risk patients before the onset of infection.

Generally, susceptibility to infection is enhanced for hospitalized patients submitted to procedures that involve: the disruption of the anatomical defenses, including surgery/transplantation, cytotoxic chemotherapies, the introduction of central venous catheters, parenteral nutrition, the insertion of indwelling devices (for example prosthetic

heart valves) which are susceptible to develop biofilms (that are more resistant to drugs and capable of greater tissue invasion). In addition, or burn injury and prolonged periods without feeding can lead to gut mucosal wasting (from lack of use) and exposure to broad spectrum antibiotics, which wipes out the normal bacterial flora and also represent risk factors [245-254].

In fact, despite the widespread belief that only immunocompromised patients are susceptible to fungal infection, patients with profound defects in immunity (neutropenic, corticosteroid-treated, treated with cancer chemotherapy, infected with HIV, etc.) represent only 10–20% of occurring *Candida* disseminated candidiasis [255-257]. And even those patients can benefit from vaccination since there is extensive literature confirming the immunogenicity and efficacy of vaccines in patients with extremely weakened immune systems, for example, those with active leukemia, HIV infections, or receiving immune-suppressing corticosteroids [258-263].

Of course commensal host colonization by *Candida* is the first step in the pathogenesis of disseminated candidiasis of endogenous origin. Patients with higher colonization burdens and more sites colonized have a proportional higher risk of developing candidemia. Indeed, treatments that lower colonization burden simultaneously decrease the risk of fungemia [264, 265].

6.2. *C. albicans* cell wall surface proteins (CWSP)

The cell wall of *C. albicans* is not only a dynamic structure that confers osmotic stabilization, protection against mechanical stress and morphological plasticity, important for the transitions that many fungi undergo, but is also a significant source of candidal antigens [266].

Structurally, the cell wall is constituted by three major polysaccharides, chitin, glucans and mannans (Figure 8). In *C. albicans,* these polysaccharides are organized as two layers: an inner skeletal layer of chitin and β-1,3-linked glucan covalently linked to an outer layer of β1,6-glucan [267]. Attached to this meshwork of structural polysaccharides the outer layer is enriched with cell wall proteins (CWP). The CWPs are normally highly glycosylated with mannose-containing polysaccharides (sometimes called mannan), and carbohydrates can account for up to 90% of their molecular mass [268].

This proteins can be grouped in three main classes, two of them covalently coupled to

cell wall polysaccharides: glycosyl-phosphatidylinositol cell wall proteins (GPI-CWPs) are the more abundant and generally indirectly linked to β-1,3-glucan through a connecting β-1,6-glucan moiety, and Pir proteins (proteins with *i*nternal *r*epeats, Pir-CWPs), which are presumed to be directly linked to β-1,3-glucan through the γ-carboxyl group of glutamic acids, arising from specific glutamines [269].

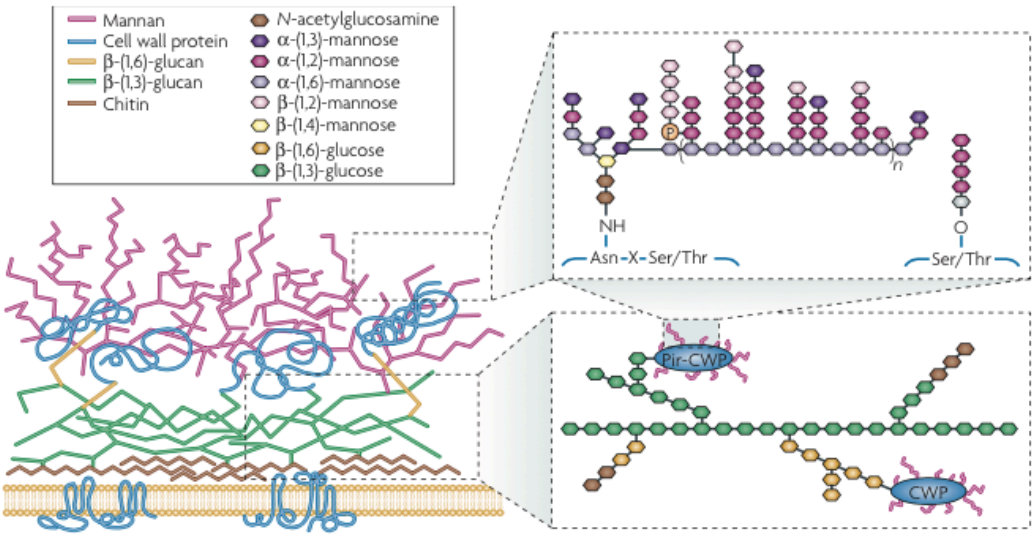

Figure 8: The structure of the *Candida albicans* cell wall (adapted from Netea et al. 2008 [268]).

The third class of proteins lacks the covalent attachment to the polysaccharide matrix and can be released from intact cells using a reducing agent. This suggests that they might be disulphide-linked to other cell wall proteins [270, 271].

Both carbohydrate and protein moieties are able to trigger immune responses [272]. In particular, the cell wall proteins of *C. albicans* are highly glycosylated with elaborate carbohydrate structures comprised of α- and β-linked mannose units. Protein mannosylation, occurs during protein synthesis in the endoplasmic reticulum (ER) and is further elaborated as the protein is passed through the Golgi apparatus [273]. Mannoproteins, including O-glycosylated oligosaccharide and N-glycosylated polysaccharide moieties, involve phosphodiester groups that confer to the outer surface of yeasts numerous negatively charged components [274].

The glycosylated proteins represent 30-40% of the cell wall dry weight and due to its outer location are readily recognized by the host immune cells, triggering and modulating the anti-Candida host immune responses, and therefore considered as the most important pathogen-associated molecular patterns (PAMPs) of *C. albicans* [275-277], inducing mainly

Th1-type cytokine profiles [278]. In fact, it is known that cell wall proteins are recognized by immune cells and therefore relevant as antigens and vaccine targets [279, 280].

6.3. Immune response to *C. albicans* infection

C. albicans is an effective colonizer of the human body, very well adapted to its host. The immune system does not remain ignorant of commensal fungi, and so a balanced between pro-and anti-inflammatory signals is required for the conservation of such a stable host-fungi interaction. For that immune system responses to *C. albicans* are based in two main strategies: resistance and tolerance. The resistance compromises the ability to limit fungal burden, and tolerance the ability to limit the host damage cause by the immune response or other mechanism [281].

The initial mechanism of innate immunity against *Candida* infections includes the barrier function of the skin and mucosal epithelial surfaces [282]. After disturbance of these barriers, elimination of fungi by the innate immune cells, especially by macrophages and neutrophils, is crucial for impaired host defense against candidiasis. Microbial antagonism, defensins, collectins and the complement system also play an important role in the innate resistance to fungal infections [283].

The innate recognition of fungi by phagocytes is achieved largely through the sensing of cell wall constituent (Table 3) [268]. Indeed, it is known that alterations in the cell wall composition, that varies between different fungal species and between the different morphological forms of the same species, affects phagocyte migration towards the fungus [284-286].

Table 3: Pattern recognition receptors sensing *C. albicans* PAMPS at the membrane level. (adapted from Brown et al 2011[287] and Netea et al. 2010 [288])

PRR	*C. albicans* PAMP(s)	Cytokines secreted	Type of response
TLR2	Mannan,	IL-10, TGFβ,	Treg
	Phospholipomannan, GXM	TNF, IL-12, IL-1, 1L-6.IL-8	Th1
TLR4	Mannan, O-mannan, GXM	TNF, IL-12, IL-1, 1L-6.IL-8	Th1
Dectin-1[a]	β-1,3-glucan	IFN type 1 family IL-12, IL-10,	Treg
		TNF, IL-1, IL-23, Il-6	Th17
Dectin-2	α-mannan	TNF, IL-1	DC activation
DC-SIGN	Mannan, galactomannan	IL-10	
Mannose receptor	Mannan, N-mannan, GlcNAc, glycoprotein	TNF, IL-1, IL-23, Il-6	Th17
CD14	Mannan, GXM	TNF, IL-12, IL-1, 1L-6.IL-8	
FcγR	Mannan, GXM	TNF, IL-1, IL-23, Il-6	Th17
Mincle	α-mannose	TNF, IL-1, IL-23, Il-6	Th17
SCARF	Mannan, β-glucan	TNF/IL-8	
CD36	β-glucan	TNF/IL-8	
Uknown	Chitin	IL-44	Th2
CD36	β-glucan	TNF/IL-8	
Uknown	Chitin	IL-44	Th2

Phagocytic clearance of opsonized and non-opsonized fungal pathogens may be considered to consist of four distinct stages; (i) accumulation of phagocytes at the site where fungal cells are located; (ii) PAMP recognition through membrane bound and soluble PRRs (PRRs involved in *C. albicans recognition* and the respective cell wall PAMPs are depicted in table 3) (iii) engulfment of fungal cells bound to the phagocyte cell membrane, and (iv) processing of engulfed cells within phagocytes by fusion with lysosomal vesicles to form the phagolysosome, an organelle with acidic pH and several antimicrobial compounds [289]. Degradation of phagocytized *C. albicans* cells is carried out by oxidative mechanisms, including generation of reactive oxygen and nitrogen intermediates, as nitric oxide, and by

non-oxidative mechanisms, such as antimicrobial peptides [290]. Conversely, in order to manipulate host immune responses and survive, or even replicate within the host, fungal pathogens employ several strategies to avoid phagocytes recognition and killing by masking cell wall PAMPS among others. Moreover, many fungi resist to phagocytic killing producing anti-oxidant enzymes, such as catalase and superoxide dismutase, and/or by inducing protective responses, such as DNA damage repair systems and heat shock proteins, that help the fungal cell cope with oxidative damage [291].

One of the major virulence attributes of *C. albicans* is its ability to reversibly switch between yeast and filamentous forms that is known to contribute to the fungus pathogenicity [287]. Whereas the yeast form may be the mode of proliferation in infected tissues, the hyphal forms are used to adhere and invade epithelial cells during mucosal infections, resulting in extensive damage to host cells. Moreover, this yeast to hyphae transitions is also induced upon phagocytosis by macrophages, allowing pathogen evasion from immune capture.[292]

For efficient control of *C. albicans* infections an activated innate immune system is not sufficient. The evidence suggests that both innate and adaptive responses integrate to produce effective anti-fungal protection [293, 294]. Upon interaction of fungi with the different PRRs, activated phagocytes, such as DCs, initiate the adaptive immune response via secretion of pro-inflammatory cytokines and chemokines and presentation of antigens and ultimately initiate Th-cell differentiation [295].

T-cell activation is a crucial step in the development of optimal protective immunity against *C. albicans*. Although, both $CD4^+$ and $CD8^+$ T cells are necessary for elimination of fungal cells, in the primary stages of disease, the presence of $CD4^+$ T cells are important for the survival of the host. Although $CD8^+$ T cells are believed to produced cytokines crucial for fungal defense their role in candidiasis is not clearly defined [296] .

It is accepted that antifungal $CD4^+$ T helper 1 (Th1)-mediated responses play a central role in *C. albicans* defenses, providing control of fungal burden through the concerted action of several cytokines such and INF-γ (interferon gamma), IL-6 (interleukin 6), TNF-α (Tumor necrosis factor alpha), and IL-12, required for optimal activation of phagocytes at the site of infection and necessary for the formation of some protective antibodies against the fungus [2, 281]. Interestingly, though protective immunity against *C. albicans* is primarily mediated by Th1 cells, some Th2 cytokines, such as IL-4 are required for the maintenance of the anti-fungal immune protection [281, 297, 298]. Regulatory T-cells (Treg) are involved in the induction of memory protective immunity by allowing the balance between the two types of responses, limiting collateral damage to tissues and restoring a homeostatic environment,

down-regulating the antifungal Th1 reactivity. Secretion of IL-10 represents one of the mechanisms by which Treg cells mediate suppression and control inflammatory responses [299]. Activation of Th17 cells, characterized by the production of interleukin-17 (IL-17), also occurs in fungal infections. Th17 cells mobilize neutrophils and induce the production of defensins, which greatly contributes to efficient control of an infection at different body sites [300].

Although, cell-mediated immunity is acknowledged as the predominant host defense mechanism against fungal infections, antibodies can play a decisive role in the overall resistance to fungi [301].

The mechanism(s) by which specific antibodies mediate protection against fungi is a contentious issue. It has been observed that the protective potential of antibodies with enhanced phagocytosis and killing of the fungus is dependent on a multiple and perhaps interdependent characteristics such as epitope specificity, isotype, serum titer, and ability to rapidly and efficiently fix complement to the fungal surface [302-304]. In this sense, several researchers reported antibody-mediated protection against *Candida* infections, using different antigen targets, such as mannans, glucans, heat-shock proteins, Saps, and adhesins, with the purpose of producing monoclonal or recombinant antibodies as potential novel treatments [305-309].

6.4. Delivery systems used in *C. albicans* vaccination strategies

As proof of interest in the development of vaccines against *C. albicans* is the numerous vaccine candidates that have been reported [310-319]. However, despite extensive investigations, only two are in clinical trials, and none have yet been approved by regulatory agencies for either active or passive immunization in humans.

In the effort to use safer and simpler fungal antigens that could be used as novel strategies for vaccination, adjuvants have become relevant as immunostimulators to elicit successful protective immune responses.

Several highly innovative strategies that take advantage of delivery systems have been published in recent years and the most important will be selectively highlighted herein. Of note, is the fact that the majority of this strategies lack the knowledge of the physiochemical and biological properties of the particles that are formed after mixing the antigens with the delivery systems. However, it is important to consider the adequate selection of adjuvant and

antigen, and to characterized and optimized the final particle in order to improve the immunogenicity and obtain the desire vaccine-specific immune responses with minimal toxicity associated.

6.4.1 *C. albicans* vaccination strategies that take advantage of aluminium adjuvant delivery systems

NDV-3 is a cell wall protein based-vaccine strategy composed by the N- terminal portion of the *Candida albicans* agglutinin-like sequence 3 protein (Als3p) formulated with an aluminum hydroxide adjuvant in phosphate-buffered saline. Of note is the fact that initial studies were preformed using Freund's adjuvant. Preclinical studies demonstrated that NDV-3 vaccine antigen protects mice from oropharyngeal, vaginal and intravenous challenge with *C. albicans* and other selected species of *Candida.* IFN-γ and IL-17A were necessary for vaccine-induced protection in mice [320]. Interestingly, 'cross-kingdom' protection against *S. aureaus* was demonstrated [321]. The results obtained with this strategy led to a Phase I clinical trial in human subjects performed by NovaDigm Therapeutics. NDV-3 proved to be safe and generally well-tolerated in healthy adults, eliciting quick and robust B- and T-cell immune responses [322].

In another strategy the use of the N-terminus of *C. albicans* cell surface prHyr1 protein (rHyr1p-N) mixed with alum significantly improved the survival and reduced the fungal burden of hematogenously disseminated candidiasis in both immunocompetent and immunocompromised mice. Furthermore, using a passive immunotherapy strategy**,** a pooled of rabbit anti-Hyr1p polyclonal antibodies raised against 8 different peptide regions of rHyr1p-N, also protected mice from a hematogenously disseminated candidiasis model. These antibodies directly neutralized the Hyr1p virulence function, rather than enhanced opsonophagocytosis for subsequent killing by neutrophil *in vitro*. Both active and passive immunization novel strategies against *Candida* infections can be design using the rHyr1p-N vaccine [323].

6.4.2 *C. albicans* vaccination strategies that take advantage of emulsions adjuvant delivery systems

Lam–CRM conjugate is a vaccine formulation design to protect against a variety of human pathogenic fungi, including *C. albicans*, and is based on laminarin (Lam), a well-

characterized but poorly immunogenic β-glucan from the brown alga *Laminaria digitata,* conjugated with the nontoxic mutant protein of diphtheria toxin CRM197 (a carrier protein used in some glyco-conjugate bacterial vaccines), using Freund's Complete Adjuvant (FCA) as an adjuvant. This Lam–CRM conjugate proved to be immunogenic and protective against both *C. albicans* systemic and vaginal infections in mice. Furthermore, the protective role of the anti-β -glucan antibodies was confirmed when passive transfer of whole immune serum, immune vaginal fluid, and the affinity-purified anti-glucan IgG fractions provided protection in naive mice [307].

MF59, the oil-in-water adjuvant, has been also tested in combination with Laminarin-CRM conjugate in various experimental vaccines. Administrated systemically, this adjuvanted conjugate stimulated protective immune responses against vaginal candidiasis [324]. The protection was associated with the production of serum and vaginal anti-β-glucan IgG antibodies as inferred by the efficacy of passive transfer of immune vaginal fluid and passive protection by an anti-β-1,3-glucan mAb [324].

Another highly innovative approach against *Candida* infections has been developed by Xin et al. [325]. These investigators synthetize six peptides from *C. albicans* cell wall proteins and conjugated which one with fungal cell wall β -mannan trisaccharide emulsified in CFA creating six new adjuvanted glycopeptide conjugates. Five conjugates protected mice against murine disseminated candidiasis using a dendritic cell (DC)-based immunization approach. The beta-(Man)(3)-Fba, beta-(Man)(3)-Met6 and beta-(Man)(3)-Hwp1 induced protection evidenced by survival and reduced kidney fungal burden, the beta-(Man)(3)-Eno1 and beta-(Man)(3)-Gap1 gave moderate protection. In particular, for beta-(Man)(3)-Fba conjugate, protection was uniquely acquired through immunity against the carbohydrate and the Fba peptide.

6.4.3 *C. albicans* vaccination strategies that take advantage of liposomal adjuvant delivery systems

Multilamellar liposomes were used for encapsulation of a mannan extract from *C. albicans* and used to vaccinate mice. Liposomes based on phosphatidylcholine and cholesterol (3.2:1) were used for entrapment of the extract. Vaccinated mice showed more resistance to disseminated candidiasis than did mice vaccinated with the free extract. In addition, antiserum from immunized animals protected naive BALB/cByJ mice against *C. albicans* serotype A and B strains and *C. tropicalis* [326].

In another study, *C. albicans* cytosolic proteins (Cp) were entrapped either in plasma beads, liposomes or in liposomes further entrapped in plasma beads. The efficacy of the different formulations in protecting mice against a lethal challenge of *C. albicans* was determined, showing that the preparation containing liposomized Cp entrapped in plasma beads was more immunogenic and imparted superior protection in immunized mice, as evaluated by the survival rate and fungal burden in systemic circulation and vital organs, compared with the results obtain with the Cp entrapped only in plasma beads or only in the liposomes. This vaccination strategy successfully elicits desired cell mediated and antibody humoral responses [246].

Another liposomal vaccine was formulated with *C. albicans* ribosomes and the lipids dimyristoylphosphatidylcholine (DMPC) and dimyristoylphosphatidylglycerol (DMPG) (9:1 molar ratio). Some of the evaluated formulations contained lipid-A as an additional adjuvant. The efficacy of these vaccines in mice was evaluated using the survival rate against a challenge with *C. albicans*; the induction of delayed type hypersensitivity (DTH) and the anti-*Candida* antibody titer. Unimmunized mice and mice vaccinated with ribosomes supplemented with Incomplete Freud's Adjuvant (IFA) were used for comparison. The results indicate that the liposomal vaccines were at least as effective as the IFA-based vaccine with a survival rate that ranged between 60-80% [327].

6.4.4 *C. albicans* vaccination strategies that take advantage of virosomes adjuvant delivery systems

A novel vaccine candidate (PEV7; Pevion Biotech) with the aim to prevent recurrent vulvaginitis is in clinical trial since 2010. This vaccine is based on a recombinant, truncated form of Sap2p, a secreted aspartyl proteinase, incorporated into virosomes. Prior to virosome assembly, antigen rtSap2 was conjugated to 1,2-dipalmitoyl-sn- glycero-3-phosphoethanolamine (DPPE) moieties and then mixed with synthetic lipids and then combined with the influenza envelope components at the desired concentration. In a rat model of candidal vaginitis, PEV7 induced significant, long-lasting, likely antibody-mediated protection following intravaginal immunization. PEV7 was also found to be safe in a repeated-dose toxicological study in rats [328]. Although a full description Phase I trial results is not currently in the public domain and interim data indicate that PEV7 it is well tolerated and is 'effective' at low doses.

REFERENCES

1. **Delany, I., Rappuoli, R., and De Gregorio, E.**, Vaccines for the 21st century. EMBO Mol Med, 2014. **6**(6): p. 708-20.
2. **Mochon, A.B. and Cutler, J.E.**, Is a vaccine needed against *Candida albicans*? Med Mycol, 2005. **43**(2): p. 97-115.
3. **Black, M., Trent, A., Tirrell, M., and Olive, C.**, Advances in the design and delivery of peptide subunit vaccines with a focus on toll-like receptor agonists. Expert Rev Vaccines, 2010. **9**(2): p. 157-73.
4. **Perrie, Y., Kirby, D., Bramwell, V.W., and Mohammed, A.R.**, Recent developments in particulate-based vaccines. Recent Pat Drug Deliv Formul, 2007. **1**(2): p. 117-29.
5. **O'Hagan, D.T. and De Gregorio, E.**, The path to a successful vaccine adjuvant--'the long and winding road'. Drug Discov Today, 2009. **14**(11-12): p. 541-51.
6. **Reed, S.G., Bertholet, S., Coler, R.N., and Friede, M.**, New horizons in adjuvants for vaccine development. Trends Immunol, 2009. **30**(1): p. 23-32.
7. **Perrie, Y., Mohammed, A.R., Kirby, D.J., McNeil, S.E., and Bramwell, V.W.**, Vaccine adjuvant systems: enhancing the efficacy of sub-unit protein antigens. Int J Pharm, 2008. **364**(2): p. 272-80.
8. **Hoebe, K., Janssen, E., and Beutler, B.**, The interface between innate and adaptive immunity. Nat Immunol, 2004. **5**(10): p. 971-4.
9. **Castellino, F., Galli, G., Del Giudice, G., and Rappuoli, R.**, Generating memory with vaccination. Eur J Immunol, 2009. **39**(8): p. 2100-5.
10. **Moser, M. and Leo, O.**, Key concepts in immunology. Vaccine, 2010. **28 Suppl 3**: p. C2-13.
11. **Clem, A.S.**, Fundamentals of vaccine immunology. J Glob Infect Dis, 2011. **3**(1): p. 73-8.
12. **McCullough, K.C. and Summerfield, A.**, Basic concepts of immune response and defense development. ILAR J, 2005. **46**(3): p. 230-40.
13. **Janeway, C.A., Jr.**, Presidential Address to The American Association of Immunologists. The road less traveled by: the role of innate immunity in the adaptive immune response. J Immunol, 1998. **161**(2): p. 539-44.
14. **Janeway, C.A., Jr.**, Approaching the asymptote? Evolution and revolution in immunology. Cold Spring Harb Symp Quant Biol, 1989. **54 Pt 1**: p. 1-13.

15. **Shishido, S.N., Varahan, S., Yuan, K., Li, X., and Fleming, S.D.**, Humoral innate immune response and disease. Clin Immunol, 2012. **144**(2): p. 142-58.
16. **Sarma, J.V. and Ward, P.A.**, The complement system. Cell Tissue Res, 2011. **343**(1): p. 227-35.
17. **Kaveri, S.V., Silverman, G.J., and Bayry, J.**, Natural IgM in immune equilibrium and harnessing their therapeutic potential. J Immunol, 2012. **188**(3): p. 939-45.
18. **Jouault, T., Sarazin, A., Martinez-Esparza, M., Fradin, C., Sendid, B., and Poulain, D.**, Host responses to a versatile commensal: PAMPs and PRRs interplay leading to tolerance or infection by *Candida albicans*. Cell Microbiol, 2009. **11**(7): p. 1007-15.
19. **Bourgeois, C., Majer, O., Frohner, I.E., Tierney, L., and Kuchler, K.**, Fungal attacks on mammalian hosts: pathogen elimination requires sensing and tasting. Curr Opin Microbiol, 2010. **13**(4): p. 401-8.
20. **Akira, S.**, Toll-like receptor signaling. J Biol Chem, 2003. **278**(40): p. 38105-8.
21. **Stuart, L.M. and Ezekowitz, R.A.**, Phagocytosis: elegant complexity. Immunity, 2005. **22**(5): p. 539-50.
22. **Segal, A.W. and Coade, S.B.**, Kinetics of oxygen consumption by phagocytosing human neutrophils. Biochem Biophys Res Commun, 1978. **84**(3): p. 611-7.
23. **Kumar, H., Kawai, T., and Akira, S.**, Pathogen recognition by the innate immune system. Int Rev Immunol, 2011. **30**(1): p. 16-34.
24. **Mancini, R.J., Stutts, L., Ryu, K.A., Tom, J.K., and Esser-Kahn, A.P.**, Directing the immune system with chemical compounds. ACS Chem Biol, 2014. **9**(5): p. 1075-85.
25. **Storni, T., Kundig, T.M., Senti, G., and Johansen, P.**, Immunity in response to particulate antigen-delivery systems. Adv Drug Deliv Rev, 2005. **57**(3): p. 333-55.
26. **Arango Duque, G. and Descoteaux, A.**, Macrophage cytokines: involvement in immunity and infectious diseases. Front Immunol, 2014. **5**: p. 491.
27. **Chaplin, D.D.**, Overview of the immune response. J Allergy Clin Immunol, 2010. **125**(2 Suppl 2): p. S3-23.
28. **Akira, S.**, Innate immunity and adjuvants. Philos Trans R Soc Lond B Biol Sci, 2011. **366**(1579): p. 2748-55.
29. **Ollila, J. and Vihinen, M.**, B cells. Int J Biochem Cell Biol, 2005. **37**(3): p. 518-23.
30. **Love, P.E. and Bhandoola, A.**, Signal integration and crosstalk during thymocyte migration and emigration. Nat Rev Immunol, 2011. **11**(7): p. 469-77.

31. **Germain, R.N.**, MHC-dependent antigen processing and peptide presentation: providing ligands for T lymphocyte activation. Cell, 1994. **76**(2): p. 287-99.
32. **Janeway, C.A., Jr. and Bottomly, K.**, Signals and signs for lymphocyte responses. Cell, 1994. **76**(2): p. 275-85.
33. **Corthay, A.**, A three-cell model for activation of naive T helper cells. Scand J Immunol, 2006. **64**(2): p. 93-6.
34. **Fu, H., Wang, A., Mauro, C., and Marelli-Berg, F.**, T lymphocyte trafficking: molecules and mechanisms. Front Biosci (Landmark Ed), 2013. **18**: p. 422-40.
35. **Williams, M.A., Cheadle, C., Watkins, T., Tailor, A., Killedar, S., Breysse, P., Barnes, K.C., and Georas, S.N.**, TLR2 and TLR4 as Potential Biomarkers of Environmental Particulate Matter Exposed Human Myeloid Dendritic Cells. Biomark Insights, 2007. **2**: p. 226-40.
36. **Curtsinger, J.M. and Mescher, M.F.**, Inflammatory cytokines as a third signal for T cell activation. Curr Opin Immunol, 2010. **22**(3): p. 333-40.
37. **Bettelli, E., Carrier, Y., Gao, W., Korn, T., Strom, T.B., Oukka, M., Weiner, H.L., and Kuchroo, V.K.**, Reciprocal developmental pathways for the generation of pathogenic effector TH17 and regulatory T cells. Nature, 2006. **441**(7090): p. 235-8.
38. **Crotty, S.**, T follicular helper cell differentiation, function, and roles in disease. Immunity, 2014. **41**(4): p. 529-42.
39. **Zhu, J. and Paul, W.E.**, Heterogeneity and plasticity of T helper cells. Cell Res, 2010. **20**(1): p. 4-12.
40. **Shrikant, P.A., Rao, R., Li, Q., Kesterson, J., Eppolito, C., Mischo, A., and Singhal, P.**, Regulating functional cell fates in CD8 T cells. Immunol Res, 2010. **46**(1-3): p. 12-22.
41. **Banchereau, J., Bazan, F., Blanchard, D., Briere, F., Galizzi, J.P., van Kooten, C., Liu, Y.J., Rousset, F., and Saeland, S.**, The CD40 antigen and its ligand. Annu Rev Immunol, 1994. **12**: p. 881-922.
42. **Noelle, R.J.**, CD40 and its ligand in host defense. Immunity, 1996. **4**(5): p. 415-9.
43. **Calame, K.L., Lin, K.I., and Tunyaplin, C.**, Regulatory mechanisms that determine the development and function of plasma cells. Annu Rev Immunol, 2003. **21**: p. 205-30.
44. **Amzel, L.M. and Poljak, R.J.**, Three-dimensional structure of immunoglobulins. Annu Rev Biochem, 1979. **48**: p. 961-97.

45. **Ramon, G.**, Sur l'augmentation anormale de l'antitoxine chez les chevaux producteurs de serum antidiphtierique. Bulletin de la Societe du Centres Medicaux et Veterinaire 1925. **101**: p. 227-234.
46. **Mohan, T., Verma, P., and Rao, D.N.**, Novel adjuvants & delivery vehicles for vaccines development: a road ahead. Indian J Med Res, 2013. **138**(5): p. 779-95.
47. **Kenney, R.T. and Edelman, R.**, Survey of human-use adjuvants. Expert Rev Vaccines, 2003. **2**(2): p. 167-88.
48. **O'Hagan, D.T.**, Recent developments in vaccine delivery systems. Curr Drug Targets Infect Disord, 2001. **1**(3): p. 273-86.
49. **Reed, S.G.**, Vaccine adjuvants. Expert Rev Vaccines, 2013. **12**(7): p. 705-6.
50. **Brito, L.A., Malyala, P., and O'Hagan, D.T.**, Vaccine adjuvant formulations: a pharmaceutical perspective. Semin Immunol, 2013. **25**(2): p. 130-45.
51. **Brito, L.A. and O'Hagan, D.T.**, Designing and building the next generation of improved vaccine adjuvants. J Control Release, 2014. **190**: p. 563-79.
52. **Cox, J.C. and Coulter, A.R.**, Adjuvants--a classification and review of their modes of action. Vaccine, 1997. **15**(3): p. 248-56.
53. **Fraser, C.K., Diener, K.R., Brown, M.P., and Hayball, J.D.**, Improving vaccines by incorporating immunological coadjuvants. Expert Rev Vaccines, 2007. **6**(4): p. 559-78.
54. **Awate, S., Babiuk, L.A., and Mutwiri, G.**, Mechanisms of action of adjuvants. Front Immunol, 2013. **4**: p. 114.
55. **Reed, S.G., Orr, M.T., and Fox, C.B.**, Key roles of adjuvants in modern vaccines. Nat Med, 2013. **19**(12): p. 1597-608.
56. **Henriksen-Lacey, M., Bramwell, V.W., Christensen, D., Agger, E.M., Andersen, P., and Perrie, Y.**, Liposomes based on dimethyldioctadecylammonium promote a depot effect and enhance immunogenicity of soluble antigen. J Control Release, 2010. **142**(2): p. 180-6.
57. **McKee, A.S., Munks, M.W., MacLeod, M.K., Fleenor, C.J., Van Rooijen, N., Kappler, J.W., and Marrack, P.**, Alum induces innate immune responses through macrophage and mast cell sensors, but these sensors are not required for alum to act as an adjuvant for specific immunity. J Immunol, 2009. **183**(7): p. 4403-14.
58. **Calabro, S., Tortoli, M., Baudner, B.C., Pacitto, A., Cortese, M., O'Hagan, D.T., De Gregorio, E., Seubert, A., and Wack, A.**, Vaccine adjuvants alum and MF59

induce rapid recruitment of neutrophils and monocytes that participate in antigen transport to draining lymph nodes. Vaccine, 2011. **29**(9): p. 1812-23.

59. **Mosca, F., Tritto, E., Muzzi, A., Monaci, E., Bagnoli, F., Iavarone, C., O'Hagan, D., Rappuoli, R., and De Gregorio, E.**, Molecular and cellular signatures of human vaccine adjuvants. Proc Natl Acad Sci U S A, 2008. **105**(30): p. 10501-6.
60. **Seubert, A., Monaci, E., Pizza, M., O'Hagan, D.T., and Wack, A.**, The adjuvants aluminum hydroxide and MF59 induce monocyte and granulocyte chemoattractants and enhance monocyte differentiation toward dendritic cells. J Immunol, 2008. **180**(8): p. 5402-12.
61. **Morel, S., Didierlaurent, A., Bourguignon, P., Delhaye, S., Baras, B., Jacob, V., Planty, C., Elouahabi, A., Harvengt, P., Carlsen, H., Kielland, A., Chomez, P., Garcon, N., and Van Mechelen, M.**, Adjuvant System AS03 containing alpha-tocopherol modulates innate immune response and leads to improved adaptive immunity. Vaccine, 2011. **29**(13): p. 2461-73.
62. **Kool, M., Soullie, T., van Nimwegen, M., Willart, M.A., Muskens, F., Jung, S., Hoogsteden, H.C., Hammad, H., and Lambrecht, B.N.**, Alum adjuvant boosts adaptive immunity by inducing uric acid and activating inflammatory dendritic cells. J Exp Med, 2008. **205**(4): p. 869-82.
63. **Didierlaurent, A.M., Morel, S., Lockman, L., Giannini, S.L., Bisteau, M., Carlsen, H., Kielland, A., Vosters, O., Vanderheyde, N., Schiavetti, F., Larocque, D., Van Mechelen, M., and Garcon, N.**, AS04, an aluminum salt- and TLR4 agonist-based adjuvant system, induces a transient localized innate immune response leading to enhanced adaptive immunity. J Immunol, 2009. **183**(10): p. 6186-97.
64. **Guery, J.C., Ria, F., and Adorini, L.**, Dendritic cells but not B cells present antigenic complexes to class II-restricted T cells after administration of protein in adjuvant. J Exp Med, 1996. **183**(3): p. 751-7.
65. **Morefield, G.L., Sokolovska, A., Jiang, D., HogenEsch, H., Robinson, J.P., and Hem, S.L.**, Role of aluminum-containing adjuvants in antigen internalization by dendritic cells in vitro. Vaccine, 2005. **23**(13): p. 1588-95.
66. **Flach, T.L., Ng, G., Hari, A., Desrosiers, M.D., Zhang, P., Ward, S.M., Seamone, M.E., Vilaysane, A., Mucsi, A.D., Fong, Y., Prenner, E., Ling, C.C., Tschopp, J., Muruve, D.A., Amrein, M.W., and Shi, Y.**, Alum interaction with dendritic cell membrane lipids is essential for its adjuvanticity. Nat Med, 2011. **17**(4): p. 479-87.

67. **Nordly, P., Madsen, H.B., Nielsen, H.M., and Foged, C.**, Status and future prospects of lipid-based particulate delivery systems as vaccine adjuvants and their combination with immunostimulators. Expert Opin Drug Deliv, 2009. **6**(7): p. 657-72.

68. **De Smedt, T., Pajak, B., Muraille, E., Lespagnard, L., Heinen, E., De Baetselier, P., Urbain, J., Leo, O., and Moser, M.**, Regulation of dendritic cell numbers and maturation by lipopolysaccharide in vivo. J Exp Med, 1996. **184**(4): p. 1413-24.

69. **Copland, M.J., Baird, M.A., Rades, T., McKenzie, J.L., Becker, B., Reck, F., Tyler, P.C., and Davies, N.M.**, Liposomal delivery of antigen to human dendritic cells. Vaccine, 2003. **21**(9-10): p. 883-90.

70. **Shah, J.A., Darrah, P.A., Ambrozak, D.R., Turon, T.N., Mendez, S., Kirman, J., Wu, C.Y., Glaichenhaus, N., and Seder, R.A.**, Dendritic cells are responsible for the capacity of CpG oligodeoxynucleotides to act as an adjuvant for protective vaccine immunity against *Leishmania* major in mice. J Exp Med, 2003. **198**(2): p. 281-91.

71. **Werninghaus, K., Babiak, A., Gross, O., Holscher, C., Dietrich, H., Agger, E.M., Mages, J., Mocsai, A., Schoenen, H., Finger, K., Nimmerjahn, F., Brown, G.D., Kirschning, C., Heit, A., Andersen, P., Wagner, H., Ruland, J., and Lang, R.**, Adjuvanticity of a synthetic cord factor analogue for subunit Mycobacterium tuberculosis vaccination requires FcRgamma-Syk-Card9-dependent innate immune activation. J Exp Med, 2009. **206**(1): p. 89-97.

72. **Sun, H., Pollock, K.G., and Brewer, J.M.**, Analysis of the role of vaccine adjuvants in modulating dendritic cell activation and antigen presentation in vitro. Vaccine, 2003. **21**(9-10): p. 849-55.

73. **Kool, M., Petrilli, V., De Smedt, T., Rolaz, A., Hammad, H., van Nimwegen, M., Bergen, I.M., Castillo, R., Lambrecht, B.N., and Tschopp, J.**, Cutting edge: alum adjuvant stimulates inflammatory dendritic cells through activation of the NALP3 inflammasome. J Immunol, 2008. **181**(6): p. 3755-9.

74. **Shi, Y., Evans, J.E., and Rock, K.L.**, Molecular identification of a danger signal that alerts the immune system to dying cells. Nature, 2003. **425**(6957): p. 516-21.

75. **Shakya, A.K. and Nandakumar, K.S.**, Applications of polymeric adjuvants in studying autoimmune responses and vaccination against infectious diseases. J R Soc Interface, 2013. **10**(79): p. 20120536.

76. **Martinon, F., Mayor, A., and Tschopp, J.**, The inflammasomes: guardians of the body. Annu Rev Immunol, 2009. **27**: p. 229-65.

77. **Olive, C.**, Pattern recognition receptors: sentinels in innate immunity and targets of new vaccine adjuvants. Expert Rev Vaccines, 2012. **11**(2): p. 237-56.

78. **Franchi, L., Eigenbrod, T., Munoz-Planillo, R., and Nunez, G.**, The inflammasome: a caspase-1-activation platform that regulates immune responses and disease pathogenesis. Nat Immunol, 2009. **10**(3): p. 241-7.

79. **Eisenbarth, S.C., Colegio, O.R., O'Connor, W., Sutterwala, F.S., and Flavell, R.A.**, Crucial role for the Nalp3 inflammasome in the immunostimulatory properties of aluminium adjuvants. Nature, 2008. **453**(7198): p. 1122-6.

80. **Franchi, L. and Nunez, G.**, The Nlrp3 inflammasome is critical for aluminium hydroxide-mediated IL-1beta secretion but dispensable for adjuvant activity. Eur J Immunol, 2008. **38**(8): p. 2085-9.

81. **Ellebedy, A.H., Lupfer, C., Ghoneim, H.E., DeBeauchamp, J., Kanneganti, T.D., and Webby, R.J.**, Inflammasome-independent role of the apoptosis-associated speck-like protein containing CARD (ASC) in the adjuvant effect of MF59. Proc Natl Acad Sci U S A, 2011. **108**(7): p. 2927-32.

82. **Embry, C.A., Franchi, L., Nunez, G., and Mitchell, T.C.**, Mechanism of impaired NLRP3 inflammasome priming by monophosphoryl lipid A. Sci Signal, 2011. **4**(171): p. ra28.

83. **Eng, N.F., Bhardwaj, N., Mulligan, R., and Diaz-Mitoma, F.**, The potential of 1018 ISS adjuvant in hepatitis B vaccines: HEPLISAV review. Hum Vaccin Immunother, 2013. **9**(8): p. 1661-72.

84. **Szarewski, A.**, Cervarix(R): a bivalent vaccine against HPV types 16 and 18, with cross-protection against other high-risk HPV types. Expert Rev Vaccines, 2012. **11**(6): p. 645-57.

85. **Christensen, D., Korsholm, K.S., Rosenkrands, I., Lindenstrom, T., Andersen, P., and Agger, E.M.**, Cationic liposomes as vaccine adjuvants. Expert Rev Vaccines, 2007. **6**(5): p. 785-96.

86. **Ferreira, S.A., Gama, F.M., and Vilanova, M.**, Polymeric nanogels as vaccine delivery systems. Nanomedicine, 2013. **9**(2): p. 159-73.

87. **Glenny, A.T. and Sudmersen, H.J.**, Notes on the Production of Immunity to Diphtheria Toxin. J Hyg (Lond), 1921. **20**(2): p. 176-220.

88. **Marrack, P., McKee, A.S., and Munks, M.W.**, Towards an understanding of the adjuvant action of aluminium. Nat Rev Immunol, 2009. **9**(4): p. 287-93.

89. **De Gregorio, E., Tritto, E., and Rappuoli, R.**, Alum adjuvanticity: unraveling a century old mystery. Eur J Immunol, 2008. **38**(8): p. 2068-71.

90. **Mbow, M.L., De Gregorio, E., and Ulmer, J.B.**, Alum's adjuvant action: grease is the word. Nat Med, 2011. **17**(4): p. 415-6.

91. **Brewer, J.M.**, (How) do aluminium adjuvants work? Immunol Lett, 2006. **102**(1): p. 10-5.

92. **Oleszycka, E. and Lavelle, E.C.**, Immunomodulatory properties of the vaccine adjuvant alum. Curr Opin Immunol, 2014. **28**: p. 1-5.

93. **Sun, J., Song, X., and Hu, S.**, Ginsenoside Rg1 and aluminum hydroxide synergistically promote immune responses to ovalbumin in BALB/c mice. Clin Vaccine Immunol, 2008. **15**(2): p. 303-7.

94. **Hornung, V., Bauernfeind, F., Halle, A., Samstad, E.O., Kono, H., Rock, K.L., Fitzgerald, K.A., and Latz, E.**, Silica crystals and aluminum salts activate the NALP3 inflammasome through phagosomal destabilization. Nat Immunol, 2008. **9**(8): p. 847-56.

95. **Monie, T.P., Bryant, C.E., and Gay, N.J.**, Activating immunity: lessons from the TLRs and NLRs. Trends Biochem Sci, 2009. **34**(11): p. 553-61.

96. **Garcia, A. and De Sanctis, J.B.**, An overview of adjuvant formulations and delivery systems. APMIS, 2014. **122**(4): p. 257-67.

97. **Langer, R.**, Polymeric delivery systems for controlled drug release. . Chem. Engi. Communicat., 1980. **6(1–3)**: p. 1–48

98. **Gregory, A.E., Titball, R., and Williamson, D.**, Vaccine delivery using nanoparticles. Front Cell Infect Microbiol, 2013. **3**: p. 13.

99. **Couvreur, P., Barratt, G., Fattal, E., Legrand, P., and Vauthier, C.**, Nanocapsule technology: a review. Crit Rev Ther Drug Carrier Syst, 2002. **19**(2): p. 99-134.

100. **McGinity, J.W. and O'Donnell, P.B.**, Preparation of microspheres by the solvent evaporation technique. Adv Drug Deliv Rev, 1997. **28**(1): p. 25-42.

101. **Sahoo, S.K., Panyam, J., Prabha, S., and Labhasetwar, V.**, Residual polyvinyl alcohol associated with poly (D,L-lactide-co-glycolide) nanoparticles affects their physical properties and cellular uptake. J Control Release, 2002. **82**(1): p. 105-14.

102. **Lu, J.M., Wang, X., Marin-Muller, C., Wang, H., Lin, P.H., Yao, Q., and Chen, C.**, Current advances in research and clinical applications of PLGA-based nanotechnology. Expert Rev Mol Diagn, 2009. **9**(4): p. 325-41.

103. **Chiang, C.H. and Yeh, M.K.**, Contribution of poly(amino acids) to advances in pharmaceutical biotechnology. Curr Pharm Biotechnol, 2003. **4**(5): p. 323-30.

104. **Murugappan, S., Patil, H.P., Kanojia, G., ter Veer, W., Meijerhof, T., Frijlink, H.W., Huckriede, A., and Hinrichs, W.L.**, Physical and immunogenic stability of spray freeze-dried influenza vaccine powder for pulmonary delivery: comparison of inulin, dextran, or a mixture of dextran and trehalose as protectants. Eur J Pharm Biopharm, 2013. **85**(3 Pt A): p. 716-25.

105. **Sharma, S., Benson, H.A., Mukkur, T.K., Rigby, P., and Chen, Y.**, Preliminary studies on the development of IgA-loaded chitosan-dextran sulphate nanoparticles as a potential nasal delivery system for protein antigens. J Microencapsul, 2013. **30**(3): p. 283-94.

106. **Arthanari, S., Mani, G., Peng, M.M., and Jang, H.T.**, Chitosan-HPMC-blended microspheres as a vaccine carrier for the delivery of tetanus toxoid. Artif Cells Nanomed Biotechnol, 2014: p. 1-7.

107. **Arca, H.C., Gunbeyaz, M., and Senel, S.**, Chitosan-based systems for the delivery of vaccine antigens. Expert Rev Vaccines, 2009. **8**(7): p. 937-53.

108. **Jain, S., O'Hagan, D.T., and Singh, M.**, The long-term potential of biodegradable poly(lactide-co-glycolide) microparticles as the next-generation vaccine adjuvant. Expert Rev Vaccines, 2011. **10**(12): p. 1731-42.

109. **Luzardo-Alvarez, A., Merkle, H.P., and Gander, B.**, Responses of cultured macrophages to microspheres. J Control Release, 2005. **101**(1-3): p. 347-9.

110. **O'Hagan, D.T. and Rappuoli, R.**, Novel approaches to vaccine delivery. Pharm Res, 2004. **21**(9): p. 1519-30.

111. **Manocha, M., Pal, P.C., Chitralekha, K.T., Thomas, B.E., Tripathi, V., Gupta, S.D., Paranjape, R., Kulkarni, S., and Rao, D.N.**, Enhanced mucosal and systemic immune response with intranasal immunization of mice with HIV peptides entrapped in PLG microparticles in combination with Ulex Europaeus-I lectin as M cell target. Vaccine, 2005. **23**(48-49): p. 5599-617.

112. **Malyala, P. and Singh, M.**, Micro/nanoparticle adjuvants: preparation and formulation with antigens. Methods Mol Biol, 2010. **626**: p. 91-101.

113. **Keijzer, C., Spiering, R., Silva, A.L., van Eden, W., Jiskoot, W., Vervelde, L., and Broere, F.**, PLGA nanoparticles enhance the expression of retinaldehyde dehydrogenase enzymes in dendritic cells and induce FoxP3(+) T-cells in vitro. J Control Release, 2013. **168**(1): p. 35-40.

114. **Schijns, V.E., Strioga, M., and Ascarateil, S.**, Oil-based emulsion vaccine adjuvants. Curr Protoc Immunol, 2014. **106**: p. 2 18 1-7.

115. **Jensen, F.C., Savary, J.R., Diveley, J.P., and Chang, J.C.**, Adjuvant activity of incomplete Freund's adjuvant. Adv Drug Deliv Rev, 1998. **32**(3): p. 173-186.

116. **Chu, R.S., Targoni, O.S., Krieg, A.M., Lehmann, P.V., and Harding, C.V.**, CpG oligodeoxynucleotides act as adjuvants that switch on T helper 1 (Th1) immunity. J Exp Med, 1997. **186**(10): p. 1623-31.

117. **Silva, A.L., Rosalia, R.A., Varypataki, E., Sibuea, S., Ossendorp, F., and Jiskoot, W.**, Poly-(lactic-co-glycolic-acid)-based particulate vaccines: Particle uptake by dendritic cells is a key parameter for immune activation. Vaccine, 2015. **33**(7): p. 847-54.

118. **Wang, Q.M., Sun, S.H., Hu, Z.L., Yin, M., Xiao, C.J., and Zhang, J.C.**, Improved immunogenicity of a tuberculosis DNA vaccine encoding ESAT6 by DNA priming and protein boosting. Vaccine, 2004. **22**(27-28): p. 3622-7.

119. **O'Hagan, D.T., Wack, A., and Podda, A.**, MF59 is a safe and potent vaccine adjuvant for flu vaccines in humans: what did we learn during its development? Clin Pharmacol Ther, 2007. **82**(6): p. 740-4.

120. **Podda, A. and Del Giudice, G.**, MF59-adjuvanted vaccines: increased immunogenicity with an optimal safety profile. Expert Rev Vaccines, 2003. **2**(2): p. 197-203.

121. **Deng, J., Cai, W., and Jin, F.**, A novel oil-in-water emulsion as a potential adjuvant for influenza vaccine: development, characterization, stability and in vivo evaluation. Int J Pharm, 2014. **468**(1-2): p. 187-95.

122. **Dar, P., Kalaivanan, R., Sied, N., Mamo, B., Kishore, S., Suryanarayana, V.V., and Kondabattula, G.**, Montanide ISA 201 adjuvanted FMD vaccine induces improved immune responses and protection in cattle. Vaccine, 2013. **31**(33): p. 3327-32.

123. **Hamouda, T., Chepurnov, A., Mank, N., Knowlton, J., Chepurnova, T., Myc, A., Sutcliffe, J., and Baker, J.R.**, Efficacy, immunogenicity and stability of a novel intranasal nanoemulsion-adjuvanted influenza vaccine in a murine model. Hum Vaccin, 2010. **6**(7): p. 585-94.

124. **Lovgren, K. and Morein, B.**, The requirement of lipids for the formation of immunostimulating complexes (iscoms). Biotechnol Appl Biochem, 1988. **10**(2): p. 161-72.

125. **Kensil, C.R., Soltysik, S., Wheeler, D.A., and Wu, J.Y.**, Structure/function studies on QS-21, a unique immunological adjuvant from Quillaja saponaria. Adv Exp Med Biol, 1996. **404**: p. 165-72.

126. **Myschik, J., Lendemans, D.G., McBurney, W.T., Demana, P.H., Hook, S., and Rades, T.**, On the preparation, microscopic investigation and application of ISCOMs. Micron, 2006. **37**(8): p. 724-34.

127. **Sun, H.X., Xie, Y., and Ye, Y.P.**, ISCOMs and ISCOMATRIX. Vaccine, 2009. **27**(33): p. 4388-401.

128. **Skene, C.D. and Sutton, P.**, Saponin-adjuvanted particulate vaccines for clinical use. Methods, 2006. **40**(1): p. 53-9.

129. **Sanders, M.T., Brown, L.E., Deliyannis, G., and Pearse, M.J.**, ISCOM-based vaccines: the second decade. Immunol Cell Biol, 2005. **83**(2): p. 119-28.

130. **Sjolander, A., Drane, D., Maraskovsky, E., Scheerlinck, J.P., Suhrbier, A., Tennent, J., and Pearse, M.**, Immune responses to ISCOM formulations in animal and primate models. Vaccine, 2001. **19**(17-19): p. 2661-5.

131. **Drane, D., Gittleson, C., Boyle, J., and Maraskovsky, E.**, ISCOMATRIX adjuvant for prophylactic and therapeutic vaccines. Expert Rev Vaccines, 2007. **6**(5): p. 761-72.

132. **Cruz-Bustos, T., Gonzalez-Gonzalez, G., Morales-Sanfrutos, J., Megia-Fernandez, A., Santoyo-Gonzalez, F., and Osuna, A.**, Functionalization of immunostimulating complexes (ISCOMs) with lipid vinyl sulfones and their application in immunological techniques and therapy. Int J Nanomedicine, 2012. **7**: p. 5941-56.

133. **Moser, C., Amacker, M., and Zurbriggen, R.**, Influenza virosomes as a vaccine adjuvant and carrier system. Expert Rev Vaccines, 2011. **10**(4): p. 437-46.

134. **de Bruijn, I.A., Nauta, J., Gerez, L., and Palache, A.M.**, The virosomal influenza vaccine Invivac: immunogenicity and tolerability compared to an adjuvanted influenza vaccine (Fluad in elderly subjects. Vaccine, 2006. **24**(44-46): p. 6629-31.

135. **Lopez-Macias, C.**, Virus-like particle (VLP)-based vaccines for pandemic influenza: performance of a VLP vaccine during the 2009 influenza pandemic. Hum Vaccin Immunother, 2012. **8**(3): p. 411-4.

136. **Buonaguro, L., Devito, C., Tornesello, M.L., Schroder, U., Wahren, B., Hinkula, J., and Buonaguro, F.M.**, DNA-VLP prime-boost intra-nasal immunization induces cellular and humoral anti-HIV-1 systemic and mucosal immunity with cross-clade neutralizing activity. Vaccine, 2007. **25**(32): p. 5968-77.

137. **Yang, F., Wang, F., Guo, Y., Zhou, Q., Wang, Y., Yin, Y., and Sun, S.**, Enhanced capacity of antigen presentation of HBc-VLP-pulsed RAW264.7 cells revealed by proteomics analysis. J Proteome Res, 2008. **7**(11): p. 4898-903.

138. **Sominskaya, I., Skrastina, D., Dislers, A., Vasiljev, D., Mihailova, M., Ose, V., Dreilina, D., and Pumpens, P.**, Construction and immunological evaluation of multivalent hepatitis B virus (HBV) core virus-like particles carrying HBV and HCV epitopes. Clin Vaccine Immunol, 2010. **17**(6): p. 1027-33.

139. **Hernandez, B.Y., Ton, T., Shvetsov, Y.B., Goodman, M.T., and Zhu, X.**, Human papillomavirus (HPV) L1 and L1-L2 virus-like particle-based multiplex assays for measurement of HPV virion antibodies. Clin Vaccine Immunol, 2012. **19**(9): p. 1348-52.

140. **Bangham, A.D., Standish, M.M., and Watkins, J.C.**, Diffusion of univalent ions across the lamellae of swollen phospholipids. J Mol Biol, 1965. **13**(1): p. 238-52.

141. **Elbayoumi, T.A. and Torchilin, V.P.**, Current trends in liposome research. Methods Mol Biol, 2010. **605**: p. 1-27.

142. **Gregoriadis, G.**, Drug entrapment in liposomes. FEBS Lett, 1973. **36**(3): p. 292-6.

143. **Allison, A.G. and Gregoriadis, G.**, Liposomes as immunological adjuvants. Nature, 1974. **252**(5480): p. 252.

144. **Gregoriadis, G. and Allison, A.C.**, Entrapment of proteins in liposomes prevents allergic reactions in pre-immunised mice. FEBS Lett, 1974. **45**(1): p. 71-4.

145. **Allison, A.C. and Gregoriadis, G.**, Liposomes as immunological adjuvants. Recent Results Cancer Res, 1976(56): p. 58-64.

146. **Gregoriadis, G. and Davis, C.**, Stability of liposomes in vivo and in vitro is promoted by their cholesterol content and the presence of blood cells. Biochem Biophys Res Commun, 1979. **89**(4): p. 1287-93.

147. **Gregoriadis, G.**, Engineering liposomes for drug delivery: progress and problems. Trends Biotechnol, 1995. **13**(12): p. 527-37.

148. **Gregoriadis, G. and Senior, J.**, The phospholipid component of small unilamellar liposomes controls the rate of clearance of entrapped solutes from the circulation. FEBS Lett, 1980. **119**(1): p. 43-6.

149. **Whitesides, G.M. and Grzybowski, B.**, Self-assembly at all scales. Science, 2002. **295**(5564): p. 2418-21.

150. **Ranade, V.V.**, Drug delivery systems. 1. site-specific drug delivery using liposomes as carriers. J Clin Pharmacol, 1989. **29**(8): p. 685-94.

151. **Lipowsky, R.**, The conformation of membranes. Nature, 1991. **349**(6309): p. 475-81.
152. **Tanford, C.**, The hydrophobic effect and the organization of living matter. Science, 1978. **200**(4345): p. 1012-8.
153. **Israelachvili, J. and Wennerstrom, H.**, Role of hydration and water structure in biological and colloidal interactions. Nature, 1996. **379**(6562): p. 219-25.
154. Tanford, C., *The hydrophobic effect: formation of micelles and biological membranes,*, ed. n. ed. 1991: Krieger Publishing Company.
155. **Gubernator, J.**, Active methods of drug loading into liposomes: recent strategies for stable drug entrapment and increased in vivo activity. Expert Opin Drug Deliv, 2011. **8**(5): p. 565-80.
156. **Frolov, V.A., Shnyrova, A.V., and Zimmerberg, J.**, Lipid polymorphisms and membrane shape. Cold Spring Harb Perspect Biol, 2011. **3**(11): p. a004747.
157. **Israelachvili, J.N., Mitchell, D.J., and Ninham, B.W.**, Theory of self-assembly of hydrocarbon amphiphiles into micelles and bilayers. J. Chem. Soc. Faraday Trans.2, 1976. **72**: p. 1525-1568.
158. **Mouritsen, O.G.**, Lipids, curvature, and nano-medicine. Eur J Lipid Sci Technol, 2011. **113**(10): p. 1174-1187.
159. **Gruner, S.M., Cullis, P.R., Hope, M.J., and Tilcock, C.P.**, Lipid polymorphism: the molecular basis of nonbilayer phases. Annu Rev Biophys Biophys Chem, 1985. **14**: p. 211-38.
160. **Hafez, I.M. and Cullis, P.R.**, Roles of lipid polymorphism in intracellular delivery. Adv Drug Deliv Rev, 2001. **47**(2-3): p. 139-48.
161. **Elizondo, E., Moreno, E., Cabrera, I., Cordoba, A., Sala, S., Veciana, J., and Ventosa, N.**, Liposomes and other vesicular systems: structural characteristics, methods of preparation, and use in nanomedicine. Prog Mol Biol Transl Sci, 2011. **104**: p. 1-52.
162. **Lindblom, G. and Oradd, G.**, Lipid lateral diffusion and membrane heterogeneity. Biochim Biophys Acta, 2009. **1788**(1): p. 234-44.
163. **Kranenburg, M. and Smit, B.**, Phase behavior of model lipid bilayers. J Phys Chem B, 2005. **109**(14): p. 6553-63.
164. **Huang, C. and Li, S.**, Calorimetric and molecular mechanics studies of the thermotropic phase behavior of membrane phospholipids. Biochim Biophys Acta, 1999. **1422**(3): p. 273-307.

165. **Kohli, A.G., Kierstead, P.H., Venditto, V.J., Walsh, C.L., and Szoka, F.C.**, Designer lipids for drug delivery: from heads to tails. J Control Release, 2014. **190**: p. 274-87.

166. **Patil, Y.P. and Jadhav, S.**, Novel methods for liposome preparation. Chem Phys Lipids, 2014. **177**: p. 8-18.

167. **Gomez-Hens, A. and Fernandez-Romero, J.M.**, Analytical methods for the control of liposomal delivery systems. Trends Anal Chem, 2006. **25**: p. 167–178.

168. **Kulkarni, S.B., Betageri, G.V., and Singh, M.**, Factors affecting microencapsulation of drugs in liposomes. J Microencapsul, 1995. **12**(3): p. 229-46.

169. **Wacker, M.**, Nanocarriers for intravenous injection--the long hard road to the market. Int J Pharm, 2013. **457**(1): p. 50-62.

170. **Akbarzadeh, A., Rezaei-Sadabady, R., Davaran, S., Joo, S.W., Zarghami, N., Hanifehpour, Y., Samiei, M., Kouhi, M., and Nejati-Koshki, K.**, Liposome: classification, preparation, and applications. Nanoscale Res Lett, 2013. **8**(1): p. 102.

171. **Szoka, F., Jr. and Papahadjopoulos, D.**, Procedure for preparation of liposomes with large internal aqueous space and high capture by reverse-phase evaporation. Proc Natl Acad Sci U S A, 1978. **75**(9): p. 4194-8.

172. **Batzri, S. and Korn, E.D.**, Single bilayer liposomes prepared without sonication. Biochim Biophys Acta, 1973. **298**(4): p. 1015-9.

173. **Meure, L.A., Foster, N.R., and Dehghani, F.**, Conventional and dense gas techniques for the production of liposomes: a review. AAPS PharmSciTech, 2008. **9**(3): p. 798-809.

174. **Brunner, J., Skrabal, P., and Hauser, H.**, Single bilayer vesicles prepared without sonication. Physico-chemical properties. Biochim Biophys Acta, 1976. **455**(2): p. 322-31.

175. **Mayer, L.D., Hope, M.J., Cullis, P.R., and Janoff, A.S.**, Solute distributions and trapping efficiencies observed in freeze-thawed multilamellar vesicles. Biochim Biophys Acta, 1985. **817**(1): p. 193-6.

176. **Kirby, C. and Gregoriadis, G.**, Dehydration-rehydration vesicles—a simple method for high-yield drug entrapment in liposomes. Nat Biotechnol 1984. **2**: p. 979–984. .

177. **Woodbury, D.J., Richardson, E.S., Grigg, A.W., Welling, R.D., and Knudson, B.H.**, Reducing liposome size with ultrasound: bimodal size distributions. J Liposome Res, 2006. **16**(1): p. 57-80.

178. **Zasadzinski, J.A.N.**, Transmission Electron-Microscopy Observations of Sonication-Induced Changes in Liposome Structure. Biophysical Journal, 1986. **49**(6): p. 1119-1130.

179. **Hope, M.J., Bally, M.B., Webb, G., and Cullis, P.R.**, Production of large unilamellar vesicles by a rapid extrusion procedure: characterization of size distribution, trapped volume and ability to maintain a membrane potential. Biochim Biophys Acta, 1985. **812**(1): p. 55-65.

180. **Berger, N., Sachse, A., Bender, J., Schubert, R., and Brandl, M.**, Filter extrusion of liposomes using different devices: comparison of liposome size, encapsulation efficiency, and process characteristics. Int J Pharm, 2001. **223**(1-2): p. 55-68.

181. **Henriksen-Lacey, M., Korsholm, K.S., Andersen, P., Perrie, Y., and Christensen, D.**, Liposomal vaccine delivery systems. Expert Opin Drug Deliv, 2011. **8**(4): p. 505-19.

182. **Heyes, J.A., Niculescu-Duvaz, D., Cooper, R.G., and Springer, C.J.**, Synthesis of novel cationic lipids: effect of structural modification on the efficiency of gene transfer. J Med Chem, 2002. **45**(1): p. 99-114.

183. **Bhattacharya, S. and Bajaj, A.**, Advances in gene delivery through molecular design of cationic lipids. Chem Commun (Camb), 2009(31): p. 4632-56.

184. **Ghosh, Y.K., Visweswariah, S.S., and Bhattacharya, S.**, Nature of linkage between the cationic headgroup and cholesteryl skeleton controls gene transfection efficiency. FEBS Lett, 2000. **473**(3): p. 341-4.

185. **Frezard, F.**, Liposomes: from biophysics to the design of peptide vaccines. Braz J Med Biol Res, 1999. **32**(2): p. 181-9.

186. **Gregoriadis, G., McCormack, B., Obrenovic, M., Saffie, R., Zadi, B., and Perrie, Y.**, Vaccine entrapment in liposomes. Methods, 1999. **19**(1): p. 156-62.

187. **Torchilin, V.P.**, Recent advances with liposomes as pharmaceutical carriers. Nat Rev Drug Discov, 2005. **4**(2): p. 145-60.

188. **Ahsan, F., Rivas, I.P., Khan, M.A., and Torres Suarez, A.I.**, Targeting to macrophages: role of physicochemical properties of particulate carriers--liposomes and microspheres--on the phagocytosis by macrophages. J Control Release, 2002. **79**(1-3): p. 29-40.

189. **Joseph, A., Itskovitz-Cooper, N., Samira, S., Flasterstein, O., Eliyahu, H., Simberg, D., Goldwaser, I., Barenholz, Y., and Kedar, E.**, A new intranasal influenza vaccine based on a novel polycationic lipid--ceramide carbamoyl-spermine

(CCS) I. Immunogenicity and efficacy studies in mice. Vaccine, 2006. **24**(18): p. 3990-4006.

190. **Henriksen-Lacey, M., Christensen, D., Bramwell, V.W., Lindenstrom, T., Agger, E.M., Andersen, P., and Perrie, Y.**, Comparison of the depot effect and immunogenicity of liposomes based on dimethyldioctadecylammonium (DDA), 3beta-[N-(N',N'-Dimethylaminoethane)carbomyl] cholesterol (DC-Chol), and 1,2-Dioleoyl-3-trimethylammonium propane (DOTAP): prolonged liposome retention mediates stronger Th1 responses. Mol Pharm, 2011. **8**(1): p. 153-61.
191. **Latif, N. and Bachhawat, B.K.**, The effect of surface charges of liposomes in immunopotentiation. Biosci Rep, 1984. **4**(2): p. 99-107.
192. **Ghaffar, K.A., Giddam, A.K., Zaman, M., Skwarczynski, M., and Toth, I.**, Liposomes as nanovaccine delivery systems. Curr Top Med Chem, 2014. **14**(9): p. 1194-208.
193. **Dong, L., Liu, F., Fairman, J., Hong, D.K., Lewis, D.B., Monath, T., Warner, J.F., Belser, J.A., Patel, J., Hancock, K., Katz, J.M., and Lu, X.**, Cationic liposome-DNA complexes (CLDC) adjuvant enhances the immunogenicity and cross-protective efficacy of a pre-pandemic influenza A H5N1 vaccine in mice. Vaccine, 2012. **30**(2): p. 254-64.
194. **Bernstein, D.I., Farley, N., Bravo, F.J., Earwood, J., McNeal, M., Fairman, J., and Cardin, R.**, The adjuvant CLDC increases protection of a herpes simplex type 2 glycoprotein D vaccine in guinea pigs. Vaccine, 2010. **28**(21): p. 3748-53.
195. **Carroll, T.D., Matzinger, S.R., Barry, P.A., McChesney, M.B., Fairman, J., and Miller, C.J.**, Efficacy of influenza vaccination of elderly rhesus macaques is dramatically improved by addition of a cationic lipid/DNA adjuvant. J Infect Dis, 2014. **209**(1): p. 24-33.
196. **Chang, S., Warner, J., Liang, L., and Fairman, J.**, A novel vaccine adjuvant for recombinant flu antigens. Biologicals, 2009. **37**(3): p. 141-7.
197. **Firouzmand, H., Badiee, A., Khamesipour, A., Heravi Shargh, V., Alavizadeh, S.H., Abbasi, A., and Jaafari, M.R.**, Induction of protection against leishmaniasis in susceptible BALB/c mice using simple DOTAP cationic nanoliposomes containing soluble *Leishmania* antigen (SLA). Acta Trop, 2013. **128**(3): p. 528-35.
198. **Sanchez, V., Gimenez, S., Haensler, J., Geoffroy, C., Rokbi, B., Seguin, D., Lissolo, L., Harris, B., Rizvi, F., Kleanthous, H., Monath, T., Cadoz, M., and Guy, B.**, Formulations of single or multiple H. pylori antigens with DC Chol adjuvant

induce protection by the systemic route in mice. Optimal prophylactic combinations are different from therapeutic ones. FEMS Immunol Med Microbiol, 2001. **30**(2): p. 157-65.

199. **Watson, D.S., Endsley, A.N., and Huang, L.**, Design considerations for liposomal vaccines: influence of formulation parameters on antibody and cell-mediated immune responses to liposome associated antigens. Vaccine, 2012. **30**(13): p. 2256-72.
200. **Schwendener, R.A.**, Liposomes as vaccine delivery systems: a review of the recent advances. Ther Adv Vaccines, 2014. **2**(6): p. 159-82.
201. **Tanaka, T., Legat, A., Adam, E., Steuve, J., Gatot, J.S., Vandenbranden, M., Ulianov, L., Lonez, C., Ruysschaert, J.M., Muraille, E., Tuynder, M., Goldman, M., and Jacquet, A.**, DiC14-amidine cationic liposomes stimulate myeloid dendritic cells through Toll-like receptor 4. Eur J Immunol, 2008. **38**(5): p. 1351-7.
202. **Kunitake, T. and Okahata, Y.J.**, A totally synthetic bilayer membrane. Am. Chem. Soc. , 1977. **99**: p. 3860–3861.
203. **Okuyama, K., Soboi, Y., Iljima, K.N., Hirabayashi, K., Kunitake, T., and Kajiyama, T.**, Molecular and Crystal Structure of the Lipid-Model Amphiphile Dioctadecyldimethylammonium Bromide Monohydrate. Bulletin of the Chemical Society of Japan, 1988. **61**: p. 1485-1490.
204. **Feitosa, E. and Brown, W.**, Fragment and Vesicle Structures in Sonicated Dispersions of Dioctadecyldimethylammonium Bromide. Langmuir, 1997. **13**: p. 4810-4816.
205. **Schulz, P.C., Rodriguez, J.L., Soltero-Martinez, F.A., Puig, J.E., and Proverbio, Z.E.**, Phase Behaviour of the Dioctadecylammonium Bromide-Water System. Journal of Thermal Analysis, 1998. **51**: p. 49- 62.
206. **Feitosa, E., Barreleiro, P.C.A., and Olofsson, G.**, Phase Transition in Dioctadecyldimethylammonium Bromide and Chloride Vesicles Prepared by Different Methods. Chemistry and Physics of Lipids, 2000. **105**: p. 201-213.
207. **Benatti, C.R., Feitosa, E., Fernandez, R.M., and Lamy-Freund, M.T.**, Structural and thermal characterization of dioctadecyldimethylammonium bromide dispersions by spin labels. Chem Phys Lipids, 2001. **111**(2): p. 93-104.
208. **Oliveira, A.C., Martens, T.F., Raemdonck, K., Adati, R.D., Feitosa, E., Botelho, C., Gomes, A.C., Braeckmans, K., and Real Oliveira, M.E.**, Dioctadecyldimethylammonium:monoolein nanocarriers for efficient in vitro gene silencing. ACS Appl Mater Interfaces, 2014. **6**(9): p. 6977-89.

209. **Oliveira, A.C., Neves Silva, J.P., Coutinho, P.J., Gomes, A.A., Coutinho, O.P., and Real Oliveira, M.E.**, Monoolein as helper lipid for non-viral transfection in mammals. J Control Release, 2010. **148**(1): p. e91-2.

210. **Lincopan, N. and Carmona-Ribeiro, A.M.**, Lipid-covered drug particles: combined action of dioctadecyldimethylammonium bromide and amphotericin B or miconazole. J Antimicrob Chemother, 2006. **58**(1): p. 66-75.

211. **Carmona-Ribeiro, A.M.**, Lipid bilayer fragments and disks in drug delivery. Curr Med Chem, 2006. **13**(12): p. 1359-70.

212. **Vieira, D.B. and Carmona-Ribeiro, A.M.**, Cationic lipids and surfactants as antifungal agents: mode of action. J Antimicrob Chemother, 2006. **58**(4): p. 760-7.

213. **Vieira, D.B. and Carmona-Ribeiro, A.M.**, Cationic nanoparticles for delivery of amphotericin B: preparation, characterization and activity in vitro. J Nanobiotechnology, 2008. **6**: p. 6.

214. **Lincopan, N., Espindola, N.M., Vaz, A.J., and Carmona-Ribeiro, A.M.**, Cationic supported lipid bilayers for antigen presentation. Int J Pharm, 2007. **340**(1-2): p. 216-22.

215. **Lincopan, N., Espindola, N.M., Vaz, A.J., da Costa, M.H., Faquim-Mauro, E., and Carmona-Ribeiro, A.M.**, Novel immunoadjuvants based on cationic lipid: Preparation, characterization and activity in vivo. Vaccine, 2009. **27**(42): p. 5760-71.

216. **Lincopan, N., Santana, M.R., Faquim-Mauro, E., da Costa, M.H., and Carmona-Ribeiro, A.M.**, Silica-based cationic bilayers as immunoadjuvants. BMC Biotechnol, 2009. **9**: p. 5.

217. **van Dissel, J.T., Joosten, S.A., Hoff, S.T., Soonawala, D., Prins, C., Hokey, D.A., O'Dee, D.M., Graves, A., Thierry-Carstensen, B., Andreasen, L.V., Ruhwald, M., de Visser, A.W., Agger, E.M., Ottenhoff, T.H., Kromann, I., and Andersen, P.**, A novel liposomal adjuvant system, CAF01, promotes long-lived Mycobacterium tuberculosis-specific T-cell responses in human. Vaccine, 2014. **32**(52): p. 7098-107.

218. **Gall, D.**, The adjuvant activity of aliphatic nitrogenous bases. Immunology, 1966. **11**(4): p. 369-86.

219. **Korsholm, K.S., Agger, E.M., Foged, C., Christensen, D., Dietrich, J., Andersen, C.S., Geisler, C., and Andersen, P.**, The adjuvant mechanism of cationic dimethyldioctadecylammonium liposomes. Immunology, 2007. **121**(2): p. 216-26.

220. **Snippe, H., de Reuver, M.J., Beunder, J.W., van der Meer, J.B., van Wichen, D.F., and Willers, J.M.**, Delayed-type hypersensitivity in rabbits. Comparison of the

adjuvants dimethyl dioctadecyl ammonium bromide and Freund's complete adjuvant. Int Arch Allergy Appl Immunol, 1982. **67**(2): p. 139-44.

221. **Henriksen-Lacey, M., Christensen, D., Bramwell, V.W., Lindenstrom, T., Agger, E.M., Andersen, P., and Perrie, Y.**, Liposomal cationic charge and antigen adsorption are important properties for the efficient deposition of antigen at the injection site and ability of the vaccine to induce a CMI response. J Control Release, 2010. **145**(2): p. 102-8.
222. **Jacquet, A., Vanderschrick, J.F., Vandenbranden, M., Elouahabi, A., Magi, M., Garcia, L., and Ruysschaert, J.M.**, Vaccination with the recombinant allergen ProDer p 1 complexed with the cationic lipid DiC14-amidine prevents allergic responses to house dust mite. Mol Ther, 2005. **11**(6): p. 960-8.
223. **Davidsen, J., Rosenkrands, I., Christensen, D., Vangala, A., Kirby, D., Perrie, Y., Agger, E.M., and Andersen, P.**, Characterization of cationic liposomes based on dimethyldioctadecylammonium and synthetic cord factor from M. tuberculosis (trehalose 6,6'-dibehenate)-a novel adjuvant inducing both strong CMI and antibody responses. Biochim Biophys Acta, 2005. **1718**(1-2): p. 22-31.
224. **Milicic, A., Kaur, R., Reyes-Sandoval, A., Tang, C.K., Honeycutt, J., Perrie, Y., and Hill, A.V.**, Small cationic DDA:TDB liposomes as protein vaccine adjuvants obviate the need for TLR agonists in inducing cellular and humoral responses. PLoS One, 2012. **7**(3): p. e34255.
225. **Kaur, R., Henriksen-Lacey, M., Wilkhu, J., Devitt, A., Christensen, D., and Perrie, Y.**, Effect of incorporating cholesterol into DDA:TDB liposomal adjuvants on bilayer properties, biodistribution, and immune responses. Mol Pharm, 2014. **11**(1): p. 197-207.
226. **Dietrich, J., Andreasen, L.V., Andersen, P., and Agger, E.M.**, Inducing dose sparing with inactivated polio virus formulated in adjuvant CAF01. PLoS One, 2014. **9**(6): p. e100879.
227. **Ingvarsson, P.T., Schmidt, S.T., Christensen, D., Larsen, N.B., Hinrichs, W.L., Andersen, P., Rantanen, J., Nielsen, H.M., Yang, M., and Foged, C.**, Designing CAF-adjuvanted dry powder vaccines: spray drying preserves the adjuvant activity of CAF01. J Control Release, 2013. **167**(3): p. 256-64.
228. **Brandt, L., Elhay, M., Rosenkrands, I., Lindblad, E.B., and Andersen, P.**, ESAT-6 subunit vaccination against Mycobacterium tuberculosis. Infect Immun, 2000. **68**(2): p. 791-5.

229. **Holten-Andersen, L., Doherty, T.M., Korsholm, K.S., and Andersen, P.**, Combination of the cationic surfactant dimethyl dioctadecyl ammonium bromide and synthetic mycobacterial cord factor as an efficient adjuvant for tuberculosis subunit vaccines. Infect Immun, 2004. **72**(3): p. 1608-17.

230. **Yu, H., Karunakaran, K.P., Jiang, X., Shen, C., Andersen, P., and Brunham, R.C.**, Chlamydia muridarum T cell antigens and adjuvants that induce protective immunity in mice. Infect Immun, 2012. **80**(4): p. 1510-8.

231. **Mayorga, O., Munoz, J.E., Lincopan, N., Teixeira, A.F., Ferreira, L.C., Travassos, L.R., and Taborda, C.P.**, The role of adjuvants in therapeutic protection against paracoccidioidomycosis after immunization with the P10 peptide. Front Microbiol, 2012. **3**: p. 154.

232. **Ridpath, J.F., Dominowski, P., Mannan, R., Yancey, R., Jr., Jackson, J.A., Taylor, L., Mediratta, S., Eversole, R., Mackenzie, C.D., and Neill, J.D.**, Evaluation of three experimental bovine viral diarrhea virus killed vaccines adjuvanted with combinations of Quil A cholesterol and dimethyldioctadecylammonium (DDA) bromide. Vet Res Commun, 2010. **34**(8): p. 691-702.

233. **van Rooij, E.M., Glansbeek, H.L., Hilgers, L.A., te Lintelo, E.G., de Visser, Y.E., Boersma, W.J., Haagmans, B.L., and Bianchi, A.T.**, Protective antiviral immune responses to pseudorabies virus induced by DNA vaccination using dimethyldioctadecylammonium bromide as an adjuvant. J Virol, 2002. **76**(20): p. 10540-5.

234. **Neves Silva, J.P., Coutinho, P.J., and Real Oliveira, M.E.**, Characterization of monoolein-based lipoplexes using fluorescence spectroscopy. J Fluoresc, 2008. **18**(2): p. 555-62.

235. **Ganem-Quintanar, A., Quintanar-Guerrero, D., and Buri, P.**, Monoolein: a review of the pharmaceutical applications. Drug Dev Ind Pharm, 2000. **26**(8): p. 809-20.

236. **Oliveira, I.M., Silva, J.P., Feitosa, E., Marques, E.F., Castanheira, E.M., and Real Oliveira, M.E.**, Aggregation behavior of aqueous dioctadecyldimethylammonium bromide/monoolein mixtures: a multitechnique investigation on the influence of composition and temperature. J Colloid Interface Sci, 2012. **374**(1): p. 206-17.

237. **Carmona-Ribeiro, A.M.**, Bilayer-forming synthetic lipids: drugs or carriers? Curr Med Chem, 2003. **10**(22): p. 2425-46.

238. **Carmona-Ribeiro, A.M.**, Biomimetic particles in drug and vaccine delivery. J Liposome Res, 2007. **17**(3-4): p. 165-72.

239. **Christensen, D., Henriksen-Lacey, M., Kamath, A.T., Lindenstrom, T., Korsholm, K.S., Christensen, J.P., Rochat, A.F., Lambert, P.H., Andersen, P., Siegrist, C.A., Perrie, Y., and Agger, E.M.**, A cationic vaccine adjuvant based on a saturated quaternary ammonium lipid have different in vivo distribution kinetics and display a distinct CD4 T cell-inducing capacity compared to its unsaturated analog. J Control Release, 2012. **160**(3): p. 468-76.

240. **Vonk, A.G., Netea, M.G., van der Meer, J.W., and Kullberg, B.J.**, Host defence against disseminated *Candida albicans* infection and implications for antifungal immunotherapy. Expert Opin Biol Ther, 2006. **6**(9): p. 891-903.

241. **Odds, F.C.**, *Candida* and candidosis: a review and bibliography. 3rd edn. Balliere Tindall, London, 1998.

242. **Pfaller, M.A. and Diekema, D.J.**, Epidemiology of invasive candidiasis: a persistent public health problem. Clin Microbiol Rev, 2007. **20**(1): p. 133-63.

243. **Horn, D.L., Neofytos, D., Anaissie, E.J., Fishman, J.A., Steinbach, W.J., Olyaei, A.J., Marr, K.A., Pfaller, M.A., Chang, C.H., and Webster, K.M.**, Epidemiology and outcomes of candidemia in 2019 patients: data from the prospective antifungal therapy alliance registry. Clin Infect Dis, 2009. **48**(12): p. 1695-703.

244. **Lionakis, M.S.**, New insights into innate immune control of systemic candidiasis. Med Mycol, 2014. **52**(6): p. 555-64.

245. **Vardakas, K.Z., Michalopoulos, A., Kiriakidou, K.G., Siampli, E.P., Samonis, G., and Falagas, M.E.**, Candidaemia: incidence, risk factors, characteristics and outcomes in immunocompetent critically ill patients. Clin Microbiol Infect, 2009. **15**(3): p. 289-92.

246. **Almirante, B., Rodriguez, D., Park, B.J., Cuenca-Estrella, M., Planes, A.M., Almela, M., Mensa, J., Sanchez, F., Ayats, J., Gimenez, M., Saballs, P., Fridkin, S.K., Morgan, J., Rodriguez-Tudela, J.L., Warnock, D.W., Pahissa, A., and Barcelona Candidemia Project Study, G.**, Epidemiology and predictors of mortality in cases of *Candida* bloodstream infection: results from population-based surveillance, barcelona, Spain, from 2002 to 2003. J Clin Microbiol, 2005. **43**(4): p. 1829-35.

247. **Pappo, I., Polacheck, I., Zmora, O., Feigin, E., and Freund, H.R.**, Altered gut barrier function to *Candida* during parenteral nutrition. Nutrition, 1994. **10**(2): p. 151-4.

248. **Wenzel, R.P.**, Nosocomial candidemia: risk factors and attributable mortality. Clin Infect Dis, 1995. **20**(6): p. 1531-4.

249. **Kralovicova, K., Spanik, S., Oravcova, E., Mrazova, M., Morova, E., Gulikova, V., Kukuckova, E., Koren, P., Pichna, P., Nogova, J., Kunova, A., Trupl, J., and Krcmery, V., Jr.**, Fungemia in cancer patients undergoing chemotherapy versus surgery: risk factors, etiology and outcome. Scand J Infect Dis, 1997. **29**(3): p. 301-4.

250. **Douglas, L.J.**, *Candida* biofilms and their role in infection. Trends Microbiol, 2003. **11**(1): p. 30-6.

251. **Mavromanolakis, E., Maraki, S., Cranidis, A., Tselentis, Y., Kontoyiannis, D.P., and Samonis, G.**, The impact of norfloxacin, ciprofloxacin and ofloxacin on human gut colonization by *Candida albicans*. Scand J Infect Dis, 2001. **33**(6): p. 477-8.

252. **Maraki, S., Mouzas, I.A., Kontoyiannis, D.P., Chatzinikolaou, I., Tselentis, Y., and Samonis, G.**, Prospective evaluation of the impact of amoxicillin, clarithromycin and their combination on human gastrointestinal colonization by *Candida* species. Chemotherapy, 2001. **47**(3): p. 215-8.

253. **Saiman, L., Ludington, E., Pfaller, M., Rangel-Frausto, S., Wiblin, R.T., Dawson, J., Blumberg, H.M., Patterson, J.E., Rinaldi, M., Edwards, J.E., Wenzel, R.P., and Jarvis, W.**, Risk factors for candidemia in Neonatal Intensive Care Unit patients. The National Epidemiology of Mycosis Survey study group. Pediatr Infect Dis J, 2000. **19**(4): p. 319-24.

254. **Nucci, M. and Marr, K.A.**, Emerging fungal diseases. Clin Infect Dis, 2005. **41**(4): p. 521-6.

255. **Kao, A.S., Brandt, M.E., Pruitt, W.R., Conn, L.A., Perkins, B.A., Stephens, D.S., Baughman, W.S., Reingold, A.L., Rothrock, G.A., Pfaller, M.A., Pinner, R.W., and Hajjeh, R.A.**, The epidemiology of candidemia in two United States cities: results of a population-based active surveillance. Clin Infect Dis, 1999. **29**(5): p. 1164-70.

256. **Zaoutis, T.E., Argon, J., Chu, J., Berlin, J.A., Walsh, T.J., and Feudtner, C.**, The epidemiology and attributable outcomes of candidemia in adults and children hospitalized in the United States: a propensity analysis. Clin Infect Dis, 2005. **41**(9): p. 1232-9.

257. **Spellberg, B.**, Vaccines for invasive fungal infections. F1000 Med Rep, 2011. **3**: p. 13.

258. **De Sousa dos Santos, S., Lopes, M.H., Simonsen, V., and Caiaffa Filho, H.H.**, *Haemophilus influenzae* type b immunization in adults infected with the human immunodeficiency virus. AIDS Res Hum Retroviruses, 2004. **20**(5): p. 493-6.

259. **Levin, M.J., Gershon, A.A., Weinberg, A., Blanchard, S., Nowak, B., Palumbo, P., Chan, C.Y., and Team, A.C.T.G.**, Immunization of HIV-infected children with varicella vaccine. J Pediatr, 2001. **139**(2): p. 305-10.

260. **Tedaldi, E.M., Baker, R.K., Moorman, A.C., Wood, K.C., Fuhrer, J., McCabe, R.E., Holmberg, S.D., and Investigators, H.I.V.O.S.**, Hepatitis A and B vaccination practices for ambulatory patients infected with HIV. Clin Infect Dis, 2004. **38**(10): p. 1478-84.

261. **Sinsalo, M., Aittoniemi, J., Kayhty, H., and Vilpo, J.**, *Haemophilus influenzae* type b (Hib) antibody concentrations and vaccination responses in patients with chronic lymphocytic leukaemia: predicting factors for response. Leuk Lymphoma, 2002. **43**(10): p. 1967-9.

262. **Klugman, K.P., Madhi, S.A., Huebner, R.E., Kohberger, R., Mbelle, N., Pierce, N., and Vaccine Trialists, G.**, A trial of a 9-valent pneumococcal conjugate vaccine in children with and those without HIV infection. N Engl J Med, 2003. **349**(14): p. 1341-8.

263. **Madhi, S.A., Kuwanda, L., Cutland, C., and Klugman, K.P.**, The impact of a 9-valent pneumococcal conjugate vaccine on the public health burden of pneumonia in HIV-infected and -uninfected children. Clin Infect Dis, 2005. **40**(10): p. 1511-8.

264. **Eggimann, P., Francioli, P., Bille, J., Schneider, R., Wu, M.M., Chapuis, G., Chiolero, R., Pannatier, A., Schilling, J., Geroulanos, S., Glauser, M.P., and Calandra, T.**, Fluconazole prophylaxis prevents intra-abdominal candidiasis in high-risk surgical patients. Crit Care Med, 1999. **27**(6): p. 1066-72.

265. **Perlroth, J., Choi, B., and Spellberg, B.**, Nosocomial fungal infections: epidemiology, diagnosis, and treatment. Med Mycol, 2007. **45**(4): p. 321-46.

266. **Klis, F.M., de Groot, P., and Hellingwerf, K.**, Molecular organization of the cell wall of *Candida albicans*. Med Mycol, 2001. **39 Suppl 1**: p. 1-8.

267. **Gow, N.A. and Hube, B.**, Importance of the *Candida albicans* cell wall during commensalism and infection. Curr Opin Microbiol, 2012. **15**(4): p. 406-12.

268. **Netea, M.G., Brown, G.D., Kullberg, B.J., and Gow, N.A.**, An integrated model of the recognition of *Candida albicans* by the innate immune system. Nat Rev Microbiol, 2008. **6**(1): p. 67-78.

269. **Chaffin, W.L.**, *Candida albicans* cell wall proteins. Microbiol Mol Biol Rev, 2008. **72**(3): p. 495-544.

270. **Cappellaro, C., Mrsa, V., and Tanner, W.**, New potential cell wall glucanases of *Saccharomyces cerevisiae* and their involvement in mating. J Bacteriol, 1998. **180**(19): p. 5030-7.

271. **Moukadiri, I., Jaafar, L., and Zueco, J.**, Identification of two mannoproteins released from cell walls of a *Saccharomyces cerevisiae* mnn1 mnn9 double mutant by reducing agents. J Bacteriol, 1999. **181**(16): p. 4741-5.

272. **Lopez-Ribot, J.L., Casanova, M., Murgui, A., and Martinez, J.P.**, Antibody response to *Candida albicans* cell wall antigens. FEMS Immunol Med Microbiol, 2004. **41**(3): p. 187-96.

273. **Mora-Montes, H.M., Lopez-Romero, E., Zinker, S., Ponce-Noyola, P., and Flores-Carreon, A.**, Heterologous expression and biochemical characterization of an alpha1,2-mannosidase encoded by the *Candida albicans* MNS1 gene. Mem Inst Oswaldo Cruz, 2008. **103**(7): p. 724-30.

274. **Gemmill, T.R. and Trimble, R.B.**, Overview of N- and O-linked oligosaccharide structures found in various yeast species. Biochim Biophys Acta, 1999. **1426**(2): p. 227-37.

275. **Hall, R.A. and Gow, N.A.**, Mannosylation in *Candida albicans*: role in cell wall function and immune recognition. Mol Microbiol, 2013. **90**(6): p. 1147-61.

276. **Netea, M.G., Gow, N.A., Munro, C.A., Bates, S., Collins, C., Ferwerda, G., Hobson, R.P., Bertram, G., Hughes, H.B., Jansen, T., Jacobs, L., Buurman, E.T., Gijzen, K., Williams, D.L., Torensma, R., McKinnon, A., MacCallum, D.M., Odds, F.C., Van der Meer, J.W., Brown, A.J., and Kullberg, B.J.**, Immune sensing of *Candida albicans* requires cooperative recognition of mannans and glucans by lectin and Toll-like receptors. J Clin Invest, 2006. **116**(6): p. 1642-50.

277. **Pietrella, D., Bistoni, G., Corbucci, C., Perito, S., and Vecchiarelli, A.**, *Candida albicans* mannoprotein influences the biological function of dendritic cells. Cell Microbiol, 2006. **8**(4): p. 602-12.

278. **Mencacci, A., Torosantucci, A., Spaccapelo, R., Romani, L., Bistoni, F., and Cassone, A.**, A mannoprotein constituent of *Candida albicans* that elicits different

levels of delayed-type hypersensitivity, cytokine production, and anticandidal protection in mice. Infect Immun, 1994. **62**(12): p. 5353-60.

279. **Xin, H., Dziadek, S., Bundle, D.R., and Cutler, J.E.**, Synthetic glycopeptide vaccines combining beta-mannan and peptide epitopes induce protection against candidiasis. Proc Natl Acad Sci U S A, 2008. **105**(36): p. 13526-31.
280. **Castillo, L., Calvo, E., Martinez, A.I., Ruiz-Herrera, J., Valentin, E., Lopez, J.A., and Sentandreu, R.**, A study of the *Candida albicans* cell wall proteome. Proteomics, 2008. **8**(18): p. 3871-81.
281. **Romani, L.**, Immunity to fungal infections. Nat Rev Immunol, 2011. **11**(4): p. 275-88.
282. **Romani, L.**, Immunity to fungal infections. Nat Rev Immunol, 2004. **4**(1): p. 1-23.
283. **Luo, S., Skerka, C., Kurzai, O., and Zipfel, P.F.**, Complement and innate immune evasion strategies of the human pathogenic fungus *Candida albicans.* Mol Immunol, 2013. **56**(3): p. 161-9.
284. **McKenzie, C.G., Koser, U., Lewis, L.E., Bain, J.M., Mora-Montes, H.M., Barker, R.N., Gow, N.A., and Erwig, L.P.**, Contribution of *Candida albicans* cell wall components to recognition by and escape from murine macrophages. Infect Immun, 2010. **78**(4): p. 1650-8.
285. **Mora-Montes, H.M., Netea, M.G., Ferwerda, G., Lenardon, M.D., Brown, G.D., Mistry, A.R., Kullberg, B.J., O'Callaghan, C.A., Sheth, C.C., Odds, F.C., Brown, A.J., Munro, C.A., and Gow, N.A.**, Recognition and blocking of innate immunity cells by *Candida albicans* chitin. Infect Immun, 2011. **79**(5): p. 1961-70.
286. **Keppler-Ross, S., Douglas, L., Konopka, J.B., and Dean, N.**, Recognition of yeast by murine macrophages requires mannan but not glucan. Eukaryot Cell, 2010. **9**(11): p. 1776-87.
287. **Brown, G.D.**, Innate antifungal immunity: the key role of phagocytes. Annu Rev Immunol, 2011. **29**: p. 1-21.
288. **Netea, M.G. and Marodi, L.**, Innate immune mechanisms for recognition and uptake of *Candida* species. Trends Immunol, 2010. **31**(9): p. 346-53.
289. **Lewis, L.E., Bain, J.M., Lowes, C., Gillespie, C., Rudkin, F.M., Gow, N.A., and Erwig, L.P.**, Stage specific assessment of *Candida albicans* phagocytosis by macrophages identifies cell wall composition and morphogenesis as key determinants. PLoS Pathog, 2012. **8**(3): p. e1002578.

290. **Cheng, S.C., Joosten, L.A., Kullberg, B.J., and Netea, M.G.**, Interplay between *Candida albicans* and the mammalian innate host defense. Infect Immun, 2012. **80**(4): p. 1304-13.

291. **Brown, A.J., Haynes, K., and Quinn, J.**, Nitrosative and oxidative stress responses in fungal pathogenicity. Curr Opin Microbiol, 2009. **12**(4): p. 384-91.

292. **Si, H., Hernday, A.D., Hirakawa, M.P., Johnson, A.D., and Bennett, R.J.**, *Candida albicans* white and opaque cells undergo distinct programs of filamentous growth. PLoS Pathog, 2013. **9**(3): p. e1003210.

293. **Cunha, C., Carvalho, A., Esposito, A., Bistoni, F., and Romani, L.**, DAMP signaling in fungal infections and diseases. Front Immunol, 2012. **3**: p. 286.

294. **van de Veerdonk, F.L., Kullberg, B.J., van der Meer, J.W., Gow, N.A., and Netea, M.G.**, Host-microbe interactions: innate pattern recognition of fungal pathogens. Curr Opin Microbiol, 2008. **11**(4): p. 305-12.

295. **Romani, L.**, Innate and adaptive immunity in *Candida albicans* infections and saprophytism. J Leukoc Biol, 2000. **68**(2): p. 175-9.

296. **Romani, L.**, Cell mediated immunity to fungi: a reassessment. Med Mycol, 2008. **46**(6): p. 515-29.

297. **Mencacci, A., Cenci, E., Del Sero, G., Fe d'Ostiani, C., Mosci, P., Trinchieri, G., Adorini, L., and Romani, L.**, IL-10 is required for development of protective Th1 responses in IL-12-deficient mice upon *Candida albicans* infection. J Immunol, 1998. **161**(11): p. 6228-37.

298. **Mencacci, A., Del Sero, G., Cenci, E., d'Ostiani, C.F., Bacci, A., Montagnoli, C., Kopf, M., and Romani, L.**, Endogenous interleukin 4 is required for development of protective CD4+ T helper type 1 cell responses to *Candida albicans*. J Exp Med, 1998. **187**(3): p. 307-17.

299. **Demengeot, J., Zelenay, S., Moraes-Fontes, M.F., Caramalho, I., and Coutinho, A.**, Regulatory T cells in microbial infection. Springer Semin Immunopathol, 2006. **28**(1): p. 41-50.

300. **Gaffen, S.L., Hernandez-Santos, N., and Peterson, A.C.**, IL-17 signaling in host defense against *Candida albicans*. Immunol Res, 2011. **50**(2-3): p. 181-7.

301. **Bromuro, C., Torosantucci, A., Chiani, P., Conti, S., Polonelli, L., and Cassone, A.**, Interplay between protective and inhibitory antibodies dictates the outcome of experimentally disseminated Candidiasis in recipients of a *Candida albicans* vaccine. Infect Immun, 2002. **70**(10): p. 5462-70.

302. **Han, Y., Kozel, T.R., Zhang, M.X., MacGill, R.S., Carroll, M.C., and Cutler, J.E.**, Complement is essential for protection by an IgM and an IgG3 monoclonal antibody against experimental, hematogenously disseminated candidiasis. J Immunol, 2001. **167**(3): p. 1550-7.

303. **Casadevall, A.**, Antibody immunity and invasive fungal infections. Infect Immun, 1995. **63**(11): p. 4211-8.

304. **Cutler, J.E.**, Defining criteria for anti-mannan antibodies to protect against candidiasis. Curr Mol Med, 2005. **5**(4): p. 383-92.

305. **Han, Y., Ulrich, M.A., and Cutler, J.E.**, *Candida albicans* mannan extract-protein conjugates induce a protective immune response against experimental candidiasis. J Infect Dis, 1999. **179**(6): p. 1477-84.

306. **Nitz, M., Ling, C.C., Otter, A., Cutler, J.E., and Bundle, D.R.**, The unique solution structure and immunochemistry of the *Candida albicans* beta -1,2-mannopyranan cell wall antigens. J Biol Chem, 2002. **277**(5): p. 3440-6.

307. **Torosantucci, A., Bromuro, C., Chiani, P., De Bernardis, F., Berti, F., Galli, C., Norelli, F., Bellucci, C., Polonelli, L., Costantino, P., Rappuoli, R., and Cassone, A.**, A novel glyco-conjugate vaccine against fungal pathogens. J Exp Med, 2005. **202**(5): p. 597-606.

308. **Han, Y., Morrison, R.P., and Cutler, J.E.**, A vaccine and monoclonal antibodies that enhance mouse resistance to *Candida albicans* vaginal infection. Infect Immun, 1998. **66**(12): p. 5771-6.

309. **Cassone, A., De Bernardis, F., and Torososantucci, A.**, An outline of the role of anti-*Candida* antibodies within the context of passive immunization and protection from candidiasis. Curr Mol Med, 2005. **5**(4): p. 377-82.

310. **Cassone, A.**, Vulvovaginal *Candida albicans* infections: pathogenesis, immunity and vaccine prospects. BJOG, 2014.

311. **Tapia, P.C.**, [NDV-3, a recombinant alum-adjuvanted vaccine for *Candida* and *Staphylococcus aureus*, is safe and immunogenic in healthy adults]. Rev Chilena Infectol, 2013. **30**(1): p. 109-10.

312. **Lipinski, T., Wu, X., Sadowska, J., Kreiter, E., Yasui, Y., Cheriaparambil, S., Rennie, R., and Bundle, D.R.**, A beta-mannan trisaccharide conjugate vaccine aids clearance of *Candida albicans* in immunocompromised rabbits. Vaccine, 2012. **30**(44): p. 6263-9.

313. **Bundle, D.R., Nycholat, C., Costello, C., Rennie, R., and Lipinski, T.**, Design of a *Candida albicans* disaccharide conjugate vaccine by reverse engineering a protective monoclonal antibody. ACS Chem Biol, 2012. **7**(10): p. 1754-63.

314. **Cutler, J.E., Corti, M., Lambert, P., Ferris, M., and Xin, H.**, Horizontal transmission of C*andida albicans* and evidence of a vaccine response in mice colonized with the fungus. PLoS One, 2011. **6**(7): p. e22030.

315. **Sandini, S., La Valle, R., Deaglio, S., Malavasi, F., Cassone, A., and De Bernardis, F.**, A highly immunogenic recombinant and truncated protein of the secreted aspartic proteases family (rSap2t) of *Candida albicans* as a mucosal anticandidal vaccine. FEMS Immunol Med Microbiol, 2011. **62**(2): p. 215-24.

316. **Luo, G., Ibrahim, A.S., Spellberg, B., Nobile, C.J., Mitchell, A.P., and Fu, Y.**, *Candida albicans* Hyr1p confers resistance to neutrophil killing and is a potential vaccine target. J Infect Dis, 2010. **201**(11): p. 1718-28.

317. **Ibrahim, A.S., Spellberg, B.J., Avanesian, V., Fu, Y., and Edwards, J.E., Jr.**, The anti-*Candida* vaccine based on the recombinant N-terminal domain of Als1p is broadly active against disseminated candidiasis. Infect Immun, 2006. **74**(5): p. 3039-41.

318. **Bystricky, S., Paulovicova, E., and Machova, E.**, *Candida albicans* mannan-protein conjugate as vaccine candidate. Immunol Lett, 2003. **85**(3): p. 251-5.

319. **Saville, S.P., Lazzell, A.L., Chaturvedi, A.K., Monteagudo, C., and Lopez-Ribot, J.L.**, Efficacy of a genetically engineered *Candida albicans* tet-NRG1 strain as an experimental live attenuated vaccine against hematogenously disseminated candidiasis. Clin Vaccine Immunol, 2009. **16**(3): p. 430-2.

320. **Lin, L., Ibrahim, A.S., Xu, X., Farber, J.M., Avanesian, V., Baquir, B., Fu, Y., French, S.W., Edwards, J.E., Jr., and Spellberg, B.**, Th1-Th17 cells mediate protective adaptive immunity against Staphylococcus aureus and *Candida albicans* infection in mice. PLoS Pathog, 2009. **5**(12): p. e1000703.

321. **Spellberg, B., Ibrahim, A.S., Yeaman, M.R., Lin, L., Fu, Y., Avanesian, V., Bayer, A.S., Filler, S.G., Lipke, P., Otoo, H., and Edwards, J.E., Jr.**, The antifungal vaccine derived from the recombinant N terminus of Als3p protects mice against the bacterium *Staphylococcus aureus*. Infect Immun, 2008. **76**(10): p. 4574-80.

322. **Schmidt, C.S., White, C.J., Ibrahim, A.S., Filler, S.G., Fu, Y., Yeaman, M.R., Edwards, J.E., Jr., and Hennessey, J.P., Jr.**, NDV-3, a recombinant alum-

adjuvanted vaccine for *Candida* and *Staphylococcus aureus*, is safe and immunogenic in healthy adults. Vaccine, 2012. **30**(52): p. 7594-600.

323. **Luo, G., Ibrahim, A.S., French, S.W., Edwards, J.E., Jr., and Fu, Y.**, Active and passive immunization with rHyr1p-N protects mice against hematogenously disseminated candidiasis. PLoS One, 2011. **6**(10): p. e25909.
324. **Pietrella, D., Rachini, A., Torosantucci, A., Chiani, P., Brown, A.J., Bistoni, F., Costantino, P., Mosci, P., d'Enfert, C., Rappuoli, R., Cassone, A., and Vecchiarelli, A.**, A beta-glucan-conjugate vaccine and anti-beta-glucan antibodies are effective against murine vaginal candidiasis as assessed by a novel in vivo imaging technique. Vaccine, 2010. **28**(7): p. 1717-25.
325. **Xin, H. and Cutler, J.E.**, Vaccine and monoclonal antibody that enhance mouse resistance to candidiasis. Clin Vaccine Immunol, 2011. **18**(10): p. 1656-67.
326. **Han, Y. and Cutler, J.E.**, Antibody response that protects against disseminated candidiasis. Infect Immun, 1995. **63**(7): p. 2714-9.
327. **Eckstein, M., Barenholz, Y., Bar, L.K., and Segal, E.**, Liposomes containing *Candida albicans* ribosomes as a prophylactic vaccine against disseminated candidiasis in mice. Vaccine, 1997. **15**(2): p. 220-4.
328. **De Bernardis, F., Amacker, M., Arancia, S., Sandini, S., Gremion, C., Zurbriggen, R., Moser, C., and Cassone, A.**, A virosomal vaccine against candidal vaginitis: immunogenicity, efficacy and safety profile in animal models. Vaccine, 2012. **30**(30): p. 4490-8.

CHAPTER III:

A new method for yeast phagocytosis analysis by flow cytometry

Adapted from:

A new method for yeast phagocytosis analysis by flow cytometry.

Catarina Carneiro[1], Catarina Vaz[1], Joana Carvalho-Pereira[1], Célia Pais[1], and Paula Sampaio[1] .

Journal of Microbiology Methods (2014) 101:56-62.

[1]Centre of Molecular and Environmental Biology (CBMA), Department of Biology, University of Minho, Braga, Portugal

ABSTRACT

Herein we developed a method based on the quenching effect of propidium iodide over Sytox-Green fluorescence to assess yeast phagocytosis by flow cytometry. It allows accurate quantification and distinction of living from dead phagocytes; internalized from non-internalized cells, maintaining yeast fluorescence within phagocytes; and the different associations between phagocytes and fungal cells.

1. INTRODUCTION

Candida species are known as common colonizers of the human gastrointestinal, respiratory, and reproductive tracts. However, in immunosuppressed patients they are by far the most common cause of fungal invasive infections. Host defense against candidiasis relies mainly on the ingestion and elimination of the yeasts by the phagocytic cells [1]. Phagocytosis of fungal pathogens is a complex process that may be divided into several distinct stages: (i) migration of phagocytes towards fungal cells; (ii) recognition of fungal pathogen-associated molecular patterns (PAMPs) through phagocyte pattern recognition receptors (PRRs); (iii) engulfment of fungal cells; and (iv) processing of engulfed cells within phagolysosomes [2]. Yeast cell wall consists of a matrix of β-glucan, chitin and mannoproteins, surrounding the plasma membrane, in which the composition and structure of cell wall mannoproteins and glucans, constitute the major yeast PAMPs [3]. However, the cell wall is a dynamic structure and changes during cell growth and transition of yeast to hypha, changing the composition and structure of their PAMPs [3]. Although this dynamic change is an advantage for the pathogen it hampers studies addressing the contribution of specific PAMPs to the different stages of the phagocytic process. Traditionally, studies focusing on phagocytes–yeast interaction use live yeast cells however, it was establish that the phagocytes recognize and respond to cell wall PAMPS present in both live or dead cells, with differences in the efficiency of phagocytosis only relevant after yeast multiplication takes place, around 45 min after co-incubation of the two types of cells [4].

Numerous methods have been developed to study yeast phagocytosis, being fluorescence microscopy and flow cytometry (FCM) the most reliable [2, 5-7]. FCM combines the advantage of being fast, able to count hundreds of cells, and easily discriminate morphological heterogeneity within cell populations [6]. In this work we evaluated the feasibility of the main phagocytosis assessing methods previously described to be adapted to FCM analysis and, to overcome some methodological limitations, we propose a new efficient method based on a combination of only two fluorochromes (Sytox Green and propidium iodide (PI) for FCM analysis of macrophage interaction with *Candida sp.* cells and show that this new methodology can be used to study the contribution of different PAMPs to the phagocytic process.

2. MATERIALS AND METHODS

2.1. Materials

All fluorescent reagents were prepared as stock solutions and then diluted in the cell incubation medium at the desired concentrations. Fluorescein isothiocyanate (FITC) (Sigma Aldrich), was freshly prepared at 750 μg/ml in 0.1 M sodium carbonate buffer (pH 9), from a 5 mg/ml dimethyl sulfoxide (DMSO) solution; Trypan Blue (TB) (Sigma Aldrich) solution (0.4%) was used directly as stock solution; 50 μM Sytox Green (Invitrogen) was prepared in 1X PBS from a 5 mM solution in DMSO; propidium iodide (PI) (Sigma Aldrich) was dissolved in sterile water at 1 mg/ml, Calcofluor White (CFW) (Sigma Aldrich) was dissolved in sterile water at 10 mg/ml stock solution. Stock solutions were stored in the dark at -20 °C. Dulbecco's Modified Eagle's medium (DMEM) was supplemented with 10% heat-inactivated fetal bovine serum (FBS) (Valbiotech), 2 mM L-glutamine, 1 mM sodium pyruvate, and 10 mM HEPES.

2.2. Preparation of yeast cells

Wild type strains of *Candida albicans* (SC5314), *Candida glabrata* (PYCC 2418), *Candida bracarensis* (153M), *Candida parapsilosis* (ATCC 22019), *Candida orthopsilosis* (HSM CAN 138), and *Candida krusei* (PYCC 3341) were used in this study. Yeast cells grown overnight at 26 °C in YEPD medium (2% glucose, 1% bactopeptone, and 2% yeast extract) were recovered by centrifugation, washed twice in sterile 1X PBS buffer and sonicated (2 cycles, 5 s) to eliminate aggregates.

To fix cell wall PAMPs, yeast cells were incubated for 10 min in formol/ethanol (1:9) and washed five times with 1X PBS for complete removal of formol/ethanol. Yeast cells were incubated for 10 min with 1 μM Sytox Green at room temperature (RT) in the dark, washed with 1X PBS to remove unbound dye, and brought to the desired cell density in complete DMEM.

Live-cells were labeled with FITC or CFW. FITC, previously prepared at a concentration of 50 μg/ml, was added directly to the yeast cells pellet and incubated for 10 min at room temperature in the dark. CFW was added to yeast cells at a final concentration of 5 μg/ml and incubated for 5 min at room temperature in the dark. Labeled cells were then

washed with 1X PBS to remove unbound dye, and brought to the desired cell density in complete DMEM.

2.3. Analyses of labeled yeast cells and quenching effect

Sytox Green, CFW or FITC labeled yeasts were incubated with TB at a final concentration of 120 µg/ml or with PI at a final concentration of 6 µg/ml, in order to validate the quenching efficiency of TB or PI over Sytox Green, CFW or FITC. As neither TB nor PI enters viable cells, the internalized yeast cells will retain the original unquenched fluorescence. The pH fluorescence stability of the labeling dyes was evaluated by incubating labeled yeasts in a solution with 1 mM of acetic acid pH of 3.9. The yeast cells were then analyzed by fluorescence microscopy or/and by flow cytometry.

2.4. Preparation of J774A.1 macrophage cell line

The murine macrophage-like cell line J774A.1 was cultured in complete DMEM at 37 °C in a 5% CO2 atmosphere. After confluent growth, macrophage cells were recovered, washed, and resuspended in complete DMEM to a final concentration of 5×10^5 cells/ml. For fluorescence microscopy assays, 1 ml of the resulting cell suspension was transferred to 24-well tissue culture plates containing clean sterile glass coverslips (Ø13 mm). For flow cytometry (FCM) 3 ml of the cell suspension were transferred to a 6-well tissue culture plate, and for confocal microscopy, 0.2 ml of the cells were plated in a microscopy chamber plate (Ibidi). Cells were then incubated overnight, at 37 °C in a 5% CO2 atmosphere, to allow macrophage adherence. In the following day, phagocytic cells were washed twice with 1X PBS buffer to remove non-adherent cells, and cells were promptly used for phagocytic assays. Triplicates were done in each plate.

2.5. Phagocytosis of *Candida* cells

Macrophages were incubated with labeled yeast suspensions at MOI of 1M:5Y for 30 min, at 37 °C and 5% CO_2. After incubation plates were kept on ice to stop phagocytosis, and wells rinsed twice with 1X PBS to remove unbound yeasts. Macrophages and associated

yeasts were then incubated with TB at a final concentration of 120 μg/ml or with PI at a final concentration of 6 μg/ml, for 5 min at RT. Cells were analyzed by fluorescence microscopy (Leica DM5000B), confocal microscopy (Leica SP2 AOBS SE) and by flow cytometry (FCM) (EPICS XL-MCL, Beckman-Coulter Corporation). Fluorescence microscopy images were analyzed using ImageJ cell counter software. Confocal microscopy images were analyzed using Fiji software. FCM data was analyzed by using Flowing software (version 2.5; Turku Centre for Biotechnology, University of Turku), as indicated in the following section.

The statistical significance values were tested by means of repeated ANOVA measures. Multiple comparisons were performed according to the Bonferroni test using GraphPad Prism 5 software (GraphPad Software, Inc., La Jolla, CA).

2.6. Flow cytometry (FCM) analysis

FCM analysis was performed on an EPICS XL-MCL (Beckman-Coulter Corporation, Hialeah, FL, USA) flow cytometer. At least twenty thousand cells were analyzed per sample at low flow rate. An acquisition protocol was defined to measure forward scatter (FSC), side scatter (SSC), green fluorescence and red fluorescence on a logarithmic scale. Each sample was collected for 30 s at the slowest flow rate to minimize the coincidental appearance of free yeasts and macrophages in the laser beam. A FSC threshold was set to gate out debris. Macrophages and free yeast cells were discriminated by combined measurements of FSC and SSC. Macrophages were gated in R1 area and free yeast cells in R2 area. The control with macrophages alone was used to define the R1 gates.

The percentage of yeast particles interacting with macrophages was calculated from dot plot analysis of Sytox Green fluorescence intensity vs. PI fluorescence intensity of R1-gated events by using Flowing software. The percentage of macrophages with attached yeast particles (M_{YA}) was calculated using the next formula, following the red fluorescence signal:

$$M_{YA} = (M_R * 100 / M_{AF}),$$

where MR is the mean red fluorescence (calculated by number of events in quadrant Q4), gated in R1, MAF is the total number of events gated in R1. The percentage of macrophages with ingested and attached yeast particles (M_{YAI}) was assessed as follows:

$$M_{YAI} = M_{RG} * 100 / M_{AF}$$

where MRG is the mean green and red fluorescence (calculated by number of events in quadrant Q3), gated in R1. The percentage of macrophages with only ingested yeast particles (M_{YI}) was assessed as follows:

$$M_{YI} = M_G * 100 / M_{AF}$$

where MG is the mean green fluorescence (calculated by number of events in quadrant Q2) gated in R1. The percentage of phagocytosis, macrophages with ingested yeast particles (M_{YI}), was assessed as follows:

$$M_{YF} = M_{YI} + M_{YA}$$

3. RESULTS AND DISCUSSION

3.1. Analyses of labeled yeast cells and quenching effect

The challenge in developing an in vitro method to assess phagocytosis of yeast cells based on flow cytometry (FCM) relies on the difficulty to distinguish between internalized and non-internalized yeasts, and on the stability of the fluorochrome within the hostile environment of the phagolysosome both reducing the accuracy of phagocytosis measurements [6]. In this view, these two characteristics were analyzed with several fluorochrome combinations in order to assess their utility for phagocytosis measurements by FCM.

One way to distinguish between internalized and non-internalized yeasts is by taking advantage of the quenching effect of some dyes over the emitted fluorescence of another dye. So, first we tested the ability of TB or PI in quenching FITC fluorescence on labeled yeast cells. We observed that TB, although not completely, was able to quench FITC fluorescence, as described in previous studies [8, 9] but FITC fluorescence is no longer detected upon incubation at a lower pH (Figure 1A), as previously reported [10]. PI was not able to quench FITC fluorescence (supplementary information Figure 1A). Thus, both combinations FITC/PI and FITC/TB were discarded for phagocytosis measurements by FCM. The quenching effect of TB over CFW-stained yeast cells was also tested and results confirmed previous data that TB quenches CFW fluorescence [4] but, CFW fluorescence is significantly reduced at lower pH (Figure 1B). Once again, PI failed as a quenching dye, being unable to quench CFW fluorescence (Figure 1B).

Traditionally, studies focusing on phagocytes–yeast interaction use live yeast cells, however, it was already establish that the innate immune cells recognize and respond to cell wall PAMPs in both, live or dead cells. The major difference described is in the efficiency of phagocytosis but this difference is only relevant after yeast multiplication takes place [4]. However, inactivating treatments based on heat killing by boiling result in the release of matricial cell wall surface components [11], which are extremely important for phagocyte recognition. On the contrary, inactivating treatments based on fixation of the cell wall components conserve the PAMPs in such a way that enables antibody recognition [12]. In this sense, in the present study yeast cells were inactivated by a fixation method that does not alter the fungal cell wall structure.

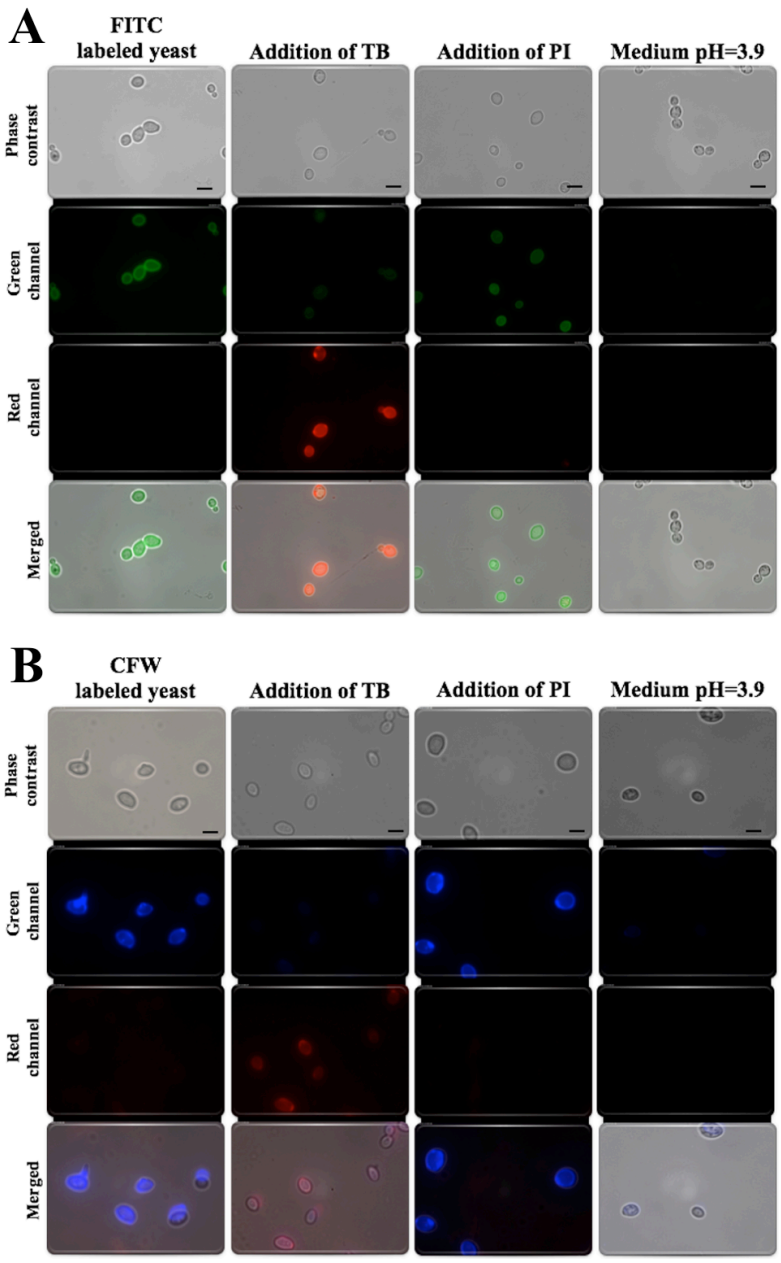

Figure 1: Analysis of yeast cells labeling, quenching effect and fluorochrome stability at low pH. The effect of TB, PI, or medium pH in the fluorescence of: **A)** FITC labeled yeast cells, **B)** CFW labeled yeast cells. The scale bar represents 7.5 µm.

The use of dead yeast cells allowed the exploitation of viability fluorescent dyes such as Sytox Green for yeast labeling, avoiding the surface exposure of the dyes. Sytox Green is a high affinity nuclear stain that penetrates cells and intercalates with nucleic acids, staining the cell. The ability of TB or PI to quench the Sytox Green-stained yeast cells was also assessed (Figure 2). As can be observed in the figure, TB incompletely quenches Sytox Green fluorescence, however the quenching effect over Sytox Green labeled yeasts is remarkably

evident when PI is used. Additionally, no significant reduction of fluorescence was observed when Sytox Green labeled yeast cells were incubated at pH 3.9 (Figure 2).

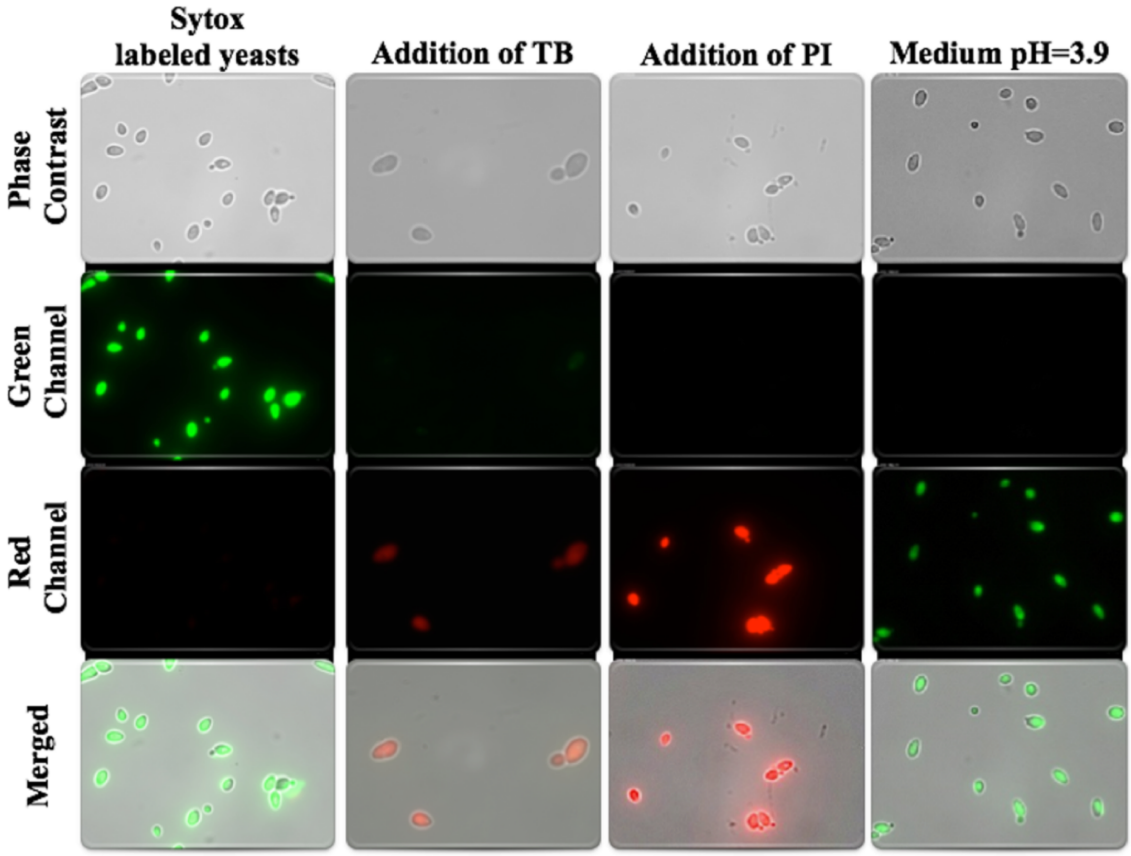

Figure 2: Analysis of yeast cells labeling, quenching effect, and fluorochrome stability at low pH. Effect of TB, PI, or medium pH in the fluorescence of Sytox Green labeled yeast cells. The scale bar represents 7.5 µm.

Since Sytox Green/PI combination is more adequate for flow cytometry analyses than Sytox Green/TB, the quenching effect and pH stability of the Sytox Green/PI protocol were confirmed by FCM. Non-stained yeast cells were gated (Figure 3A) and used to calibrate yeast auto-fluorescence in the cytometer (Figure 3B). After incubation with Sytox Green, 99.97% of the yeast cells are labeled, validating Sytox Green label efficiency (Figure 3C). The incubation of Sytox Green labeled cells with PI shifted the fluorescence of 99.25% of the cells to PI positive, while only 0.75% remained Sytox Green positive (Figure 3D), confirming our previous results of an almost complete quenching of the Sytox Green fluorescence.

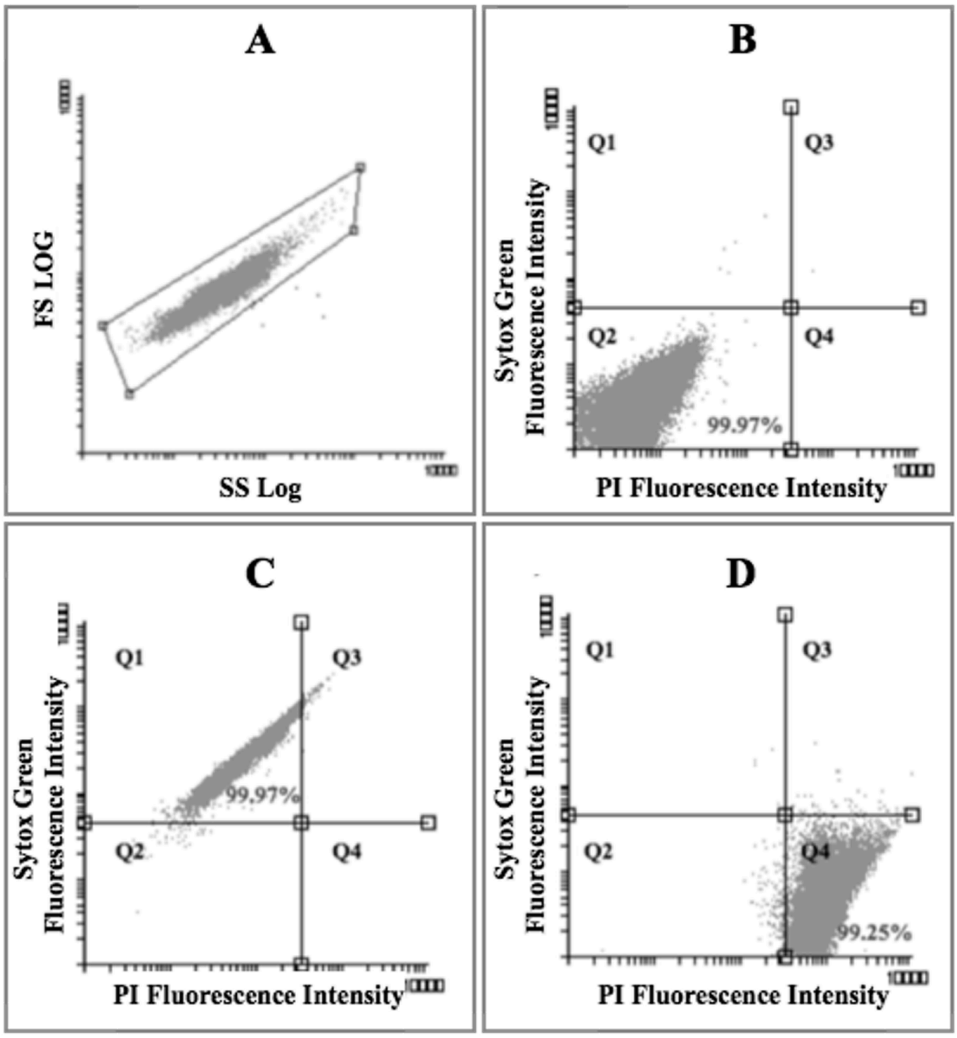

Figure 3: FCM analysis of PI quenching effect over Sytox Green labeled yeast cells. **(A)** Gated non-stained yeast cells used for **(B)** auto-fluorescence calibration. **(C)** Sytox Green labeled yeasts showing green fluorescence (Q1) and (D) Sytox Green/PI double-stained yeast cells showing red florescence (Q4).

The mean fluorescence (MFI) of Sytox Green yeast cells incubated at pH 3.9 showed a slight decrease in intensity but yeast cells remained Sytox Green stained, supporting our previous observations (Figure 4).

In order to evaluate the efficiency of Sytox Green/PI protocol in a phagocytosis assay, fixed *C. albicans* cells stained with Sytox Green were incubated with macrophages for 30 min and then stained with PI. The murine macrophage-like cell line J774A.1 was selected for this study, since it is widely used in phagocytic studies and no significant differences regarding the ability to engulf yeast cells are described, in comparison with primary phagocytic culture, at least within the time point used in our study [2].

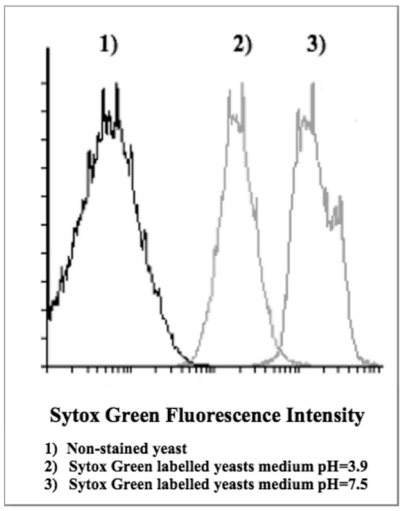

Figure 4: FCM analysis of fluorescence stability at low pH in Sytox Green labeled yeast cells. Histogram overlay of Sytox Green Medium Fluorescence Intensity (MFI) of non-labeled yeast cells (1), labeled yeast cells at pH of 7.5 (2), and labeled yeast cells at pH of 3.9 (3).

The confocal microscopy analysis after phagocytosis revealed, as expected, that without fluorescence distinction of internalized from non-internalized yeast cells is imprecise (Figure 5Ai). The PI quenching effect of the non-internalized yeast cells (Figure 5Aiii), and the integrity of the Sytox Green fluorescence of *C. albicans* cells inside live macrophages (Figure 5Aii) are clearly visible and critical for the accurate distinction. In order to confirm that Sytox Green labeled yeast cells were indeed inside macrophages, an ortho-stack 3D visualization of the cells is represented in Figure 5B (supplementary information Movie S1). In view of these results, the presented protocol will enable differentiation of: (i) non labeled phagocytes, representing phagocytes with no interaction with yeast cells; (ii) Sytox Green labeled phagocytes, representing phagocytes that have only internalized yeast cells; (iii) PI labeled phagocytes, representing phagocytes that have only attached yeast cells; and (iv) Sytox Green and PI labeled phagocytes, representing phagocytes that have both internalized and attached yeast cells.

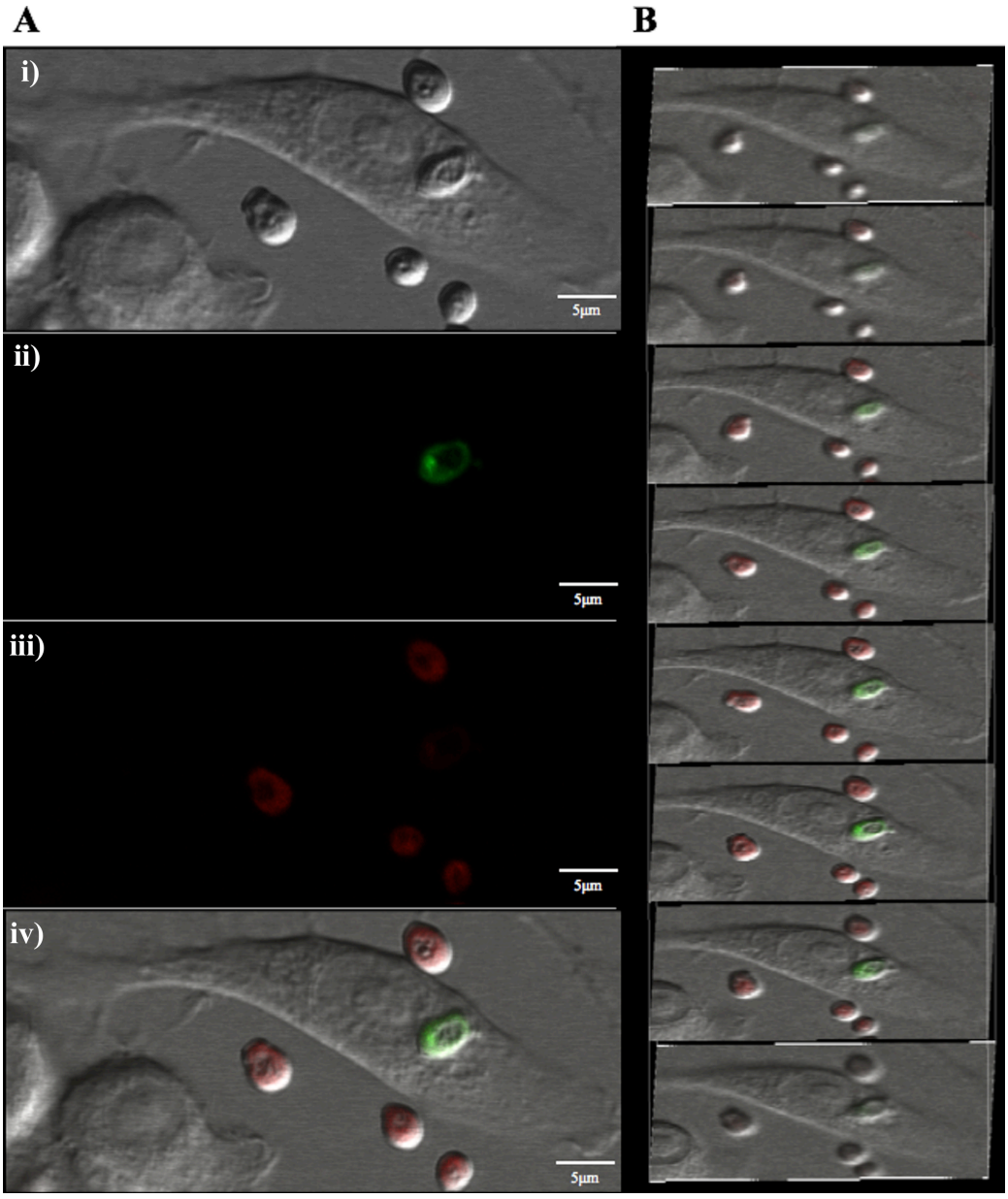

Figure 5: Confocal phagocytosis analysis. **(A)** Confocal microscopy image of J774A.1 macrophage with internalized and adhered yeast cells showing the PI quenching effect on yeast cells after phagocytosis. Intracellular yeast remains Sytox Green fluorescent after 30 min of incubation and extracellular yeast cells are PI stained. i) Nomarski image, ii) Sytox Green fluorescence, iii) PI fluorescence and iv) Merged image. **(B)** Z-stack images were analyzed to confirm internalization. The scale bar represents 5 µm.

3.2. FCM analysis of the phagocytosis assay with different *Candida* species

In order to test this new FCM phagocytosis protocol, assays were performed using different *Candida* species: *C. albicans*, *C. glabrata*, *C. bracarensis*, *C. parapsilosis*, *C. orthopsilosis*, and *C. krusei*. The % of phagocytes with internalized yeast cells, the % of phagocytes that have both internalized and attached yeast cells, and the % of phagocytes that

have only attached yeast cells were calculated. Before incubation with yeast cells macrophage auto-fluorescence was calibrated with a suspension of non-stained macrophages. Then, PI stained macrophages were evaluated and two populations clearly distinguishable, one representing dead macrophages (PI positive), which was not analyzed, and the other, the live macrophages, designated as R1 (P1 negative) (Figure 6A). The non stained R1 macrophages were indeed PI negative and were further analyzed in a second dot plot, by plotting Sytox Green fluorescence against PI fluorescence. The majority of the cells (97.39%) gated in a quadrant (Q2) were used to define the limits of Sytox Green and PI negative cells (Figure 6B). The other quadrants will gate the distinct phagocytes–yeast interactions: phagocytes that have only internalized yeast cells (Q1), phagocytes representing phagocytes that have both internalized and attached yeast cells (Q3), and phagocytes that have only attached yeast cells (Q4). In a first approach, *C. albicans* FCM assessed phagocytosis was performed to test the protocol. Dot plot of macrophages after incubation with the yeast cells showed an additional population, the free yeast cells (R2), that were not analyzed (Figure 5C). In order to quantify *C. albicans* phagocytosis, the R1 cell population was selected and the fluorescence intensity of Sytox Green vs. PI analyzed, by using the previously defined gate limits (Figure 5D). Four distinct phagocytes–yeast interactions could be quantified: in Q1 the phagocytes that have only internalized yeast cells (M_{YI}, 57.6%); in Q2 the phagocytes with no interaction with yeast cells (M_{YNO}, 42.7%); in Q3 the phagocytes with both internalized and attached yeast cells (M_{YAI}, 8.7%); and in Q4 the phagocytes with only attached yeast cells (M_{YA}, 1.50%). These results confirmed that the new fluorochrome combination is suitable for flow cytometry phagocytosis assays of fixed yeast cells.

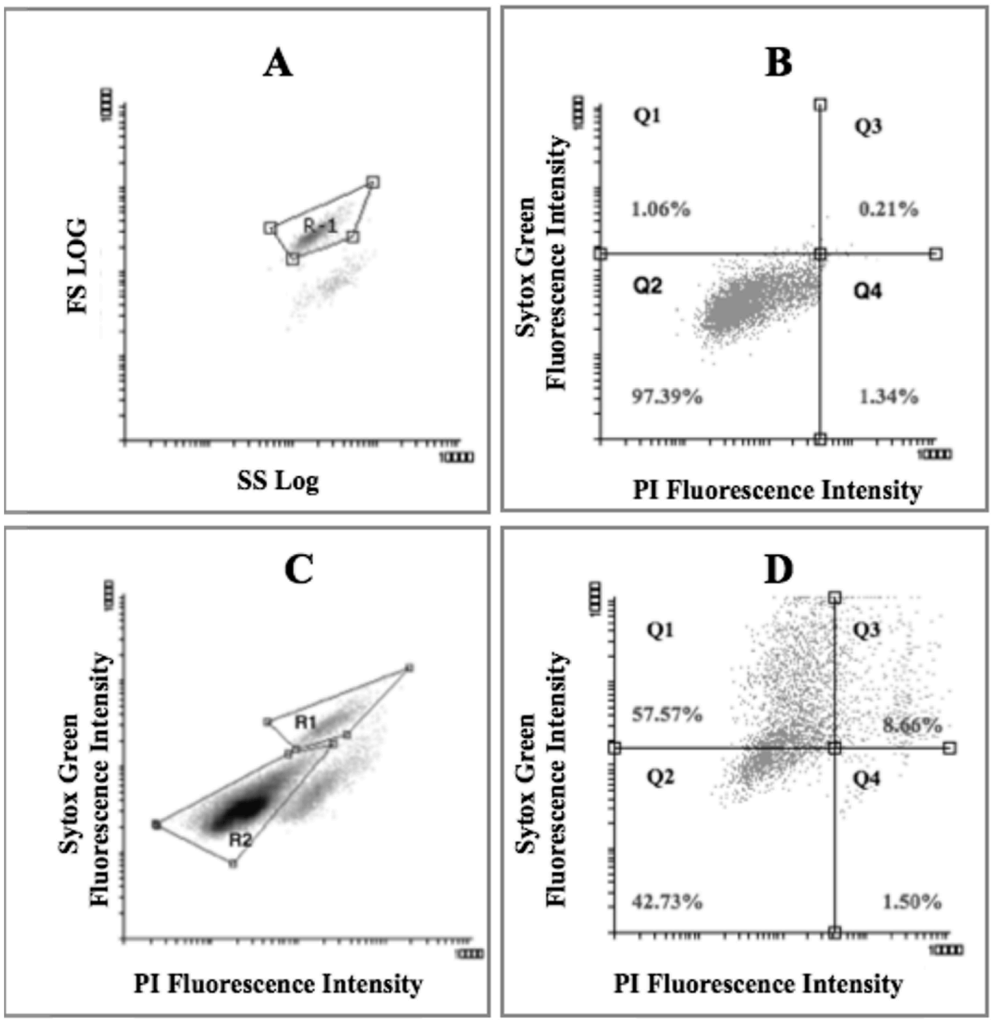

Figure 6: Macrophage *Candida spp.* phagocytosis assay by flow cytometry. **(A)** Dot plot of macrophage cells alone stained with PI that were used to gate live cells (R1) and **(B)** calibrate auto- fluorescence. **(C)** Dot plot of macrophages after 30 min of incubation with yeast cells, showing a clear distinction between live macrophages (R1) and yeast cells (R2). **(D)** Analysis of R1 population after phagocytosis allows the identification of macrophages without yeast interaction (M_{YNO}) in quadrant Q2; macrophages with ingested yeast cells (M_{YI}) in quadrant Q1; macrophages with ingested and adhered yeast cells (M_{YAI}) in quadrant Q3, and macrophages with only adhered cells (M_{YA}) in quadrant Q4.

Following this confirmation, the protocol was extended to evaluate phagocytosis quantified by the new protocol in different *Candida* species. As expected, different species presented different ratios of macrophage ingestion and/or adhered yeast cells (Figure 7). *C. orthopsilosis* was the species with the higher percentage of ingested/adhered cells followed by *C. krusei*, *C. bracarensis* and *C. parapsilosis*, while *C. glabrata* and *C. albicans* were the species with the lower percentage. These results are in accordance with several studies that demonstrated that the immune cells respond differently. These results are in accordance with several studies that demonstrated that the immune cells respond differently to individual *Candida* species in part, due to differences in cell wall PAMP components and

organization [13-18]. It was also described that phagocytosis was more efficient using *C. parapsilosis* as a target than *C. albicans* yeasts [19]. *C. krusei* was more phagocytized than *C. albicans* or *C. glabrata* [20], and *C. orthopsilosis* was less resistant to phagocytic host defenses than C. parapsilosis [21].

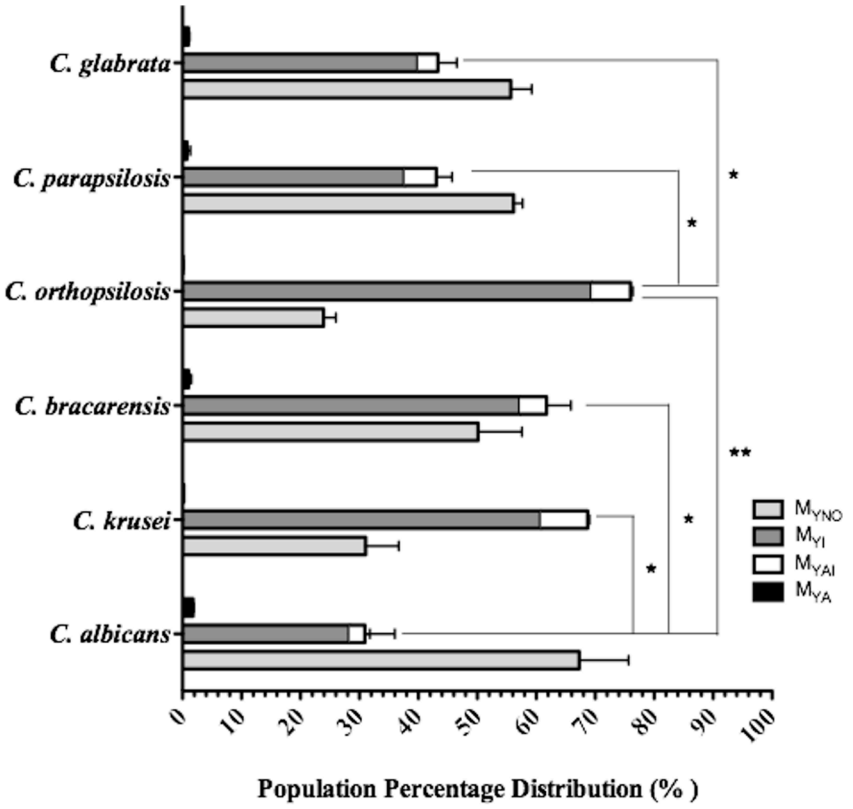

Figure 7: Phagocytosis assay with cells from different *Candida* species. Analysis of the interactions of J774A.1 macrophages with formol/ethanol (1:9) killed *Candida spp.* cells after 30 min of incubation. The light gray bars (M_{YNO}) represent the % of macrophages with no interaction with yeast cells; The gray bars (M_{YI}) macrophages with internalized yeast cells; white bars (M_{YAI}) macrophages with internalized and adhered yeast cells and the black bars (M_{YA}) macrophages with only adhered cells. The gray bar together with the white bar represents the % of phagocytosis. Each bar is the average of two independent experiments. The significance of the results between the different species is indicated in this figure (*P<0.05, **P<0.01).

For methodology comparison, confocal microscopy images were taken and analyzed to assess the percentage of macrophages with internalized *C. albicans*, *C. parapsilosis* and *C. orthopsilosis* yeast cells. At least 500 macrophages were counted in each slide and results confirmed that *C. orthopsilosis* is easily internalized followed by *C. parapsilosis* and by *C. albicans* (Figure 8). The percentages of internalization were slightly lower than those observed with FCM, probably due to the fact that the number of macrophages counted was 10 times lower than those assessed by flow cytometry.

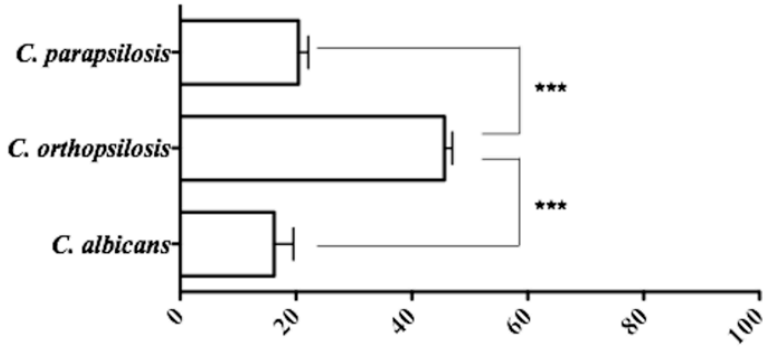

Figure 8: Quantification of macrophage *Candida spp*. phagocytosis by fluorescence microscopy. Macrophages were incubated with Sytox green stained yeast cells for 30 minutes, at 37°C and 5% CO2. After incubation macrophages and associated yeasts were incubated with Propidium iodide (PI) for 5 minutes at RT. Cells were then analyzed by fluorescence microscopy, images taken and the number of macrophages with internalized yeast counted manually using ImageJ cell counter software. Each bar is the average of two experiments ± standard error.

4. CONCLUSION

In conclusion, we proposed a new, fast and simple method to study the interaction between phagocytes and *Candida spp.* yeast cells and to quantify phagocytosis. The method is based on the quenching effect of PI over Sytox Green fluorescence and allows a clear distinction between internalized and non-internalized yeast cells with the advantage of maintaining Sytox Green fluorescence upon internalization of the yeast by phagocytic cells. Using only these two fluorochromes we could accurately distinguish and quantify various parameters simultaneously, in a single infection experiment: i) phagocyte survival and ii) the association of phagocytes to fungal cells: phagocytes that have only internalized yeast cells, phagocytes that have only attached yeast cells, and phagocytes that have both, internalized and attached yeast cells. In addition, this method proved to be efficient for evaluation of differences in the phagocytosis of distinct *Candida* species. Although the comparative virulence among different *Candida* species is not entirely dependent on its recognition and internalization by phagocytes, the innate immune system plays an important role in controlling *Candida* infections, and this technique may help to elucidate some PAMPs characteristics that may be involved in the virulence process. Contrary to microscopy, which may be too cumbersome for analyzing a large number of strains, this method allows the high-throughput screening of yeast strains from different species, including mutants. Such studies would significantly enhance our understanding of the molecular mechanisms involved in the interaction between yeasts and host phagocytes.

Supplementary data to this chapter can be found online at: https://www.dropbox.com/s/vlg3beikjde18qq/Movie%20S1.avi?dl=0

Movie S1: Video microscopy of the confocal Z-stack microscopy sections of J774A.1 macrophage yeast phagocytosis, showing that the extracellular yeast cells are PI stained while the phagocytized yeast remain Sytox Green fluorescent even after 30 min of incubation (AVI).

ACKNOWLEDGMENTS

We thank Professor Paula Sampaio from IBMC (Institute for Molecular and Cell Biology) for helping with the confocal microscopy.

REFERENCES

1. **Romani, L.**, Immunity to fungal infections. Nat Rev Immunol, 2011. **11**(4): p. 275-88.
2. **Lewis, L.E., Bain, J.M., Lowes, C., Gillespie, C., Rudkin, F.M., Gow, N.A., and Erwig, L.P.**, Stage specific assessment of *Candida albicans* phagocytosis by macrophages identifies cell wall composition and morphogenesis as key determinants. PLoS Pathog, 2012. **8**(3): p. e1002578.
3. **Chaffin, W.L., Lopez-Ribot, J.L., Casanova, M., Gozalbo, D., and Martinez, J.P.**, Cell wall and secreted proteins of *Candida albicans*: identification, function, and expression. Microbiol Mol Biol Rev, 1998. **62**(1): p. 130-80.
4. **Dementhon, K., El-Kirat-Chatel, S., and Noel, T.**, Development of an in vitro model for the multi-parametric quantification of the cellular interactions between *Candida* yeasts and phagocytes. PLoS One, 2012. **7**(3): p. e32621.
5. **Hampton, M.B. and Winterbourn, C.C.**, Methods for quantifying phagocytosis and bacterial killing by human neutrophils. J Immunol Methods, 1999. **232**(1-2): p. 15-22.
6. **Lehmann, A.K., Sornes, S., and Halstensen, A.**, Phagocytosis: measurement by flow cytometry. J Immunol Methods, 2000. **243**(1-2): p. 229-42.
7. **Linden, J.R., Kunkel, D., Laforce-Nesbitt, S.S., and Bliss, J.M.**, The role of galectin-3 in phagocytosis of *Candida albicans* and *Candida parapsilosis* by human neutrophils. Cell Microbiol, 2013. **15**(7): p. 1127-42.
8. **Busetto, S., Trevisan, E., Patriarca, P., and Menegazzi, R.**, A single-step, sensitive flow cytofluorometric assay for the simultaneous assessment of membrane-bound and ingested *Candida albicans* in phagocytosing neutrophils. Cytometry A, 2004. **58**(2): p. 201-6.
9. **Warolin, J., Essmann, M., and Larsen, B.**, Flow cytometry of *Candida albicans* for investigations of surface marker expression and phagocytosis. Ann Clin Lab Sci, 2005. **35**(3): p. 302-11.
10. **Hoch, H.C., Galvani, C.D., Szarowski, D.H., and Turner, J.N.**, Two new fluorescent dyes applicable for visualization of fungal cell walls. Mycologia, 2005. **97**(3): p. 580-8.
11. **Sarazin, A., Poulain, D., and Jouault, T.**, In vitro pro- and anti-inflammatory responses to viable *Candida albicans* yeasts by a murine macrophage cell line. Med Mycol, 2010. **48**(7): p. 912-21.

12. **Murciano, C., Yanez, A., Gil, M.L., and Gozalbo, D.**, Both viable and killed *Candida albicans* cells induce in vitro production of TNF-alpha and IFN-gamma in murine cells through a TLR2-dependent signalling. Eur Cytokine Netw, 2007. **18**(1): p. 38-43.
13. **Sheth, C.C., Hall, R., Lewis, L., Brown, A.J., Odds, F.C., Erwig, L.P., and Gow, N.A.**, Glycosylation status of the *C. albicans* cell wall affects the efficiency of neutrophil phagocytosis and killing but not cytokine signaling. Med Mycol, 2011. **49**(5): p. 513-24.
14. **Mora-Montes, H.M., McKenzie, C., Bain, J.M., Lewis, L.E., Erwig, L.P., and Gow, N.A.**, Interactions between macrophages and cell wall oligosaccharides of *Candida albicans*. Methods Mol Biol, 2012. **845**: p. 247-60.
15. **McKenzie, C.G., Koser, U., Lewis, L.E., Bain, J.M., Mora-Montes, H.M., Barker, R.N., Gow, N.A., and Erwig, L.P.**, Contribution of *Candida albicans* cell wall components to recognition by and escape from murine macrophages. Infect Immun, 2010. **78**(4): p. 1650-8.
16. **Kuhn, D.M. and Vyas, V.K.**, The *Candida glabrata* adhesin Epa1p causes adhesion, phagocytosis, and cytokine secretion by innate immune cells. FEMS Yeast Res, 2012. **12**(4): p. 398-414.
17. **Keppler-Ross, S., Douglas, L., Konopka, J.B., and Dean, N.**, Recognition of yeast by murine macrophages requires mannan but not glucan. Eukaryot Cell, 2010. **9**(11): p. 1776-87.
18. **de Groot, P.W., Kraneveld, E.A., Yin, Q.Y., Dekker, H.L., Gross, U., Crielaard, W., de Koster, C.G., Bader, O., Klis, F.M., and Weig, M.**, The cell wall of the human pathogen *Candida glabrata*: differential incorporation of novel adhesin-like wall proteins. Eukaryot Cell, 2008. **7**(11): p. 1951-64.
19. **Destin, K.G., Linden, J.R., Laforce-Nesbitt, S.S., and Bliss, J.M.**, Oxidative burst and phagocytosis of neonatal neutrophils confronting *Candida albicans* and *Candida parapsilosis*. Early Hum Dev, 2009. **85**(8): p. 531-5.
20. **Wellington, M., Bliss, J.M., and Haidaris, C.G.**, Enhanced phagocytosis of *Candida* species mediated by opsonization with a recombinant human antibody single-chain variable fragment. Infect Immun, 2003. **71**(12): p. 7228-31.
21. **Sabino, R., Sampaio, P., Carneiro, C., Rosado, L., and Pais, C.**, Isolates from hospital environments are the most virulent of the *Candida parapsilosis* complex. BMC Microbiol, 2011. **11**: p. 180.

CHAPTER IV:

DODAB:monoolein as protein delivery systems: the role of monoolein

DODAB:monoolein as protein delivery systems: the role of monoolein

Catarina Carneiro[1], Alexandra Correia[2], Tânia Lima[1], Manuel Vilanova[2,3], Célia Pais[1], Andreia C, Gomes[1,5], M. Elisabete C.D. Real Oliveira[4,5], Paula Sampaio[1*]

(manuscript in preparation)

[1]Centre of Molecular and Environmental Biology (CBMA), Department of Biology, University of Minho, 4710-057 Braga, Portugal

[2] IBMC-Instituto de Biologia Molecular e Celular, Rua do Campo Alegre 823, Porto, Portugal

[3] Instituto de Ciências Biomédicas de Abel Salazar (ICBAS), Universidade do Porto, Rua de Jorge Viterbo Ferreira n.º 228, 4050-313 Porto, Portugal

[4]Centre of Physics (CFUM) University of Minho, Campus of Gualtar, 4710-057 Braga, Portugal

[5]NanoDelivery I&D in Biotechnology, Biology Department, Campus of Gualtar, 4710-057 Braga, Portugal

ABSTRACT

The introduction of a helper lipid into cationic liposomes formulation is essential for liposomal membrane stabilization and for minimization of cationic lipids cytotoxicity associated. The purpose of this study was to investigate the role of monooleoyl-rac-glycerol (monoolein, MO) content in DODAB:MO liposomes. The introduction of MO leads to an increase in the mean size and in PDI values, except for DODAB:MO (1:2) liposomes were the liposomes exhibited a more homogenous population with a mean size of 139 ± 14.0 nm. In addition, an increase in MO content decreased the cytotoxic effect associated with DODAB and improved internalization efficiency. Accordingly, we demonstrated that DODAB:MO liposomes loaded with BSA (BSA LNPs) benefit with an increase in MO molar fraction in terms of colloidal stability, cellular viability and uptake. In addition, incorporation of BSA into DODAB:MO liposomes leads to a reorganization of the liposomal bilayer, forming rigid rich DODAB domains separated from fluids rich MO domains. In terms of macrophage uptake both empty liposomes and BSA LNPs were internalized by endocytosis and BSA uptake per cell was increased upon BSA loading in DODAB:MO liposomes. Finally, and according with the previous characteristics we choose DODAB:MO (1:2) and demonstrated its adjuvant ability in activating antigen presenting cells by enhancing the expression of three activation markers, CD86 and CD80 co-stimulatory molecules and MHC class II molecules.

1. INTRODUCTION

Cationic liposomes have been used extensively as drug and vaccine delivery systems [1, 2]. The cationic surfactant dioctadecyldimethylammonium bromide (DODAB) is a synthetic amphiphilic molecule composed of a hydrophilic positively charged dimethylammonium group (head) attached to two hydrophobic 18-carbon alkyl chains (tail). In aqueous buffers, DODAB molecules self-assemble into closed liposomal vesicular bilayers [3]. Being a cationic molecule, DODAB induces dose-dependent cytotoxicity requiring dose minimization for administration *in vivo*. The introduction of a helper lipid to formulate drugs or vaccines at reduced charged lipid doses is essential for minimization of the cytotoxic effect associated with cationic lipids [4-6]. Moreover, in salt solutions, such as phosphate buffer saline (PBS), DODAB liposomes can instantaneously aggregate due to insufficient electrostatic repulsion forces [7].

Monooleoyl-rac-glycerol (monoolein, MO) was first proposed as helper lipid in a DODAB liposomal formulation for use as non-viral transfection system [3]. MO has the ability to exist in several different phases, with one-, two- and three- dimensional periodicity, such as the lamellar (L_α), inverted micelles (L_2), hexagonal (H_2), and bicontinuous cubic phases, under rather easily accessible temperature and pressure conditions [8, 9].

Phase scan imaging shows that DODAB liposomal formulations benefit from the structural richness of MO content, revealing that with higher MO proportion are dominated by densely packed cubic-oriented structures [10]. This enhancement in the structural complexity of DODAB liposomes can be used for tailored design of protein delivery systems.

Encapsulation of macromolecules, proteins and other drugs into developed systems is of great interest for pharmaceutics and biotechnology due to its capability to use such systems as micro- and nanocarriers, not only for controlled drug delivery but also for use as adjuvants in vaccination strategies [11, 12]. Subunit proteins or synthetic peptides are normally used for the development of immunoprotective strategies. Unfortunately, their effective implementation is limited, due to their poor immunogenicity, when administered without a carrier for the targeted delivery of antigens to immune competent cells [13, 14]. Therefore, understanding the behavior of the empty delivery system as well as the interaction between the antigen and the delivery system is highly necessary, since this would allow for optimization of the efficacy, stability and safety of new formulations.

In this study, we investigate the role of MO in the improvement of DODAB liposomes as antigen delivery systems. Bovine serum albumin (BSA) was used as model protein in

order to assess the effect of MO on the colloidal stability of the liposomal BSA loaded nanoparticles (BSA LNPs), cell viability and internalization efficiency. Finally, we validated the use of DODAB:MO liposomes as carriers with the ability to enhance antigen activation of antigen presenting cells (APCs).

2. MATERIALS AND METHODS

2.1. Materials

Dioctadecyldimethylammonium bromide (DODAB) was purchased from Tokyo Kasei (Japan). 1-monooleoyl-rac-glycerol (MO), Hanks' balanced salt solution (HBSS), Trypan Blue, BSA-FITC conjugate, BSA were supplied by Sigma–Aldrich (St. Louis, MO, USA). Dulbecco's Modified Eagle's medium (DMEM) was supplemented with 10% heat-inactivated fetal bovine serum (FBS) (Valbiotech), 2 mM L-glutamine, 1 mM sodium pyruvate, and 10 mM HEPES (all from Sigma–Aldrich (St. Louis, MO, USA). Wheat Germ Agglutinin (WGA) Alexa Fluor® 633 Conjugate (λem=647nm) was provided by Alfagene (Carcavelos, Portugal), Rhodamine DHPE (Lissamine™ λem=580nm) and ethanol (high spectral purity) was purchased from Uvasol (Leicester, United Kingdom). Dulbecco's Modified Eagle's Medium (DMEM) was supplemented with 10% heat-inactivated fetal bovine serum (FBS), 2 mM L-glutamine, (all from Sigma-Aldrich), HEPES-Buffer solution pH=7.5 supplied by VWR Internacional (Radnor, PA, USA).

2.2. Extraction of complex fungal antigens from cell wall surface of *C. albicans*

C. albicans strain SC5314, kindly provided by Prof. Joachim Morschhauser (Wurzburg, Germany), was obtained from a 2 day YPD agar (2% D-glucose, 1% Difco yeast extract, 2% peptone and 2% agar) (w/v) culture incubated at 26 °C. The following procedures used for antigen extraction were all performed in a sterile environment using apyrogenic solutions. The fungal antigens were released from whole intact cells by DTT treatment as described previously [15].

2.3. Preparation and characterization of liposomes

2.3.1 Preparation of Liposomes by the Lipid-Film Method

DODAB:MO based liposomes were prepared using the lipid-film hydration method [16]. Five different MO molar fractions (χMO) were used: 0.2 (DOBAB:MO molar ratio 4:1), 0.330 (DOBAB:MO molar ratio 2:1), 0.5 (DOBAB:MO molar ratio 1:1), 0.66

(DOBAB:MO molar ratio 1:2) and 0.8 (DOBAB:MO molar ratio 1:4). The χMO is given by the following eq. [10]:

$$\chi \mathrm{MO} = \frac{[\mathrm{MO}]}{[\mathrm{DODAB}]+[\mathrm{MO}]}$$

Briefly, DODAB and MO were dissolved in ethanol and mixed in a round-bottom flask, followed by removal of the solvent by rotary evaporation at 55 ºC. Liposomes formed after hydration of the lipid film with 25 mM HEPES buffer pH 7.5 at 55 ºC as previously described [15]. The dispersion was then placed in a bath sonicator during 2 min. The liposomal stock dispersion was prepared at a 4 mM total lipid concentration. For liposomal BSA loaded nanoparticles (BSA LNPs) formation (protein to lipid ratio of 0,376 mol/mol) equal volumes of liposomal stock dispersion and 0.75mM BSA stock solution were co-incubated at 55 ºC for 1 h. Empty liposomes were always used at 2 mM, after addition of equal volumes of 25 mM HEPES buffer pH 7.5 to the liposomal stock dispersion. For the studies with the CWSP, the same preparation method was used and similar concentrations of antigen and empty liposomes were used (protein to lipid ratio of 0,376 mol/mol).

2.3.2 **Size, Polydispersity Index and ζ -Potential**

The ζ-potential and the mean size of all formulations were determined by dynamic light scattering (DLS) at 25 ºC with a Malvern ZetaSizer Nano ZS particle analyzer. The Malvern Dispersion Technology Software (DTS) was used with multiple narrow mode (high-resolution) data processing, and mean size (nm), polydispersity index (PDI) and error values were determined. The liposomes surface charge was measured indirectly by ζ-potential analysis, using electrophoretic light scattering (ELS) at 25 ºC. DTS with monomodal mode data processing was used to determine average ζ-potential (mV) and error values. All characterization was undertaken in triplicate.

2.3.3 **Differential Scanning Calorimetry (DSC)**

DSC was used to determine the gel-to-liquid crystalline phase transition temperature (T_m) of the liposomes or liposomal nanoparticles in suspension. These measurements were performed on a VP-DSC (MicroCal, Northampton, MA) calorimeter equipped with 0.542 mL twin cells for the reference and sample solutions. The formulations were prepared as

described in section 2.3.1 and total lipid concentration was maintained at 2 mM for all measurements, which were performed at the scan rate of 1 °C/min and temperature range of 5−55°C. The T_m was determined as the temperature at which the excess heat capacity, Cp, was at its maximum. The change in enthalpy (ΔH) was determined by integrating the area under the baseline-corrected Cp curve obtained for each sample.

2.3.4 Cryo-SEM analysis

The morphology of the liposomes was evaluated by cryogenic scanning electron microscopy (cryo-SEM) using a High resolution Scanning Electron Microscope with X- Ray Microanalysis (JEOL JSM 6301F/ Oxford INCA Energy 350/ Gatan Alto 2500). Aliquots of 4 µl of empty liposomes (total lipid concentration of 2 mM) were placed into carbon film grids, rapidly cooled (plunging into sub-cooled nitrogen – slush nitrogen) and transferred under vacuum to the cold stage of the preparation chamber. The samples were fractured, sublimated ('etched') for 120 seconds at -90 °C and coated with Au/Pd by sputtering for 40 seconds. Samples were transferred into the SEM chamber and studied at a temperature of -150°C. Micrographs were captured at an acceleration voltage of 15 kV and a working distance of 15 mm with a secondary electron in the lens detector.

2.4. *"In vitro"* analyses

The *in vitro* studies were performed using the murine macrophage cell line RAW 264.7. The cell line was maintained in complete medium, DMEM supplemented with 10% FBS, 2 mM L-glutamine, 1 mM sodium pyruvate, and 10 mM HEPES, at 37°C in a 5% CO_2 atmosphere. After confluent growth, macrophage cells were recovered, washed and re-suspended in complete medium to the desired cell concentration.

2.4.1 Cytotoxicity analysis

RAW 264.7 macrophages were plated onto 96-well tissue culture plates (Falcon) at $1x10^5$ cells/well and incubated to adhere overnight at 37ºC in a humidified atmosphere of 5 % CO_2. Three different concentrations of empty liposomes (40 µM, 80 µM or 160 µM) were evaluated. In addition, using the same protein to lipid ratio (0.376 mol/mol), three different concentrations of BSA LNPs were used (15:40; 30:80; 60:160, protein:lipid, µM: µM).

Cell viability was assessed using 3-[4,5-dimethylthiazol-2-yl]-2,5-diphenyltetrazolium bromide (MTT) assay and Lactate Dehydrogenase (LDH) assay after 24 h of incubation, according to the manufacturer's instructions.

MTT is a water-soluble tetrazolium salt, which is converted to an insoluble purple formazan by cleavage of the tetrazolium ring by succinate dehydrogenase within the mitochondria. Enzymatic activity was quantified after solubilization of MTT formazan with DMSO:ethanol (1:1) solution and absorbance measured at 570 nm. Untreated cells were used as a control of viability (100%) and cells treated with DMEM:DMSO (4:1) as a control of cytotoxicity (100%) as previously described [17].

The membrane cell integrity was analyzed using the LDH leakage assay, quantified by measuring the lactate dehydrogenase activity in the extracellular medium as previously described [18]. Briefly, the extracellular enzyme activity was assessed at 30 ºC on a microplate reader (Spectra Max 340PC), by following for 3 min, the rate of conversion of reduced nicotinamide adenine dinucleotide (0.28 mM NADH) to oxidized nicotinamide adenine dinucleotide (NAD+), at 340 nm. Pyruvate 0.32 mM (in phosphate buffer, pH 7.4) was used as substrate. Data were expressed as percentage of the control (cells without treatment, 100% cellular viability) from at least two independent experiments.

2.4.2 **Cellular Uptake**

Cellular uptake of liposomes, at 37 °C or at 4 ºC (at 4 ºC cells were also incubated with 10 mM of sodium azide to the medium) was quantified by flow cytometry. For analyses of empty liposomes internalization Rhodamine DHPE (at a molar ratio of 1:200) was incorporated into the DODAB:MO liposomes during the preparation phase. RAW 264.7 cells were seeded into 24-multiwell plates at a density of 5×10^5 cells per well in complete cell culture medium. Immediately before liposome addition, cells were washed and medium replaced. Cells were incubated with Rhodamine DHPE labeled empty liposomes (final concentration of 40 μM) or BSA-FITC LNPs (15:40 protein:lipid (μM: μM)). After 40 min incubation, cells were placed on ice and washed with PBS 1X and scrapped in FCM Buffer (2%FBS, 10 mM sodium azide in 25% PBS 1X). Before analysis, 0,6% of Trypan Blue (0.36 ng/ml) was added to the samples in order to quench the fluorescence of non-internalized liposomes. A control without cells, only with the formulations alone, was analyzed for validation of Trypan Blue quenching.

For confocal microscopy analyses, Rhodamine DHPE (at a molar ratio of 1:200) was incorporated into DODAB:MO liposomes during the preparation phase. Macrophages were plated in a microscopy chamber plate (Ibidi) at 3×10^5 cells/well and left to adhere overnight at 37 ºC in a humidified atmosphere of 5% CO_2. Immediately prior to incubation with labeled liposomes, RAW 264.7 macrophages were labeled with Wheat Germ Agglutinin Alexa Fluor® 633 Conjugate (2.5 μg/ml) for 10 min and then washed twice with HBSS. The microscopy chamber plate was then placed in the integrated chamber (37 ºC, 5% CO_2) of the LSM 780 Carl Zeiss Microscope and 8 μl of empty labeled liposomes (total lipid concentration of 888μg /ml) were added to the adhered macrophages. A z-stack image after 40 min were obtained and images were analyzed using ZEN 2012 lite software (ZEISS).

2.4.3 **ROS production**

RAW 264.7 macrophages were plated onto 24-well tissue culture plates (Falcon) at 5×10^5 cells/well, incubated with empty liposomes (final concentration 80 μM) during 1h. Using Superoxide Detection Kit from Enzo Life Sciences (NY, USA) superoxide production was assessed in live cells using flow cytometry according to manufacture instructions.

2.5. Stimulation of Bone Marrow Dendritic Cells (BMDCs)

Bone marrow cells were collected from femurs and tibias of BALB/c mice by flushing with cold RPMI 1640 (Sigma). Cells (1×106/mL) were cultured in 6-well plates in RPMI medium supplemented with 15% (v/v) J558-cell supernatant, 10% FBS (PAA), penicillin (100 U.I./mL)-streptomycin (100 μg/ml) (Sigma), and L- Glutamine (2 mM) (Sigma) and incubated at 37 ºC and 5% CO_2. Half of the medium was renewed every two days. At day 6, BMDCs were detached and distributed in 96-well round bottom plates adjusted at a concentration of 2×10^5 cells/well in supplemented RPMI medium. Immediately after being seeded, cells were stimulated with: empty liposomes (final concentration 160 μM); BSA (final concentration 160 μM); BSA LNPs (final concentration 60:160 protein: lipid molar ratio (μM: μM)); fungal antigens (at the same final concentration used for free BSA); fungal antigens LNPs (at the same final concentration used for BSA LNPs). LPS (1μg/ml) (Sigma) and unstimulated cells were used as positive and negative controls of activation, respectively. For the assessment of cell surface markers, after stimulation the BMDCs were collected from the culture plates, washed twice in Hanks's Balanced Salt

Solution (Sigma) and incubated with specific cell surface antibodies. The following monoclonal antibodies (mAbs), at previously determined optimal dilutions, for immunofluorescence cytometry [19] were used: fluorescein isothiocyanate (FITC) hamster anti-mouse CD11c (HL3), PE anti-mouse CD80 (B7-1) (16-10A1); PE anti-mouse CD86 (B7-2) (GL1); PE anti-mouse I-Ad/I-Ed-MHC class II (clone 2G9); all from BD (Biosciences Pharmingen, San Diego, CA). The analyzed cell samples were always pre-incubated with anti-FcγR mAb before the antibody incubation to prevent non-specific antibody binding. All cytometric measurements were performed in an EPICS XL flow cytometer using the EXPO32ADC software (Beckman Coulter). The collected data files were converted using FACS CONVERT, v1.0 (Becton Dickinson) and analyzed using CELL QUEST software, v3.2.1f1 (Becton Dickinson).

2.6. Statistical analyses

Data were analyzed using analysis of variance (ANOVA) followed by the Bonferroni test to compare the mean values of different groups, using GraphPad Prism 5 software (GraphPad Software, Inc., La Jolla, CA). Unless otherwise stated, results shown are from three independent experiments with three replicates. Differences were considered significant when the p value was less than 0.05.

3. RESULTS AND DISCUSSION

3.1. The effect of χMO in DODAB:MO empty liposomes

3.1.1 Characterization of empty liposomes

The physicochemical properties of DODAB liposomes after MO incorporation at different molar fractions were study by dynamic light scattering (DLS), electrophoretic light scattering (ELS) and differential scanning calorimetry (DSC). Five different DODAB:MO liposome formulations were used, DOBAB:MO molar ratios 4:1, 2:1, 1:1, 1:2 and 1:4. The average size of these liposomes, prepared by the thin film method followed by a sonication step was relatively small, all formulations presented sizes smaller than 500 nm, except DODAB:MO 1:4 liposomes, that presented a mean size of 2880 ± 699 nm, a significant increase ($P<0.0001$) in comparison with all other molar ratios (Figure 1). The values for polydispersity index (PDI) ranged from 1.0 ± 0.01 for DODAB:MO 1:4 liposomes to 0.2 ± 0.06 relatively for DODAB:MO 1:2 liposomes (Figure 1).

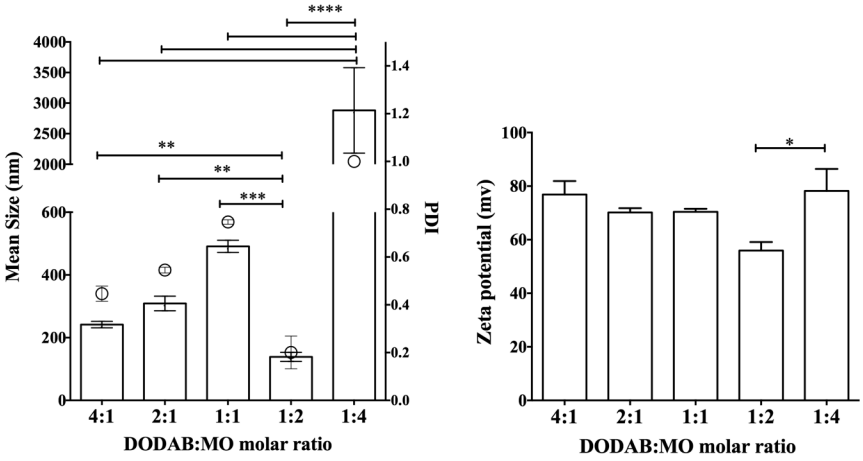

Figure 1: Effect of χMO in DODAB:MO liposomes mean size (bars), PDI (spherical symbols) and ζ-potential (bars). Significant differences in the mean size and in the ζ-potential between the different ratios are represented above the lines by: *P<0.05, **P<0.01 and ***P<0.001. All values shown are the average values from three independent experiments ± SD

All MO-based liposomes tested have a high net positive charge (> +55mV) clearly resulting from the cationic nature of DODAB. DODAB:MO (1:2) liposomes presented the lowest surface charge (+55.9 ± 3.2 mV) and DODAB:MO (1:4) liposomes presenting the highest surface charge (+78.2 ± 8.2 mV) (Figure 1).

In previous studies, we established that, for χMO < 0.5, MO is distributed in the lamellar phase of DODAB and bilayer-based structures dominate, whereas for χMO > 0.5, DODAB and MO self-assembled into lamellar and bicontinuous inverted cubic mesophases [10, 20]. This implies a lipid phase separation and could explain the high ζ-potential values observed for DODAB:MO (1:4) molar ratio.

Overall, an increase in the amount of MO until DODAB:MO (1:1) leads to an increase in the mean size and in PDI values, except for DODAB:MO (1:2) liposomes were the liposomes exhibited a more homogenous population with a mean size of 139 ± 14.0 nm.

3.1.2 The effect of χMO in DODAB:MO liposomes cytotoxicity, uptake and ROS production by macrophages.

One of the main concerns in the design of any cellular delivery system is their associated cytotoxicity. In this sense, the effect of MO content on the metabolic activity of RAW 264.7 cells after being exposed to three different concentrations of each of the five DODAB:MO liposome formulations, was evaluated using the MTT assay, while the impact on membrane integrity was evaluated using the LDH assay, after 24 h of co-incubation.

As represented in Figure 2, a slight decrease in cell metabolic activity is observed with increasing concentration of liposomes, particularly for the formulations where MO was present at lower percentages (<50%). However, DODAB:MO (1:2) and DODAB:MO (1:4) liposomes were well tolerated at all concentrations, showing viability values above 95 %. Cells treated with 160 μM DODAB:MO (4:1) liposomes showed only 73.9 ± 14.9 % of viability, significantly lower than values observed with all other DODAB:MO molar ratios ($P<0.01$, Figure 2). However, the membrane integrity was maintained when cells were incubation with liposomes with all other molar ratios, which confirmed the capacity of MO to lower the cytotoxicity associated with DODAB [21].

Phagocytes generate ROS by using superoxide-generating NADPH oxidase (NOX) family proteins, which play pivotal roles in host defense against bacterial and fungal pathogens [22]. After 1 hour of incubation, ROS was evident in macrophages incubated with all liposomal formulations, but the percentage of ROS producing cells was not significantly different between the liposomal preparations, ranged from 44 ± 0.8% for DODAB:MO (1:2) liposomes to 59 ± 1.5% for DODAB:MO (4:1) liposomes (Figure 3). Only with incubation with DODAB:MO (1:2) the percentage of ROS producing cells was slightly lower ($P<0.05$)

Of note is the fact that this ROS production does not seem to affect cell viability although it can be considered a marker of cell activation.

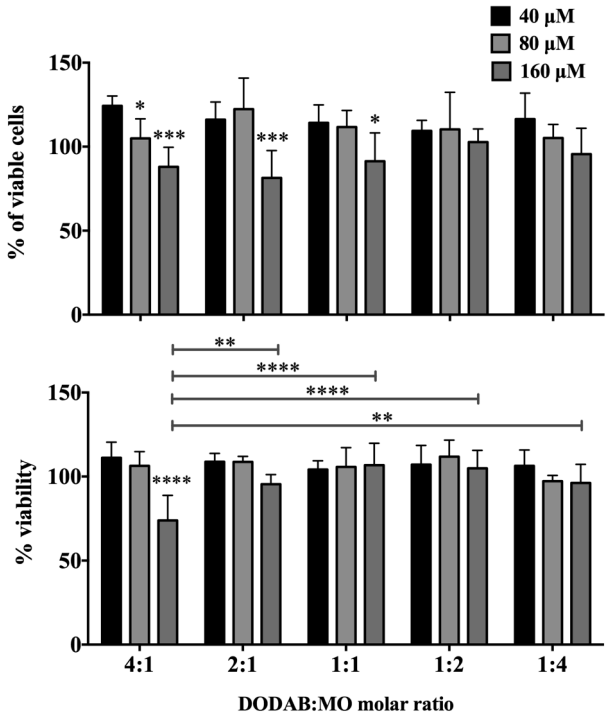

Figure 2: Viability of RAW 264.7 cells after 24 h incubation with DODAB:MO liposomes at different χMO. Viability was assessed using the MTT (in the top) and LDH (in the bottom) assay after 24 h incubation. The liposomes were diluted in the culture medium at the final concentrations of 40, 80 and 160 µM. Bars indicate the mean ± SD of two independent experiments. Significant differences between the different molar ratios are represented by (*) above the line, differences with the former concentration are represented by (*) above the bar: (*P<0.5, **P < 0.01, ***P < 0.001, ****P< 0.0001)

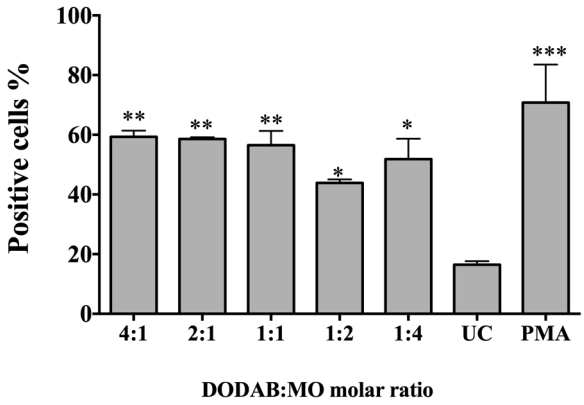

Figure 3: Percentage of cells producing ROS after 1 h incubation with DODAB:MO liposomes at different χMO. The liposomes were diluted in cell culture medium at a final concentration of 80 µM. Bars indicate the mean ± SD of two independent experiments. UC: unstimulated cells. Significant differences between the different molar ratios and control-unstimulated cells are represented by (*) above the bar: (*P<0.5, **P<0.01, ***P <0.001).

In order to elucidate the effect of MO in cellular uptake, cells were incubated with Rhodamine DHPE labeled empty liposomes at either 37 °C or 4 °C. Incubations at 4 ºC were preformed in the presence of sodium azide in medium (which helps inhibition of the energy-dependent uptake by endocytosis). At 4 ºC, and comparing with the results observed at 37 ºC, a decrease in intracellular fluorescent intensity was observed for all DODAB:MO molar ratios tested (Figure 4A), which indicates that the uptake DODAB:MO liposomes is energy-dependent. The fact that cationic liposomes are taken up by active endocytosis has been reported in other studies [23-25]. At a physiological temperature, the ability of cellular uptake of DODAB:MO liposomes was dependent of the MO content. As shown in Figure 4A, the percentage of positive cells was higher for DODAB:MO (1:1) and (1:2) ($P>0.01$) in comparison to the other molar ratios. The amount of internalized liposomes per cell (MFI) was higher for DODAB:MO (1:1) ($P> 0.0001$) in comparison to the other molar ratios (Figure 4A).

As shown in Figure 4A, at 37 ºC the percentage of fluorescently labeled cells (positive cells) tends to increase with increasing the amount of MO. The percentage of positive cells was higher for DODAB:MO (1:1) and (1:2) ($P>0.01$) in comparison with the DODAB:MO (4:1) and (2:1). Additionally, the amount of internalized liposomes per cell (MFI) increased from DODAB:MO (4:1) to (1:1), diminishing again from (1:2) to (1:4). This result indicates that at a physiological temperature, increasing the MO content favors cellular uptake of DODAB:MO liposomes, at least until molar ratio of 1:2.

In order to confirm endocytosis, internalization of DODAB:MO liposomes was visualized by confocal microscopy (Figure 4B). DODAB:MO (1:2) liposomes were chosen as evidence, since according to their good colloidal stability, efficient internalization and lack of cytotoxic effects, liposomes with this DODAB:MO molar ratio are suitable for the construction of an antigen delivery system. After 40 min of incubation, most of the Rhodamine (Rho)-labeled liposomes were seen accumulated throughout the cytoplasm, the transport endosome region and in the Golgi area next to the nucleus, which itself does not reveal any fluorescence signal (Figure 4B). Superimposition of Rho with Alexa Fluor 633 fluorescence was observed and localized liposomes within membrane-rich regions, i.e., in the cytoplasmic area and in the cellular extensions as expected in an endocytic process [26]. Figure 4C displays the view at the mid-point of cell thickness confirming that most of the Rho fluorescence is concentrated intracellularly in certain areas. Figure 4D Cryo-SEM micrographs showed that DODAB:MO (1:2) liposomes are spherical smaller-sized liposomes.

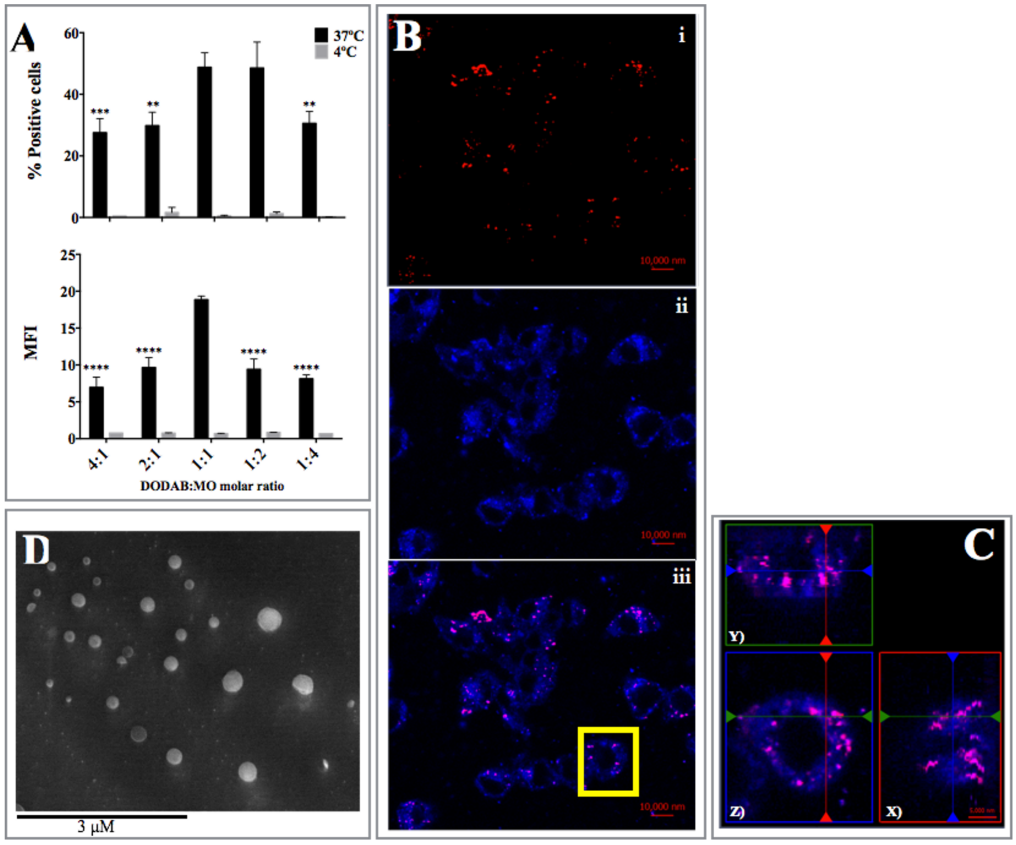

Figure 4: Cellular uptake of DODAB:MO liposomes after 40 min of incubation. **A)** Percentage of cellular uptake (in the top) and the mean fluorescence intensity (MFI) (in the bottom), at 37ºC and 4ºC, at different χMO **B)** Confocal images of Rho-DODAB:MO (1:2) liposomes cellular uptake at 37ºC: i. Rhodamine fluorescence ii. Alexa Fluor 633 fluorescence and iii. superimposition of Rhodamine and Alexa Fluor 633 fluorescence. **C)** A mid-point thickness view (X68, Y44, Z24) of the cell, indicated by a yellow rectangle in (Biii), (z). Z-axis rotations of a single transverse slice through two sections of the cell: view in the x-0-z plane (x) and view in the y-0-z plane (y). **D)** Cryo-SEM Representative image of DODAB:MO (1:2) liposomes morphology. Bars indicate the mean ± SD of two independent experiments. Significant differences between the different molar ratios and control-unstimulated cells are represent by (*) above the bar: (*P<0.5, **P<0.01, ***P<0.001, ****P<0.0001)

3.2. The effect of χMO in protein loaded DODAB:MO liposomes

3.2.1 Characterization of BSA LNPs

Cationic liposomes have the ability to adsorb oppositely charged antigens and to encapsulate hydrophobic and hydrophilic antigens due to their amphiphilic nature [21]. The model protein chosen in this study was Bovine Serum Albumin (BSA), a medium-weight protein (MW = 66 kDa) consisting of 580 amino acid residues. BSA is negatively charged with an isoelectric point of 5.3 at pH 7.4 [27]. The binding mode of the lipid–protein interaction can be determined from the effect of the protein on the gel-to-liquid crystalline lipid phase transition [28]. Dynamic light scattering (DLS), electrophoretic light scattering

(ELS) and differential scanning calorimetry (DSC) were used in order to study the interaction of BSA with the DODAB:MO liposomes with different MO content, after BSA incorporation. Figure 5 shows the mean size, PDI and the surface charge of DODAB:MO liposomes in the presence of BSA (BSA LNPs). Curiously, the adsorption of BSA to all DODAB:MO liposomes made no significant difference to the ζ-potential of the empty liposomes (Figure 5). Regarding BSA LNPs mean sizes and PDI, although these values decreased in comparison with empty liposomes, the decreases were only significant for 1:4 BSA LNPs ($P<0.0001$). In fact, for DODAB:MO (1:4) liposomes the incorporation of BSA enhanced its colloidal stability, since both mean size (< 350 nm) and PDI (<0.4) drastically decrease. With the incorporation of BSA, the effect of the MO in increasing the mean size was no longer observed.

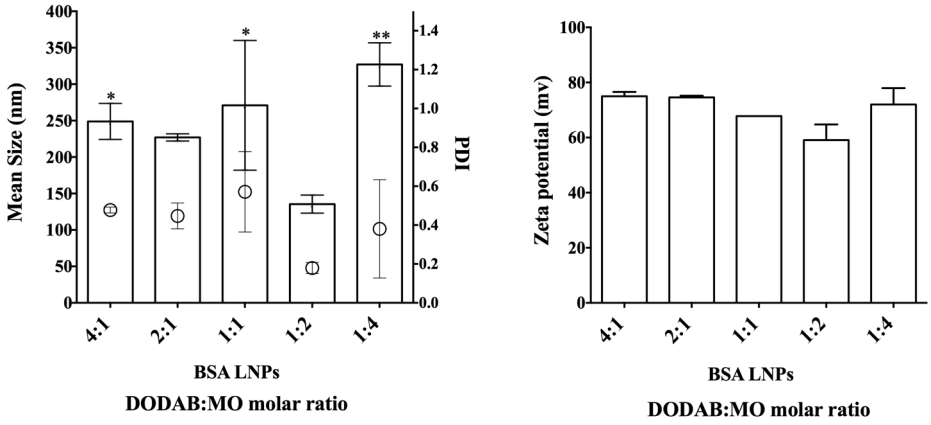

Figure 5: Effect of χMO in BSA LNPs mean size (bars), PDI (spherical symbols) and ζ-potential (bars). Significant differences in the mean size in comparison with DODAB:MO (1:2) molar ratio are represented by: *P<0.05, **P<0.01. All values shown are the average values from three independent experiments ± SD.

DODAB:MO (1:2) BSA LNPs, which compromises the most promising molar ratio so far, exhibited the lowest mean size (135 ± 12.4 nm) and the lowest PDI value (0.18 ± 0.03).

MO dispersions present no melting transition since they do not contain bilayer aggregates and are instead two-phase dispersions of a bicontinuous cubic phase in a very diluted solution [29]. It is well known that DODAB presents a pre-transition temperature (T_p) due to the tilting of the DODAB chains prior to the melting temperature which occurs at 44.4 °C, when the gel-phase dominated by ordered alkyl chain conformations melts into a high-temperature fluid-phase characterized by disordered alkyl chain conformations [10, 20, 30].

The effect of MO on the thermal behavior of the mixture of DODAB:MO was previously described using DSC [10]. The gel-to-liquid crystalline phase transition is characterized by a number of thermodynamic parameters, such as the phase transition temperature (T_m) and the enthalpy of the calorimetric event (ΔH) and, in some cases, a pre-transition temperature is also observed. In the present study, the effect of BSA in the thermal behavior of DODAB:MO liposomes, at different χMO, was studied by DSC (Figure 6 and Table 1).

Table 1: The effect of BSA in the gel-to-Liquid Crystalline Transition Temperature (T_m) and variation in Enthalpy (ΔH_m) of DODAB:MO liposomes, as assessed by DSC in the Heating Mode.

		Pre-transitions						Main Transition		
DODAB:MO	Liposomes	T_p* (°C)	ΔH_p (kJ/mo)	$\Delta T_{1/2}$ (°C)	T_p (°C)	ΔH_p (kJ/mo)	$\Delta T_{1/2}$ (°C)	T_m (°C)	ΔH_m (kJ/mol)	$\Delta T_{1/2}$ (°C)
Pure DODAB	Empty	-	-	-	36	33.3	1.1	44.4	47.4	0.59
4:1	Empty*							46.4	47.4	0.59
	BSA loaded	32.3	3.04	5.5	40.2	0.46	3.7	53.3	30.2	0.49
2:1	Empty*	-	-	-	-	-	-	47.1	25.4	0.8
	BSA loaded	-	-	-	33.5	8.21	7.6	53.4	20.1	0.41
1:1	Empty*	-	-	-	30.3	1.95	1.26	45.4	21.2	1.61
	BSA loaded	28.6	0.82	5.2	43	4.06	9	53.5	14.1	0.41
1:2	Empty*	-	-	-	-	-	-	46.5	11.6	0.98
	BSA loaded	-	-	-	35.6	1.74	4.3	53.2	7.1	1
1:4	Empty*	-	-	-	-	-	-	-	-	-
	BSA loaded	26.8	0.87	6.9	37.6	0.59	2.3	52.9	2.7	0.7

* Empty liposomes values present in the table were previously reported [10].

Table 1 shows, in detail, the gel-to-liquid crystalline phase transition properties of DODAB:MO liposomes, at different χMO, in the presence of BSA. The properties of empty liposomes with similar χMO, were described in previous studies [10, 20] and are also present in Table 1 for comparison.

For all DODAB:MO molar ratios, BSA induced great changes in the enthalpy and T_m suggesting the occurrence of strong interactions between BSA with the lipid bilayer. The T_m increased and the ΔH decreased in comparison with empty liposomes (Figure 6 and Table 1). T_m was nevertheless still detected even for the highest molar fraction of MO (DODAB:MO (1:4)), indicating the presence of some rigid bilayers at higher MO content

The increase in T_m values indicates that the incorporation of BSA leads to the reorganization of the bilayer with the separation of a MO rich domain (more fluid) from the DODAB rich domain (more rigid). Furthermore, a decrease in $\Delta T_{1/2,}$ as observed by a reduction of the peak diameter, suggests that BSA incorporation speeds the phage transition probably due to the formation of DODAB rich domains. In fact, the effect of proteins on the

transition temperature and shape of the DSC peaks can also provide information on the miscibility of lipids and proteins. In accordance with these results, the proteins well mixed with the gel phase, displayed an upward shift of thermogram broadening the high-temperature side [31]. Consequently, for the same BSA LNPs, the T_p found in pure DODAB appears at higher temperatures. Interestingly, for BSA LNPs formulations with excess of DODAB, DODAB:MO (4:1), equal molar fraction DODAB:MO (1:1) or excess of MO, DODAB:MO (1:4) the appearance of a second pre-transition peak (T_p*) is observed.

These results suggest that at these χMO, we may have the same phase separation leading to co-existence of DODAB-rich and MO-rich domains. In fact, for empty DODAB:MO (1:4) liposomes no transition peak was observed [10] suggesting the presence of some BSA LNPs-MO rich (fluid) and also the convergence of DODAB-rich domains upon protein interaction, which could explain the reappearance of the peak. In fact, it was already reported that specific interactions between a protein/peptide with lipid molecules could induce the formation of domains within lipid membranes and the appearance of shoulders or double peaks in the DSC [32, 33]. In DODAB:MO (2:1) and (1:2) BSA LNPs, the Tp found in pure DODAB is reduced for lower values, although no Tp exists for the corresponding empty liposomes [10]. This again suggests that a phase separation occurs between DODAB and MO molecules upon BSA interaction.

The decrease in enthalpy suggests that in BSA/cationic lipid interaction may occur two competing effects: charge-neutralization interaction at the bilayer surface, due to electrostatic forces which cause the packing and stabilization of the gel-state bilayer, and a hydrophobic interaction caused by a partial insertion of BSA into the lipid bilayer core. DLS studies reveal that BSA incorporation lead to slight decreased in mean size and PDI of LNPS than can be associated with the packing and stabilization effect.

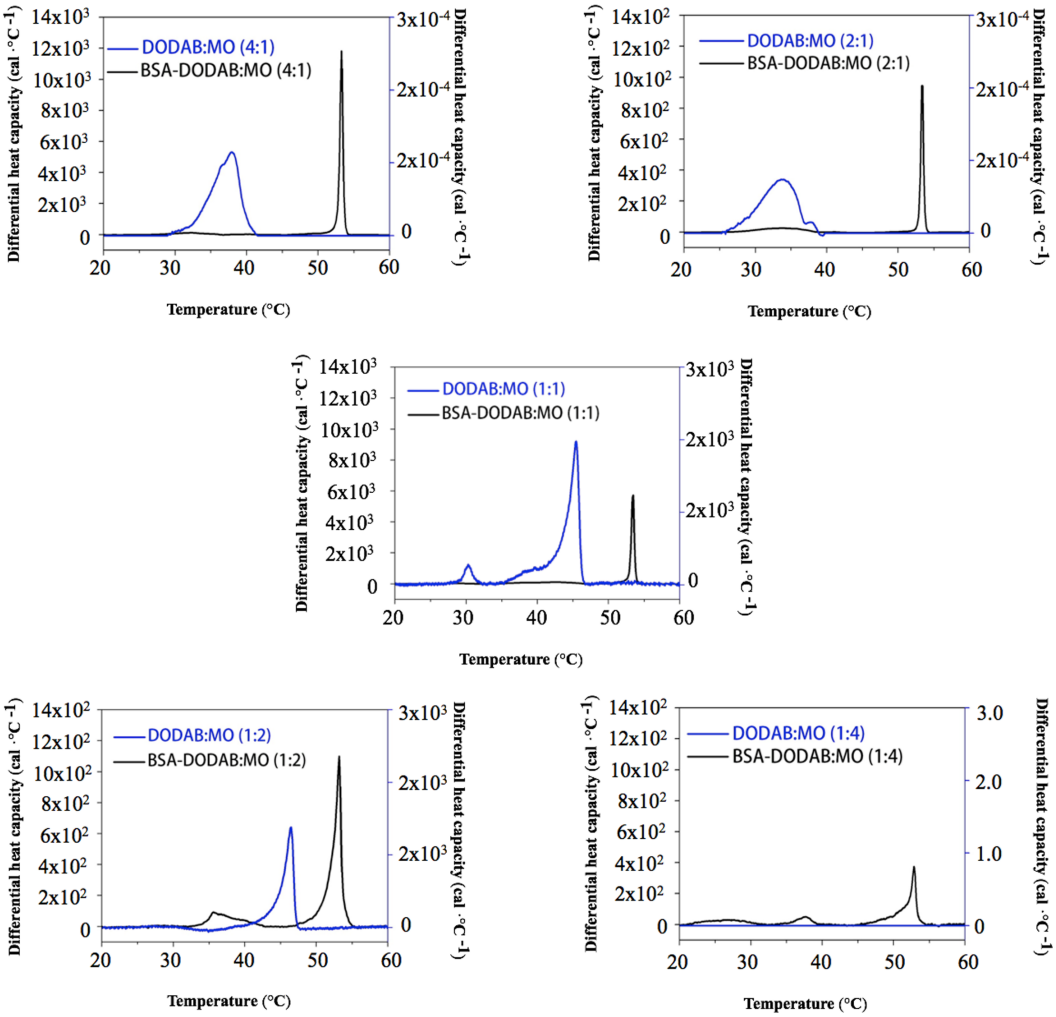

Figure 6: The effect of BSA on the DSC thermograms of DODAB:MO liposomes, at different χMO, obtained in the heating mode, at scan rate 1 °C/ min. The left Y-axis indicates differential heat capacity values for the BSA NLPs (black) and the right Y-axis indicates differential heat capacity values for the empty liposomes (blue) as previously described [10].

Moreover, BSA incorporation in the bilayers can restrain the swing of surrounding DODAB molecules preventing their contribution to the phase transition decreasing enthalpy [34]. The same authors also suggested that hydrophobic interaction between BSA and liposomal bilayer membrane is likely to be between the 'domain III' and/or 'hydrophobic hole' of BSA and the hydrocarbon region of liposomal bilayer membranes [34]. In fact, different studies suggested that the presence of substances that insert, or even only penetrate to some extent into the hydrophobic core of the bilayer promote a decrease in cooperativity (ΔH decreases) [35, 36].

3.2.2 The effect of χMO in liposomal BSA nanoparticles (BSA LNPs) cytotoxicity and BSA uptake.

The cytotoxicity of the BSA LNPs was evaluated on the metabolic activity of RAW 264.7 cells after being exposed to three different concentrations of each of the five DODAB:MO molar ratios, using the MTT assay, while the impact on membrane integrity was evaluated using the LDH assay, after 24h of co-incubation.

In general, cell viability after incubation with BSA LNPs was above 93%, indicating no cytotoxic effect (Figure 7). However, contrary to what was observed for empty liposomes, the clear dependence of cell viability on the content of MO was not observed.

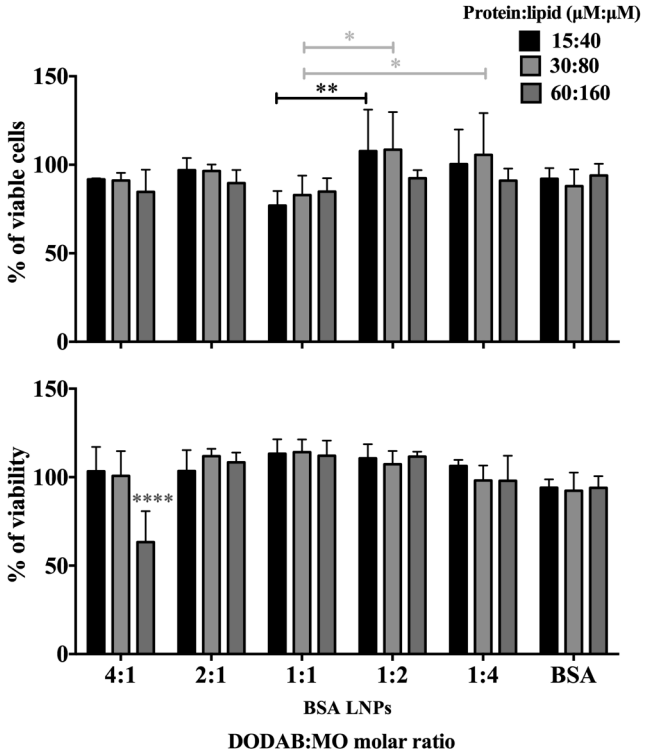

Figure 7: Viability of RAW 264.7 cells after 24 h incubation with BSA LNPs at different χMO. Viability was assessed using the MTT (in the top) and LDH (in the bottom). The liposomes were diluted in the cells medium and the final concentration is indicated by means of protein to lipid molar ratio. Free BSA was used at the same concentrations. The bars indicate the mean ± SD of two independent experiments. Significant differences between the different molar ratios are represented by (*) above the line, differences with the former concentration are represented by (*) above the bar: (*P<0.5, **P<0.01, ***P<0.001, ****P<0.0001)

The only formulation with a higher cytotoxic effect was DODAB:MO (4:1) BSA LNPs at the higher concentration, that seems to affect cell membrane integrity (Figure 7). Nevertheless, comparing all result from this analysis, cell viability was higher than 90% for

DODAB:MO (1:2) and (1:4) BSA LNPs, supporting the tolerability of the cells towards liposomes that incorporated higher proportions of MO.

In order to evaluate the effect of MO presence in BSA internalization, DODAB:MO (1:2) BSA LNPs were chosen, due to the characteristics described previously, and for comparison, the inverted χMO: DODAB:MO (2:1) BSA LNPs was also included in this analysis. After 40 min of exposure at 37ºC to FITC–BSA LNPs or FITC–BSA solution, the percentage of FITC positive cells was significantly higher ($P<0.05$) for FITC–BSA solution and for DODAB:MO (1:2) BSA LNPs in comparison to cells incubated with DODAB:MO (2:1) BSA LNPs (Figure 8). In contrast, the mean fluorescence intensity (MFI), that indicates the amount of FITC-BSA internalized per cell, was higher when BSA was loaded in DODAB:MO (2:1) ($P<0.0001$) or (1:2) ($P<0.001$) liposomes, increasing from 120 ± 5.0 for the free BSA to 152 ± 5.6 for DODAB:MO (1:2) reaching 243 ± 7.0 for DODAB:MO (2:1) liposomes. These results are in agreement with several studies pointing out that cationic liposomes bound avidly to murine antigen presenting cells (APCs) and consequently mediate enhanced cellular adsorption and uptake of antigens [25, 37].

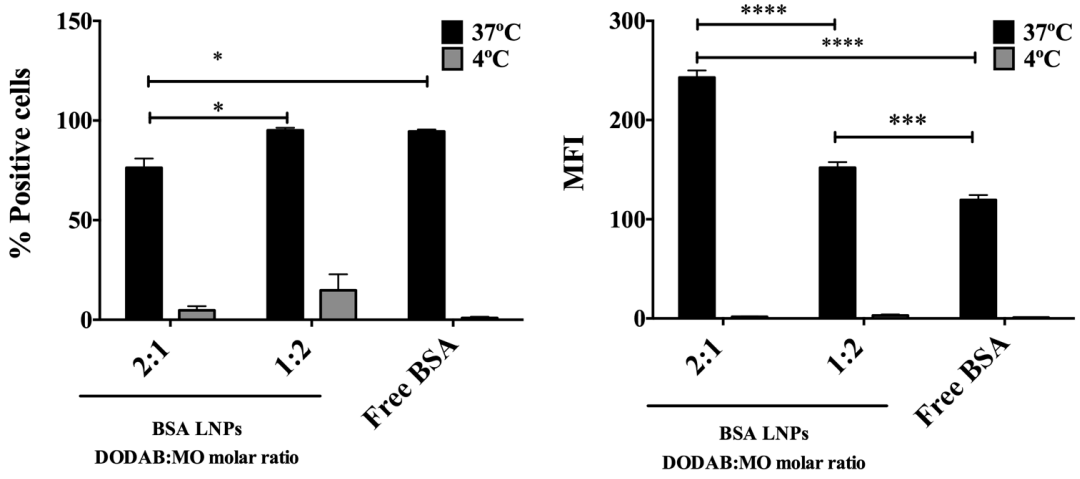

Figure 8: Effect of χMO in the cellular uptake of BSA LNPs after 40 min of incubation at 37 ºC and 4 ºC. Percentage of cellular uptake (left) and the mean fluorescence intensity (MFI) (right). The bars indicate the mean ± SD of two independent experiments. Significant differences are represented by (*) above the line: (*P<0.5, **P<0.01, ***P<0.001, ****P<0.0001)

Considering the results obtained, DODAB:MO (1:2) liposomes prove to be superior when successfully delivered the FITC-BSA to 95.2 ± 1.2% of the cells in contrast to 76 ± 4.6% reached by DODAB:MO (2:1) BSA LNPs, leading to a more homogeneous and efficient delivery. This result is in agreement with our previous indication that empty

liposomes with a higher amount of MO favors cellular uptake. The same tendency was observed, for these two χMO in DODAB:MO liposomes in a Small interfering RNA (siRNA) transfection assay , in a different strategy [20]. These observations suggest that differences in the structural organization of the liposomes due to different χMO can interfere with the internalization efficiency.

Exposure to FITC–BSA LNPs or FITC–BSA solution at 4 ºC, resulted in negligible increase in FITC fluorescence above cellular auto-fluorescence, indicating that fluorescence associated with the cells at 37 ºC is a result of active uptake rather than superficial adhesion, similar to what was observed for empty liposomes. Moreover, the uptake pathway for particles internalization is mainly determined by the particle size [38]. The BSA LNPs used in this study, as previously mentioned, exhibit sizes larger than 50 nm and smaller than 500 nm, which is the exact range defined for macrophage particle uptake to occur mainly via endocytosis (including clathrin-, caveolae-mediated, non-mediated endocytosis etc) [38].

3.2.3 **Activation of Bone marrow dendritic cells (BMDCs)**

Dendritic cells (DCs) constitute the most important class of antigen presenting cells (APCs) of the immune system and the activation of these cells seems to play a major role in the initiation of the adaptive immune response. In fact, DCs are responsible for capturing, processing and presenting antigens, through MHC pathways, to $CD4^+$ and $CD8^+$ T lymphocytes [39, 40].

After showing that that DODAB:MO (1:2) liposomes enhanced BSA internalization by macrophages, and in order to test if this efficiency was associated with a functional enhancement of APCs activation, DODAB:MO (1:2) BSA LNPs were incubated for 24 h with BMDCs and the of activation markers were assessed by measuring surface expression of co-stimulatory (CD80 and CD86) and MHC class II molecules. As it can be seen in Figure 9A, the loading of BSA in liposomes did not cause any effect in BMDCs activation. In fact, several studies have demonstrated that dendritic cells are remarkably potent at initiating and directing adaptive immune responses but only when the antigen is captured in the presence of microbial products or inflammatory stimuli, being tolerant in the absence of these signals [41, 42].

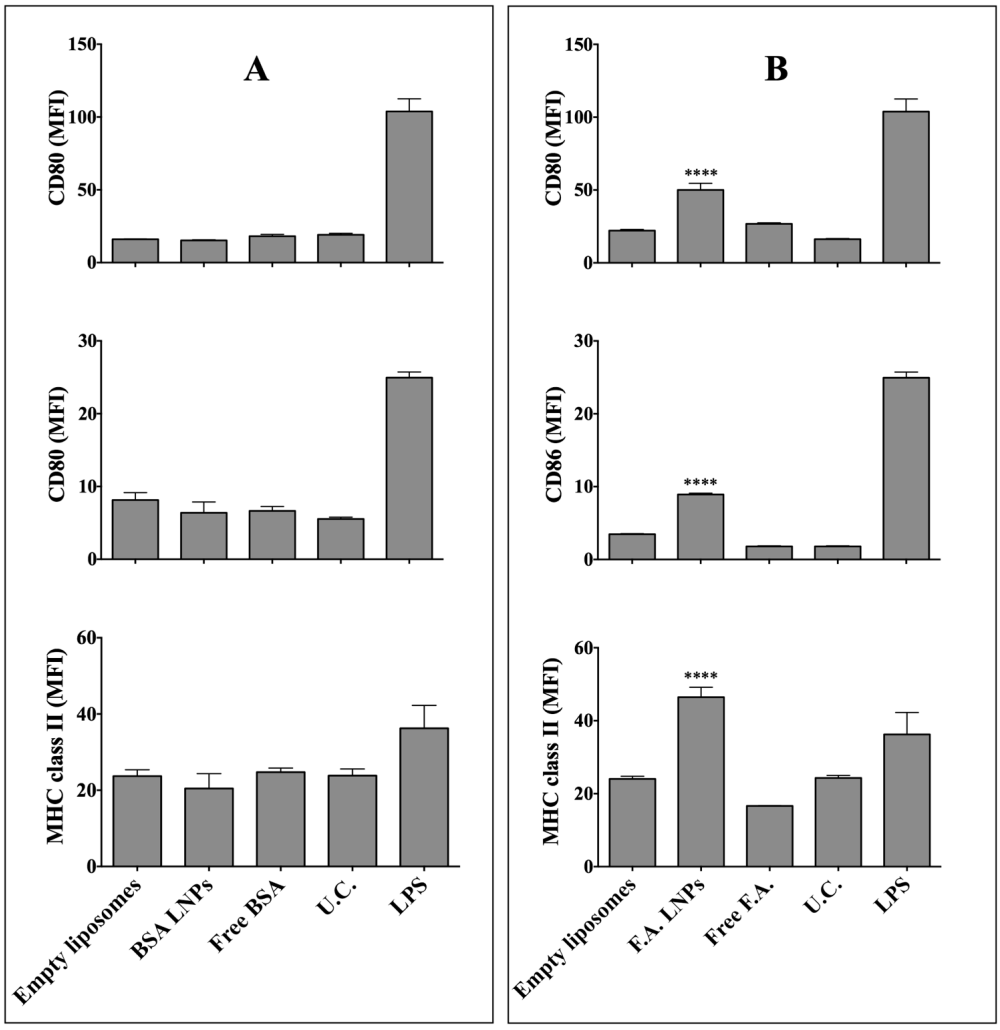

Figure 9: BMDCs isolated from BALB/c mice were stimulated *in vitro* with empty liposomes A) BSA LNPs or free BSA for; B) fungal antigens (F.A.) LNPs or free fungal. All at DODAB:MO (1:2) molar ratio during 24 h. BMDCs were gated on $CD11c^{+}$ cells and analyzed for expression of co-stimulatory and MHC class II molecules. Bars represent the mean ± SD of mean fluorescence intensity (MFI) from two independent experiments. U.C.: unstimulated cells. Only significant differences between fungal antigens loaded in LNPs and free antigens are represent by (#), between the two time points at the same concentration by (*) above the bars and between concentration by (*) above the line: **P<0.01; ***P<0.001 and ****P<0.0001. U.C.: unstimulated cells

In order to clarify if DODAB:MO liposomes could enhance the immunogenicity of microbial antigens, the same liposomes, DODAB:MO (1:2) liposomes were loaded with complex fungal antigens (F.A.). Complex F.A. were obtained from C. *albicans* cell wall, which due to its outer location is readily recognized by the host immune cells, triggering and modulating the anti-*Candida* host immune responses, and therefore constitutes the most important pathogen-associated molecular patterns (PAMPs) of *C. albicans* [43, 44]. These complex fungal antigens display a mean size of 88.7 ± 5.1 nm and a PDI of 0.63 ± 0.01, characterized by DLS. Fungal antigens DODAB:MO (1:2) LNPs present a mean size of 223 ± 37 nm and a PDI of 0.19 ± 0.015, relatively similar to BSA LNPs. After 24 h of

incubation with BMDCs a pronounced improvement in the activation promoted by the free fungal antigens is achieved for both activation markers and MHC class II molecules with their incorporation in DODAB:MO (1:2) liposomes ($P<0.0001$) (Figure 9B).

This improvement in the activation suggests that after being captured by DCs the LNPs collapse within the intracellular acidic compartments, releasing the fungal antigens intracellularly in a way that enabled processing by the MHC class II dependent pathway. Furthermore, expression of activation markers (CD80 and CD86) represents important surface molecules for T cell activation [45]. The fact LNPs enhance their expression indicates that DODAB:MO liposomes can have tremendous potential as adjuvant delivery systems in development of new vaccines.

Consistent with the current study, other proposed delivery systems have been shown to have an adjuvant activity for DCs activation, such as layered double hydroxides [46], salidroside (*a component from Rhodiola rosea L plant*) liposome formulations [47], polyanhydride nanoparticles[48], poly (D,L-lactic-co-glycolic acid) (PLGA) nanoparticles with entrapped with monophosphoryl lipid A (MPL) [49], cationized gelatin nanoparticles (GNPs) [50].

4. CONCLUSION

Based on presented findings we therefore established that an increase in MO content is important for the improvement of DODAB:MO liposomes colloidal stability and in contrary a decrease in MO content affects cell viability and internalization efficiency. BSA incorporation in DODAB:MO liposomes leads to a reorganization of the liposomal bilayer with the separation of a MO rich domain (more fluid) from the DODAB rich domain (more rigid). Moreover, according to the obtained results we show that both empty liposomes and BSA LNPs are internalized in an energy depend process and BSA uptake per cell is increased upon BSA loading in DODAB:MO liposomes. Finally, according we the previous characteristics we selected the more suitable molar fraction of MO and showed that DODAB:MO (1:2 molar ratio) liposomes can be used, in the future, as delivery system to promote vaccine delivery in immune cells, since they not only act as nanocarries but also as antigen adjuvants that induced significantly more effective APC activation than free microbial antigens.

ACKNOWLEDGEMENTS

We thank Professor Eduardo F. Marques, Faculdade de Ciências, Universidade do Porto, Professor Claudia Botelho, Centre of Biological Engineering, Minho University, and Professor Eloi Feitosa. Physics Department/IBILCE, São Paulo State University, for technical support with the Cryo-SEM, confocal microscopy, and Differential scanning calorimetry analysis, respectively.

REFERENCES

1. **Davidsen, J., Rosenkrands, I., Christensen, D., Vangala, A., Kirby, D., Perrie, Y., Agger, E.M., and Andersen, P.**, Characterization of cationic liposomes based on dimethyldioctadecylammonium and synthetic cord factor from *M. tuberculosis* (trehalose 6,6'-dibehenate)-a novel adjuvant inducing both strong CMI and antibody responses. Biochim Biophys Acta, 2005. **1718**(1-2): p. 22-31.
2. **Ingvarsson, P.T., Schmidt, S.T., Christensen, D., Larsen, N.B., Hinrichs, W.L., Andersen, P., Rantanen, J., Nielsen, H.M., Yang, M., and Foged, C.**, Designing CAF-adjuvanted dry powder vaccines: spray drying preserves the adjuvant activity of CAF01. J Control Release, 2013. **167**(3): p. 256-64.
3. **Neves Silva, J.P., Coutinho, P.J., and Real Oliveira, M.E.**, Characterization of monoolein-based lipoplexes using fluorescence spectroscopy. J Fluoresc, 2008. **18**(2): p. 555-62.
4. **Carmona-Ribeiro, A.M.**, Bilayer-forming synthetic lipids: drugs or carriers? Curr Med Chem, 2003. **10**(22): p. 2425-46.
5. **Carmona-Ribeiro, A.M.**, Biomimetic particles in drug and vaccine delivery. J Liposome Res, 2007. **17**(3-4): p. 165-72.
6. **Carmona-Ribeiro, A.M.**, Lipid bilayer fragments and disks in drug delivery. Curr Med Chem, 2006. **13**(12): p. 1359-70.
7. **Ogris, M., Steinlein, P., Kursa, M., Mechtler, K., Kircheis, R., and Wagner, E.**, The size of DNA/transferrin-PEI complexes is an important factor for gene expression in cultured cells. Gene Ther, 1998. **5**(10): p. 1425-33.
8. **Kulkarni, C.V., Wachter, W., Iglesias-Salto, G., Engelskirchen, S., and Ahualli, S.**, Monoolein: a magic lipid? Phys Chem Chem Phys, 2011. **13**(8): p. 3004-21.
9. **Ganem-Quintanar, A., Quintanar-Guerrero, D., and Buri, P.**, Monoolein: a review of the pharmaceutical applications. Drug Dev Ind Pharm, 2000. **26**(8): p. 809-20.
10. **Oliveira, I.M., Silva, J.P., Feitosa, E., Marques, E.F., Castanheira, E.M., and Real Oliveira, M.E.**, Aggregation behavior of aqueous dioctadecyldimethylammonium bromide/monoolein mixtures: a multitechnique investigation on the influence of composition and temperature. J Colloid Interface Sci, 2012. **374**(1): p. 206-17.

11. **Henriksen-Lacey, M., Korsholm, K.S., Andersen, P., Perrie, Y., and Christensen, D.**, Liposomal vaccine delivery systems. Expert Opin Drug Deliv, 2011. **8**(4): p. 505-19.
12. **Carmona-Ribeiro, A.M.**, Preparation and characterization of biomimetic nanoparticles for drug delivery. Methods Mol Biol, 2012. **906**: p. 283-94.
13. **Perrie, Y., Mohammed, A.R., Kirby, D.J., McNeil, S.E., and Bramwell, V.W.**, Vaccine adjuvant systems: enhancing the efficacy of sub-unit protein antigens. Int J Pharm, 2008. **364**(2): p. 272-80.
14. **Perrie, Y., Kirby, D., Bramwell, V.W., and Mohammed, A.R.**, Recent developments in particulate-based vaccines. Recent Pat Drug Deliv Formul, 2007. **1**(2): p. 117-29.
15. **Carneiro, C., Correia, A., Collins, T., Vilanova, M., Pais, C., Gomes, A.C., Real Oliveira, M.E., and Sampaio, P.**, DODAB:monoolein liposomes containing *Candida albicans* cell wall surface proteins: A novel adjuvant and delivery system. Eur J Pharm Biopharm, 2015. **89**: p. 190-200.
16. **Bangham, A.D., Standish, M.M., and Watkins, J.C.**, Diffusion of univalent ions across the lamellae of swollen phospholipids. J Mol Biol, 1965. **13**(1): p. 238-52.
17. **Carneiro, C., Correia, A., Collins, T., Vilanova, M., Pais, C., Gomes, A.C., Real Oliveira, M.E., and Sampaio, P.**, DODAB:monoolein liposomes containing *Candida albicans* cell wall surface proteins: A novel adjuvant and delivery system. Eur J Pharm Biopharm, 2014.
18. **Silva, J.P., Oliveira, A.C., Casal, M.P., Gomes, A.C., Coutinho, P.J., Coutinho, O.P., and Oliveira, M.E.**, DODAB:monoolein-based lipoplexes as non-viral vectors for transfection of mammalian cells. Biochim Biophys Acta, 2011. **1808**(10): p. 2440-9.
19. **Teixeira, L., Botelho, A.S., Mesquita, S.D., Correia, A., Cerca, F., Costa, R., Sampaio, P., Castro, A.G., and Vilanova, M.**, Plasmacytoid and conventional dendritic cells are early producers of IL-12 in Neospora caninum-infected mice. Immunol Cell Biol, 2010. **88**(1): p. 79-86.
20. **Oliveira, A.C., Martens, T.F., Raemdonck, K., Adati, R.D., Feitosa, E., Botelho, C., Gomes, A.C., Braeckmans, K., and Real Oliveira, M.E.**, Dioctadecyldimethylammonium:monoolein nanocarriers for efficient in vitro gene silencing. ACS Appl Mater Interfaces, 2014.

21. **Lincopan, N., Espindola, N.M., Vaz, A.J., da Costa, M.H., Faquim-Mauro, E., and Carmona-Ribeiro, A.M.**, Novel immunoadjuvants based on cationic lipid: Preparation, characterization and activity in vivo. Vaccine, 2009. **27**(42): p. 5760-71.
22. **Segal, A.W.**, How neutrophils kill microbes. Annu Rev Immunol, 2005. **23**: p. 197-223.
23. **Wrobel, I. and Collins, D.**, Fusion of cationic liposomes with mammalian cells occurs after endocytosis. Biochim Biophys Acta, 1995. **1235**(2): p. 296-304.
24. **Friend, D.S., Papahadjopoulos, D., and Debs, R.J.**, Endocytosis and intracellular processing accompanying transfection mediated by cationic liposomes. Biochim Biophys Acta, 1996. **1278**(1): p. 41-50.
25. **Korsholm, K.S., Agger, E.M., Foged, C., Christensen, D., Dietrich, J., Andersen, C.S., Geisler, C., and Andersen, P.**, The adjuvant mechanism of cationic dimethyldioctadecylammonium liposomes. Immunology, 2007. **121**(2): p. 216-26.
26. **Martina, M.S., Nicolas, V., Wilhelm, C., Menager, C., Barratt, G., and Lesieur, S.**, The in vitro kinetics of the interactions between PEG-ylated magnetic-fluid-loaded liposomes and macrophages. Biomaterials, 2007. **28**(28): p. 4143-53.
27. **Takeda, K., Wada, A., Yamamoto, K., Moriyama, Y., and Aoki, K.**, Conformational change of bovine serum albumin by heat treatment. J Protein Chem, 1989. **8**(5): p. 653-9.
28. **Papahadjopoulos, D., Moscarello, M., Eylar, E.H., and Isac, T.**, Effects of proteins on thermotropic phase transitions of phospholipid membranes. Biochim Biophys Acta, 1975. **401**(3): p. 317-35.
29. **Caffrey, M.**, A lipid's eye view of membrane protein crystallization in mesophases. Curr Opin Struct Biol, 2000. **10**(4): p. 486-97.
30. **Feitosa, E., Barreleiro, P.C., and Olofsson, G.**, Phase transition in dioctadecyldimethylammonium bromide and chloride vesicles prepared by different methods. Chem Phys Lipids, 2000. **105**(2): p. 201-13.
31. **Canadas, O. and Casals, C.**, Differential scanning calorimetry of protein-lipid interactions. Methods Mol Biol, 2013. **974**: p. 55-71.
32. **Joanne, P., Galanth, C., Goasdoue, N., Nicolas, P., Sagan, S., Lavielle, S., Chassaing, G., El Amri, C., and Alves, I.D.**, Lipid reorganization induced by membrane-active peptides probed using differential scanning calorimetry. Biochim Biophys Acta, 2009. **1788**(9): p. 1772-81.

33. **Saenz, A., Canadas, O., Bagatolli, L.A., Johnson, M.E., and Casals, C.**, Physical properties and surface activity of surfactant-like membranes containing the cationic and hydrophobic peptide KL4. FEBS J, 2006. **273**(11): p. 2515-27.
34. **Tsunoda, T., Imura, T., Kadota, M., Yamazaki, T., Yamauchi, H., Kwon, K.O., Yokoyama, S., Sakai, H., and Abe, M.**, Effects of lysozyme and bovine serum albumin on membrane characteristics of dipalmitoylphosphatidylglycerol liposomes. Colloids Surf B Biointerfaces, 2001. **20**(2): p. 155-163.
35. **Gardikis, K., Hatziantoniou, S., Viras, K., Wagner, M., and Demetzos, C.**, A DSC and Raman spectroscopy study on the effect of PAMAM dendrimer on DPPC model lipid membranes. Int J Pharm, 2006. **318**(1-2): p. 118-23.
36. **Mouritsen, O.G. and Jorgensen, K.**, Dynamical order and disorder in lipid bilayers. Chem Phys Lipids, 1994. **73**(1-2): p. 3-25.
37. **Barnier-Quer, C., Elsharkawy, A., Romeijn, S., Kros, A., and Jiskoot, W.**, Adjuvant effect of cationic liposomes for subunit influenza vaccine: influence of antigen loading method, cholesterol and immune modulators. Pharmaceutics, 2013. **5**(3): p. 392-410.
38. **Xiang, S.D., Scholzen, A., Minigo, G., David, C., Apostolopoulos, V., Mottram, P.L., and Plebanski, M.**, Pathogen recognition and development of particulate vaccines: does size matter? Methods, 2006. **40**(1): p. 1-9.
39. **Vangasseri, D.P., Cui, Z., Chen, W., Hokey, D.A., Falo, L.D., Jr., and Huang, L.**, Immunostimulation of dendritic cells by cationic liposomes. Mol Membr Biol, 2006. **23**(5): p. 385-95.
40. **Banchereau, J. and Steinman, R.M.**, Dendritic cells and the control of immunity. Nature, 1998. **392**(6673): p. 245-52.
41. **Palm, N.W. and Medzhitov, R.**, Pattern recognition receptors and control of adaptive immunity. Immunol Rev, 2009. **227**(1): p. 221-33.
42. **Platt, C.D., Ma, J.K., Chalouni, C., Ebersold, M., Bou-Reslan, H., Carano, R.A., Mellman, I., and Delamarre, L.**, Mature dendritic cells use endocytic receptors to capture and present antigens. Proc Natl Acad Sci U S A, 2010. **107**(9): p. 4287-92.
43. **Hall, R.A. and Gow, N.A.**, Mannosylation in *Candida albicans*: role in cell wall function and immune recognition. Mol Microbiol, 2013. **90**(6): p. 1147-61.
44. **Netea, M.G., Gow, N.A., Munro, C.A., Bates, S., Collins, C., Ferwerda, G., Hobson, R.P., Bertram, G., Hughes, H.B., Jansen, T., Jacobs, L., Buurman, E.T., Gijzen, K., Williams, D.L., Torensma, R., McKinnon, A., MacCallum, D.M.,**

Odds, F.C., Van der Meer, J.W., Brown, A.J., and Kullberg, B.J., Immune sensing of *Candida albicans* requires cooperative recognition of mannans and glucans by lectin and Toll-like receptors. J Clin Invest, 2006. **116**(6): p. 1642-50.

45. **Ridge, J.P., Di Rosa, F., and Matzinger, P.**, A conditioned dendritic cell can be a temporal bridge between a CD4+ T-helper and a T-killer cell. Nature, 1998. **393**(6684): p. 474-8.
46. **Li, A., Qin, L., Wang, W., Zhu, R., Yu, Y., Liu, H., and Wang, S.**, The use of layered double hydroxides as DNA vaccine delivery vector for enhancement of anti-melanoma immune response. Biomaterials, 2011. **32**(2): p. 469-77.
47. **Zhao, X., Lu, Y., Tao, Y., Huang, Y., Wang, D., Hu, Y., Liu, J., Wu, Y., Yu, Y., and Liu, C.**, Salidroside liposome formulation enhances the activity of dendritic cells and immune responses. Int Immunopharmacol, 2013. **17**(4): p. 1134-40.
48. **Vela Ramirez, J.E., Roychoudhury, R., Habte, H.H., Cho, M.W., Pohl, N.L., and Narasimhan, B.**, Carbohydrate-functionalized nanovaccines preserve HIV-1 antigen stability and activate antigen presenting cells. J Biomater Sci Polym Ed, 2014. **25**(13): p. 1387-406.
49. **Elamanchili, P., Lutsiak, C.M., Hamdy, S., Diwan, M., and Samuel, J.**, "Pathogen-mimicking" nanoparticles for vaccine delivery to dendritic cells. J Immunother, 2007. **30**(4): p. 378-95.
50. **Zwiorek, K., Bourquin, C., Battiany, J., Winter, G., Endres, S., Hartmann, G., and Coester, C.**, Delivery by cationic gelatin nanoparticles strongly increases the immunostimulatory effects of CpG oligonucleotides. Pharm Res, 2008. **25**(3): p. 551-62.

CHAPTER V

DODAB:monoolein liposomes containing *Candida albicans* cell wall surface proteins: a novel adjuvant and delivery system

Adapted from:

DODAB:monoolein liposomes containing *Candida albicans* cell wall surface proteins: a novel adjuvant and delivery system

Catarina Carneiro[1], Alexandra Correia[2], Tony Collins[1], Manuel Vilanova[2,3], Célia Pais[1], Andreia C, Gomes[1,5], M. Elisabete C.D. Real Oliveira[4,5], Paula Sampaio[1*]

European Journal of Pharmaceutics and Biopharmaceutics (2015) 89:190-200.

[1]Centre of Molecular and Environmental Biology (CBMA), Department of Biology, University of Minho, 4710-057 Braga, Portugal

[2] IBMC-Instituto de Biologia Molecular e Celular, Rua do Campo Alegre 823, Porto, Portugal

[3] Instituto de Ciências Biomédicas de Abel Salazar (ICBAS), Universidade do Porto, Rua de Jorge Viterbo Ferreira n.º 228, 4050-313 Porto, Portugal

[4]Centre of Physics (CFUM) University of Minho, Campus of Gualtar, 4710-057 Braga, Portugal

[5]NanoDelivery I&D in Biotechnology, Biology Department, Campus of Gualtar, 4710-057 Braga, Portugal

ABSTRACT

We describe the preparation and characterization of DODAB:MO-based liposomes and demonstrate their adjuvant potential and use in antigen delivery. Liposomes loaded with *C. albicans* proteins assembled as stable negatively charged spherical liposomal nanoparticles (LNPs) with a mean size of 280 nm. High adsorption efficiency (91.0 ± 9.0%) is attained with high lipid concentrations. The LNPs were non-toxic, avidly taken up by macrophage cells and accumulated in membrane rich regions with an internalization time of 20 min. Immunized mice displayed strong humoral and cell-mediated immune responses, producing antibodies (IgGs) against specific cell wall proteins, Cht3p and Xog1p. DODAB:MO-based liposomes loaded with *C. albicans* proteins have an excellent immunogenic potential and can be explored for the development of an immunoprotective strategy against *Candida* infections.

1. INTRODUCTION

Delivery systems are frequently used in vaccine formulations to ensure efficient antigen delivery and induction of an adequate immune response. In fact, delivery systems have been applied in marketed vaccines for over 70 years to protect and carry antigens as well as to act as adjuvants for molecules with low immunogenicity [1, 2]. Currently, many options for delivery systems are available, including liposomes, polymer-based micro- and nanoparticles, virosomes, immune stimulating complexes **(**ISCOMS) and many more [3-6]. Of these, liposomes can also act as immunological adjuvants [7] and are the most widely investigated delivery system for phagocyte-targeted therapies [8, 9]. Liposomes offer a flexible system for manipulation and enable the preparation of vesicles with varying lamellarities, physical characteristics, adsorption efficiencies, and antigen encapsulation abilities [3]. In addition, liposomes are biodegradable and biocompatible and may be functionalized to provide cell targeting specificity and antigen protection [10, 11].

Cationic liposomes have been used extensively as drug and vaccine delivery systems [12, 13]. Various types of cationic lipids may be used in the preparation of liposomes, varying in the charge of the hydrophilic head group, the number and/or length of fatty acid chains (tail) and/or their degree of saturation. The cationic surfactant dioctadecyldimethylammonium bromide (DODAB) is a synthetic amphiphilic lipid composed of a hydrophilic positively charged dimethylammonium group (head) attached to two hydrophobic 18-carbon alkyl chains (tail). In aqueous buffers, DODAB molecules self-assembles into closed liposomal vesicular bilayers [14]. DODAB cationic vesicles have been used as carriers in drug delivery [15, 16] as well as adjuvants for vaccination, displaying higher colloid stability than alum and better efficacy in inducting higher cellular immune responses [17-19]. However, cationic liposomes alone may be associated with *in vivo* cytotoxicity [18, 20] and, in salt solutions, such as phosphate buffer saline (PBS), can instantaneously aggregate due to insufficient electrostatic repulsion forces [21]. To overcome these problems, several stabilizers including trehalose 6,6'-dibehenate (TDB) [12], and silica [19] have been used to increase DODAB liposomes colloidal stability, minimize cytotoxicity by dilution effect and increase adjuvant efficacy. In previous studies, we have demonstrated that monooleoyl-rac-glycerol (monoolein, MO) could also be used as a stabilizer as it conferred fluidity to the DODAB system by favoring lipid chain mobility [22]. In fact, we have successfully used DODAB:MO as a mammalian cell transfection system and as a system for in vitro gene silencing [16, 23]. MO is particularly interesting because it exhibits

two inverted bicontinuous cubic phases and as a result forms non-lamellar vesicles with negative curvature [24]**.** This characteristic decreases the structural rigidity of DODAB vesicles causing an increase in the lateral mobility of the lipid chain which in turn improves the fusion of the liposomes with cell membranes [16]. Tuning MO content in DODAB:MO formulations is also very advantageous in terms of formulation development for drug/protein delivery purposes, since MO has been described as an enhancer of proteins solubilization [25-28].

Fungal cell wall protein antigens constitute excellent candidates for vaccine development as the cell wall is a unique microbial feature with an important role in antigen presentation and immunomodulation [29]. Currently, several vaccine strategies against *Candida* have been investigated, using several cell wall antigens varying from proteins carriers conjugated with laminarin [30, 31] or mannoproteins conjugates [32] to recombinant cell surface proteins or peptides, such as Hyr1p [33], or the surface adhesins family of proteins (Als proteins) [34-36]. These studies administered these antigens with several adjuvants or carriers such as complete Freund's adjuvant (CFA), aluminum hydroxide gel or MPL (lipid A; monophosphoryl) [37-39]. Other studies also reported the used of β-mercaptoethanol (β -ME) extracts containing *Candida* cell wall proteins mixed with Ribi Adjuvant System [40]. However, despite the extensive investigation, more studies are needed to develop a safe and efficient a vaccine against *Candida* infections.

In the present study, we developed and explored a DODAB:MO lipid based delivery system loaded with dithiothreitol (DTT) extracted *C. albicans* cell wall surface proteins (CWSP) and determined its immunogenicity for future use against deleterious fungal infections.

2. MATERIAL AND METHODS

2.1. Materials

Dioctadecyldimethylammonium bromide (DODAB) was purchased from Tokyo Kasei (Japan). 1-monooleoyl-rac-glycerol (MO), Hanks' balanced salt solution (HBSS), glutaraldehyde, propidium iodide (PI) and DTT were supplied by Sigma–Aldrich (St. Louis, MO, USA). Wheat Germ Agglutinin Alexa Fluor® 633 Conjugate (λem=647nm) was provided by Alfagene (Carcavelos, Portugal), Rhodamine DHPE (Lissamine™ λem=580nm) and Tris-HCI Buffer by Invitrogen/Molecular Probes (Eugene, OR, USA) and ethanol (high spectral purity) was purchased from Uvasol (Leicester, United Kingdom). Dulbecco's Modified Eagle's Medium (DMEM) was supplemented with 10% heat-inactivated fetal bovine serum (FBS), 2 mM L-glutamine, (all from Sigma-Aldrich), HEPES-Buffer solution pH=7.5 supplied by VWR Internacional (Radnor, PA, USA) and 1mM sodium pyruvate by Merck (Frankfurt, Germany).

2.2. Extraction of yeast cell wall surface proteins

C. albicans strain SC5314, kindly provided by Prof. Joachim Morschhauser (Wurzburg, Germany), was obtained from a 2 day YPD agar (2 % D-glucose, 1% Difco yeast extract, 2% peptone and 2% agar) (w/v) culture incubated at 26 °C. The following procedures used for CWSP extraction were all performed in a sterile environment using apyrogenic solutions. The CWSP were released from whole intact cells by DTT treatment as described previously [41] with some modifications. Briefly, yeast cells were grown in YPD medium at 26 °C, 180 ×g, to the start of the stationary growth phase. Cells were then harvested by fugation and washed twice with 50 mM-Tris–HCl pH 7.5 buffer. Subsequently, cells were resuspended in the same buffer supplemented with 2 mM dithiothreitol (DTT), shaken vigorously for 2 h at 4 °C and centrifuged at 7943*g* for 15min. The yeast pellet obtained was used for assessment of membrane integrity while the yeast CWSP in the supernatant were concentrated and retained. Membrane integrity was assessed by incubating cells with PI (6 μg/ml) and analysis by flow cytometry (EPICS XL-MCL, Beckman-Coulter Corporation). Supernatant proteins were concentrated with a 3 kDa Amicon centrifugal filter supplied by Millipore (Madrid, Spain) at 4 °C, washed with 25 mM HEPES-buffer solution pH=7.5 and

quantified by means of the Bradford assay [42]. The concentrated proteins obtained were stored at -80 °C in aliquots of 100 μg/ml.

2.3. Western Blot

Extracted proteins were subjected to 12% SDS-polyacrylamide gel electrophoresis and transferred to polyvinylidene fluoride membranes (hybond-P; Amersham). The membranes were blocked with 3% BSA in Tris-saline buffer (w/v) containing 0.05% Tween (v/v) for 2 h at room temperature. Membranes were then incubated overnight at 4 ºC with a pool of antisera (1:250) from immunized mice. Bound antibodies were detected with goat anti-mouse Igs AP conjugate and membranes were developed using the conventional method with nitroblue tetrazolium (NBT)/5-bromo-4-chloro-3-indolylphosphate (BCIP) (Roche) in 100 mM Tris, 100 mM NaCl, and 5 mM $MgCl_2$, pH 9.5. A broad range SDS-PAGE molecular weight (MW) marker (15-250 kDa) was used (Bio-Rad).

2.4. Identification of the proteins

The protein bands, excised from the gel, were destained, reduced, alkylated and digested with trypsin (Promega, 6.7ng/μl) overnight at 37 ºC. The tryptic peptides were desalted and concentrated using POROS R2 (Applied Biosystems) and eluted directly onto the MALDI plate using 0.6μl of 5mg/ml CHCA (alpha-cyano-4-hydroxycinnamic acid, Sigma) in 50% (v/v) acetonitrile and 5% (v/v) formic acid. The data was acquired in positive reflector MS and MS/MS modes using a 4800plus MALDI-TOF/TOF (AB Sciex) mass spectrometer and using 4000 Series Explorer Software v.3.5.3 (Applied Biosystems). External calibration was performed using Pepmix1 (Laser BioLabs). The twenty-fifth most intense precursor ions from the MS spectra were selected for MS/MS analysis. The MS/MS data were analyzed using Protein Pilot Software v. 4.5 (ABSciex) with the Mascot search engine (MOWSE algorithm). The search parameters were as follows: monoisotopic peptide mass values were considered, maximum precursor mass tolerance (MS) of 50 ppm and a maximum fragment mass tolerance (MS/MS) of 0.3 Da. The searches were performed against SwissProt database with or without taxonomic restriction for Fungi. A maximum of two missed cleavage was allowed. Carboxyamidomethylation of cysteines and oxidation of methionines, were set as fixed and variable modifications, respectively.

Protein identification was only accepted when significant protein homology scores were obtained ($P<0.05$) and at least one peptide was fragmented with a significant individual ion score ($P<0.05$). This data was obtained at the Mass Spectrometry Unit (UniMS), at ITQB/iBET, Oeiras, Portugal.

2.5. Preparation and characterization of CWSP-loaded liposomes

DODAB:MO based liposomes were prepared using the lipid-film hydration method as previously described [43]. DODAB and MO, at a DODAB molar fraction (χDODAB) of 0.33, were dissolved in ethanol and mixed in a round-bottom flask. The χDODAB is given by the following equation [25]:

$$\chi\mathrm{DODAB} = \frac{[\mathrm{DODAB}]}{[\mathrm{DODAB}]+[\mathrm{MO}]}$$

The solvent was removed by rotary evaporation at 55 ºC and liposomes formed after hydration of the lipid film with 25 mM HEPES pH 7.5 at 55 ºC. The dispersion was then placed in a bath sonicator during 2 min .The liposomal stock dispersion was prepared at a total lipid concentration of 1774 μg/ml. Using 5 μg/ml of CWSP, seven different formulations containing different protein/lipid ratio (w/w), 0.006, 0.011, 0.014, 0.028, 0.056 and 0.113 were prepared (Table 1). The formulations were then incubated for 1h at 55 ºC. The *z*-average diameter of all formulations was determined by dynamic light scattering at 25 ºC with a Malvern ZetaSizer Nano ZS particle analyzer. The Malvern Dispersion Technology Software (DTS) was used with multiple narrow mode (high-resolution) data processing, and mean size (nm), polydispersity index (PDI) and error values were determined. The liposomal nanoparticle (LNP) surface charge was measured indirectly by ζ-potential analysis at 25 ºC using DTS with mono-modal mode data processing to determine average ζ-potential (mV) and error values. For several studies, an up-scale of some formulations, using 50 μg/ml of protein, was necessary but in all cases the protein-to-lipid weight ratios was maintained as described in Table 1.

2.5.1 Quantification of protein adsorption to liposomes

The prepared formulations were pelleted by ultracentrifugation (100,000*g* for 1 h), the

pellet submitted to TCA protein precipitation (Thermo Scientific Pierce), and the concentration of CWSP determined using the BCA Protein Assay Kit (Thermo Scientific Pierce) according to the manufacturer's instructions. The empty liposomes were used as negative control in order to exclude lipid interference in the protein quantification method.

2.5.2 **Cryo-SEM analysis of liposomes**

The morphology of the liposomes was evaluated by cryogenic scanning electron microscopy (cryo-SEM) using a High resolution Scanning Electron Microscope with X-Ray Microanalysis (JEOL JSM 6301F/ Oxford INCA Energy 350/ Gatan Alto 2500). Aliquots of 4 μl of empty liposomes (total lipid concentration of 888 μg/ml) or 4 μl of formulation ADS1 LNPs (50 μg/ml of CWSP and 888 μg/ml of lipids, CWSP:Lipid weight ratio of 0.056) were placed into carbon film grids, rapidly cooled (plunging into sub-cooled nitrogen – slush nitrogen) and transferred under vacuum to the cold stage of the preparation chamber. The samples were fractured, sublimated ('etched') for 120 seconds at -90 °C and coated with Au/Pd by sputtering for 40 seconds. Samples were transferred into the SEM chamber and studied at a temperature of -150°C.Micrographs were captured at an acceleration voltage of 15 kV and a working distance of 15 mm with a secondary electron in lens detector.

Table 1: Total lipid and of antigen concentrations for the different protein to lipid weight ratios.

CWSP:total lipid (Weight ratio)	Total lipid (μg/ml)	CWSP (μg/ml)
0.006	833	5
0.011	454.5	5
0.014	357.1	5
0.028	178.5	5
0.056	88.8	5
0.113	44.2	5
0.376	13.3	5

Equal volumes of CWSP were added to the liposomes dispersions and the final concentrations of the formulations are presented. For some experiments, the concentration of total lipid and of CWSP was increased but protein to lipid ratio was maintained.

2.6. Macrophage studies

The *in vitro* studies were performed using the murine macrophage cell line J774A.1 as previously described [44]. This cell line was cultured in complete DMEM at 37°C in a 5% CO_2 atmosphere. After confluent growth, macrophage cells were recovered, washed and re-suspended in complete DMEM to the desired final concentration.

2.6.1 Cytotoxicity analysis

Macrophages were plated onto 96-well tissue culture plates (Falcon) at $3x10^5$ cells/well and incubated to adhere overnight at 37 ºC in a humidified atmosphere of 5% CO_2. Different concentrations of empty liposomes, CWSP alone and two LNPs, ADS1 (CWSP:Lipid weight ratio of 0.056) and ADS2 (CWSP:Lipid weight ratio of 0.376), were added to the cells. Cell viability was analyzed by the 3-(4,5-dimethyl- thiazol-2-yl)-2,5-diphenyltetrazolium bromide (MTT) assay [45] following 24 h and 48 h incubation with the different formulations, at different concentrations. MTT formazan was solubilized by adding DMSO:ethanol (1:1) solution and absorbance measured at 570 nm. Untreated cells were used as a control of viability (100%) and cells treated with DMEM:DMSO (4:1) as a control of cytotoxicity (100%). Results were expressed as percentage of viability according to the following equation:

$$Viability(\%) = \frac{Experimental\ value\ (average) - Control\ of\ cytotoxicity\ (average)}{Control\ of\ viability\ (average) - Control\ of\ cytotoxicity\ (average)} \times 100$$

2.6.2 Microscopy analysis of internalized liposomes

For confocal microscopy, Rhodamine DHPE was incorporated into the DODAB:MO liposome (at a molar ratio of 1:200) during the preparation phase, as described in section 2.3. Labeled liposomes were then pelleted by ultracentrifugation (100,000*g* for 1 h) to remove unbound dye and resuspended in the same buffer volume. This labeled liposome stock dispersion was used to prepare the various protein to lipids weight ratios formulations, as described in section 2.3. Macrophages were plated in a microscopy chamber plate (Ibidi) at 3×10^5 cells/well and left to adhere overnight at 37 ºC in a humidified atmosphere of 5% CO_2. Immediately prior to incubation with liposomes, the macrophages were labeled with Wheat Germ Agglutinin Alexa Fluor® 633 Conjugate (2.5 µg/ml) for 10 min and then washed twice

with HBSS. The microscopy chamber plate was then placed in the integrated chamber (37 ºC, 5% CO_2) of the LSM 780 Carl Zeiss Microscope and 8 µl of DODAB:MO (1:2) empty labeled liposomes (total lipid concentration of 888 µg /ml) and 8 µl of labeled ADS1 or ADS2 LNPs were added to the adhered macrophages. A time-lapse imaging video and a z-stack image after 75 min were obtained and images were analyzed using ZEN 2012 lite software (ZEISS).

For scanning electron microscopy (SEM), macrophages were plated at 5×10^5 cells/well onto 24-well tissue culture plates (Falcon) containing clean sterile glass coverslips (Ø13 mm) and left to adhere overnight at 37 ºC in a humidified atmosphere of 5% CO_2. 8 µl of DODAB:MO (1:2) empty liposomes (total lipid concentration of 888 µg/ml), 8 µl of ADS1 or ADS2 LNPs were added to the adhered macrophages. After 30 min, cells were washed with 1× PBS and fixed according to Hoess et al [46] with some modifications. Briefly, cells were fixed with 2% glutaraldehyde in PBS (v/v) for 2h at 4 ºC and dehydrated through a series of 10 min incubations in increasing ethanol concentrations (10, 30, 50, 70, 90 and 100%). Desiccation was carried out with two mixtures of hexamethyldisilazane:ethanol (1:2, 2:1) (v/v) and pure hexamethyldisilazane for 3 min each followed by air-drying. Glass coverslips were mounted onto aluminium stubs, sputter-coated with gold and observed with an S-360 scanning electron microscope (Leo, Cambridge, USA).

2.6.3 **Cytokine production**

Macrophages were plated onto 96-well tissue culture plates (Falcon) at 3×10^5 cells/well, incubated with the prepared lipid formulations and the release of pro-inflammatory cytokine TNF-α was quantified after 2, 6 and 24 h of incubation. The Mouse TNFα Elisa Kit (Thermo Scientific) (Sensitivity: 9 pg/mL) was used according to the manufacturer's instructions. Macrophages incubated with 1µg/ml LPS were used as a positive control and macrophages alone as a negative control.

2.7. Immunization procedures

Female BALB/c mice, 8 to 10 weeks old, were purchased from Charles River (Barcelona, Spain) and kept under specific-pathogen-free conditions at the Animal Facility of the Instituto de Ciências Biomédicas Abel Salazar, Porto, Portugal. All procedures involving mice were performed according to the European Convention for the Protection of Vertebrate

Animals used for Experimental and other Scientific Purposes (ETS 123), the 86/609/EEC directive and Portuguese rules (DL 129/92).

2.7.1 Immunization protocol

Eight BALB/c mice per group, total of 4 groups, were injected subcutaneously three times with a 2-week intervening period, with 200µl of one of the following preparations: CWSP alone (50 µg/ml); DODAB:MO (1:2) empty liposomes (total lipid concentration of 888 µg/ml), ADS1 or ADS2. Following the last immunization, serum was collected by retro-orbital bleeding and mice humanely terminated by placing them in a closed chamber filled with CO_2. Spleens were aseptically removed and total splenocytes obtained by homogenization of the tissue in HBSS buffer.

2.7.2 Quantification of CWSP Specific Antibody Isotypes

Specific anti-CWSP immunoglobulins in the collected serum were quantified by an enzyme-linked immunosorbent assay (ELISA) according to Ferreirinha et al. [47]. Briefly, polystyrene microtiter plates (Nunc, Roskilde, Denmark) were coated with 5 µg/ml of CWSP and incubated overnight. Wells were then saturated for 1 h at room temperature with 1% BSA in PBS (w/v) and serial dilutions of the serum samples were plated and incubated for 2 h at room temperature. After washing, alkaline phosphatase-coupled monoclonal goat anti-mouse IgG1 and IgG2a (Southern Biotechnology Associates, Birmingham, AL) were added and incubated for 30 min at room temperature. After washing, the bound antibodies were detected by development with a substrate solution containing p-nitrophenyl phosphate (Sigma) during 30 min, and the reaction stopped by addition of 0.1 M EDTA, pH 8. The absorbance was measured at 405 nm, subtracting for each well the value of the absorbance at 570 nm. The antibody titers were expressed as the reciprocal of the highest dilution with an absorbance 2X higher than the value of the control (no serum added).

2.7.3 Analysis of Cytokine Production

Splenocytes isolated from mice were washed, re-suspended in RPMI 1640-FCS and seeded at 1×10^6 cells/ml in 96-well flat-bottom plates (Nunc). Spleen cells were stimulated *ex vivo* for 6 days with CWSP (5 µg/ml) at 37 °C in 5% CO_2. The culture supernatants were collected and IFN-γ (Sensitivity: 2 pg/mL), IL-17 (Sensitivity: 5 pg/mL), IL-10 (Sensitivity:

5.22 pg/mL) and IL-4 (Sensitivity: 2 pg/mL) levels quantified with Duo-Set ELISA kits (all from R&D Systems, Minneapolis, MN) according to the manufacturer's instructions.

2.7.4 **Proliferation of Splenocytes ex Vivo**

After *ex-vivo* stimulation with 5μg/mL CWSP, splenocytes were incubated with polystyrene monodisperse microparticles (Fluka) and the number of splenocytes determined by Flow Cytometry ((Beckman-Coulter Corporation, Hialeah, FL, USA) according to the manufacturer's instructions. CD3 was used as a positive control for proliferation.

2.8. Statistical Analyses

Data were analyzed using analysis of variance (ANOVA) followed by the Bonferroni test to compare the mean values of different groups, using GraphPad Prism 5 software (GraphPad Software, Inc., La Jolla, CA). Unless otherwise stated, results shown are from three independent experiments with three replicates. Differences were considered significant when the p value was less than 0.05.

3. RESULTS

3.1. Characterization of CWSP-loaded liposomes

In previous studies, we observed that DODAB:MO formulations with an enriched MO content assembled mainly as vesicles with lamellar structures containing inverted non-lamellar structures. This morphology is observed probably because MO is preferentially localized in the interior of the lipidic structures, due to its natural negative curvature [16, 23]. These structures will offer a high surface area that may be advantageous for entrapping/adsorbing antigens for vaccine development.

In the present study, we used liposomes based on DODAB and MO with a χDODAB of 0.33 to prepare antigen delivery systems (ADS) and evaluated the adjuvant potential of this lipid formulation. *C. albicans* CWSP obtained by using the reducing agent DTT were selected as antigens for the DODAB:MO delivery systems. Flow cytometry analysis of *C. albicans* cells after the extraction treatment confirmed the membrane integrity of yeast cells (>99% PI negative) (Figure 1), thereby ensuring that the majority of the extracted proteins are derived from the surface of the yeast cell and that cytoplasmic protein contamination is low.

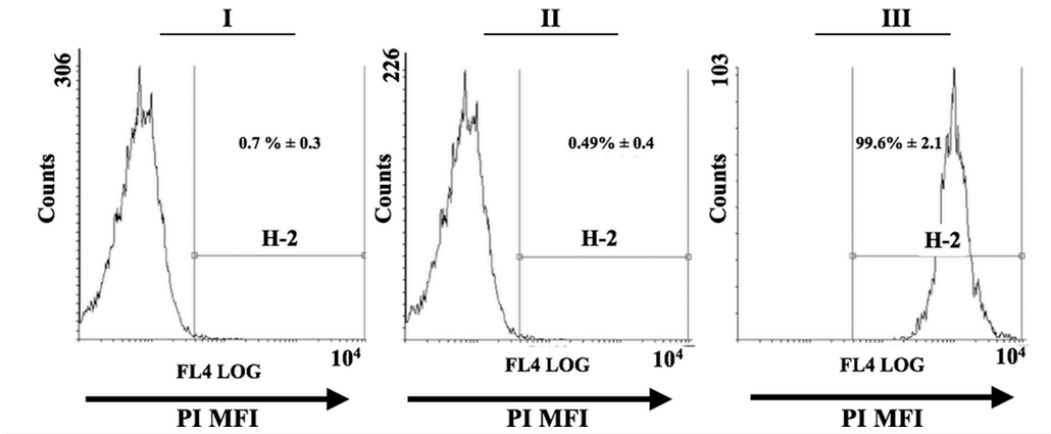

Figure 1: (A) Flow cytometry evaluation of membrane integrity of *C. albicans*. Cells were stained with the propidium iodide (PI), a membrane impermeant dye, before (I) and after (II) treatment with DTT used for CWSP extraction. Membrane disrupted, by heat, *C. albicans* cells were used as a negative control (III). In the histograms, PI stained cells percentage is indicated and gated in H-2. Histograms are a representative example from one of three independent experiments (mean ± SD). No less than 20 000 cells were analyzed per condition.

This method yielded 3 ± 0.04 μg of proteins/g of cell dry weight and DLS and ζ-potential measurements suggested polydisperse (PDI) (0.63 ± 0.01), negatively charged (-14 ± 0.70 mV) proteins with a mean size of 88.76 ± 5.1. The DLS size distributions of the extracted CWSP and can be found in supplementary information (Figure 2).

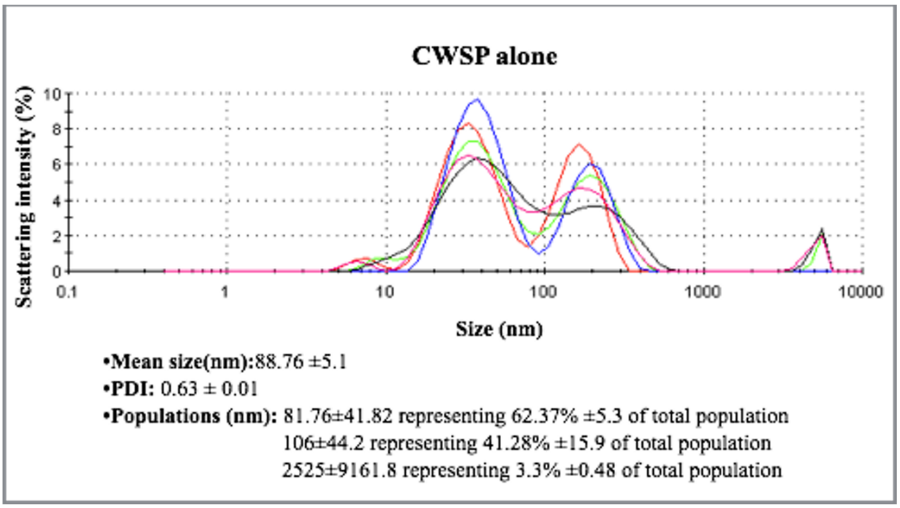

Figure 2: DLS size distributions of CWSP. The mean size, PDI and populations size are indicated. The DLS image is a representative result of three independent experiments (mean ± SEM).

DODAB:MO liposomes were relatively polydisperse, PDI ~ 0.39 ± 0.01, with a main (95 ± 6%) population size of around 245 ± 18 nm and were highly positively charged (+52 ± 2.4 mV). Since the protein-to-lipid weight ratio is highly decisive for the aggregation behavior of the liposomes [48], seven different formulations were prepared and characterized. Figure 3 includes a schematic representation of the possible protein-to-lipid interactions observed at different protein-lipid weight ratios. Analyses of the mean size and ζ- potential of these formulations indicated that at protein/lipid weight ratios below 0.014, an increase in the liposomal nanoparticle (LNP) size and heterogeneity is observed in comparison with the naked liposomes (Figure 3). The mean size of the LNPs at the lowest protein/lipid ratio (0.006) was approximately 200 nm, similar to the empty liposomes, what confirms a small adsorption of the protein at this point. The PDI of these LNPs revealed however a more polydisperse population in comparison with the naked vesicles, which can be explained by the presence of a high amount of liposomes competing for the proteins. However, at protein/lipid ratio from 0.006 to 0.014, the mean size of the LNPs increased significantly, from 207.2 ± 49.8 nm to 4143 ± 1903 nm, and this increase was characterized by aggregation

at room temperature (data not shown). It is also important to mention that the increase in mean size and PDI was accompanied by a decrease in ζ-potential from 51.1 ± 1.02 mV (naked liposomes) to 22.7 ± 1.1 mV (at weight ratio 0.014).

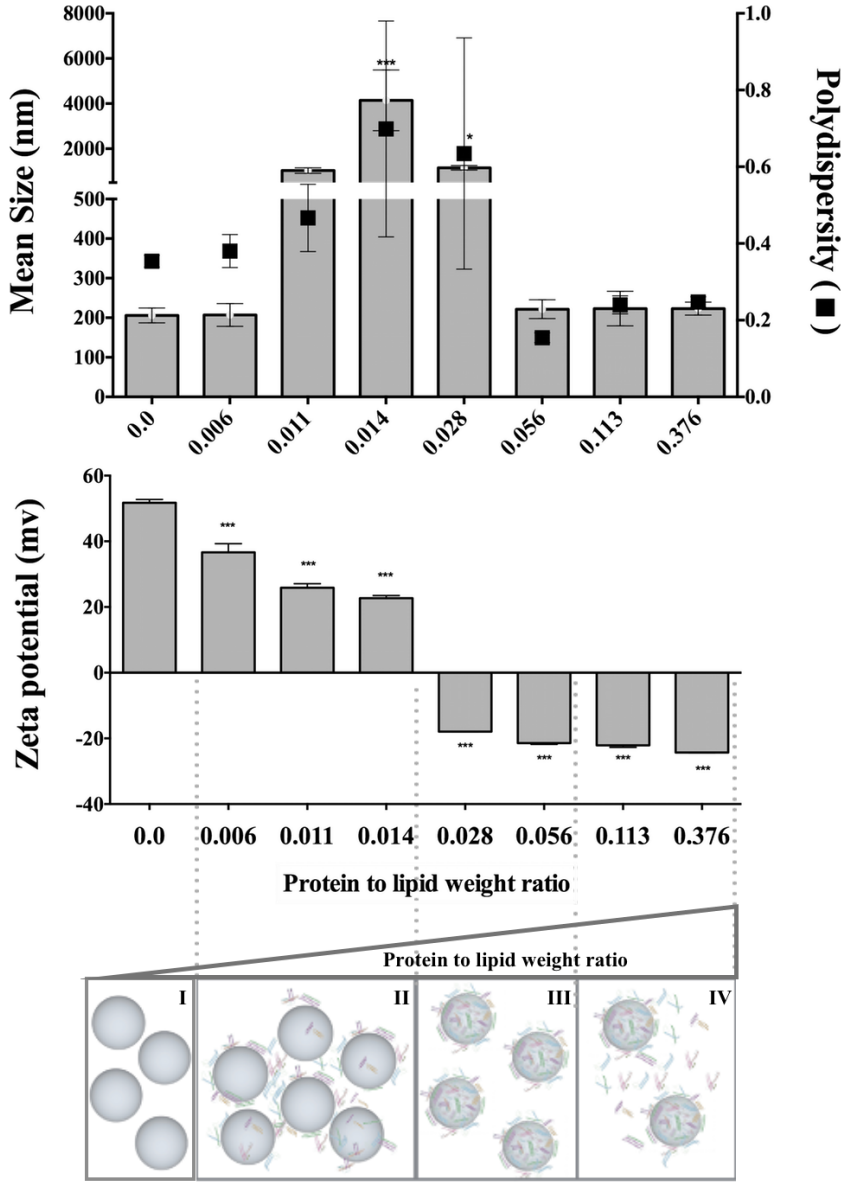

Figure 3: Representative mean size, PDI and ζ-potential of DODAB:MO LNPs at different protein-to-lipid weight ratios. At the bottom, a schematic representation of the possible interactions between proteins and liposomes: (I) empty liposomes, (II) at low protein to lipid weight ratios, liposomes and proteins interact forming unstable aggregates, (III) at intermediate protein to lipid weight ratios, liposomes adsorb more proteins, forming a protein corona around the liposomal surface that stabilizes liposomes and reduces liposome-to-liposome interactions, and (IV) at high, protein to lipid weight ratios, liposomes with a protein corona are formed and free proteins remain in solution. Significant differences between the different formulations and the empty liposomes are: */P<0.05, and ***P<0.001. All values shown are the average values from three independent experiments ± SEM.

In contrast, a LNP size reduction is observed at protein/lipid weight ratios of 0.028 and above, ranging from 1157 ± 143.5 nm to 223.1 ± 23.1 nm. In addition, at these protein/lipid ratios the ζ-potential became negative, ranging from -17.95 ± 0.07 mV to -24.03 ± 0.14 mV. This is a clear indication that, by decreasing the concentration of lipids the positive charge of this LNPs is shielded by the negative residues of the adsorbed proteins and the vesicles become negatively charged. The DLS size distributions of DODAB:MO liposomes at the different protein/lipid weight ratios are represented in Figure 4.

The morphology of the liposomal structures was determined by Cryo-SEM (Figure 5) and demonstrated that the DODAB:MO microstructure is clearly dominated by spherical vesicles of variable sizes, as already observed by DLS assays. Large vesicles (≥ 500 nm) were also detected, in some of which it is possible to observe smaller vesicles inside. It was also observed that the vesicles with a protein-to-lipid weight ratio of 0.056 had a mean particle size of around 350 nm, showing that the addition of proteins did not changed the main morphology; it only reduced the mean size of the LNPs.

Based on physicochemical properties (Figure 3), negatively charged LNPs with mean sizes around 200 nm, and acceptable PDI values were selected. The LNPs with a protein/lipid weight ratio of 0.056, designated as ADS1 (antigen delivery system 1), and the LNPs with a protein/lipid ratio of 0.376, designated as ADS2 (antigen delivery system 2) were selected. These were the LNPs with the highest (833 μg/ml) and lowest (125 μg/ml) lipid concentrations, respectively, that meet the criteria defined.

After selecting the formulations, the protein adsorption was quantified. ADS1 and ADS2 LNPs presented different degrees of antigen adsorption efficiency: 91.0 ± 9.0% for the former and 16.5 ± 4.5% for the latter, showing that an increase in the protein/lipid ratio reduced the protein adsorption. In order to confirm this trend the adsorption efficiency of the protein/lipid weight ratio 0.113 was quantified and, as expected, an intermediate value of 45.2 ± 4.9% was obtained.

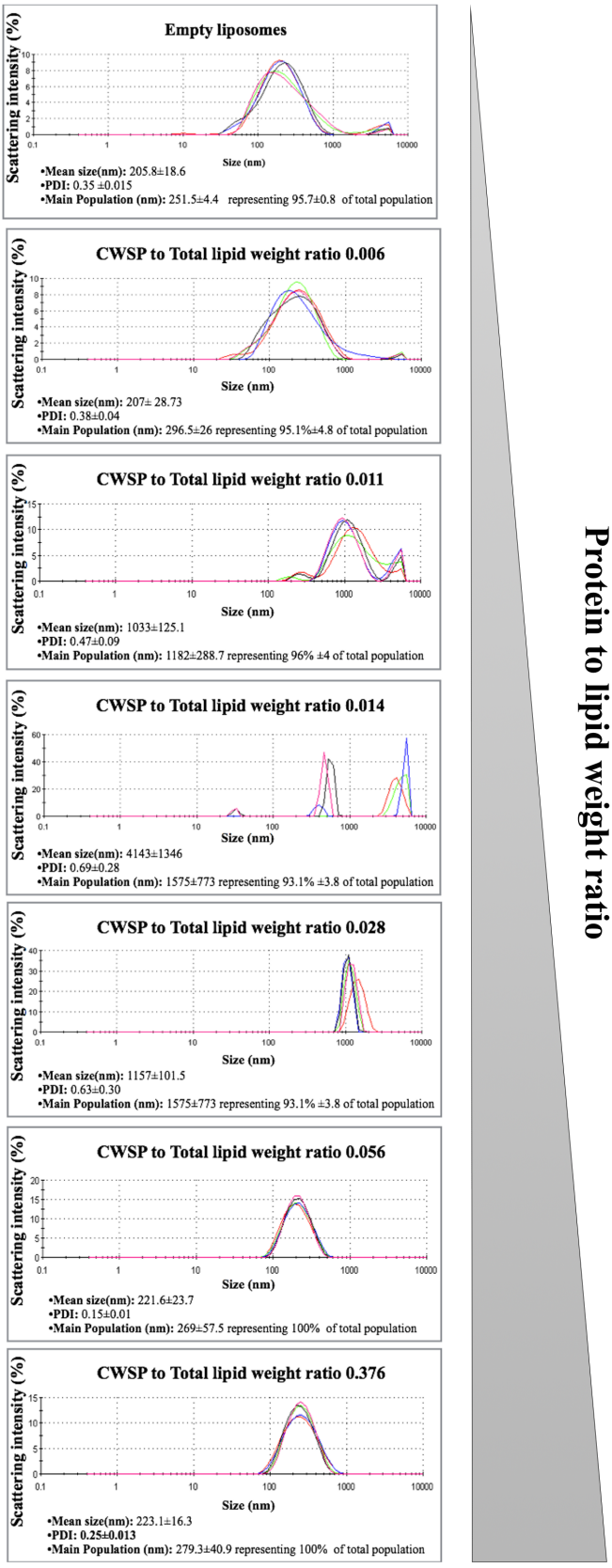

Figure 4: DLS size distributions of DODAB:MO liposomes at different protein-to-lipid weight ratios. The mean size, PDI and main population size are indicated. The DLS image is a representative result of three independent experiments (mean ± SEM).

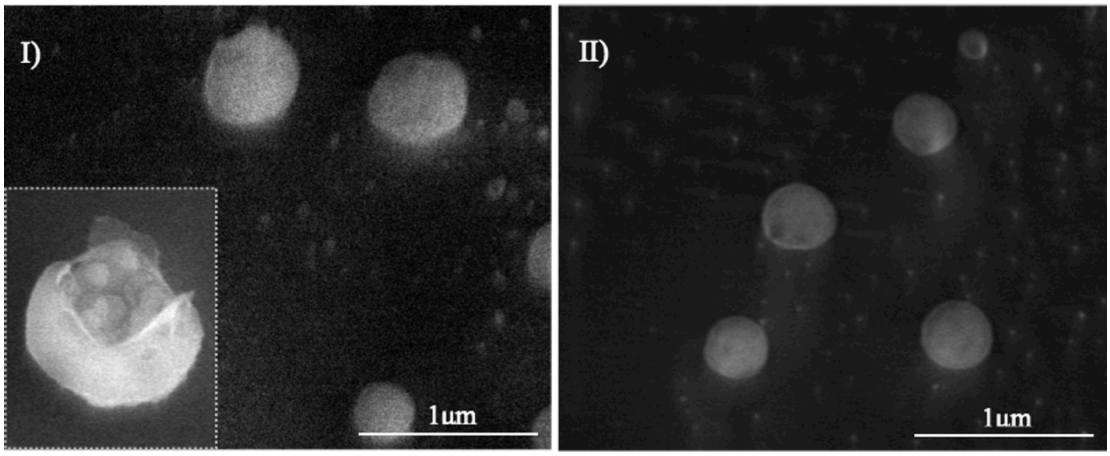

Figure 5: Representative image of DODAB:MO liposomes morphology observed by Cryo-SEM. I) Liposomes alone (36 μg/ml of total lipid) with the insert showing an open liposome and, II) liposomes (final concentration 36 μg/ml of total lipid) after incubation with the antigenic proteins (final concentration 2 μg/ml).

3.2. In vitro activation of phagocytic cells

Before evaluating the immunostimulatory potential of the formulations their associated cytotoxicity was considered. Figure 6 shows cell viability values above 81% for all formulations and lipid concentrations upon 24 and 48 h of co-incubation, indicating that the CWSP and ADSs systems are not cytotoxic to these cells.

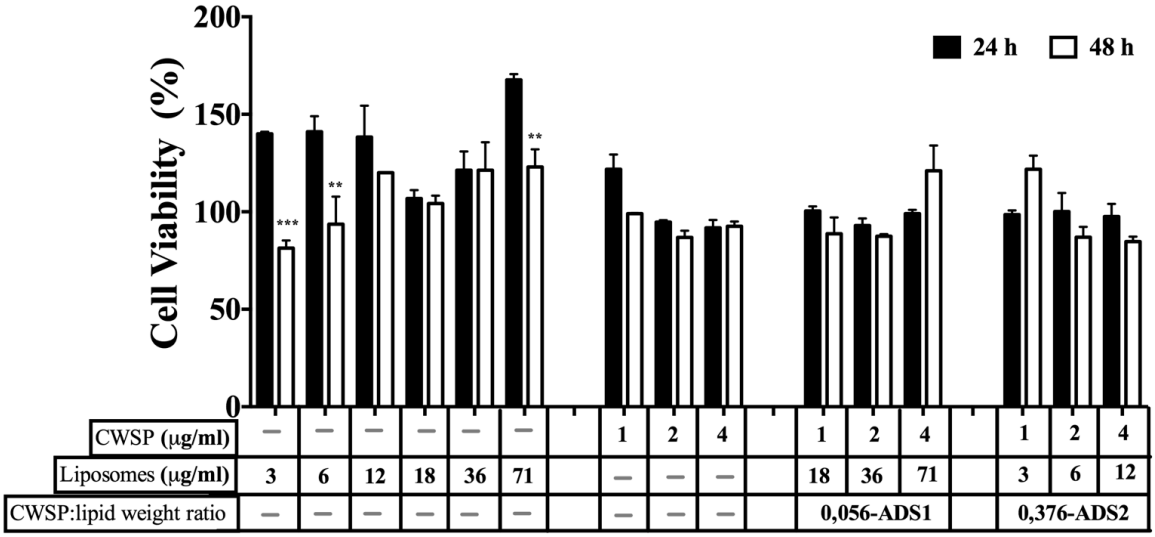

Figure 6. The effect of different concentrations of empty liposomes, CWSP, ADS1 or ADS2, on the viability of J774A.1 cells. Viability was assessed using the MTT assay after 24 h and 48 h incubation. The liposomes, CWSP and the ADSs were diluted in the cells medium and the final concentration is indicated in the x-axis. Results indicate the mean ± SEM of three independent experiments. Significant differences between the two time points, 24 h and 48 h of incubation, are indicated: (**P<0.01, ***P<0.001).

We also characterized macrophage morphology after one hour of incubation with the different formulations by scanning electron microscopy (SEM) and found these to be similar to that of the control cells (Figure 7), in agreement with the toxicity results.

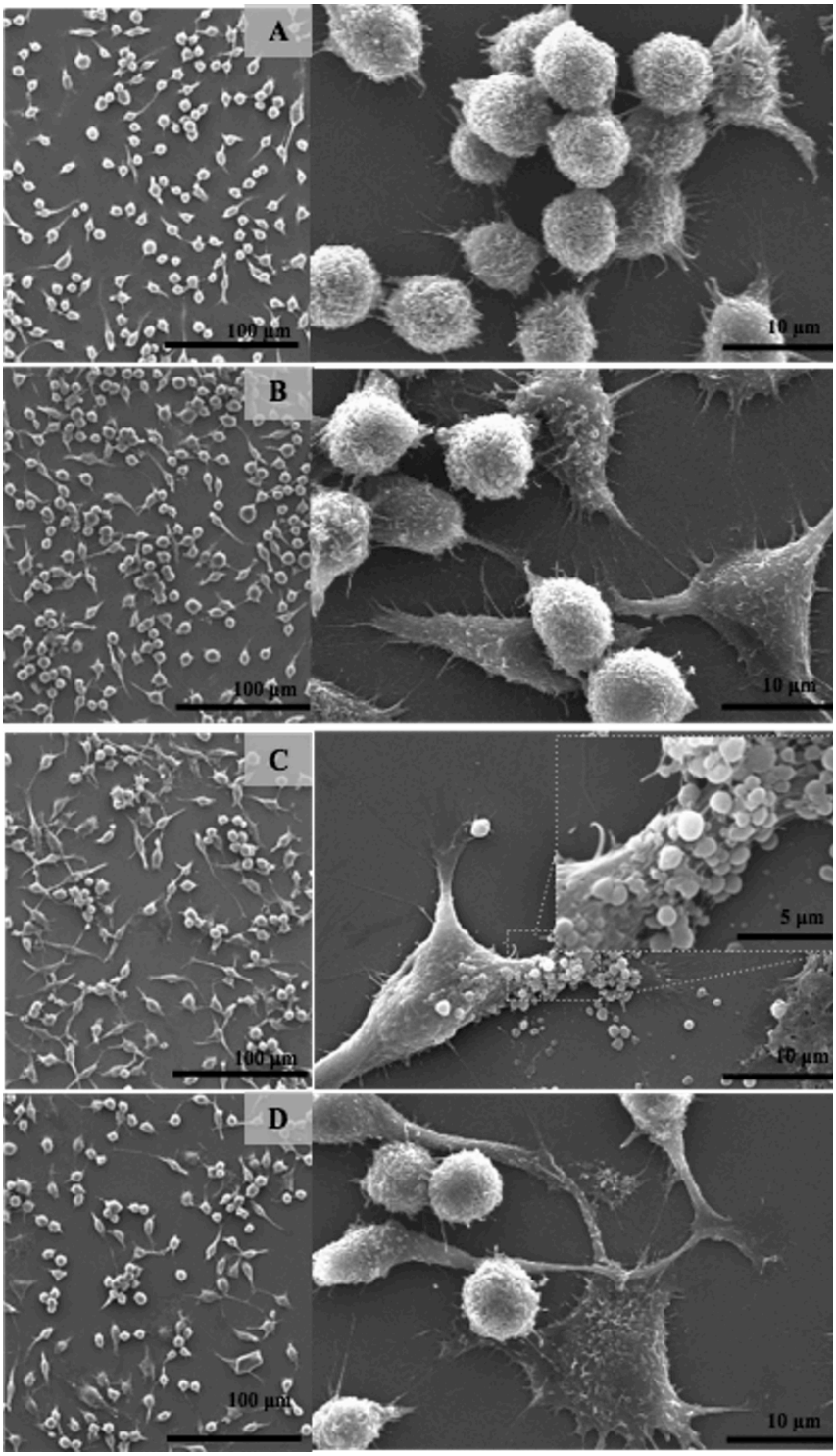

Figure 7: Representative SEM photomicrographs of macrophage cell morphology untreated (A); after 1 h incubation with empty liposomes (36 µg/ml) (B); after 1 h incubation with ADS1 (2:36 µg/ml; CWSP:Lipid) (C) or ADS2 (2:6 µg /ml; CWSP:Lipid) (D) .

ADS1 LNPs uptake by J447 cells was monitored for 70 min by confocal microscopy in order to determine uptake by macrophages (Figure 8A). A gradual intracellular accumulation of rhodamine labeled LNPs was observed with time, showing that ADS1 is efficiently taken up by macrophages (Supplementary data Movie S1).

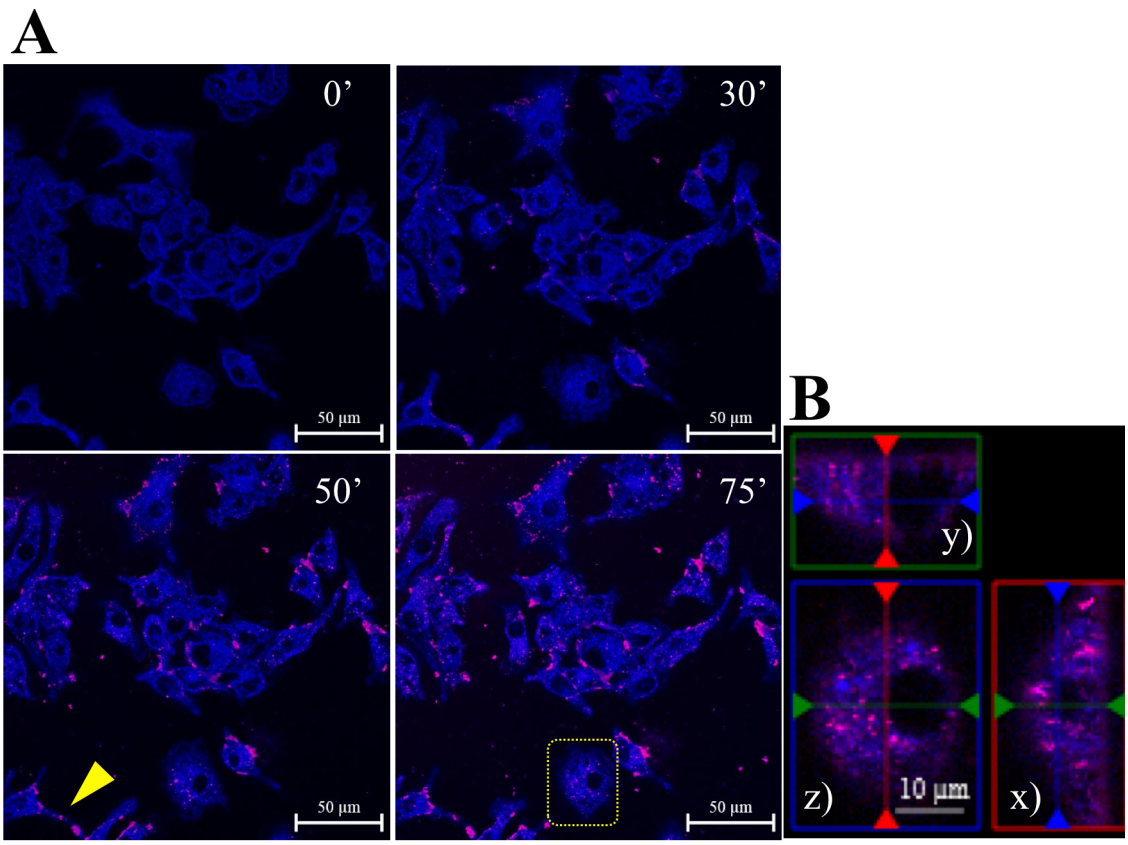

Figure 8: A representative confocal microscopy image of ADS1 uptake, by J774A.1 cells. (A) Uptake as a function of incubation time over 75 min. Rhodamine labeled ADS1 (red) superimposed with Alexa Fluor® 633 Conjugate labeled macrophages (blue). B) A mid-point thickness view (22.8 µm x 20.7 µm x 0.7 µm) of the cell, indicated by a rectangle in (A), shows rhodamine fluorescence superimposed with Alexa Fluor® 633 Conjugate fluorescence (z). Z-axis rotations of a single transverse slice through two sections of the cell: view in the x-0-z plane (x) and view in the y-0-z plane (y) are also presented.

Interestingly, an image viewed at the mid-point of cell thickness shows that most of the rhodamine fluorescence did not spread uniformly and seemed to concentrate intra-cellularly in discrete sites (Figure 8B). Rhodamine fluorescence appears to be distributed throughout the cytoplasm, the transport endosome region and in the Golgi area next to the nucleus, which itself does not reveal any fluorescence signal. By analyzing co-localization with Alexa Fluor 633 the fluorescence was observed to be within membrane-rich regions, i.e., in the cytoplasmic area and in the cellular extensions (Figure 8A - arrow head), resembling

the pattern seen after endocytosis described previously [49]. The internalization of a labeled ADS1 was estimated to be around 20 min, in agreement with other studies that assessed endocytosis of a liposome to occur within 30 min (Figure 9) [49, 50].

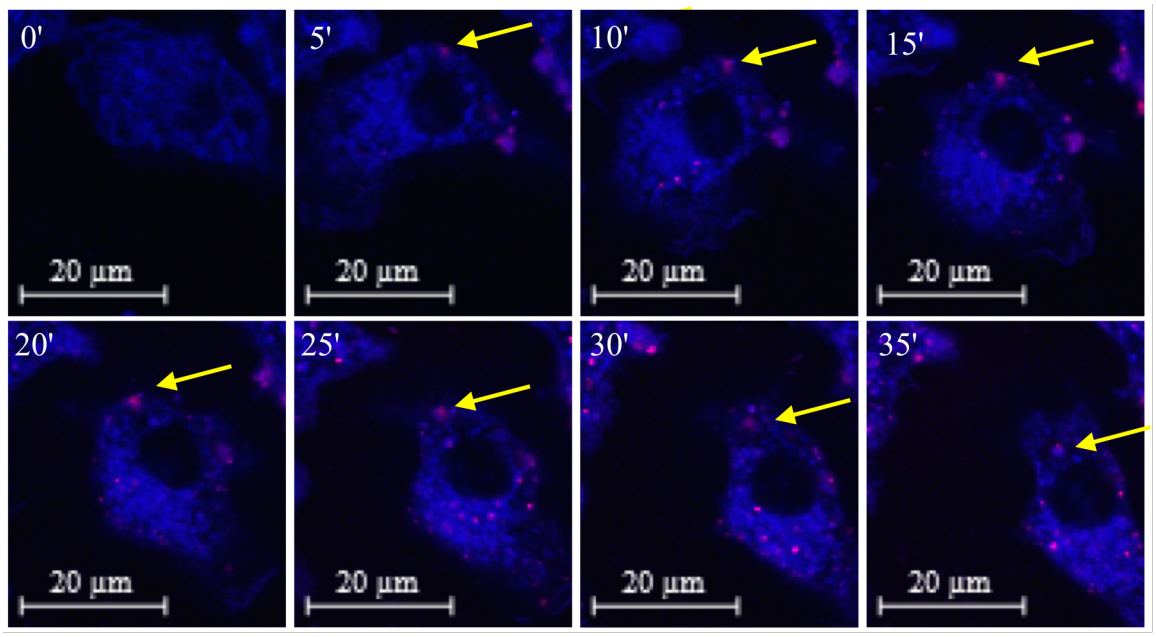

Figure 9: Representative confocal microscopy image of a time-resolved magnification of Rhodamine labeled ADS1, indicated by the yellow arrow in Figure 8A, penetrating a J774A.1 cell during 35 min. (38.66 µm x 42.61µm).

Secretion of pro-inflammatory cytokines, namely TNF-α, by the macrophages was quantified by ELISA after co-incubation with the different formulations (Figure 10). Untreated cells and cells stimulated with liposomes alone produced residual or no TNF-α. CWSP significantly ($P<0.01$) potentiated the production of TNF-α in a time dependent manner in comparison with lipids alone. ADS2 LNPs also induced TNF-α production as expected since free CWSP are also present in this formulation, but the levels were significantly lower than for CWSP ($P<0.05$). ADS1 LNPs however failed to enhance the basal levels of TNF-α production.

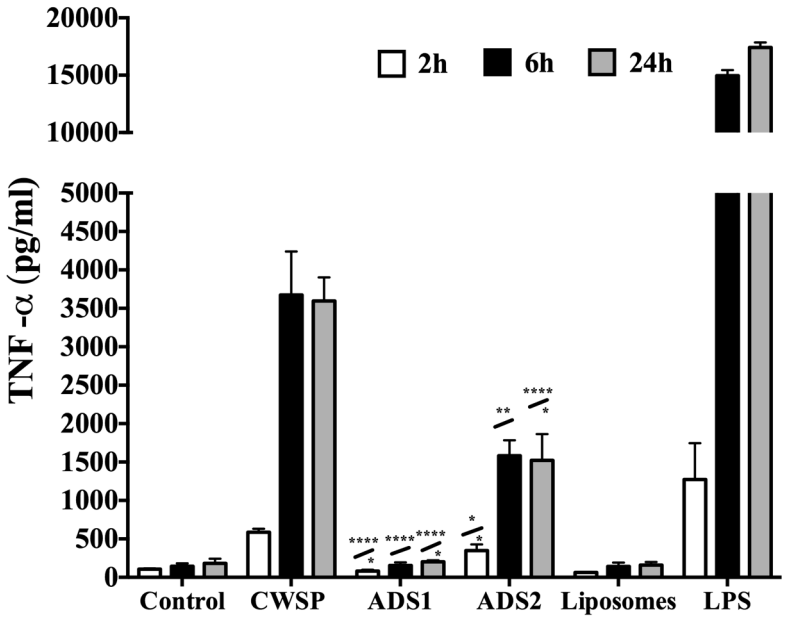

Figure 10: Production of TNF-α by J774A.1 cells after incubation with CWSP (2 μg/ml), liposomes alone (36 μg/ml), ADS1 (2:36 μg/ml; CWSP:Lipid), ADS2 (2:6 μg/ml; CWSP:Lipid), or LPS (1 μg/ml) for 2, 6 and 24 h. Results indicate the mean ± SEM of three measurements and represent three independent experiments. Significant differences between ADSs and the CWSP are shown above the symbol / and significant differences between the ADSs are shown below /: *P<0.05, **P<0.01, and ****P<0.0001.

3.3. Immunological characterization of CWSP-loaded liposomes

The potential of the ADSs to act as adjuvant/antigen delivery vehicles *in vivo*, was analyzed by determining both humoral and cell mediated immune responses elicited by the loaded CWSP. The humoral response was analyzed by quantification of CWSP-specific IgG1 and IgG2a antibody production, after immunization with ADS1, ADS2, CWSP alone or empty liposomes (Figure 11). Immunization with ADS2 induced similar levels of IgGs as immunization with the proteins alone (P>0.05). On the contrary, the IgG response of mice immunized with ADS1 was significantly higher (P<0.05) than the response observed with proteins alone.

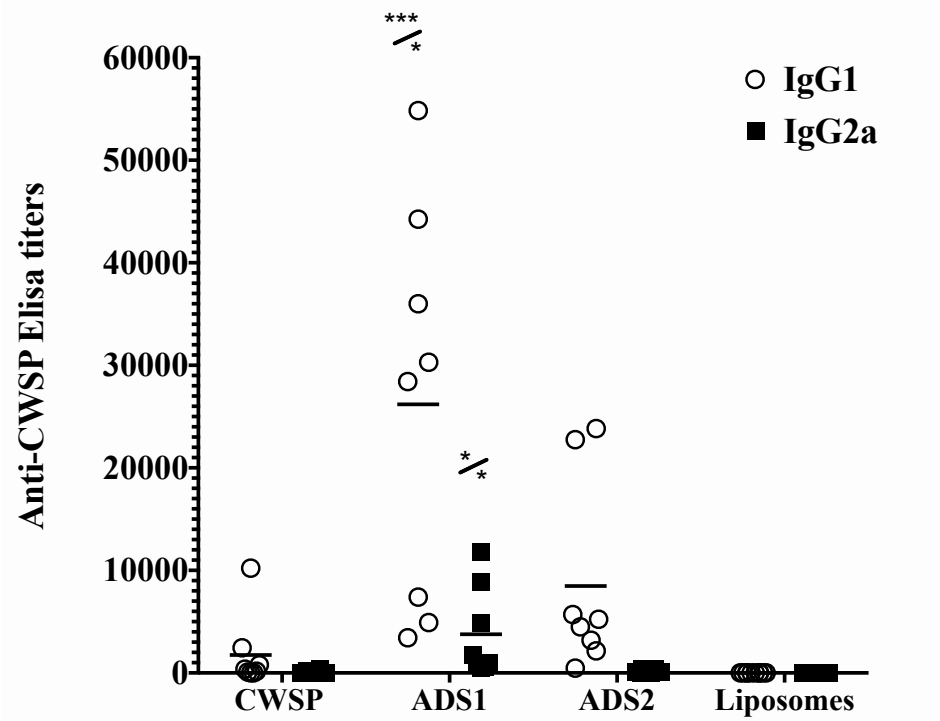

Figure 11: Anti-CWSP specific IgG1 and IgG2a responses in serum of mice immunized with 200 µl of the following: CWSP alone (50 µg/ml), ADS1 (50:888 µg/ml; CWSP:Lipid), ADS2 (50:133 µg/ml; CWSP:Lipid), or empty liposomes (888 µg/ml). The antibody titers are expressed as the reciprocal highest dilution with an absorbance 2X higher than the value of the control (no serum added). Each point represents an individual mouse. Horizontal lines correspond to the mean value in each group. Results are representative of two independent experiments. Significant differences between the ADSs LNPs and the CWSP are shown above the symbol / and significant differences between the ADSs LNPs are shown below /: *P<0.05, **P<0.01 and ***P<0.001.

Comparing the two systems, immunization with ADS1 resulted in significantly higher levels of IgG1 and IgG2a than immunization with ADS2 (P<0.05). IgG1 was the predominantly produced isotype as the ratio of IgG1:IgG2a in mice immunized with the CWSP was 21.4. However, in mice immunized with ADS1, the IgG1:IgG2a ratio was three times lower as compared to the one detected when using free-proteins, indicating that immunization with ADS1 shifted the immune response to a Th1-type (P<0.05) in comparison with mice immunized with the CWSP alone.

Cell mediated immune responses to CWSP delivered by the prepared liposomes were evaluated by splenocytes proliferation analysis and subsequent quantification of cytokine secretion after antigen re-stimulation. Results showed that, after re-stimulation, splenocytes from all groups of mice, except from mice immunized with empty liposomes, exhibited a higher (P<0.05) proliferative response in comparison with the respective non re-stimulated controls (Figure 12).

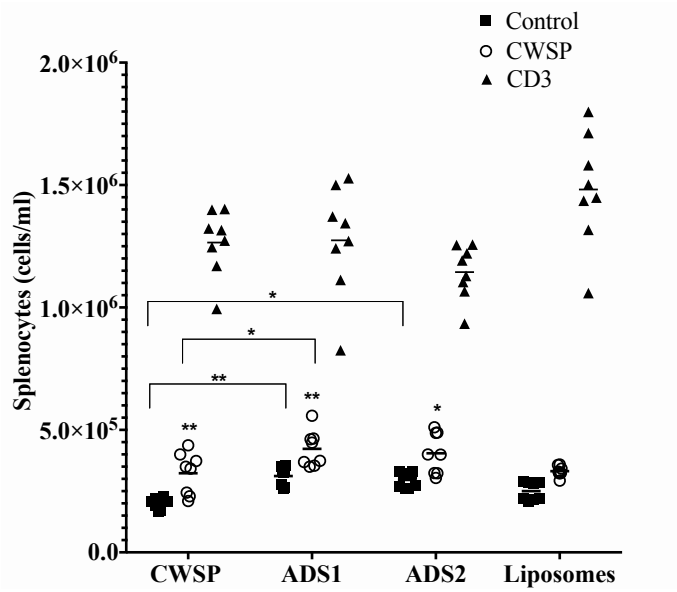

Figure 12: Splenocytes proliferation after re-stimulation with CWSP (5 μg/ml) after 6 days incubation. Controls are cells incubated in the same conditions without re-stimulation and CD3 was used as a positive control for proliferation. Each point represents an individual mouse. Results are representative of two independent experiments. Significant differences between control and re-stimulated cells are indicated above the bars and differences between the groups are indicated above the horizontal line: *P<0.05, **P<0.01.

Splenocytes from mice immunized with ADS1 showed the highest levels of proliferation and only these presented a significant proliferation (P<0.05) in comparison with cells from CWSP immunized mice. Quantification of IFN-γ and IL-17 was performed after re-stimulation with CWSP as indicators of a Th1 or Th17-type polarized response, respectively, while IL-4 and IL-10 were used as indicators of a Th2 pathway. Re-stimulated splenocytes derived from mice immunized with ADS1 or ADS2 secreted IFN-γ and IL-17A, while splenocytes from mice immunized with CWSP or liposomes alone failed to do so (Figure 13). Importantly, the levels of these cytokines were much higher in mice immunized with ADS1 (380.0 pg/ml of IFN-γ and 124.0 pg/ml of IL-17A) than with ADS2 (41.6 pg/ml of IFN-γ and 2.0 pg/ml of IL-17A) (P<0.05).

The production of IL-4 and IL-10 was investigated as an indicator of Th2 polarization. Low levels of IL-4 were detected in splenocytes of mice immunized with ADS1 (31 pg/ml) and ADS2 (11.6 pg/ml) while residual or no production was observed in mice immunized with CWSP or liposomes alone. IL-10 levels were similar in all groups (between 55.1 and 99.6 pg/ml) except for the group of mice injected with lipids alone where only residual levels were observed (1.7 pg/ml).

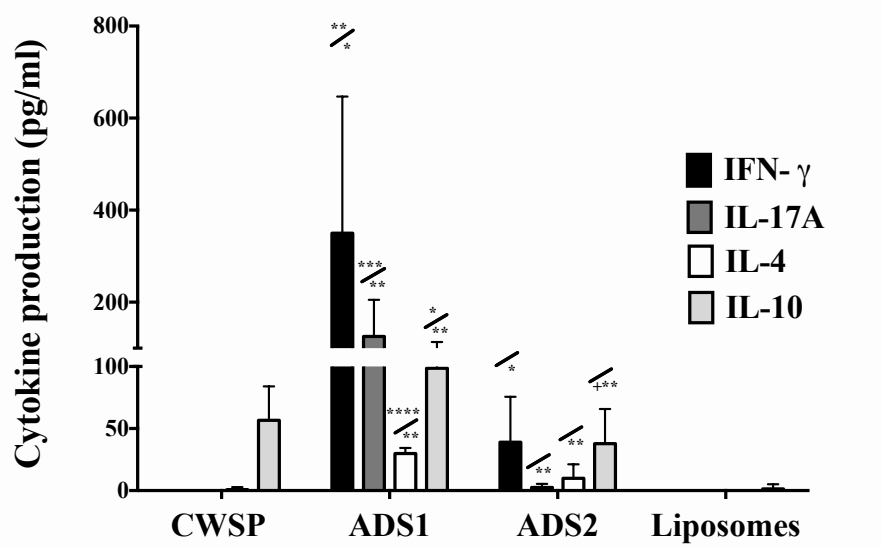

Figure 13: Cytokine production from CWSP re-stimulated splenocytes derived from mice immunized with 200 µl of the following: CWSP alone (50 µg/ml), ADS1 (50:888 µg/ml; CWSP:Lipid), ADS2 (50:133 µg/ml; CWSP:Lipid), or empty liposomes (888 µg/ml). Bars denote mean cytokine levels, and error bars denote SD of 8 mice per group. Results are representative of two independent experiments. Significant differences between the systems and the CWSP are shown above the symbol / and significant differences between systems are shown below the symbol /: *P<0.05, **P<0.01 and ***P<0.001.

As expected, no significant differences were observed regarding levels of IL-4 or IL-10 between mice immunized with CWSP and ADS2. Comparing both ADSs LNPs, the levels of IL-4 and IL-10 secreted by splenocytes of mice immunized with ADS1 were higher than of mice immunized with ADS2 (P<0.01).

3.4. Analysis of antibody specificities by Western blotting

In order to determine whether the different ADS LNPs were similarly capable of delivering proteins, immunoblotting assays were performed by combining the CWSP proteins as antigens with the serum from immunized mice. Reactivity of serum obtained from mice immunized with CWSP revealed the presence of antibodies specific for protein bands located at a molecular weight of circa 60 kDa, for a protein band of approximately 40 kDa and for others less intensely, between 10 and 15 kDa (Figure 14).

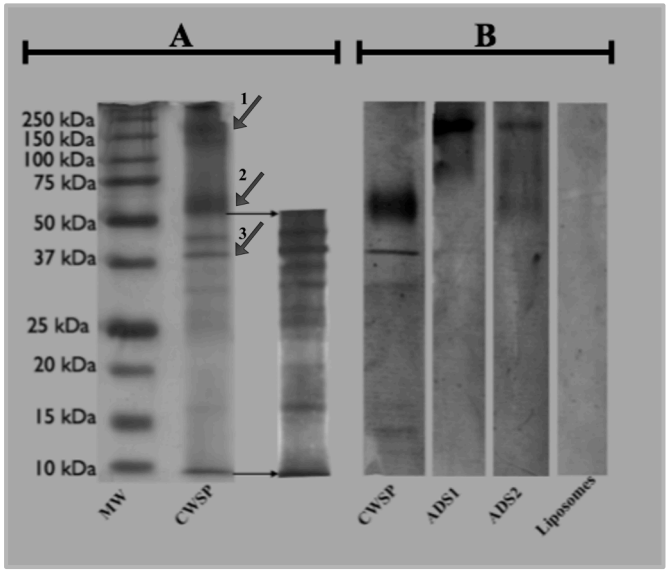

Figure 14: Western blot analysis of the *C. albicans* cell wall surface proteins (CWSP) used in the preparation of the LNPs. Proteins were separated on 12% SDS-PAGE, (between the black arrows a profile with increased resolution of the low molecular weight proteins is shown) (A), and transferred onto a PVDF membrane to be probed with serum from mice immunized with CWSP, ADS1, ADS2 or liposomes alone (B).

Curiously, serum from mice immunized with ADS1 contained antibodies mainly reactive with a protein (or proteins) with a molecular weight of approximately 200 kDa, while serum from mice immunized with ADS2 mainly contained antibodies specific for this protein but also for proteins with a molecular weight of ~ 60 kDa, as observed for the serum of mice immunized with CWSP. The reactivity detected with serum of mice immunized with ADS2 is in agreement with the fact that, with this lipid formulation, only 16% of the proteins are entrapped and most is free, as in mice immunized with CWSP alone. Protein sequence analysis revealed that the protein that was mainly identified by antibodies induced by ADS1 was Cht3p (60.0 kDa) (Figure 14, band 1), the major chitinase that has been reported to be present at *C. albicans* cell wall [51]. In contrast, the protein identified by serum of mice immunized with CWSP with a molecular weight circa 40 kDa was Xog1p (50 kDa) identified as exo-1, 3-beta-glucanase (Figure 14, band 3), which has also been identified at *C. albicans* cell wall [52]. Unfortunately, the other protein identified by the serum of CWSP immunized mice with a molecular weight ~ 60 kDa (Figure 14, band 2) could not be identified by the method applied due to the presence of several proteins in that molecular weight range. Nevertheless it is clear that the ADS1 favors the induction of antibodies against Cht3p, a protein with none or very low reactivity to be delivered alone.

4. DISCUSSION

In this study, we evaluated *"in vivo"* for the first time the ability of DODAB:MO liposomes to act simultaneously as protein delivery vehicles and immunoadjuvants. In previous studies, we observed that the introduction of MO in DODAB based liposomes at a molar fraction lower than 0.5, allowed the liposomes to assemble mainly into spherical densely packed nanoparticles [25]. These DODAB:MO based liposomes offer a high surface area that may be advantageous for adsorbing antigens for vaccine development. Therefore in the present study, we used these liposomes to prepare antigen delivery systems (ADS) with *C. albicans* cell wall surface proteins (CWSP) as antigens and evaluated their adjuvant potential. Indeed, the surface of *C. albicans* is a significant source of candidal antigens [53] and previous studies have shown that the major cell wall components that elicit a response from the host immune system are proteins and mannoproteins, in which both the carbohydrate and protein moieties are able to trigger the response [54-56].

The characterization of the prepared formulations revealed interesting features for these LNPs. At low protein/lipid weight ratios (<0.014; higher lipid concentrations) an increase in the LNPs mean size and heterogeneity is observed, in comparison with the naked liposomes, accompanied by a decrease in ζ-potential. This can be explained stepwise considering the decreasing effect of liposomes concentration for a fixed amount of protein. For the lowest protein/lipid weight ratio (0.006) there is the highest amount of cationic liposomes, and hence the ζ-potential presents positive values although slightly smaller comparing to the naked vesicles of DODAB:MO, indicating the beginning of some charge shielding made by the protein negatively charged residues. This charge neutralization may reduce the repulsion of the liposomes that tend to aggregate and thus the increase in size and PDI is due to the formation of aggregates of different sizes. In addition, the protein adsorbed at the surface might behave as linker between some positively charged LNPs promoting the aggregation, as represented in the schematic drawing proposed (Figure 3II). At ratio of 0.028 and above (lower lipid concentrations) the LNPs are now negatively charged, the size is reducing stabilizing at a protein/lipid ratio of 0.056 with lower PDI and colloidal stability. This stabilization of liposomes against aggregation may be due to the adsorption of a protein layer around the surface of the liposomes and could result in a progressive coating of the cationic head groups of the liposomes with the negatively charged CWSP and thereby forming a protein corona as already suggested by other authors [48, 57, 58]. In fact, one of the main advantages of using positively charged liposomes lies on its ability to adsorb

oppositely charged antigens. Furthermore, complexation of liposomes with the CWSP might also occur by the hydrophobic effect since some of these proteins might exhibit a substantial proportion of hydrophobic alpha-helix domains as secondary structures, which will be prone to interact with hydrophobic borders of the DODAB:MO layers. In fact, the main protein recognized by the serum of mice immunized with ADS1, the Cht3, is indicated as a probable unstable protein, considering the method of Guruprasad et al. [59].

In a previous work we characterized the DODAB:MO liposome system used in this study by Cryo-TEM and showed the presence of larger and smaller vesicles with some internal structures [25]. Indeed, cryo-SEM performed in this work confirmed spherical vesicles of variable sizes, and in some, smaller vesicles inside, in accordance with Cryo-TEM observations. In addition, Cryo-SEM showed that the addition of proteins doesn't change the main morphology of the liposomes but instead stabilizes the LNPs to a more uniform size.

One of the advantages of using liposomes is the possibility of quantitative evaluation of CWSP adsorption by means of ultracentrifugation to separate free from adsorbed proteins. ADS1 showed an adsorption efficiency of more than 90% and ADS2 around 17% with ADS1 being thus an excellent vehicle for CWSP adsorption. We also observed that from the 50 μg/ml of CWSP initially added, the amount of protein effectively adsorbed into ADS1 and ADS2 equals 45.5 and 8.25 μg/ml, respectively, resulting in an effective ratio of protein/lipid of 0.05 for ADS1 and 0.06 for ADS2, when taking into account the amount of lipid used to prepare the LNPs. Since ADS1 and ADS2 present similar LNPs sizes it appears that the stabilizing protein corona is achieved at a protein/lipid ratio of around 0.05 - 0.06 and that addition of more liposomes doesn't significantly increased the proteins absorbed, instead, the formulations aggregate and precipitation ensues. As expected, at an intermediate weight ratio of 0.113 approximately 45% of CWSP added were adsorbed confirming the optimal ratio for protein corona formation. A schematic representation of the possible LNPs structures, based on electrostatic interactions with the CWSP, is presented in figure 3.

The immunostimulatory potential of these DODAB:MO based formulations was evaluated but firstly their cytotoxic effect was examined. Cationic liposomes are well known for their toxicity in comparison to neutral or anionic liposomes and DODAB liposomes were previously shown to be cytotoxic to macrophage cultures at concentrations ≥ 50 μg/ml [60]. However, since the concentration of DODAB needed for the preparation of the formulations, used in this study, is reduced by the introduction of MO, the cytotoxic effects associated to high doses of DODAB were avoided and all formulations showed viabilities above 80%. Indeed, cationic liposomes cytotoxic effects are well-described [61] and that is why the

interest in neutral and anionic liposomes is increasing [62]. However, the adsorption of CWSP masked the cationic charge of liposomes and that might be the reason why pronounced toxicity was avoided when ADS where incubated with the cells. Moreover, the negative charge of ADSs didn't interfere with cell uptake. In fact, ADS1 was avidly internalized by macrophages as observed by the gradually intracellular accumulation of rhodamine labeled ADS1, stained with Alexa Fluor 633, in discrete sites membrane-rich regions. This pattern of internalization is similar to endocytosis pattern observed in other studies [49, 50] and was estimated to occur within 20 min, in agreement with other studies that assessed endocytosis of a liposome within 30 min [49, 50]. The mean size of the two LNPs selected may also contribute for adequate cell uptake since size range for optimal uptake of antigens and elicitation of a cellular response by dendritic cells have been determined to be below 500 nm [18, 63].

After confirmation of internalization, it was important to evaluate if the LNPs were able to activate macrophages. Our studies indicated that only, ADS2 and the CWSP were able to induce the production of the pro-inflammatory cytokine, TNF-α, in J774A.1 cells. Only residual TNF-α was obtained upon incubation of these cells with ADS1 or liposomes alone. Several studies have already reported that the cell wall components of *C. albicans* have the capacity to induce the release of pro-inflammatory cytokines upon incubation with phagocytic cells [64-67]. The fact that ADS1, contrary to ADS2, fails to stimulate these cells is probably due to all CWSP being entrapped/protected and unavailable to activate, whereas free non-encapsulated CWSP (approx.83%) are believed to be present in ADS2. Therefore, as discussed previously, the phagocytic cells rapidly internalize ADS1, but fail to activate TNF-α secretion. Similarly to these observations, it was previously described that a *C. albicans* recombinant mannoprotein was transported into the compartments of endosomes and lysosomes, degraded and loaded on major histocompatibility molecules without stimulating pro-inflammatory cytokines production [68]. The lack of evident TNF-α production could be an interesting feature of that delivery system by preventing deleterious side effects that could result from excessive inflammation still allowing antigen-delivery and the generation of an immune response [69].

Due to the results of the studies on the activation of macrophages it was thus important to evaluate whether the liposomes were able to activate the immune system *in vivo* and generate humoral and cellular responses. As expected, immunization with CWSP and ADS2 induced similar levels of IgGs, while immunization with ADS1 induced significantly

higher levels of IgGs than immunization with ADS2 ($P<0.05$). The ratio of IgG1:IgG2a in mice immunized with the CWSP was 21.4, suggesting a Th2-type immune response was generated. However, in mice immunized with ADS1, this ratio was three times lower in comparison with the one detected when using free-proteins, indicating that immunization with ADS1, promoted a shifted in the Th1/Th2 balance towards the Th1 type ($P<0.05$), as observed in previous studies with DODAB based liposomes [12]. These results show that increasing the amount of DODAB:MO liposomes used to incorporate the CWSP (ADS1) is effective in enhancing not only the levels of CWSP-IgGs but also the balance towards a Th1-type response, which is known to be protective in *C. albicans* infections [70]. In accordance with this, splenocytes of ADS1 immunized mice produced higher levels of IFN-γ and Il-17 than splenocytes from mice immunized with the other formulations after re-stimulation with the proteins. These are important indicators of T-cell activation and protective immunity and numerous vaccine studies have shown their importance in *C. albicans* vaccine efficacy [71-74]. Finally, activation of a cell-mediated immune response was also shown by the observation of splenocytes proliferation after specific re-stimulation ($P<0.05$).

An important feature of using different formulations to deliver proteins is the evaluation of whether the antibodies induced by the different liposomes/CWSP are reactive against the same proteins. In our work, immunoblotting using CWSP as antigens revealed major differences in the serum CWSP-specific antibodies produced by the different groups of immunized mice. Serum from ADS1 immunized mice showed a pattern of CWSP-specific antibodies that hybridized mainly with a high molecular weight protein identified as Cht3p (*C. albicans* cell wall chitinase). Although the molecular weight estimated in our analysis was of around 150 -200 kDa, the molecular weight of this protein has been estimated to be around 60.0 kDa. This discrepancy is probably due to glycosylation of the protein, indeed it has been described that CHT3 has four N-glycosylation sites (Asn-Xaa-Ser/Thr) and several sites for 0-mannosylation [75]. In contrast, serum from mice immunized with CWSP alone presented antibodies against proteins around 60 kDa (not identified) and the 50 kDa Xog1p (*C. albicans* exo-1,3-beta-glucanase). Curiously, ADS2 showed a pattern of hybridization that appears to include the range of proteins that hybridize with serum from mice immunized with CWSP alone and with ADS1. The differences in the hybridization patterns between the ADS1 and ADS2 are in agreement with the fact that ADS2 entraps only 16% of the CWSP while most is free, as in mice immunized with CWSP alone and ADS1 entraps 91% of the CWSP, presenting a different pattern. The major difference between Xog1p and Cht3p, besides the molecular weight, is the fact that Cht3p is unstable *in vitro*. These results reveal

interesting features for these liposomal formulations, showing that these liposomes not only enhance the immune response against proteins from the pathogenic yeast *C. albicans* but also adsorb and efficiently deliver a protein considered to be unstable *in vitro*, that otherwise was not efficiently delivered.

5. CONCLUSIONS

In this study, we prepared and evaluated *"in vivo"* for the first time the ability of DODAB:MO liposomes to act simultaneously as protein delivery vehicles and immunoadjuvants. The selected LNPs were stable, non-cytotoxic, avidly taken up by macrophages and showed a good adjuvant activity, inducing both strong antibody responses and cell-mediated immunity. In contrast to immunization with CWSP alone, these systems induced high levels of IL-17 and IFN-γ but low levels of IL-10, indicating polarization towards a Th1-type immune response and confirming their immunoadjuvant potential. Additionally, these systems favored the induction of antibodies against proteins different to those induced by CWSP alone, with mainly a protein(s), probably glycosylated, of high molecular weight being observed. The advantage of these liposomes may be associated with the fact that, as particulate carriers, they entrap and therefore protect the specific protein(s) against degradation.

Supplementary data to this chapter can be found online at
https://www.dropbox.com/s/39xq9jsvvn4yun3/Movie%20S1%20%281%29.avi?dl=0
Movie S1: Video microscopy of ADS1 uptake by J774A.1 cells as a function of incubation time over 75 min.

ACKNOWLEDGEMENTS

We thank Professor Eduardo F. Marques, Faculdade de Ciências, Universidade do Porto, and Professor Claudia Botelho, Centre of Biological Engineering, Minho University, for technical support with the Cryo-SEM and confocal microscopy analysis, respectively. We thank also Deborah Penque from the Laboratório de Proteómica, Instituto Nacional de Saúde Dr. Ricardo Jorge INSA I.P, Lisbon, Portugal, and Patrícia Alves from the Mass Spectrometry Unit (UniMS), at ITQB/iBET, Oeiras, Portugal, for their help with the proteins identification. This work was supported by FEDER through POFC – COMPETE and by national funds from FCT through the projects PEst-OE/BIA/UI4050/2014, PEst-C/FIS/UI0607/2013 (CFUM) and PTDC/QUI/69795/2006, while Catarina Carneiro holds scholarship SFRH/BD/69068/2010. We acknowledge NanoDelivery-I&D em Bionanothecnologia, Lda. for access to their equipment.

REFERENCES

1. **Henriksen-Lacey, M., Korsholm, K.S., Andersen, P., Perrie, Y., and Christensen, D.**, Liposomal vaccine delivery systems. Expert Opin Drug Deliv, 2011. **8**(4): p. 505-19.
2. **Azmi, F., Ahmad Fuaad, A.A., Skwarczynski, M., and Toth, I.**, Recent progress in adjuvant discovery for peptide-based subunit vaccines. Hum Vaccin Immunother, 2013. **10**(3).
3. **Mohammed, A.R., Bramwell, V.W., Kirby, D.J., McNeil, S.E., and Perrie, Y.**, Increased potential of a cationic liposome-based delivery system: enhancing stability and sustained immunological activity in pre-clinical development. Eur J Pharm Biopharm, 2010. **76**(3): p. 404-12.
4. **Gregory, A.E., Titball, R., and Williamson, D.**, Vaccine delivery using nanoparticles. Front Cell Infect Microbiol, 2013. **3**: p. 13.
5. **Joshi, V.B., Geary, S.M., and Salem, A.K.**, Biodegradable particles as vaccine delivery systems: size matters. AAPS J, 2013. **15**(1): p. 85-94.
6. **Garcia, A. and De Sanctis, J.B.**, An overview of adjuvant formulations and delivery systems. APMIS, 2014. **122**(4): p. 257-67.
7. **Allison, A.C.**, Immunological adjuvants and their modes of action. Arch Immunol Ther Exp (Warsz), 1997. **45**(2-3): p. 141-7.
8. **Daftarian, P.M., Stone, G.W., Kovalski, L., Kumar, M., Vosoughi, A., Urbieta, M., Blackwelder, P., Dikici, E., Serafini, P., Duffort, S., Boodoo, R., Rodriguez-Cortes, A., Lemmon, V., Deo, S., Alberola, J., Perez, V.L., Daunert, S., and Ager, A.L.**, A targeted and adjuvanted nanocarrier lowers the effective dose of liposomal amphotericin B and enhances adaptive immunity in murine cutaneous leishmaniasis. J Infect Dis, 2013. **208**(11): p. 1914-22.
9. **Jain, N.K., Mishra, V., and Mehra, N.K.**, Targeted drug delivery to macrophages. Expert Opin Drug Deliv, 2013. **10**(3): p. 353-67.
10. **Ghaffar, K.A., Giddam, A.K., Zaman, M., Skwarczynski, M., and Toth, I.**, Liposomes As Nanovaccine Delivery Systems. Curr Top Med Chem, 2014.
11. **Vabbilisetty, P. and Sun, X.L.**, Liposome surface functionalization based on different anchoring lipids via Staudinger ligation. Org Biomol Chem, 2014. **12**(8): p. 1237-44.

12. **Davidsen, J., Rosenkrands, I., Christensen, D., Vangala, A., Kirby, D., Perrie, Y., Agger, E.M., and Andersen, P.**, Characterization of cationic liposomes based on dimethyldioctadecylammonium and synthetic cord factor from *M. tuberculosis* (trehalose 6,6'-dibehenate)-a novel adjuvant inducing both strong CMI and antibody responses. Biochim Biophys Acta, 2005. **1718**(1-2): p. 22-31.
13. **Ingvarsson, P.T., Schmidt, S.T., Christensen, D., Larsen, N.B., Hinrichs, W.L., Andersen, P., Rantanen, J., Nielsen, H.M., Yang, M., and Foged, C.**, Designing CAF-adjuvanted dry powder vaccines: spray drying preserves the adjuvant activity of CAF01. J Control Release, 2013. **167**(3): p. 256-64.
14. **Neves Silva, J.P., Coutinho, P.J., and Real Oliveira, M.E.**, Characterization of monoolein-based lipoplexes using fluorescence spectroscopy. J Fluoresc, 2008. **18**(2): p. 555-62.
15. **Hussain, M.J., Wilkinson, A., Bramwell, V.W., Christensen, D., and Perrie, Y.**, Th1 immune responses can be modulated by varying dimethyldioctadecylammonium and distearoyl-sn-glycero-3-phosphocholine content in liposomal adjuvants. J Pharm Pharmacol, 2014. **66**(3): p. 358-66.
16. **Oliveira, A.C., Martens, T.F., Raemdonck, K., Adati, R.D., Feitosa, E., Botelho, C., Gomes, A.C., Braeckmans, K., and Real Oliveira, M.E.**, Dioctadecyldimethylammonium:monoolein nanocarriers for efficient in vitro gene silencing. ACS Appl Mater Interfaces, 2014.
17. **Carmona-Ribeiro, A.M.**, Biomimetic particles in drug and vaccine delivery. J Liposome Res, 2007. **17**(3-4): p. 165-72.
18. **Lincopan, N., Espindola, N.M., Vaz, A.J., da Costa, M.H., Faquim-Mauro, E., and Carmona-Ribeiro, A.M.**, Novel immunoadjuvants based on cationic lipid: Preparation, characterization and activity in vivo. Vaccine, 2009. **27**(42): p. 5760-71.
19. **Lincopan, N., Santana, M.R., Faquim-Mauro, E., da Costa, M.H., and Carmona-Ribeiro, A.M.**, Silica-based cationic bilayers as immunoadjuvants. BMC Biotechnol, 2009. **9**: p. 5.
20. **Carmona-Ribeiro, A.M.**, Bilayer-forming synthetic lipids: drugs or carriers? Curr Med Chem, 2003. **10**(22): p. 2425-46.
21. **Ogris, M., Steinlein, P., Kursa, M., Mechtler, K., Kircheis, R., and Wagner, E.**, The size of DNA/transferrin-PEI complexes is an important factor for gene expression in cultured cells. Gene Ther, 1998. **5**(10): p. 1425-33.

22. **Silva, J.P., Oliveira, I.M., Oliveira, A.C., Lucio, M., Gomes, A.C., Coutinho, P.J., and Oliveira, M.E.**, Structural dynamics and physicochemical properties of pDNA/DODAB:MO lipoplexes: effect of pH and anionic lipids in inverted non-lamellar phases versus lamellar phases. Biochim Biophys Acta, 2014. **1838**(10): p. 2555-67.

23. **Silva, J.P., Oliveira, A.C., Casal, M.P., Gomes, A.C., Coutinho, P.J., Coutinho, O.P., and Oliveira, M.E.**, DODAB:monoolein-based lipoplexes as non-viral vectors for transfection of mammalian cells. Biochim Biophys Acta, 2011. **1808**(10): p. 2440-9.

24. **Sagalowicz, L., Mezzenga, R., and Leser, M.E.**, Investigating reversed liquid crystalline mesophases. Curr. Opin. Colloid Interface Sci., 2006. **11**: p. 224–229.

25. **Oliveira, I.M., Silva, J.P., Feitosa, E., Marques, E.F., Castanheira, E.M., and Real Oliveira, M.E.**, Aggregation behavior of aqueous dioctadecyldimethylammonium bromide/monoolein mixtures: a multitechnique investigation on the influence of composition and temperature. J Colloid Interface Sci, 2012. **374**(1): p. 206-17.

26. **Lynch, M.L., Ofori-Boateng, A., Hippe, A., Kochvar, K., and Spicer, P.T.**, Enhanced loading of water-soluble actives into bicontinuous cubic phase liquid crystals using cationic surfactants. J Colloid Interface Sci, 2003. **260**(2): p. 404-13.

27. **Caffrey, M.**, A lipid's eye view of membrane protein crystallization in mesophases. Curr Opin Struct Biol, 2000. **10**(4): p. 486-97.

28. **Ai, X. and Caffrey, M.**, Membrane protein crystallization in lipidic mesophases: detergent effects. Biophys J, 2000. **79**(1): p. 394-405.

29. **El-Kirat-Chatel, S., Beaussart, A., Alsteens, D., Sarazin, A., Jouault, T., and Dufrene, Y.F.**, Single-molecule analysis of the major glycopolymers of pathogenic and non-pathogenic yeast cells. Nanoscale, 2013. **5**(11): p. 4855-63.

30. **Pietrella, D., Rachini, A., Torosantucci, A., Chiani, P., Brown, A.J., Bistoni, F., Costantino, P., Mosci, P., d'Enfert, C., Rappuoli, R., Cassone, A., and Vecchiarelli, A.**, A beta-glucan-conjugate vaccine and anti-beta-glucan antibodies are effective against murine vaginal candidiasis as assessed by a novel in vivo imaging technique. Vaccine, 2010. **28**(7): p. 1717-25.

31. **Torosantucci, A., Bromuro, C., Chiani, P., De Bernardis, F., Berti, F., Galli, C., Norelli, F., Bellucci, C., Polonelli, L., Costantino, P., Rappuoli, R., and Cassone,**

A., A novel glyco-conjugate vaccine against fungal pathogens. J Exp Med, 2005. **202**(5): p. 597-606.

32. **Paulovicova, L., Paulovicova, E., Karelin, A.A., Tsvetkov, Y.E., Nifantiev, N.E., and Bystricky, S.**, Humoral and cell-mediated immunity following vaccination with synthetic *Candida* cell wall mannan derived heptamannoside-protein conjugate: immunomodulatory properties of heptamannoside-BSA conjugate. Int Immunopharmacol, 2012. **14**(2): p. 179-87.
33. **Luo, G., Ibrahim, A.S., Spellberg, B., Nobile, C.J., Mitchell, A.P., and Fu, Y.**, *Candida albicans* Hyr1p confers resistance to neutrophil killing and is a potential vaccine target. J Infect Dis, 2010. **201**(11): p. 1718-28.
34. **Ibrahim, A.S., Spellberg, B.J., Avenissian, V., Fu, Y., Filler, S.G., and Edwards, J.E., Jr.**, Vaccination with recombinant N-terminal domain of Als1p improves survival during murine disseminated candidiasis by enhancing cell-mediated, not humoral, immunity. Infect Immun, 2005. **73**(2): p. 999-1005.
35. **Spellberg, B., Ibrahim, A.S., Yeaman, M.R., Lin, L., Fu, Y., Avanesian, V., Bayer, A.S., Filler, S.G., Lipke, P., Otoo, H., and Edwards, J.E., Jr.**, The antifungal vaccine derived from the recombinant N terminus of Als3p protects mice against the bacterium *Staphylococcus aureus.* Infect Immun, 2008. **76**(10): p. 4574-80.
36. **Luo, G., Ibrahim, A.S., French, S.W., Edwards, J.E., Jr., and Fu, Y.**, Active and passive immunization with rHyr1p-N protects mice against hematogenously disseminated candidiasis. PLoS One, 2011. **6**(10): p. e25909.
37. **Xin, H., Dziadek, S., Bundle, D.R., and Cutler, J.E.**, Synthetic glycopeptide vaccines combining beta-mannan and peptide epitopes induce protection against candidiasis. Proc Natl Acad Sci U S A, 2008. **105**(36): p. 13526-31.
38. **Xin, H. and Cutler, J.E.**, Vaccine and monoclonal antibody that enhance mouse resistance to candidiasis. Clin Vaccine Immunol, 2011. **18**(10): p. 1656-67.
39. **Paulovicova, E., Paulovicova, L., Pilisiova, R., Bystricky, S., Yashunsky, D.V., Karelin, A.A., Tsvetkov, Y.E., and Nifantiev, N.E.**, Synthetically prepared glycooligosaccharides mimicking *Candida albicans* cell wall glycan antigens - novel tools to study host-pathogen interactions. FEMS Yeast Res, 2013.
40. **Thomas, D.P., Viudes, A., Monteagudo, C., Lazzell, A.L., Saville, S.P., and Lopez-Ribot, J.L.**, A proteomic-based approach for the identification of *Candida*

albicans protein components present in a subunit vaccine that protects against disseminated candidiasis. Proteomics, 2006. **6**(22): p. 6033-41.

41. **Insenser, M.R., Hernaez, M.L., Nombela, C., Molina, M., Molero, G., and Gil, C.**, Gel and gel-free proteomics to identify *Saccharomyces cerevisiae* cell surface proteins. J Proteomics, 2010. **73**(6): p. 1183-95.
42. **Bradford, M.M.**, A rapid and sensitive method for the quantitation of microgram quantities of protein utilizing the principle of protein-dye binding. Anal Biochem, 1976. **72**: p. 248-54.
43. **Bangham, A.D., Standish, M.M., and Watkins, J.C.**, Diffusion of univalent ions across the lamellae of swollen phospholipids. J Mol Biol, 1965. **13**(1): p. 238-52.
44. **Sabino, R., Sampaio, P., Carneiro, C., Rosado, L., and Pais, C.**, Isolates from hospital environments are the most virulent of the *Candida parapsilosis* complex. BMC Microbiol, 2011. **11**: p. 180.
45. **Madesh, M. and Balasubramanian, K.A.**, A microtiter plate assay for superoxide using MTT reduction method. Indian J Biochem Biophys, 1997. **34**(6): p. 535-9.
46. **Hoess, A., Teuscher, N., Thormann, A., Aurich, H., and Heilmann, A.**, Cultivation of hepatoma cell line HepG2 on nanoporous aluminum oxide membranes. Acta Biomater, 2007. **3**(1): p. 43-50.
47. **Ferreirinha, P., Dias, J., Correia, A., Perez-Cabezas, B., Santos, C., Teixeira, L., Ribeiro, A., Rocha, A., and Vilanova, M.**, Protective effect of intranasal immunization with *Neospora caninum* membrane antigens against murine neosporosis established through the gastrointestinal tract. Immunology, 2014. **141**(2): p. 256-67.
48. **Perrie, Y., Kastner, E., Kaur, R., Wilkinson, A., and Ingham, A.J.**, A case-study investigating the physicochemical characteristics that dictate the function of a liposomal adjuvant. Hum Vaccin Immunother, 2013. **9**(6).
49. **Martina, M.S., Nicolas, V., Wilhelm, C., Menager, C., Barratt, G., and Lesieur, S.**, The in vitro kinetics of the interactions between PEG-ylated magnetic-fluid-loaded liposomes and macrophages. Biomaterials, 2007. **28**(28): p. 4143-53.
50. **Daleke, D.L., Hong, K., and Papahadjopoulos, D.**, Endocytosis of liposomes by macrophages: binding, acidification and leakage of liposomes monitored by a new fluorescence assay. Biochim Biophys Acta, 1990. **1024**(2): p. 352-66.
51. **Hernaez, M.L., Ximenez-Embun, P., Martinez-Gomariz, M., Gutierrez-Blazquez, M.D., Nombela, C., and Gil, C.**, Identification of *Candida albicans*

exposed surface proteins in vivo by a rapid proteomic approach. J Proteomics, 2010. **73**(7): p. 1404-9.

52. **Tsai, P.W., Yang, C.Y., Chang, H.T., and Lan, C.Y.**, Characterizing the role of cell-wall beta-1,3-exoglucanase Xog1p in *Candida albicans* adhesion by the human antimicrobial peptide LL-37. PLoS One, 2011. **6**(6): p. e21394.
53. **Gauglitz, G.G., Callenberg, H., Weindl, G., and Korting, H.C.**, Host defence against *Candida albicans* and the role of pattern-recognition receptors. Acta Derm Venereol, 2012. **92**(3): p. 291-8.
54. **de Groot, P.W., Bader, O., de Boer, A.D., Weig, M., and Chauhan, N.**, Adhesins in human fungal pathogens: glue with plenty of stick. Eukaryot Cell, 2013. **12**(4): p. 470-81.
55. **Lopez-Ribot, J.L., Casanova, M., Murgui, A., and Martinez, J.P.**, Antibody response to *Candida albicans* cell wall antigens. FEMS Immunol Med Microbiol, 2004. **41**(3): p. 187-96.
56. **Lowman, D.W., Greene, R.R., Bearden, D.W., Kruppa, M.D., Pottier, M., Monteiro, M.A., Soldatov, D.V., Ensley, H.E., Cheng, S.C., Netea, M.G., and Williams, D.L.**, Novel structural features in *Candida albicans* hyphal glucan provide a basis for differential innate immune recognition of hyphae versus yeast. J Biol Chem, 2014. **289**(6): p. 3432-43.
57. **Hirano, A., Yoshikawa, H., Matsushita, S., Yamada, Y., and Shiraki, K.**, Adsorption and disruption of lipid bilayers by nanoscale protein aggregates. Langmuir, 2012. **28**(8): p. 3887-95.
58. **Hamborg, M., Jorgensen, L., Bojsen, A.R., Christensen, D., and Foged, C.**, Protein antigen adsorption to the DDA/TDB liposomal adjuvant: effect on protein structure, stability, and liposome physicochemical characteristics. Pharm Res, 2013. **30**(1): p. 140-55.
59. **Guruprasad, K., Reddy, B.V., and Pandit, M.W.**, Correlation between stability of a protein and its dipeptide composition: a novel approach for predicting in vivo stability of a protein from its primary sequence. Protein Eng, 1990. **4**(2): p. 155-61.
60. **Korsholm, K.S., Agger, E.M., Foged, C., Christensen, D., Dietrich, J., Andersen, C.S., Geisler, C., and Andersen, P.**, The adjuvant mechanism of cationic dimethyldioctadecylammonium liposomes. Immunology, 2007. **121**(2): p. 216-26.
61. **Carmona-Ribeiro, A.M.**, Biomimetic nanoparticles: preparation, characterization and biomedical applications. Int J Nanomedicine, 2010. **5**: p. 249-59.

62. **Kelly, C., Jefferies, C., and Cryan, S.A.**, Targeted liposomal drug delivery to monocytes and macrophages. J Drug Deliv, 2011. **2011**: p. 727241.

63. **Xiang, S.D., Scholzen, A., Minigo, G., David, C., Apostolopoulos, V., Mottram, P.L., and Plebanski, M.**, Pathogen recognition and development of particulate vaccines: does size matter? Methods, 2006. **40**(1): p. 1-9.

64. **de Boer, A.D., de Groot, P.W., Weindl, G., Schaller, M., Riedel, D., Diez-Orejas, R., Klis, F.M., de Koster, C.G., Dekker, H.L., Gross, U., Bader, O., and Weig, M.**, The *Candida albicans* cell wall protein Rhd3/Pga29 is abundant in the yeast form and contributes to virulence. Yeast, 2010. **27**(8): p. 611-24.

65. **Pietrella, D., Bistoni, G., Corbucci, C., Perito, S., and Vecchiarelli, A.**, *Candida albicans* mannoprotein influences the biological function of dendritic cells. Cell Microbiol, 2006. **8**(4): p. 602-12.

66. **Ueno, K., Okawara, A., Yamagoe, S., Naka, T., Umeyama, T., Utena-Abe, Y., Tarumoto, N., Niimi, M., Ohno, H., Doe, M., Fujiwara, N., Kinjo, Y., and Miyazaki, Y.**, The mannan of *Candida albicans* lacking beta-1,2-linked oligomannosides increases the production of inflammatory cytokines by dendritic cells. Med Mycol, 2013. **51**(4): p. 385-95.

67. **Martinez-Esparza, M., Tapia-Abellan, A., Vitse-Standaert, A., Garcia-Penarrubia, P., Arguelles, J.C., Poulain, D., and Jouault, T.**, Glycoconjugate expression on the cell wall of tps1/tps1 trehalose-deficient *Candida albicans* strain and implications for its interaction with macrophages. Glycobiology, 2011. **21**(6): p. 796-805.

68. **Pietrella, D., Lupo, P., Rachini, A., Sandini, S., Ciervo, A., Perito, S., Bistoni, F., and Vecchiarelli, A.**, A *Candida albicans* mannoprotein deprived of its mannan moiety is efficiently taken up and processed by human dendritic cells and induces T-cell activation without stimulating proinflammatory cytokine production. Infect Immun, 2008. **76**(9): p. 4359-67.

69. **Inoue, M., Arikawa, T., Chen, Y.H., Moriwaki, Y., Price, M., Brown, M., Perfect, J.R., and Shinohara, M.L.**, T cells down-regulate macrophage TNF production by IRAK1-mediated IL-10 expression and control innate hyperinflammation. Proc Natl Acad Sci U S A, 2014. **111**(14): p. 5295-300.

70. **Spellberg, B.**, Vaccines for invasive fungal infections. F1000 Med Rep, 2011. **3**: p. 13.

71. **Hernandez-Santos, N. and Gaffen, S.L.**, Th17 cells in immunity to *Candida albicans.* Cell Host Microbe, 2012. **11**(5): p. 425-35.

72. **Romani, L.**, Immunity to fungal infections. Nat Rev Immunol, 2011. **11**(4): p. 275-88.

73. **Lin, L., Ibrahim, A.S., Xu, X., Farber, J.M., Avanesian, V., Baquir, B., Fu, Y., French, S.W., Edwards, J.E., Jr., and Spellberg, B.**, Th1-Th17 cells mediate protective adaptive immunity against Staphylococcus aureus and *Candida albicans* infection in mice. PLoS Pathog, 2009. **5**(12): p. e1000703.

74. **Spellberg, B., Ibrahim, A.S., Lin, L., Avanesian, V., Fu, Y., Lipke, P., Otoo, H., Ho, T., and Edwards, J.E., Jr.**, Antibody titer threshold predicts anti-candidal vaccine efficacy even though the mechanism of protection is induction of cell-mediated immunity. J Infect Dis, 2008. **197**(7): p. 967-71.

75. **McCreath, K.J., Specht, C.A., and Robbins, P.W.**, Molecular cloning and characterization of chitinase genes from *Candida albicans.* Proc Natl Acad Sci U S A, 1995. **92**(7): p. 2544-8.

CHAPTER VI:

Candida albicans cell wall surface proteins incorporated in DODAB:monoolein liposomes confer protection against the fungal infection in BALB/c mice

Candida albicans cell wall surface proteins incorporated in DODAB:monoolein liposomes confer protection against the fungal infection in BALB/c mice

Catarina Carneiro[1], Alexandra Correia[2], Tânia Lima[1], Manuel Vilanova[2,3], Célia Pais[1], Andreia C, Gomes[1,5], M. Elisabete C.D. Real Oliveira[4,5], Paula Sampaio[1*]

(manuscript in preparation)

[1]Centre of Molecular and Environmental Biology (CBMA), Department of Biology, University of Minho, 4710-057 Braga, Portugal

[2] IBMC-Instituto de Biologia Molecular e Celular, Rua do Campo Alegre 823, Porto, Portugal

[3] Instituto de Ciências Biomédicas de Abel Salazar (ICBAS), Universidade do Porto, Rua de Jorge Viterbo Ferreira n.º 228, 4050-313 Porto, Portugal

[4]Centre of Physics (CFUM) University of Minho, Campus of Gualtar, 4710-057 Braga, Portugal

[5]NanoDelivery I&D in Biotecnology, Biology Department, Campus of Gualtar, 4710-057 Braga, Portugal

ABSTRACT

Here, we evaluate the potential of a liposomal antigen delivery system (ADS) containing *C. albicans* cell wall surface proteins in mediate protection against systemic candidiasis. Firstly, we show that loading of the CWSP in DODAB:MO liposomes enhances and prologues the activation of dendritic cells indicating that entrapped antigen is slowly and sustained released when trapped in DODAB:MO liposomes. Then we immunized mice with free CWSP, ADS1, ADS2 or empty liposomes. The efficacy of various formulations in protecting mice against a lethal dose of *C. albicans* was determined assessing mice survival rate and kidney fungal burden. Mice immunized with ADS1 significantly extended survival time in comparison to mice immunized with either free CWSP or buffer.

Mice vaccinated with ADS1 LNPs developed a strong humoral response with specific antibodies that enhanced phagocytosis of *C. albicans* cells. In addition, this mice group developed a protective and specific Th1/Th17 response with higher frequencies of splenic $CD4^{+}IL\text{-}4^{+}$ cells and higher levels of IL-17/IL-10/IL-4 in CWSP re-stimulated splenocytes in comparison with mice immunized with free CWSP.

In this study we demonstrate that DODAB:MO liposomes enhance *C. albicans* antigens immunogenicity and that adjuvant potential was crucial in protecting mice against a systemic candidiasis

1. INTRODUCTION

Vaccines are routinely used to protect against pathogens. They generally contain antigens that mimic the disease-causing microorganism, including weakened or killed forms of the target microbe, its surface or secreted molecules. Nevertheless, the use of attenuated pathogens raises several safety issues due to possible reversion of the phenotype, and the use of single molecules may be insufficient because of antigen modifications. To overcome some of these issues, subunit vaccines, composed of nonliving or split pathogens, are being developed as immunoprotective strategies. Their effective implementation is however greatly limited by their poor immunogenicity when administered without adjuvant [1, 2]. Therefore, selecting an appropriate adjuvant or delivery system is as important as selecting the antigen candidates. For this purpose, cationic liposomes are interesting adjuvants that also serve as carriers for the targeted delivery of antigens to immune cells. These liposomes are used both as immunoadjuvants to induce cell mediated immunity or humoral immune responses to various antigens but also as delivery systems for drugs, DNA or peptides [3, 4]. In fact, cationic liposomes have the ability to tightly bind negatively charged antigen, rendering soluble antigens into a particulate form thereby lengthening their *in vivo* half-life [5, 6]. Formulating protein antigens into nanoparticles has emerged as one of the most promising strategies to trigger an immune response to vaccine antigens [4-8]. Cationic liposomes composed by surfactant dioctadecyldimethylammonium bromide (DODAB) have been used as carriers in drug delivery [7, 8] as well as adjuvants for vaccination, displaying higher colloidal stability than alum and better efficacy in inducing cellular immune responses [9-11].

Previously, we have demonstrated that monooleoyl-rac-glycerol (monoolein, MO), when used as helper lipid with DODAB, can act as a stabilizer, conferring fluidity to the DODAB nanoparticle liposomes by favoring lipid chain mobility [12]. In fact, we have successfully used DODAB:MO as a mammalian cell transfection system and as a system for *in vitro* gene silencing [8, 13]. In particular, we demonstrated that liposomes formed by DODAB and MO at DODAB:MO (1:2) molar ratio, assembled mainly as positively spherical bilamellar vesicles with some internal structures [14].

Candida albicans is an important complex opportunistic human pathogen causing infections that range from superficial mucosal lesions to life-threatening systemic diseases [15]. It is by far the most common cause of fungal invasive infections and, despite the availability of new antifungal agents, candidemia is the fourth most common bloodstream infection in hospitalized patients both in the United States and in many European countries

[16-18]. Consequently, antifungal vaccines are currently considered one of the most appealing and cost effective strategies and many laboratories are focused on the development of a vaccine against *Candida* infections [16, 19-21]. In a recent report, we described the development of two liposomal nanoparticle (LNPs) antigen delivery systems (ADS), ADS1 and ADS2, composed of DODAB:MO liposomes loaded with *C. albicans* cell wall surface proteins (CWSP) as antigens. These ADSs assembled as stable negatively charged spherical nanoparticles with an average particle size of approximately 280 nm. Their size mimicking that of natural pathogens allowed internalization and antigen presentation. Immunization with these systems resulted in an evident enhancement in both antibody responses and cell-mediated immunity when compared with freely administered CWSP [22].

In this work, we confirmed that the designed LNP vaccine is effective against systemic candidiasis. Moreover, we examined the ability of these liposomes to load and retain CWSP, their ability to deliver the antigens and enhance activation of dendritic cells, key antigen presenting cells. Moreover, *in vivo* immunization studies confirmed that these LNPs are protective against lethal systemic *C. albicans* infection, by inducing Th1/Th17 cell-mediated and humoral immunity. This study indicates that a liposomal nanoparticle based immunization with complex and heterogeneous proteins is a promising approach to improve vaccination efficacy.

2. MATERIAL AND METHODS

2.1. Materials

Dioctadecyldimethylammonium bromide (DODAB) was purchased from Tokyo Kasei (Japan). 1-monooleoyl-rac-glycerol (MO); Hanks' balanced salt solution (HBSS); glutaraldehyde; propidium iodide (PI) and DTT were supplied by Sigma–Aldrich (St. Louis, MO, USA). Tris-HCl Buffer was provided by Invitrogen/Molecular Probes (Eugene, OR, USA) and ethanol (high spectral purity) was purchased from Uvasol (Leicester, United Kingdom). Dulbecco's Modified Eagle's Medium (DMEM) was supplemented with 10% heat-inactivated fetal bovine serum (FBS), 2 mM L-glutamine, (all from Sigma-Aldrich); HEPES-Buffer solution pH 7.5 was provided by VWR International (Radnor, PA, USA) and 1 mM sodium pyruvate by Merck (Frankfurt, Germany).

2.2. *Candida albicans* and culture conditions

For cell wall surface proteins extraction, *C. albicans* strain SC5314 was used. For infection experiments *C. albicans* 124A clinical isolate was used. All strains were maintained as frozen stocks in 30% glycerol at -80°C. When needed, yeasts were obtained from a 2 day YPD agar plate (2% D-glucose, 1% Difco yeast extract, 2% peptone and 2% agar) (w/v) incubated at 30 °C.

2.3. Extraction of yeast cell wall surface proteins

All procedures used for CWSP extraction was performed in a sterile environment and using apyrogenic solutions. The CWSP were released from whole intact cells by DTT treatment as described previously [22]. The concentrated proteins obtained were stored at -80°C in aliquots of 100 μg/ml.

2.4. Preparation and characterization of CWSP-loaded liposomes

DODAB:MO based **liposomes** were prepared using the lipid-film hydration method [23]. Briefly, DODAB and MO, at a DODAB molar fraction (χDODAB) of 0.33, were dissolved in ethanol and mixed in a round-bottom flask. The solvent was removed by rotary evaporation, at a temperature 10 ºC above the main phase transition of DODAB (Tm ≈ 44 ºC), and liposomes formed after hydration of the lipid film with 25 mM HEPES pH 7.5 at 55 ºC. The dispersion was then placed in a bath sonicator during 2 min.

Two liposomal stock dispersions were prepared, stock 1, used for ADS1, at a total lipid concentration of 1774 μg/ml and stock 2, used for ADS2, at a total lipid concentration of 266 μg/ml. For the ADSs assembling, equal volumes of CWSP were added to respective stock dispersions post lipid-film hydration. For both ADSs the final concentration of CWSP was 50μg/ml. For ADS1, the final total lipid concentration was 888 μg/ml and for ADS2 was 133 μg/ml. The empty liposomes were always used at a final total lipid concentration of 888 μg/ml (Table 1). These formulations were then incubated for 1 hour, at 55 ºC, to ensure CWSP adsorption followed by a brief sonication step in a bath sonicator.

2.4.1 Quantification of protein retention

The liposomes were prepared as previously described and stored at 4 ºC. Protein retention was evaluated at different time points, 0, 3, 24, 48 and 72 h. The prepared formulations were pelleted by ultracentrifugation (100,000*g* for 1 hour), the pellet submitted to TCA protein precipitation (Thermo Scientific Pierce), and the proteins quantified with the BCA Protein Assay Kit (Thermo Scientific Pierce), according to the manufacturer's instructions. The empty liposomes were used as negative control in order to exclude lipid interference in the protein quantification method.

2.5. Stimulation of Bone Marrow Dendritic Cells (BMDCs)

Bone marrow cells were collected from femurs and tibias of BALB/c mice by flushing with cold RPMI 1640 (Sigma). Cells (1×106/mL) were cultured in 6-well plates in RPMI supplemented with 15% (v/v) J558-cell supernatant, 10% FBS (PAA), penicillin (100 U.I./mL)-streptomycin (100 μg/ml) (Sigma), and L-Glutamine (2 mM) (Sigma) and incubated at 37 ºC and 5% CO_2. Half of the medium was renewed every two days. At day 6,

BMDCs were detached and distributed in 96-well round bottom plates adjusted at a concentration of 2×10^5 cells/well in supplemented RPMI medium. Immediately after being seeded cells were stimulated with 10 µl (removed from the stock preparations indicated in Table 1) of CWPS (0.5 µg), ADS1 (0.5 µg of CWSP loaded in 8.8 µg of total lipid), ADS2 (0.5 µg of CWSP loaded in 1.33 µg of total lipid) or empty liposomes (8.8 µg of total lipid) in a final volume of 200 µl. LPS (1µg/ml) (Sigma) and un-stimulated cells were used as positive and negative controls of activation, respectively. After 6 or 24 h, the culture supernatants were removed and stored at -80 ºC. For the assessment of cell surface markers, after stimulation, the BMDC were collected from the culture plates, washed twice in Hanks's Balanced Salt Solution (Sigma) and incubated with specific cell surface antibodies. The following monoclonal antibodies (mAbs), along with the respective isotype controls were used (at previously determined optimal dilutions) [24] for immunofluorescence cytometry: fluorescein isothiocyanate (FITC) hamster anti-mouse CD11c (HL3), PE anti-mouse CD80 (B7-1) (16-10A1); PE anti-mouse CD86 (B7-2) (GL1) ; PE anti-mouse I-Ad/I-Ed (clone 2G9); all from BD Biosciences Pharmingen, San Diego, CA. The analyzed cell samples were always pre-incubated with anti-FcγR mAb before the antibody incubation to prevent non-specific antibody binding. All cytometric measurements were performed in an EPICS XL flow cytometer using the EXPO32ADC software (Beckman Coulter). The collected data files were converted using FACS CONVERT, v1.0 (Becton Dickinson) and analyzed using CELL QUEST software, v3.2.1f1 (Becton Dickinson).

The concentrations of IL-23, IL-12 and TNF-α in cell culture supernatants were quantified with the respective Mouse ELISA Ready-Set-Go kit (eBioscience, San Diego, CA) while IL-10 was quantified using the Mouse IL-10 DuoSet ELISA development system (R&D Systems, Minneapolis, MN); according to the manufacturer's instructions.

2.6. Cellular delivery of proteins by ADSs LNPs

Confocal microscopy was performed as described in our previous study [22]. Briefly, macrophages (RAW 264.7 cell line) were plated in 6-well chamber plates (Ibidi) 3 x 10^5 cells/well and left to adhere overnight at 37 °C in a humidified atmosphere of 5% CO2. Prior to LNPs preparation, DODAB:MO liposomes were labeled with Rhodamine (Rho) DHPE. Previous to incubation with Rho-DHPE labeled LNPs, macrophages were labeled with Wheat Germ Agglutinin Alexa Fluor 633 Conjugate. Labeled macrophages were then incubated

with labeled LNPs, the microscopy chamber plate placed in the integrated chamber (37 °C, 5% CO2) of LSM 780 Carl Zeiss and a mid-point cells thickness view images and z-stack images were obtained after 60 min and analyzed using ZEN 2012 lite software (ZEISS).

2.7. Immunization procedures

Female BALB/c mice, 8 to 10 weeks old, were purchased from Charles River (Barcelona, Spain) and kept under specific-pathogen-free conditions at the Animal Facility of the Instituto de Ciências Biomédicas Abel Salazar, Porto, Portugal. All procedures involving mice were performed according to the European Convention for the Protection of Vertebrate Animals used for Experimental and other Scientific Purposes (ETS 123), the 86/609/EEC directive and Portuguese rules (DL 129/92).

Nineteen BALB/c mice per group, in a total of 5 groups, were injected subcutaneously three times with a 2-week intervening period, with 200µl of one of the following preparations: CWSP alone (50 µg/ml); DODAB:MO empty liposomes (888 µg/ml), ADS1 (50:888 µg/ml; CWSP:Lipid) or ADS2 (50:133 µg/ml; CWSP:Lipid).

2.8. *C. albicans* hematogenously disseminated infections

For the survival experiment, three weeks after the last immunization, eight female BALB/c mice per group were infected intravenously (i.v.) with 1 x 10^5 *C. albicans* yeast-form cells. *C. albicans* inoculum for infection was grown in a shaking incubator for 14 h at 30 °C in Winge medium (0.2% glucose, 0.3% yeast extract). Yeast cells were harvested, washed twice with sterile, apyrogenic phosphate- buffered saline (PBS), counted in a hemocytometer, and resuspended at the appropriate concentrations. Inocula were always confirmed by CFU (colony forming units) counts on YPD agar plates at 37°C for up to 48 h. Infected mice were weighed and monitored twice daily to evaluate the progress of hematological disseminated candidemia. Moribund mice were humanely terminated, and their deaths recorded as occurring on the following day.

2.8.1 Kidney fungal burden

For the determination of organ fungal-burden, four mice per group were similarly

immunized and infected. Three and seven days *C. albicans* infection mice were sacrificed and both kidneys aseptically removed. The organs were weighed, homogenized in Hanks's Balanced Salt Solution (Sigma), and quantitatively cultured on YPD agar at 37°C. The results are expressed as log CFU per gram of tissue.

2.9. Splenocytes intracytoplasmic cytokines determination

For the determination of immunological parameters, four mice per group were similarly immunized and infected and spleens from days 0 (before infection), 3 and 7 post-infection were aseptically removed, homogenized in Hanks' balanced salt solution (Sigma) and red blood cells lysed with 0.15 M ammonium chloride. The remaining cells were counted and plated in round-bottom 96-well plates (Nunc, 1 $x10^6$ cells) in RPMI-1640 compete medium [RPMI-1640 (Sigma) supplemented with 10% fetal calf serum (PAA Laboratories), HEPES (10 mM), penicillin (200 IU/ml), streptomycin (200 g/ml) (all from Sigma) and 2-mercaptoethanol (0.1 mM) (Merk)]. Cells were incubated in a humidified atmosphere with 5% CO_2 at 37° for 5 hour under stimulation with 20 ng/ml PMA (Sigma), 200 ng/ ml ionomycin (Merk) and 10 ng/ml brefeldin A (Epicentre Biotechologies, Madison, WI). Then, cells were recovered and non-specific antibody binding was prevented by the pre-incubation with anti-FcγR mAb followed by incubation with anti-CD4 peridinin-chlorophyll protein-cychrome 5.5 (PerCP-Cy5.5)-conjugate (clone RM4- 5). Following extracellular CD4 staining cells were washed, fixed in 2% formaldehyde, washed again and permeabilized with 0.05% saponin (Sigma) in PBS solution. Intra-cytoplasmic staining was carried out with anti-interferon-γ (IFN-γ) FITC-conjugate (clone XMG1.2) (Biolegend) and anti-IL-10 phycoerythrin-conjugate (clone JES5-16E3) (BD Biosciences) or with anti-IL-4 phycoerythrin-conjugate (clone BVD4-1D11) (BD Biosciences) and anti-IL-17A FITC conjugate (clone TC11-18H10.1) (Biolegend). Antibody-labeled cells were analyzed in an EPICS XL flow cytometer using the EXPO32ADC software (Beckman Coulter). At least 150 000 events were acquired per sample. The collected data files were converted using FACS CONVERT, v1.0 (Becton Dickinson) and analyzed using CELL QUEST software, v3.2.1f1 (Becton Dickinson).

2.10. "*ex vivo*" splenocytes cytokine detection

To assess *in vitro* cytokine production by CWSP-stimulated spleen cells, 5 ml aliquots of cell suspensions prepared as described above for intra-cytoplasmic staining, were layered onto 2.5 ml of a polysucrose-sodium ditrizoate solution (Histopaque 1083®, Sigma) and centrifuged at 800*g* for 20 min at room temperature. Mononuclear cells collected from the medium–Histopaque interface were collected, washed, suspended in RPMI-1640 complete medium, plated (5x 10^5/well) in round-bottom 96-well plates, and stimulated with CWSP (final concentration of 20 μg/ml) for 3 days at 37° and 5% CO_2. The concentrations of IFN-γ, IL-4 and IL-17 in cell culture supernatants were quantified with the respective Mouse ELISA Ready-Set-Go kit (eBioscience, San Diego, CA) while IL-10 was quantified using the Mouse IL-10 DuoSet ELISA development system (R&D Systems, Minneapolis, MN); according to the manufacturer's instructions.

2.11. Phagocytosis of *C. albicans* opsonized cells

Phagocytosis analyses was assessed by flow cytometry as described by Carneiro, *et al* [25]. Briefly, fixed *C. albicans* cells were labeled with Sytox Green and opsonized (treated with 20% mice serum during 30 min at 37 °C) from mice immunized thrice with CWSP, ADS1, ADS2 or empty liposomes, then washed twice with PBS and resuspended in incomplete DMEM. RAW 264.7 macrophage were incubated with labeled yeast suspensions at MOI of 1M:5Y for 30 min, at 37 °C and 5% CO2. After incubation plates were kept on ice to stop phagocytosis, and wells rinsed twice with PBS to remove unbound yeasts. Macrophages and associated yeasts were then incubated with PI at a final concentration of 6 μg/ml, for 5 min at RT. The percentage of macrophages with internalized cells as well as the percentage of macrophages with adherent cells was determined as previously described [25] .

2.12. Statistical Analyses.

Data was analyzed using analysis of variance (ANOVA) followed by the Bonferroni test to compare the mean values of different groups, using GraphPad Prism 5 software (GraphPad Software, Inc., La Jolla, CA). Unless otherwise stated, results shown are from

three independent experiments with three replicates. Differences were considered significant when the P value was less than 0.05.

3. RESULTS

3.1. Characterization of ADS LNPs, quantification of protein retention and delivery

ADSs are liposomal nanoparticles (LNPs) prepared from DODAB:MO liposomes loaded with *C. albicans* cell wall surface antigens (CWSP) as previously described [22]. The ADS1 LNPs had a size around 223 ± 37 nm with a polydispersity index (PDI) of 0.19 ± 0.015, while ADS2 LNPs had a similar size, 255 ± 46 nm, but were more polydisperse, 0.25 ± 0.017 (Table 1). These LNPs were negatively charged, with ADS1 presenting a ζ-potential value of -18.3 ± 1.5 mV and ADS2 a ζ-potential value of -21.8 ± 1.5 mV, while DODAB:MO empty liposomes exhibited a ζ-potential value of 54.6 ± 3.2 mV, showing that antigenic proteins (CWSP) are surface adsorbed to liposomes.

Table 1: Composition, mean size and ζ-potential of ADSs liposomal nanoparticles.

	ADS1	**ADS2**	**CWSP**	**Empty liposomes**
Total lipid (μg/ml)	888	133	-	888
CWSP added (μg/ml)	50	50	50	-
Mean size (nm)	223±37	255±46	88.7±5.1	176.8±23
PDI	0.19±0.015	0.25±0.017	0.63±0.01	0.24±0.08
ζ-potential(mv)	-18.3±1.5	-21.8±1.4	-14±0.7	54.6±3.2

DODAB:MO liposomes were mixed with CWSP for 1 hour to prepare ADS1 and ADS2 and mean size and ζ-potential were measured by dynamic light scattering on a ZetaSizer NanoZS. PDI: polydispersity index.

Owing to the complexity of *Candida* cell wall antigens and their surface localization, we now focused on the stability over time of the proteins associated with the liposomes when stored at 4 ºC. Immediately after LNPs assembling (time 0), ADS1 presents 91 ± 12% of the proteins adsorbed while ADS2 shows only 25 ± 12% (Fig. 1). Although at 48h approximately 12,6% of CWSP was released from the surface of ADS1 liposomes, no significant change is observed over 72h after preparation. Thus, in this study, both systems, ADS1 and ADS2, were always used within 48h after preparation to ensure the % of CWSP absorbed. This result highlights the fact that the interactions between DODAB:MO liposomes and CWSP proteins are strong and protein adsorption on to ADS1 or ADS2 LNPs is stable, at least over a range of 72h after liposomes preparation and storage at 4 ºC.

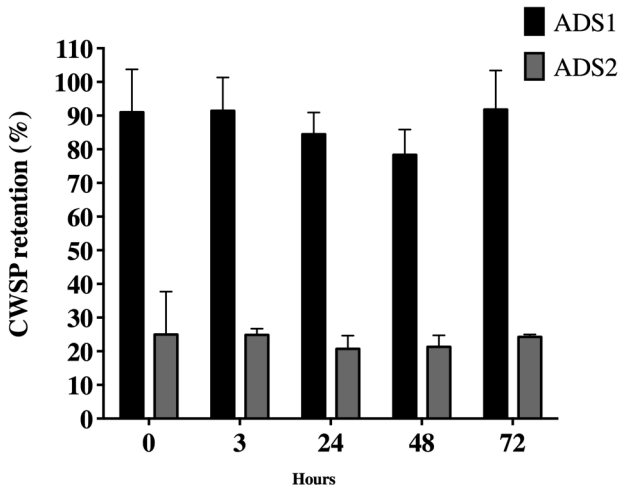

Figure 1: Percentage of CWSP retention in ADSs liposomal nanoparticles (LNPs)(ADS1 and ADS2) over time. LNPs were prepared, stored at 4 ºC, and retention of CWSP (antigen) was monitored during 72 h after preparation. Results represent percentage retention of initial antigen added (50 µg/ml for both ADSs). All values shown are the average values from two independent experiments with two replicates mean ± SD.

In our previous study we have shown that the prepared LNPs were non-toxic and avidly internalized by J774A.1 macrophages, indicating that LNPs are able to efficiently deliver antigens into this macrophages cell line [22]. In this study we confirmed that after 60 min of incubation, ADS1 also effectively delivered CWSP into the RAW 264.7 macrophage by confocal microscopy (Figure 2).

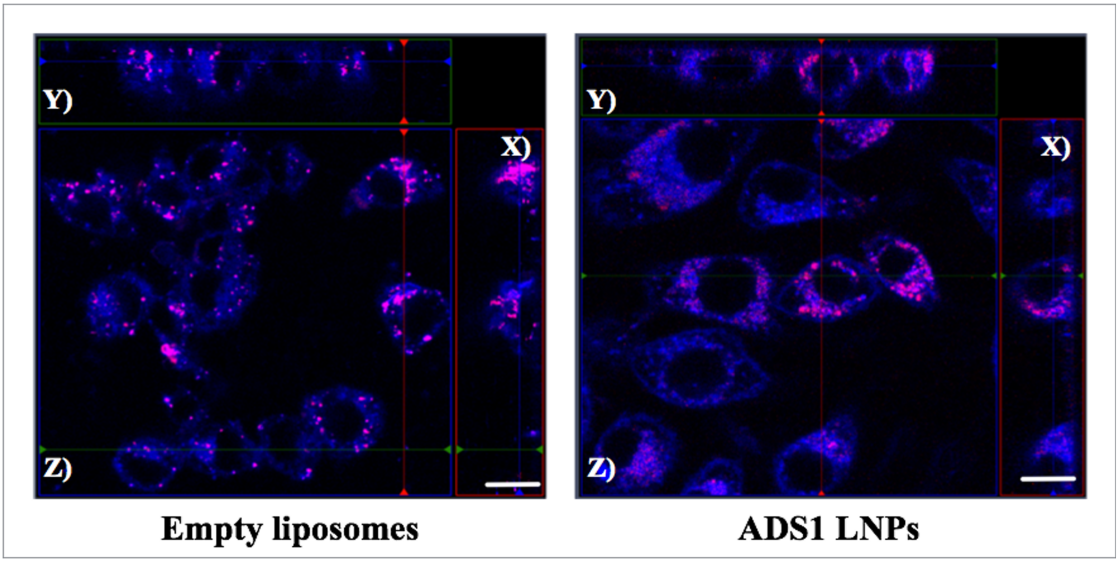

Figure 2: Cellular uptake of empty liposomes and ADS1 LNPs after 1 h min of incubation. Representation of a mid-point thickness view (X68, Y44, Z24) (z). Z-axis rotations of a single transverse slice through two sections of the cell: view in the x-0-z plane (x) and view in the y-0-z plane (y). The scale bar represents 10 nm.

3.2. Immunostimulatory efficiency of ADSs LNPs on dendritic cells

The activation of antigen presenting cells (APCs), such as dendritic cells (DCs) and macrophages, is one of the fundamental steps towards an effective *in vivo* immune response. Thus, it is important to evaluate the ability of these LNPs vaccine formulations to activate APCs *in vitro*. Therefore, BMDCs activation was assessed by measuring surface expression of co-stimulatory CD80 and CD86) and MHC class II molecules, and by quantifying pro-inflammatory cytokines TNF-α, IL-12 and IL-23 and anti-inflammatory cytokine IL-10 from the culture supernatants, after incubation with the LNPs.

Figure 3A shows that after 6 h cells stimulated with CWSP and LNPs already significantly enhanced the expression of all surface activation markers analyzed ($P<0.05$) in comparison with un-stimulated cells or cells stimulated with empty liposomes. At this time point, the LNPs enhanced activation promoted by free antigenic proteins but only regarding CD80 expression ($P<0.01$). However, after 24 h of incubation a remarked enhancement in the activation promoted by the free CWSP is achieved with ADS1 ($P<0.0001$, Figure 3A). CWSP and ADS2 failed to boost the activation and the effect achieved at 6h was even reduced after 24 h.

The BMDCs stimulated with either CWSP or ADS2 produced similar levels of TNF-α and IL-12 as those stimulated with LPS, a strong activator of the innate immune system and a potent inducer of inflammation [26]. These cells also produced significantly higher amounts of IL-23 and IL-10 ($P<0.01$) when compared with stimulation by ADS1 or empty liposomes (Figure 3B). After 24 h the levels of all these cytokines were maintained or even enhanced. On the contrary, stimulation with ADS1 led to intermediate levels of all cytokines, between the free proteins/ADS2 and liposomes alone (Figure 3B).

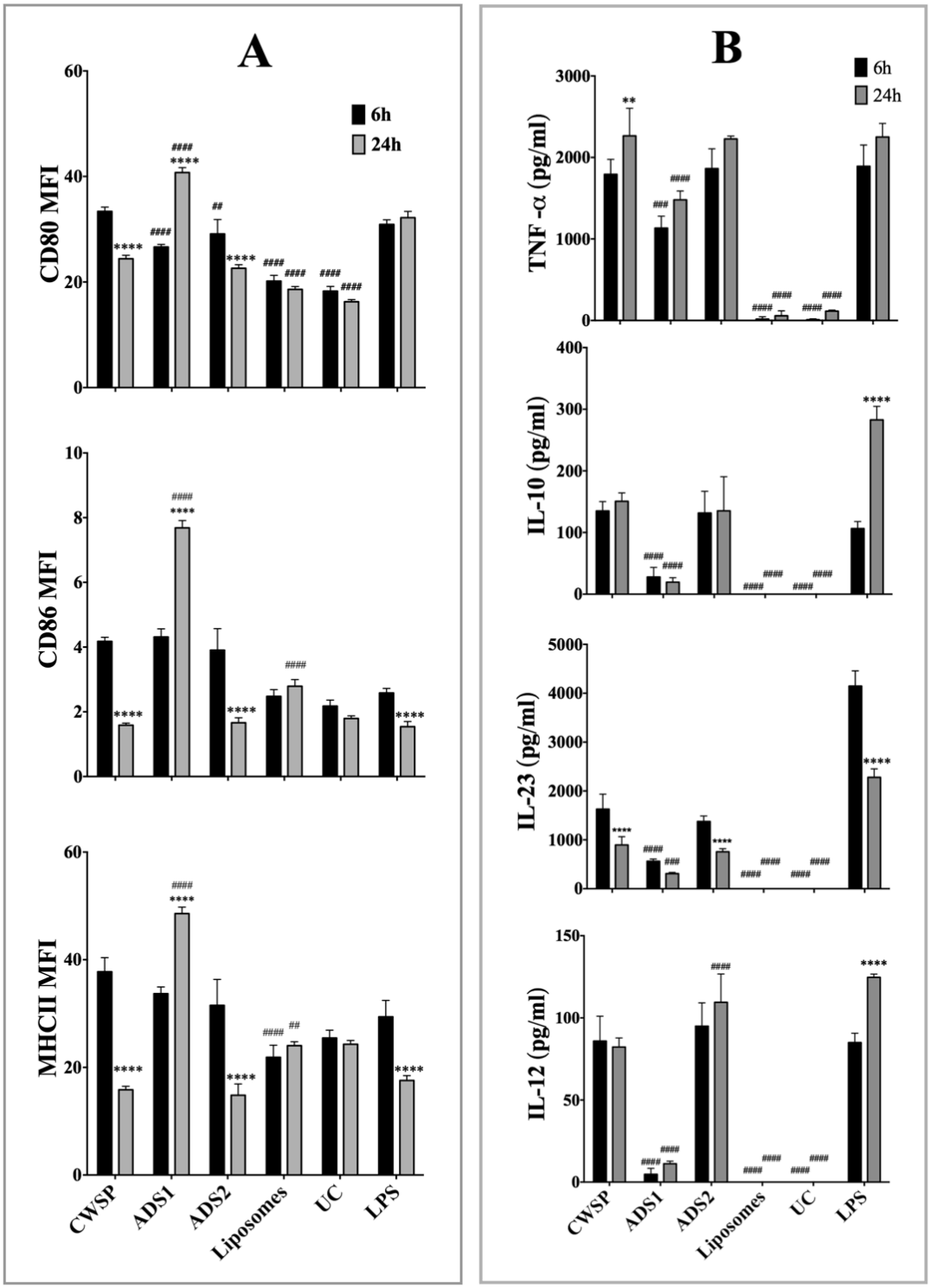

Figure 3: BMDCs activation by ADSs LNPs. BMDCs isolated from BALB/c mice were stimulated *in vitro* with CWSP, ADS1, ADS2 or Liposomes for 6 or 24 h. (**A)** BMDCs were gated on CD11c+cells and analyzed for expression of co-stimulatory (CD80, CD86) and MHC class II molecules. (**B)** Cytokine production with the indicated stimulus is represented. As references, un-stimulated cell (UC) and cells stimulated with LPS are also represented. Bars represent the mean ± SD of mean fluorescence intensity (MFI) from two independent experiments Only significant differences obtain in comparison with the free CWSP (#) and between the two time points for the same stimulus are presented: **P<0.01; ***P<0.001 and ****P<0.0001

These results suggests that both LNPs activate DCs but ADS2 and the antigens alone appear to be as inflammatory as LPS, while ADS1 activated not only reasonable amounts of cytokines but also significantly enhanced expression of co-stimulatory surface proteins.

3.3. ADSs LNPs vaccination protects against a lethal *C. albicans* infection

In order to evaluate the protective effect of LNPs vaccine against a candidemia, s.c. vaccinated and control mice were challenged with a lethal dose of *C. albicans* cells from a clinical strain obtained from a systemic infection (strain 124A, [27]), two weeks after the last immunization (a scheme of the immunization protocol is represented in Figure 4A). Mice survival was monitored over 50 days.

Infection progressed similarly in all immunized and control groups until the first week after infection, when mice immunized with HEPES-buffer began to die. As expected, mice from this control group were the first to succumb to *Candida* infection, followed by mice immunized with CWSP (Figure 4B).

ADS1 immunized mice presented a significant extended overall survival time (undefined) compared to mice immunized with CWSP (21 days, P=0.020) or with HEPES-Buffer (18 days, P=0.012). At the end of the experimental period, 62.5% of the mice immunized with ADS1 survived the infection while none of the CWSP immunized mice survived. All mice immunized with ADS2 expired at the end of the experience but presented a survival time of 30 days, between immunization with CSWP (P=0.096) and ADS1 (P=0.031).

Kidney fungal burden was evaluated and only mice immunized with ADS1 LNPs were able to significantly reduce ($P<0.01$) fungal burden from day three to seven post infection (Figure 4C). Vaccination of mice with ADS2 LNPs or CWSP also reduced fungal burden, even if without statistical significance. Although immunization with ADS1 resulted in significant reduction in CFUs, the fungal burden at day seven was still comparable to those observed in mice immunized with CWSP and ADS2.

These results demonstrate that the ADS1 LNPs vaccine protects against lethal infection even using a *C. albicans* strain different from the origin of the isolated antigens, and that protection correlated with a significant reduction in fungal burden but not total CFU counts.

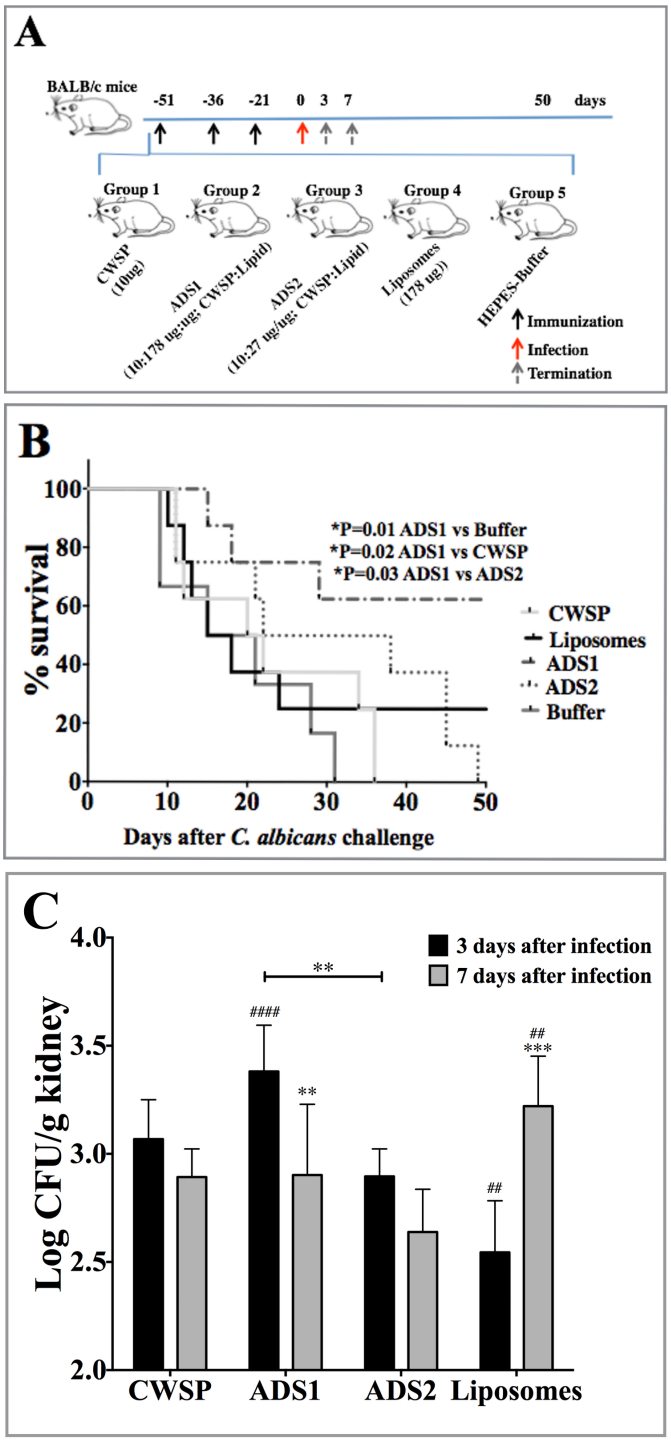

Figure 4: Mice protection after ADS LNPs vaccination. Naive BALB/c mice were immunized s.c. with CWSP, ADS1, ADS2 or empty Liposomes, boosted 2 times, with an intervening interval of 2 weeks, and infected intravenously (i.v.) with 1 x 10^5 *C. albicans* yeast-form cells, 21 days after the last s.c. immunization. At days 0, 3 and 7 after infection mice were sacrificed for immunological studies (A) Scheme of the immunization protocol. (B) Survival rates of immunized mice. Eight mice per group were used. (C) Kidney fungal burden of mice sacrificed at 3 and 7 days after *C. albicans* infection. Data are displayed as mean ± SD of four mice used per group. Only significant differences obtain in comparison with the free CWSP (#), and between the two time points for the same stimulus (*) are represented: (**P<0.01, ***P<0.001).

3.4. Production of antigen specific antibodies *in vivo*

Serum IgG titers of BALB/c mice vaccinated with ADSs LNPs or CWSP alone were quantified before and after infection. Before infection, immunization with ADS2 or with free CWSP induced similar levels of both anti-CWSP IgG1 and IgG2a. Only ADS1 induced a significant increase in serum anti-CWSP antibody titers in comparison with all other groups ($P<0.05$, Figure 5).

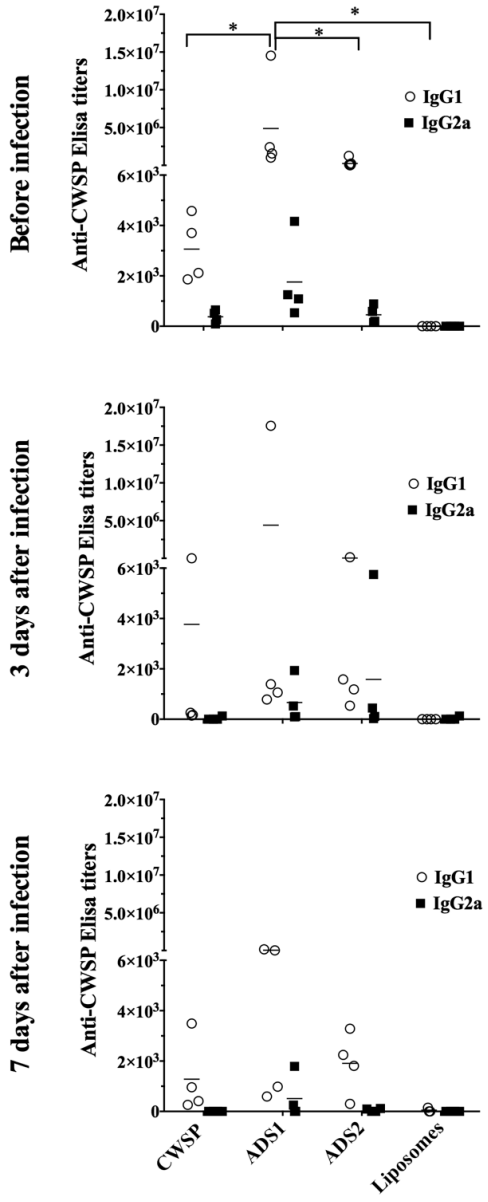

Figure 5: CWSP-specific IgGs antibody titers. Specific anti-CWSP IgG1 and IgG2a were quantified in mice immunized s.c. with CWSP, ADS1, ADS2 or empty Liposomes. Antibody titers were measured by ELISA using sera collected 21 days after the last s.c. immunization (before infection) and 3 and 7 days post-intravenous (i.v.) infection with 1 x 10^5 *C. albicans* yeast-form cells. Data are representative of at least three independent experiments. The statistical significance between the different groups is indicated above the lines: *$P<0.05$.

After infection, a significant reduction in anti-CWSP IgGs was observed, at both time points and for all groups of mice.The efficacy of sera from immunized mice in enhancing the phagocytosis of *C. albicans* cells was tested *in vitro* by flow cytometry, with a methodology that enables the discrimination of yeast cells that are internalized from yeast cells that are only adhered to phagocytes [25]. It is clear that *C. albicans* cell pre-treated with serum from mice immunized with LNPs were significantly better internalized/adhered by macrophages than yeast cells incubated with serum from mice immunized with empty liposomes ($P<0.01$), in which no anti-CWSP IgGs were detected (Figure 6). This indicates that the enhancement in the percentage of internalized/adhered cells by macrophages may be associated to the presence of anti-CWSP IgGs. The same trend was observed when comparing cells incubated with serum from mice immunized with LNPs or with CWSP alone ($P<0.001$).

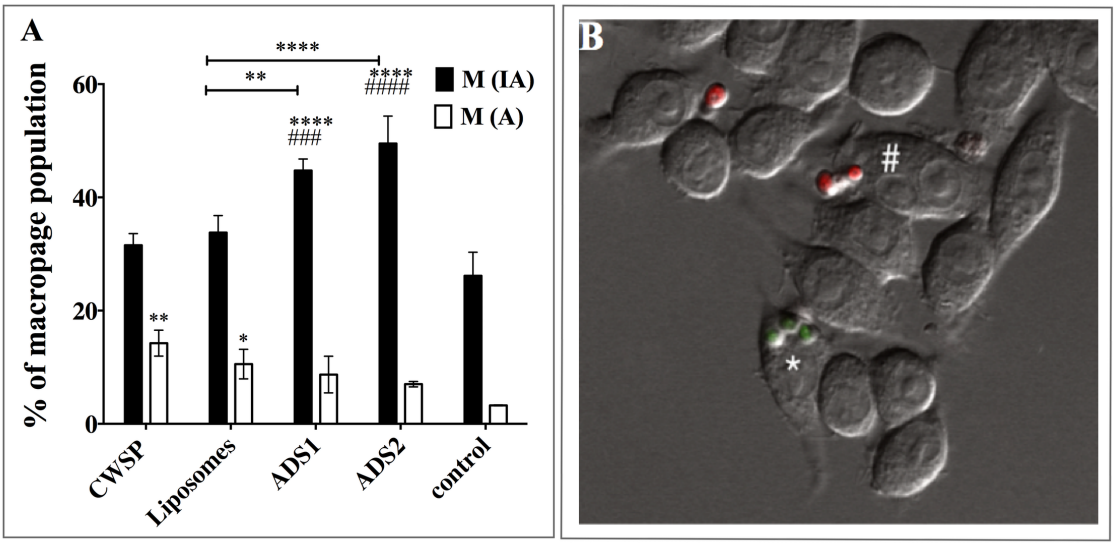

Figure 6: Antibody opsonization enhances macrophage-mediated internalization of *C. albicans* yeast cells. Serum from mice immunized with CWSP, ADS1, ADS2 or empty liposomes were used to opsonize the yeast cells before interaction with RAW264.7 (**A**) Phagocytosis was measured after 30 min of incubation, by flow cytometry. M(IA) represent the percentage of macrophages cells with internalized (Sytox Green positive fluorescence) and internalized/adhered yeast cells (Sytox Green/IP positive fluorescence); M(A), percentage of macrophage cells with only adhered yeast cells (IP positive fluorescence). Control represents non-opsonized yeast cells. (**B**) Representative image of internalized (Sytox Green positive, *) and adhered (IP positive, #) yeast cells. Bars represent mean ± SD. Significant differences between sera from ADSs and the liposomes immunized mice are represented above the lines and significant differences between sera from ADSs and the CWSP immunized mice are represented as #: *P<0.05; **P<0.01, ****P<0.0001.

Although serum from CWSP immunized mice contained anti-CWSP IgGs, no differences in the percentage of internalized/adhered yeast were observed for yeast cells

treated with this serum in comparison with cells treated with serum from mice immunized with empty liposomes. This result indicates that serum from CWSP immunized mice is not efficient in inducing cell opsonization.

According to these results, mice immunized with LNPs presented a significant increase in serum anti-CWSP antibody titers before infection that markedly enhanced *ex vivo* phagocytosis of *C. albicans* yeast cells. Immunization with ADS1 LNPs resulted in superior protection, indicating that protection seems to be correlated with opsonizing antibody titers before infection.

3.5. Splenocytes stimulation and intracellular cytokine quantification

Cell-mediated immune response is essential for the control of *C. albicans* and Th1/Th17 cytokines are critical for coordinating protective immunity against the fungus. Thus, to determine whether immunization with LNPs could induce cellular immunity, Th1 (IFN- γ), Th2 (IL-4), Treg (IL-10) and Th17 (IL-17) cytokines were analyzed in the supernatant of CWSP-re-stimulated splenocytes from immunized mice. The frequencies of splenic CD4+ T cells producing these cytokines were also assessed.

Before infection, CWSP re-stimulated splenocytes from mice immunized with ADSs LNPs produced higher levels of IFN-γ and IL-17 ($P<0.05$) in comparison with re-stimulated splenocytes from mice immunized with CWSP or liposomes (Figure 7). Although low, levels of IL-4 and IL-10 were detectable in splenocytes from mice immunized with the LNPs but, at this time point, no significant differences between groups were observed. After *C. albicans* i.v. infection, the levels of IFN-γ increased significantly for all groups of mice, at the acute phase (3 days post-infection), decreasing again by day seven to levels similar to those before infection, except for mice immunized with empty liposomes ($P<0.0001$) (Figure 7). The same pattern was observed for IL-4, but at day seven post-infection its levels remained higher than before infection for the LNPs. Only LNPs were capable of inducing significant levels of IL-17, and mice immunized with ADS1 showed the highest levels at three days post-infection ($P<0.001$), diminishing at day seven, albeit being the only group that retained significant levels of this cytokine (Figure 7).

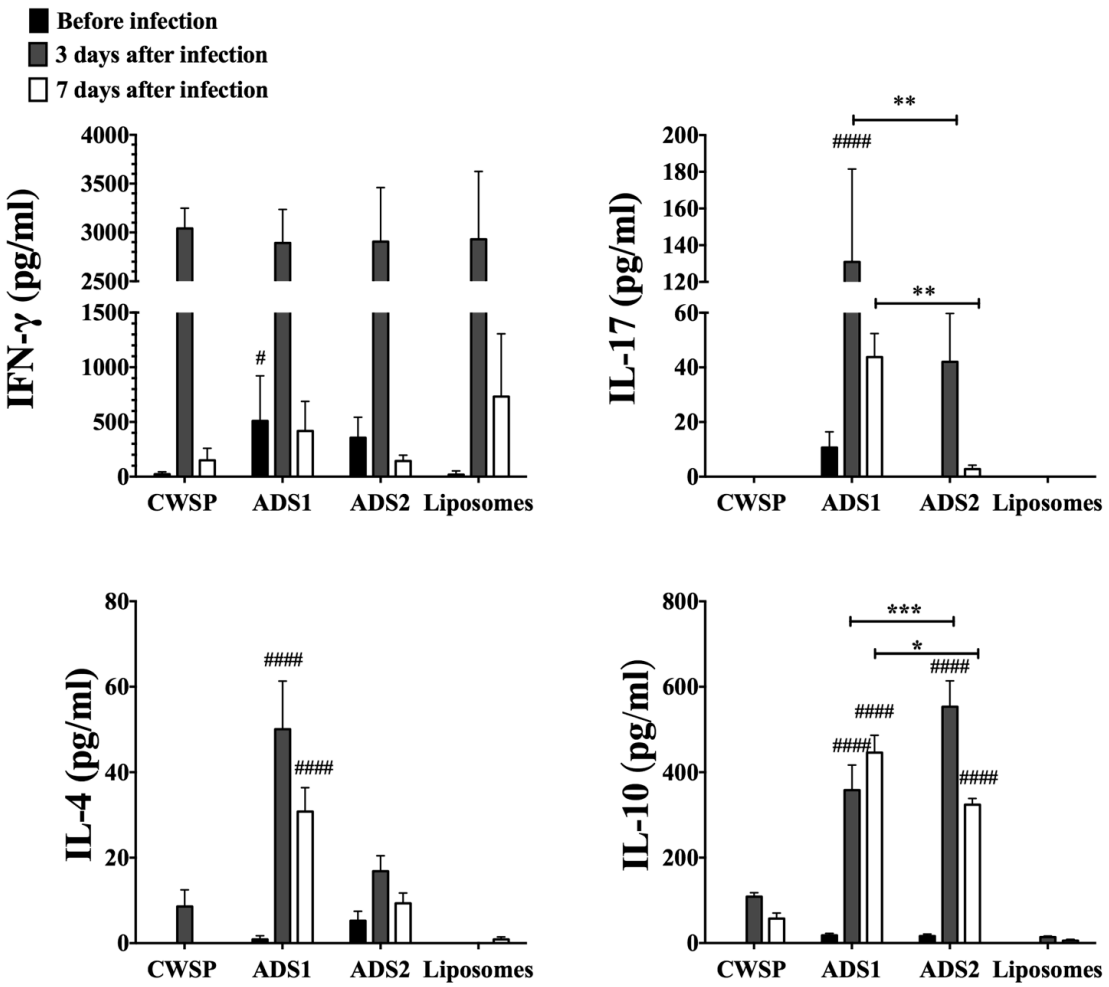

Figure 7: Cytokine production after splenocytes re-stimulation with CWSP. Splenocytes from mice s.c. immunized with CWSP, ADS1, ADS2 or liposomes were isolated 21 days after the last s.c. immunization (before infection) and 3 and 7 days post-intravenous (i.v.) infection with 1 x 10^5 *C. albicans* yeast-form cells. Re-stimulation with CWSP (20 μg/ml) was performed for 3 days and IFN- γ, IL-17, IL-4 and IL-10 quantified by ELISA. Bars represent mean ± SD of four mice used per group. Only significant differences obtain in comparison with the free CWSP (#), significant differences between the two time points for the same group of immunized mice and significant differences between ADSs are represented: **P<0.01; ***P<0.001 and ****P<0.0001.

Moreover, mice immunized with LNPs presented the highest levels of Treg IL-10, at day 3 post-infection, while for all other groups the levels of this cytokine diminished. At day seven post-infection, levels of Treg IL-10 continued to increase only in ADS1 immunized mice, being significantly higher compared to all other groups (P<0.05).

The frequency of splenic $CD4^+$ T cells producing IFN-γ increased for all groups at day 3 post-infection, in comparison with values observed before infection. At day seven, for mice immunized with CWSP, ADS1 and ADS2, the levels of $CD4^+$ T cells producing IFN-γ were significantly diminished (Figure 8A) to levels similar to those observed before infection (P<0.05), as observed in figure 7. A significant increase in the frequency of $CD4^+$ cells

secreting IL-4 ($P<0.001$) and IL-10 ($P<0.01$) was observed for mice immunized with LNPs at the acute phase of infection, in comparison with mice immunized with the free proteins or empty liposomes, remaining relatively high at day seven post-infection, particularly for ADS1 immunized mice (Figure 8A). Of note is the fact that mice immunized with ADS1 enhanced the frequency of $CD4^+$ cells expressing IL-17 at day three post-infection ($P<0.05$) in comparison with mice immunized with CWSP and empty liposomes (Figure 8B). As expected, these results are in accordance with the cytokine profile observed analyzing total splenocytes.

These results indicate that immunization with LNPs primed lymphocytes to produce pro-inflammatory Th1/Th17 cytokines particularly at the acute phase of inflammation and that prove to be decisive for the recovery and protection of mice infected with *C. albicans*.

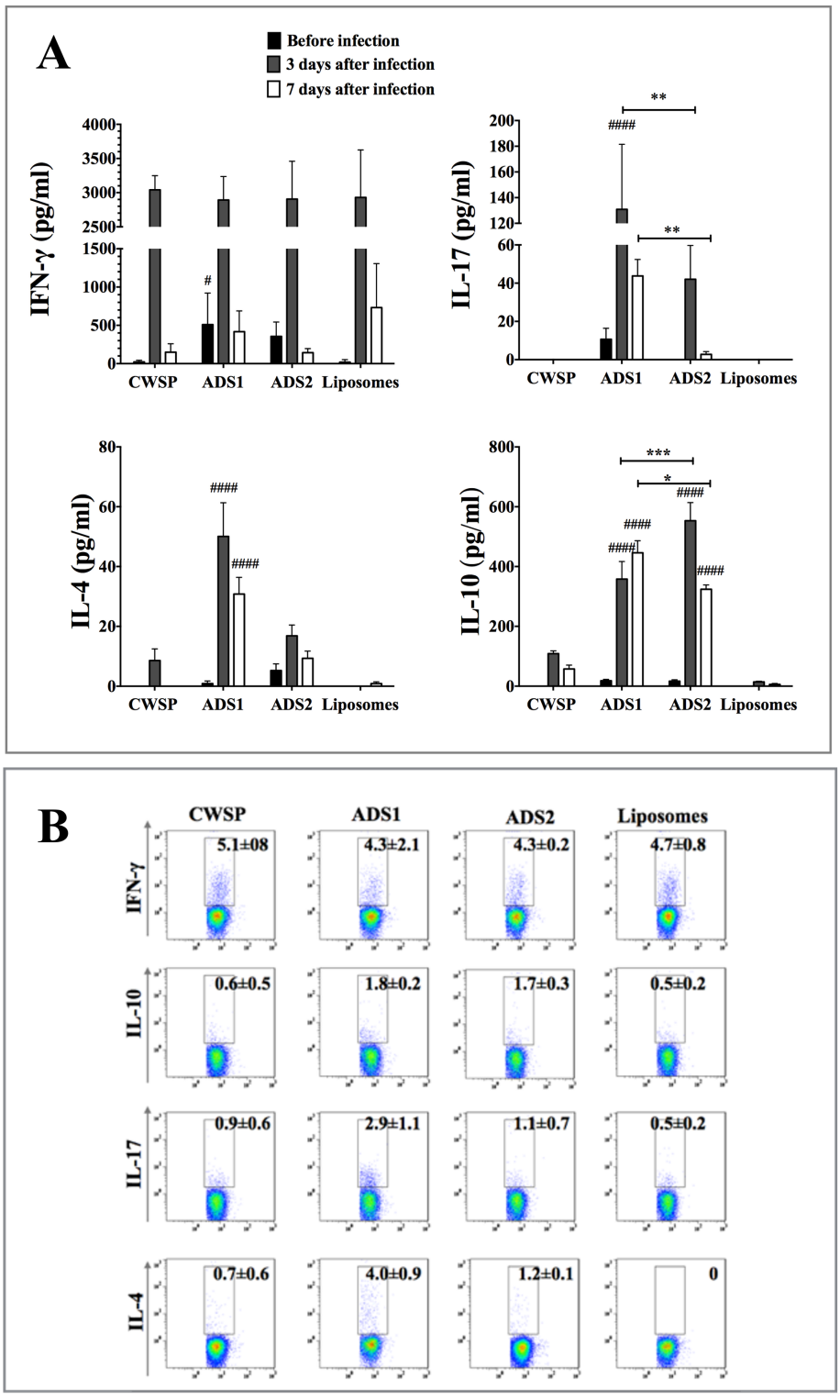

Figure 8: A) Frequency of IFN-γ^+, IL-17^+, IL-10^+, or IL-4^+ cells in splenic $CD4^+$ T cells from mice s.c. immunized with CWSP, ADS1, ADS2 or liposomes, isolated 21 days after the last s.c. immunization (before infection) and 3 and 7 days post-intravenous (i.v.) infection with 1 x 10^5 *C. albicans* yeast-form cells (**B**) Representative examples of flow cytometry analysis of intracellular IFN-γ^+, IL-17^+, IL-10^+, or IL-4^+ expression on gated splenic $CD4^+$ T cells after 3 days of infection, as indicated. Numbers inside dot plot regions represent means ± SD. Only significant differences obtain in comparison with the free CWSP (#), significant differences between the two time points for the same group of immunized mice and significant differences between ADSs are represented: **P<0.01; ***P<0.001 and ****P<0.0001.

4. DISCUSSION

The surge of *Candida* species infections coupled to higher resistance rates to antifungal drugs resulted in a tremendous increase in the prevalence of systemic candidiasis in hospitalized patients over the past two decades [28-31]. Hence, it is of paramount interest to develop a new prophylactic immunointervention against systemic candidiasis. In a previous study, we have shown the potential of DODAB:MO liposomes loaded with *C. albicans* CWSP (ADSs LNPs) in improving the immunogenicity of *Candida* antigens and therefore suggested that these liposomes could act as promising delivery systems for use in vaccination against *C. albicans* [22]. In this study, CWSP were also chosen as antigens since they ensure the diversity and complexity of *C. albicans* surface antigens. In fact, the proteins present in the fungal cell wall constitute excellent candidates for vaccine development as the cell wall plays a unique and important role in antigen presentation and immunomodulation [32]. In addition, the combination of antigens that are related to key *C. albicans* virulence attributes or biological functions may induce additive or synergistic immune responses and therefore reduce the probability of fungal immune evasion [33].

The LNPs have been prepared as two vaccine formulations, ADS1 and ADS2, differing only in the total lipid concentration used for CWSP adsorption. ADS1 is composed by approximately 7 times more total lipid than ADS2 and, as a consequence, it retains 91 ± 12% of the protein added, while ADS2 only 25 ± 12%, as previously reported [22]. Its characterization confirmed the LNPs mean sizes to be approximately 223 and 255 nm for ADS1 and ADS2 respectively, and that the antigenic proteins are adsorbed to the cationic liposomes, as shown by ζ-potential values. Furthermore, the electrostatic interactions between the cationic liposomes and the anionic proteins are strong enough to retain the antigens at the LNPs surface for at least 3 days after preparation. Importantly, the quantity of antigens loaded in the LNPs is dependent of the total lipid concentration, but the stability of the core proteins at their surface is not.

DCs constitute an important class of antigen presenting cells (APCs) of the immune system and are involved in antigen capturing, processing and subsequent presentation to antigen-specific T cells [26, 34]. DC maturation *in vitro* is characterized by up-regulation of MHC II and the co-stimulatory molecules CD80 and CD86 [35]. Un-stimulated cells $CD11c^{+}$ revealed moderate expression levels of CD80, CD86 and MHC-II molecules as shown by the mean fluorescence intensity (MFI) in the flow cytometry analysis. Incubation with the four different stimulus, CWSP, ADS1, ADS2 and empty liposomes reveal that only ADS1 was

able to significantly elevate the levels of expression of the three activation markers, in comparison cells exposed to the same concentration of free CWSP. This enhancement was only achieved after 24 h and interestingly at this time point the activation promoted by the CWSP significantly decreased, as opposed to the significant stimulation obtained with ADS1. This kinetic suggests that the delivery of CWSP in the liposomes not only enhances but also prolongs the cells activation by slow and sustained release of the entrapped antigen. Thus, the particulate nature of the ADS1 strongly improves the uptake of the entrapped antigen by DCs and their subsequent presentation to responder cells. In fact, the ability of cationic lipids to improve antigen immunogenicity is well recognized [36-38]. The fact that ADS2 fails to promote the same pattern is probably related to the lower lipid concentration used in this system, which results in just about 20% of CSWP entrapment, behaving similarly as the free CWSP.

IL-12 and IL-23 are members of a family of pro-inflammatory heterodimeric cytokines that can promote a Th1/Th17 response, inducing IFN-γ expression in $CD4^+$ T cells and maintaining Th17 effector function, respectively [39, 40]. In contrast, IL-10 might be required to limit host damage under circumstances of strong inflammation [41] and can also be associated with a Th2 polarization [42]. The cytokine profile obtained by stimulating $CD11c^+$ cells with ADS2 and free CWSP revealed a response similar to LPS, which could be considered as an exacerbated pro-inflammation. On the contrary, ADS1 seems to control that high inflammatory response once these cytokines were present but in significantly reduced levels. Furthermore, the higher levels of IL-23 and TNF-α and lower levels of IL-10 and 1L-12 suggest a Th17 polarization. In accordance with previous reports [26], incubation with empty liposomes led to production of insignificant levels of all cytokines, which indicates that the strong pro-inflammatory response was probably due to the presence of high concentrations of free proteins in the incubation solution, with CWSP and ADS2 stimuli. In fact, *C. albicans* cell wall proteins have been considered pro-inflammatory [43, 44]. The results observed with these LNPs, particularly with ADS1, encourage us to test if protection of mice from a lethal *C. albicans* systemic infection could be achieved.

In fact, after a lethal dose of *C. albicans,* only mice immunized with ADS1 LNPs showed a significant extended survival time compared to mice immunized with either free CWSP or buffer ($P<0.05$), and in fact more than 60% of mice immunized with ADS1 survived. Currently, scientific interest has grown towards the development of nanoparticles for use as adjuvants and delivery of antigens for vaccine development [45-49]. Other studies, using DODAB liposomes with monophosphoryl lipid A (MPL) or with trehalose 6,6'-

dibehenate (TDB) were used as adjuvants, also resulted in a protective immune response towards *Chlamydia* infection [50]. Similarly, in another study, the combination of DODAB with a major antigen of *Paracoccidioides brasiliensis* resulted in the lowest numbers of viable yeast cells in mice infected with *P. brasiliensis* in comparison with the use of other adjuvants such as aluminum hydroxide, CFA or flagellin [51].

Of note is the fact that only 10 μg of antigen were used per immunization in the present strategy, which is a small quantity in comparison to other studies describing the enhanced protection provide by liposomes with entrapped candida antigens [52, 53], supporting the high adjuvant potential of DODAB:MO liposomes. It is described that fungal CFU in mice kidneys increase progressively during fatal infection and decrease during nonfatal infection [54]. Consistently, the decrease of kidney fungal burden, observed at day 7, was only achieved in ADS1 immunized mice, which correlates with the survival of this group. This decrease in fungal burden with ADS1 immunization can be correlated with the fact that mice vaccinated with LNPs developed a strong humoral response with specific antibodies able to enhance phagocytosis of *C. albicans* cells. Serum from mice immunized with empty liposomes also enhanced yeast internalization, which could be accounted for both the presence of complement proteins and/or unspecific antibodies. The fact that serum from mice immunized with LNPs lead to a higher phagocytic activity than serum from mice immunized with empty liposomes, indicates that specific antibodies against CWSP play a major role in *C. albicans* recognition and internalization. This result is in agreement with studies that show that antibodies against *C. albicans* cell surface components favor internalization and killing of the fungus [55-57]. However, incubation with serum from CWSP immunized mice, which contains sufficient levels of anti-CWSP IgGs, was unable to enhance internalization/adhesion as did the serum form LNPs immunized mice. This result highlights the fact that not all antibodies have the same efficiency in the effector function of opsonizing/enhancing phagocytosis [58]. Indeed, in our previous study we have shown that the cell wall proteins identified by serum from CWSP immunized mice are different from the proteins identified by ADSs [22].

Mice vaccinated with ADS1 LNPs developed a protective and specific Th1/Th17 response with higher frequencies of splenic $CD4^{+}IL\text{-}4^{+}$ cells and higher levels of IL-17/IL-10/IL-4 in re-stimulated splenocytes in comparison with mice immunized with free CWSP. In fact, Th1 cells secrete IFN-γ but not IL-4, and the immune response is described by intense phagocytic activity while Th17 cells response is characterized by enhancement of neutrophil recruitment through secretion of IL-17 cytokine [59, 60]. Conversely, Th2 cells

secrete IL-4 but not IFN-γ suppressing the phagocytic activity [33]. Indeed, at day 3, the inflammatory response is high for all immunized mice, but it is at this time point that LNPs immunized mice show the highest amount of the anti-inflammatory cytokine IL-10. Actually, it is known that a vaccine that elicits by itself an inflammatory reaction might damage the host when the infectious agent is encountered, and IL-10 may act as a homeostatic host-driven response to keep inflammation under control [41, 61]. Moreover, a vaccine that elicited some Th2-type regulatory cytokines could provide a more balanced response [62]. Furthermore, although Th1/Th17 cells have been shown to be important in the development of protective host responses against *C. albicans* infection [60, 63] it is the balance between pro- and anti-inflammatory signaling that defines a successful fungal control [52, 64]. In the case of mice immunized with ADS1, the generation of Th1/Th17 and Th2 mix immune responses supports the idea that DODAB:MO liposomes contribute to more balanced immune responses against *Candida* infections that ultimately culminate in extended survival of mice when compared with mice immunized with free CWSP. These results reveal once more the adjuvant potential of DODAB:MO liposomes, suggesting that a decreased in their concentration could be fatal once ADS2 fails in enhancing CWSP immunogenicity.

5. CONCLUSION

This study demonstrated that DODAB:MO ADSs liposomal nanoparticles not only efficiently deliver antigens to activate BMDCs but also represents a promising new antigen vaccine delivery system. The *in vivo* results showed that a dose as low as 10 μg of antigenic proteins elicited significant humoral and cellular immune responses in BALB/c mice, conferring protection against a lethal *C. albicans* systemic infection.

REFERENCES

1. **Perrie, Y., Mohammed, A.R., Kirby, D.J., McNeil, S.E., and Bramwell, V.W.**, Vaccine adjuvant systems: enhancing the efficacy of sub-unit protein antigens. Int J Pharm, 2008. **364**(2): p. 272-80.
2. **Perrie, Y., Kirby, D., Bramwell, V.W., and Mohammed, A.R.**, Recent developments in particulate-based vaccines. Recent Pat Drug Deliv Formul, 2007. **1**(2): p. 117-29.
3. **Ghaffar, K.A., Giddam, A.K., Zaman, M., Skwarczynski, M., and Toth, I.**, Liposomes As Nanovaccine Delivery Systems. Curr Top Med Chem, 2014.
4. **Garcia, A. and De Sanctis, J.B.**, An overview of adjuvant formulations and delivery systems. APMIS, 2014. **122**(4): p. 257-67.
5. **Christensen, D., Korsholm, K.S., Andersen, P., and Agger, E.M.**, Cationic liposomes as vaccine adjuvants. Expert Rev Vaccines, 2011. **10**(4): p. 513-21.
6. **Christensen, D., Korsholm, K.S., Rosenkrands, I., Lindenstrom, T., Andersen, P., and Agger, E.M.**, Cationic liposomes as vaccine adjuvants. Expert Rev Vaccines, 2007. **6**(5): p. 785-96.
7. **Hussain, M.J., Wilkinson, A., Bramwell, V.W., Christensen, D., and Perrie, Y.**, Th1 immune responses can be modulated by varying dimethyldioctadecylammonium and distearoyl-sn-glycero-3-phosphocholine content in liposomal adjuvants. J Pharm Pharmacol, 2014. **66**(3): p. 358-66.
8. **Oliveira, A.C., Martens, T.F., Raemdonck, K., Adati, R.D., Feitosa, E., Botelho, C., Gomes, A.C., Braeckmans, K., and Real Oliveira, M.E.**, Dioctadecyldimethylammonium:monoolein nanocarriers for efficient in vitro gene silencing. ACS Appl Mater Interfaces, 2014.
9. **Carmona-Ribeiro, A.M.**, Biomimetic particles in drug and vaccine delivery. J Liposome Res, 2007. **17**(3-4): p. 165-72.
10. **Lincopan, N., Espindola, N.M., Vaz, A.J., da Costa, M.H., Faquim-Mauro, E., and Carmona-Ribeiro, A.M.**, Novel immunoadjuvants based on cationic lipid: Preparation, characterization and activity in vivo. Vaccine, 2009. **27**(42): p. 5760-71.
11. **Lincopan, N., Santana, M.R., Faquim-Mauro, E., da Costa, M.H., and Carmona-Ribeiro, A.M.**, Silica-based cationic bilayers as immunoadjuvants. BMC Biotechnol, 2009. **9**: p. 5.

12. **Silva, J.P., Oliveira, I.M., Oliveira, A.C., Lucio, M., Gomes, A.C., Coutinho, P.J., and Oliveira, M.E.**, Structural dynamics and physicochemical properties of pDNA/DODAB:MO lipoplexes: effect of pH and anionic lipids in inverted non-lamellar phases versus lamellar phases. Biochim Biophys Acta, 2014. **1838**(10): p. 2555-67.
13. **Silva, J.P., Oliveira, A.C., Casal, M.P., Gomes, A.C., Coutinho, P.J., Coutinho, O.P., and Oliveira, M.E.**, DODAB:monoolein-based lipoplexes as non-viral vectors for transfection of mammalian cells. Biochim Biophys Acta, 2011. **1808**(10): p. 2440-9.
14. **Oliveira, I.M., Silva, J.P., Feitosa, E., Marques, E.F., Castanheira, E.M., and Real Oliveira, M.E.**, Aggregation behavior of aqueous dioctadecyldimethylammonium bromide/monoolein mixtures: a multitechnique investigation on the influence of composition and temperature. J Colloid Interface Sci, 2012. **374**(1): p. 206-17.
15. **Correia, A., Lermann, U., Teixeira, L., Cerca, F., Botelho, S., da Costa, R.M., Sampaio, P., Gartner, F., Morschhauser, J., Vilanova, M., and Pais, C.**, Limited role of secreted aspartyl proteinases Sap1 to Sap6 in *Candida albicans* virulence and host immune response in murine hematogenously disseminated candidiasis. Infect Immun, 2010. **78**(11): p. 4839-49.
16. **Spellberg, B.**, Vaccines for invasive fungal infections. F1000 Med Rep, 2011. **3**: p. 13.
17. **Pfaller, M.A. and Diekema, D.J.**, Epidemiology of invasive candidiasis: a persistent public health problem. Clin Microbiol Rev, 2007. **20**(1): p. 133-63.
18. **Hajjeh, R.A., Sofair, A.N., Harrison, L.H., Lyon, G.M., Arthington-Skaggs, B.A., Mirza, S.A., Phelan, M., Morgan, J., Lee-Yang, W., Ciblak, M.A., Benjamin, L.E., Sanza, L.T., Huie, S., Yeo, S.F., Brandt, M.E., and Warnock, D.W.**, Incidence of bloodstream infections due to *Candida* species and in vitro susceptibilities of isolates collected from 1998 to 2000 in a population-based active surveillance program. J Clin Microbiol, 2004. **42**(4): p. 1519-27.
19. **Edwards, J.E., Jr.**, Fungal cell wall vaccines: an update. J Med Microbiol, 2012. **61**(Pt 7): p. 895-903.
20. **Ibrahim, A.S., Edwards, J.E., Jr., Bryant, R., and Spellberg, B.**, Economic burden of mucormycosis in the United States: can a vaccine be cost-effective? Med Mycol, 2009. **47**(6): p. 592-600.

21. **Brown, G.D., Denning, D.W., and Levitz, S.M.**, Tackling human fungal infections. Science, 2012. **336**(6082): p. 647.

22. **Carneiro, C., Correia, A., Collins, T., Vilanova, M., Pais, C., Gomes, A.C., Real Oliveira, M.E., and Sampaio, P.**, DODAB:monoolein liposomes containing *Candida albicans* cell wall surface proteins: A novel adjuvant and delivery system. Eur J Pharm Biopharm, 2015. **89**: p. 190-200.

23. **Bangham, A.D., Standish, M.M., and Watkins, J.C.**, Diffusion of univalent ions across the lamellae of swollen phospholipids. J Mol Biol, 1965. **13**(1): p. 238-52.

24. **Teixeira, L., Botelho, A.S., Mesquita, S.D., Correia, A., Cerca, F., Costa, R., Sampaio, P., Castro, A.G., and Vilanova, M.**, Plasmacytoid and conventional dendritic cells are early producers of IL-12 in Neospora caninum-infected mice. Immunol Cell Biol, 2010. **88**(1): p. 79-86.

25. **Carneiro, C., Vaz, C., Carvalho-Pereira, J., Pais, C., and Sampaio, P.**, A new method for yeast phagocytosis analysis by flow cytometry. J Microbiol Methods, 2014. **101**: p. 56-62.

26. **Vangasseri, D.P., Cui, Z., Chen, W., Hokey, D.A., Falo, L.D., Jr., and Huang, L.**, Immunostimulation of dendritic cells by cationic liposomes. Mol Membr Biol, 2006. **23**(5): p. 385-95.

27. **Sampaio, P., Santos, M., Correia, A., Amaral, F.E., Chavez-Galarza, J., Costa-de-Oliveira, S., Castro, A.G., Pedrosa, J., and Pais, C.**, Virulence attenuation of *Candida albicans* genetic variants isolated from a patient with a recurrent bloodstream infection. PLoS One, 2010. **5**(4): p. e10155.

28. **Sabino, R., Verissimo, C., Brandao, J., Alves, C., Parada, H., Rosado, L., Paixao, E., Videira, Z., Tendeiro, T., Sampaio, P., and Pais, C.**, Epidemiology of candidemia in oncology patients: a 6-year survey in a Portuguese central hospital. Med Mycol, 2010. **48**(2): p. 346-54.

29. **Xin, H., Cartmell, J., Bailey, J.J., Dziadek, S., Bundle, D.R., and Cutler, J.E.**, Self-adjuvanting glycopeptide conjugate vaccine against disseminated candidiasis. PLoS One, 2012. **7**(4): p. e35106.

30. **Iannitti, R.G., Carvalho, A., and Romani, L.**, From memory to antifungal vaccine design. Trends Immunol, 2012.

31. **Moragues, M.D., Rementeria, A., Sevilla, M.J., Eraso, E., and Quindos, G.**, *Candida* antigens and immune responses: implications for a vaccine. Expert Rev Vaccines, 2014. **13**(8): p. 1001-12.

32. **El-Kirat-Chatel, S., Beaussart, A., Alsteens, D., Sarazin, A., Jouault, T., and Dufrene, Y.F.**, Single-molecule analysis of the major glycopolymers of pathogenic and non-pathogenic yeast cells. Nanoscale, 2013. **5**(11): p. 4855-63.
33. **Cassone, A.**, Development of vaccines for *Candida albicans*: fighting a skilled transformer. Nat Rev Microbiol, 2013. **11**(12): p. 884-91.
34. **Banchereau, J. and Steinman, R.M.**, Dendritic cells and the control of immunity. Nature, 1998. **392**(6673): p. 245-52.
35. **Hackstein, H., Knoche, A., Nockher, A., Poeling, J., Kubin, T., Jurk, M., Vollmer, J., and Bein, G.**, The TLR7/8 ligand resiquimod targets monocyte-derived dendritic cell differentiation via TLR8 and augments functional dendritic cell generation. Cell Immunol, 2011. **271**(2): p. 401-12.
36. **Chen, W., Yan, W., and Huang, L.**, A simple but effective cancer vaccine consisting of an antigen and a cationic lipid. Cancer Immunol Immunother, 2008. **57**(4): p. 517-30.
37. **Christensen, D., Henriksen-Lacey, M., Kamath, A.T., Lindenstrom, T., Korsholm, K.S., Christensen, J.P., Rochat, A.F., Lambert, P.H., Andersen, P., Siegrist, C.A., Perrie, Y., and Agger, E.M.**, A cationic vaccine adjuvant based on a saturated quaternary ammonium lipid have different in vivo distribution kinetics and display a distinct CD4 T cell-inducing capacity compared to its unsaturated analog. J Control Release, 2012. **160**(3): p. 468-76.
38. **Kirby, D.J., Kaur, R., Agger, E.M., Andersen, P., Bramwell, V.W., and Perrie, Y.**, Developing solid particulate vaccine adjuvants: surface bound antigen favours a humoural response, whereas entrapped antigen shows a tendency for cell mediated immunity. Curr Drug Deliv, 2013. **10**(3): p. 268-78.
39. **Bettelli, E. and Kuchroo, V.K.**, IL-12- and IL-23-induced T helper cell subsets: birds of the same feather flock together. J Exp Med, 2005. **201**(2): p. 169-71.
40. **Dong, C.**, Diversification of T-helper-cell lineages: finding the family root of IL-17-producing cells. Nat Rev Immunol, 2006. **6**(4): p. 329-33.
41. **Romani, L. and Puccetti, P.**, Protective tolerance to fungi: the role of IL-10 and tryptophan catabolism. Trends Microbiol, 2006. **14**(4): p. 183-9.
42. **Yamazaki, S., Okada, K., Maruyama, A., Matsumoto, M., Yagita, H., and Seya, T.**, TLR2-dependent induction of IL-10 and Foxp3+ CD25+ CD4+ regulatory T cells prevents effective anti-tumor immunity induced by Pam2 lipopeptides in vivo. PLoS One, 2011. **6**(4): p. e18833.

43. **de Boer, A.D., de Groot, P.W., Weindl, G., Schaller, M., Riedel, D., Diez-Orejas, R., Klis, F.M., de Koster, C.G., Dekker, H.L., Gross, U., Bader, O., and Weig, M.**, The *Candida albicans* cell wall protein Rhd3/Pga29 is abundant in the yeast form and contributes to virulence. Yeast, 2010. **27**(8): p. 611-24.

44. **Ueno, K., Okawara, A., Yamagoe, S., Naka, T., Umeyama, T., Utena-Abe, Y., Tarumoto, N., Niimi, M., Ohno, H., Doe, M., Fujiwara, N., Kinjo, Y., and Miyazaki, Y.**, The mannan of Candida albicans lacking beta-1,2-linked oligomannosides increases the production of inflammatory cytokines by dendritic cells. Med Mycol, 2013. **51**(4): p. 385-95.

45. **Wang, G., Pan, L., Zhang, Y., Wang, Y., Zhang, Z., Lu, J., Zhou, P., Fang, Y., and Jiang, S.**, Intranasal delivery of cationic PLGA nano/microparticles-loaded FMDV DNA vaccine encoding IL-6 elicited protective immunity against FMDV challenge. PLoS One, 2011. **6**(11): p. e27605.

46. **Mahapatro, A. and Singh, D.K.**, Biodegradable nanoparticles are excellent vehicle for site directed in-vivo delivery of drugs and vaccines. J Nanobiotechnology, 2011. **9**: p. 55.

47. **Moon, J.J., Suh, H., Polhemus, M.E., Ockenhouse, C.F., Yadava, A., and Irvine, D.J.**, Antigen-displaying lipid-enveloped PLGA nanoparticles as delivery agents for a *Plasmodium vivax* malaria vaccine. PLoS One, 2012. **7**(2): p. e31472.

48. **Beg, S., Samad, A., Nazish, I., Sultana, R., Rahman, M., Ahmad, M.Z., and Akbar, M.**, Colloidal drug delivery systems in vaccine delivery. Curr Drug Targets, 2013. **14**(1): p. 123-37.

49. **Bhowmick, S., Mazumdar, T., Sinha, R., and Ali, N.**, Comparison of liposome based antigen delivery systems for protection against *Leishmania donovani*. J Control Release, 2010. **141**(2): p. 199-207.

50. **Yu, H., Karunakaran, K.P., Jiang, X., Shen, C., Andersen, P., and Brunham, R.C.**, *Chlamydia muridarum* T cell antigens and adjuvants that induce protective immunity in mice. Infect Immun, 2012. **80**(4): p. 1510-8.

51. **Mayorga, O., Munoz, J.E., Lincopan, N., Teixeira, A.F., Ferreira, L.C., Travassos, L.R., and Taborda, C.P.**, The role of adjuvants in therapeutic protection against paracoccidioidomycosis after immunization with the P10 peptide. Front Microbiol, 2012. **3**: p. 154.

52. **Ahmad, E., Fatima, M.T., Saleemuddin, M., and Owais, M.**, Plasma beads loaded with *Candida albicans* cytosolic proteins impart protection against the fungal infection in BALB/c mice. Vaccine, 2012. **30**(48): p. 6851-8.

53. **Chauhan, A., Swaleha, Z., Ahmad, N., Farazuddin, M., Vasco, A., Abida, M., and Mohammad, O.**, Escheriosome mediated cytosolic delivery of *Candida albicans* cytosolic proteins induces enhanced cytotoxic T lymphocyte response and protective immunity. Vaccine, 2011. **29**(33): p. 5424-33.

54. **Spellberg, B., Johnston, D., Phan, Q.T., Edwards, J.E., Jr., French, S.W., Ibrahim, A.S., and Filler, S.G.**, Parenchymal organ, and not splenic, immunity correlates with host survival during disseminated candidiasis. Infect Immun, 2003. **71**(10): p. 5756-64.

55. **Kozel, T.R., MacGill, R.S., Percival, A., and Zhou, Q.**, Biological activities of naturally occurring antibodies reactive with *Candida albicans* mannan. Infect Immun, 2004. **72**(1): p. 209-18.

56. **de Bernardis, F., Santoni, G., Boccanera, M., Spreghini, E., Adriani, D., Morelli, L., and Cassone, A.**, Local anticandidal immune responses in a rat model of vaginal infection by and protection against *Candida albicans.* Infect Immun, 2000. **68**(6): p. 3297-304.

57. **Paulovicova, L., Paulovicova, E., Karelin, A.A., Tsvetkov, Y.E., Nifantiev, N.E., and Bystricky, S.**, Humoral and cell-mediated immunity following vaccination with synthetic *Candida* cell wall mannan derived heptamannoside-protein conjugate: immunomodulatory properties of heptamannoside-BSA conjugate. Int Immunopharmacol, 2012. **14**(2): p. 179-87.

58. **Han, Y., Kozel, T.R., Zhang, M.X., MacGill, R.S., Carroll, M.C., and Cutler, J.E.**, Complement is essential for protection by an IgM and an IgG3 monoclonal antibody against experimental, hematogenously disseminated candidiasis. J Immunol, 2001. **167**(3): p. 1550-7.

59. **Pietrella, D., Rachini, A., Pines, M., Pandey, N., Mosci, P., Bistoni, F., d'Enfert, C., and Vecchiarelli, A.**, Th17 cells and IL-17 in protective immunity to vaginal candidiasis. PLoS One, 2011. **6**(7): p. e22770.

60. **Gaffen, S.L., Hernandez-Santos, N., and Peterson, A.C.**, IL-17 signaling in host defense against *Candida albicans*. Immunol Res, 2011. **50**(2-3): p. 181-7.

61. **Romani, L.**, Immunity to fungal infections. Nat Rev Immunol, 2011. **11**(4): p. 275-88.

62. **Li, W., Hu, X., Zhang, X., Ge, Y., Zhao, S., Hu, Y., and Ashman, R.B.**, Immunisation with the glycolytic enzyme enolase confers effective protection against *Candida albicans* infection in mice. Vaccine, 2011. **29**(33): p. 5526-33.

63. **Lin, L., Ibrahim, A.S., Xu, X., Farber, J.M., Avanesian, V., Baquir, B., Fu, Y., French, S.W., Edwards, J.E., Jr., and Spellberg, B.**, Th1-Th17 cells mediate protective adaptive immunity against *Staphylococcus aureus* and *Candida albicans* infection in mice. PLoS Pathog, 2009. **5**(12): p. e1000703.

64. **Romani, L.**, Cell mediated immunity to fungi: a reassessment. Med Mycol, 2008. **46**(6): p. 515-29.

CHAPTER VII

Concluding remarks and future perspectives

1. CONCLUDING REMARKS

Subunit vaccines, composed of nonliving or split pathogens, are being developed as immunoprotective strategies. Their effective implementation is however greatly limited because, in general, they do not sufficiently activate antigen presenting cells (APCs) and elicit an adaptive immune response. Therefore, to potentiate their immunogenicity, subunit vaccines are frequently formulated with an adjuvant. Cationic liposomes are interesting choices for the development of adjuvant delivery systems due to their ability to act as immunostimulators, inducing cell mediated immunity and humoral immune responses towards the associated antigens, and as nanocarriers for diverse drugs, DNA or different types of antigens.

Formulating protein antigens into nanocarriers has emerged as one of the most promising strategies to trigger an immune response against the carried antigens. For the efficient design of nanoparticles composed of cationic liposomes, it is important to understand the delivery system-antigen interactions. The particulate adjuvant delivery system addressed in the present study is a cationic liposomal adjuvant, which is based on the cationic surfactant dioctadecyldimethylammonium bromide (DODAB) together with monoolein (MO), a naturally-occurring neutral surfactant and helper lipid. The χMO was critical for DODAB:MO liposomes and for BSA loaded DODAB:MO liposomal nanoparticle (BSA LNPs) colloidal stability, structural organization, and reduction of cytotoxicity and improvement of phagocytic cells ability to internalize antigens. At χMO (0.66), DODAB:MO not only functioned as a delivery vehicle that mediated initial contact with the cells but also facilitated subsequent activation of APCs.

Currently, systemic infections caused by *Candida* species, mainly caused by *Candida albicans,* represent the fourth leading cause of nosocomial bloodstream infection in modern hospitals, despite the administration of antifungal agents that have potent activity *in vitro* and *in vivo* in preclinical studies. Clearly, prevention of this type of invasive fungal infections has become of paramount importance. The yeast cell wall is a unique microbial feature with an important role in antigen presentation and immunomodulation. Therefore, fungal cell wall protein antigens, exposed at the yeast surface, constitute excellent candidates for vaccine development. In fact, phagocytosis is mediated by receptors on the cell surface that recognize specific ligands on the pathogen surface. In this study, we developed a new method to assess yeast phagocytosis by flow cytometry. This method allowed a clear distinction between internalized and non-internalized yeast cells being of great usefulness

further in this thesis for comparison of phagocytosis rate between opsonized vs. non-opsonized yeast cells.

At the same χMO (0.66), DODAB:MO (1:2) liposomes were loaded with *C. albicans* cell wall surface proteins (CWSP). To understand the delivery system-antigen interactions different formulations were tested with distinct protein/lipid weight ratios. These formulations assembled as spherical liposomal nanoparticles and two were selected and further studied: ADS1 LNPs (protein/lipid weight ratio of 0.056) and ADS2 LNPs (protein/lipid ratio of 0.376). Both LNPs were stable with mean sizes around 200 nm, non-cytotoxic and avidly taken up by macrophages. Moreover, the electrostatic interactions between the cationic liposomes and the anionic proteins were strong enough to retain the antigens at the LNPs surface for at least 3 days after preparation.

The loading of the CWSP in DODAB:MO liposomes not only enhanced but also prolonged the activation of dendritic cells indicating that entrapped antigen is released in a slow and sustained manner when trapped in DODAB:MO liposomes. This behavior indicates that DODAB:MO liposomes adjuvant effect may be attributed to an increase in antigen uptake and to an enhancement of APC activation, two mechanisms already described for other types of delivery systems.

In the mouse model, immunization with the ADSs induced strong antibody responses and cell-mediated immunity. Moreover, in contrast to immunization with CWSP alone, these systems induced higher levels of IL-17 and IFN-γ but lower levels of IL-10, indicating a polarization towards a Th1/Th17-type immune response and confirming their immunoadjuvant potential. Additionally, mice immunized with LNPs displayed strong humoral responses, producing antibodies (IgGs) against proteins different to those induced by CWSP alone, in particular the cell wall chitinase Cht3p. This protein is known to be unstable *in vitro*, indicating that these liposomes not only enhance the immune response against proteins from the pathogenic yeast *C. albicans* but also adsorb and efficiently deliver a protein that otherwise was not efficiently delivered due to its instability.

Furthermore, in a mouse model of systemic candidiasis DODAB:MO ADS1 liposomal nanoparticles, with a dose as low as 10 μg of antigenic proteins, elicited significant humoral and cellular immune responses in BALB/c mice, conferring protection against a lethal *C. albicans* systemic infection.

Thus with this work we developed and characterized a novel delivery system, composed by DODAB:MO liposomes, that was able to enhance *C. albicans* antigens

immunogenicity and that adjuvant potential was crucial in protecting mice against systemic candidiasis (Figure 1).

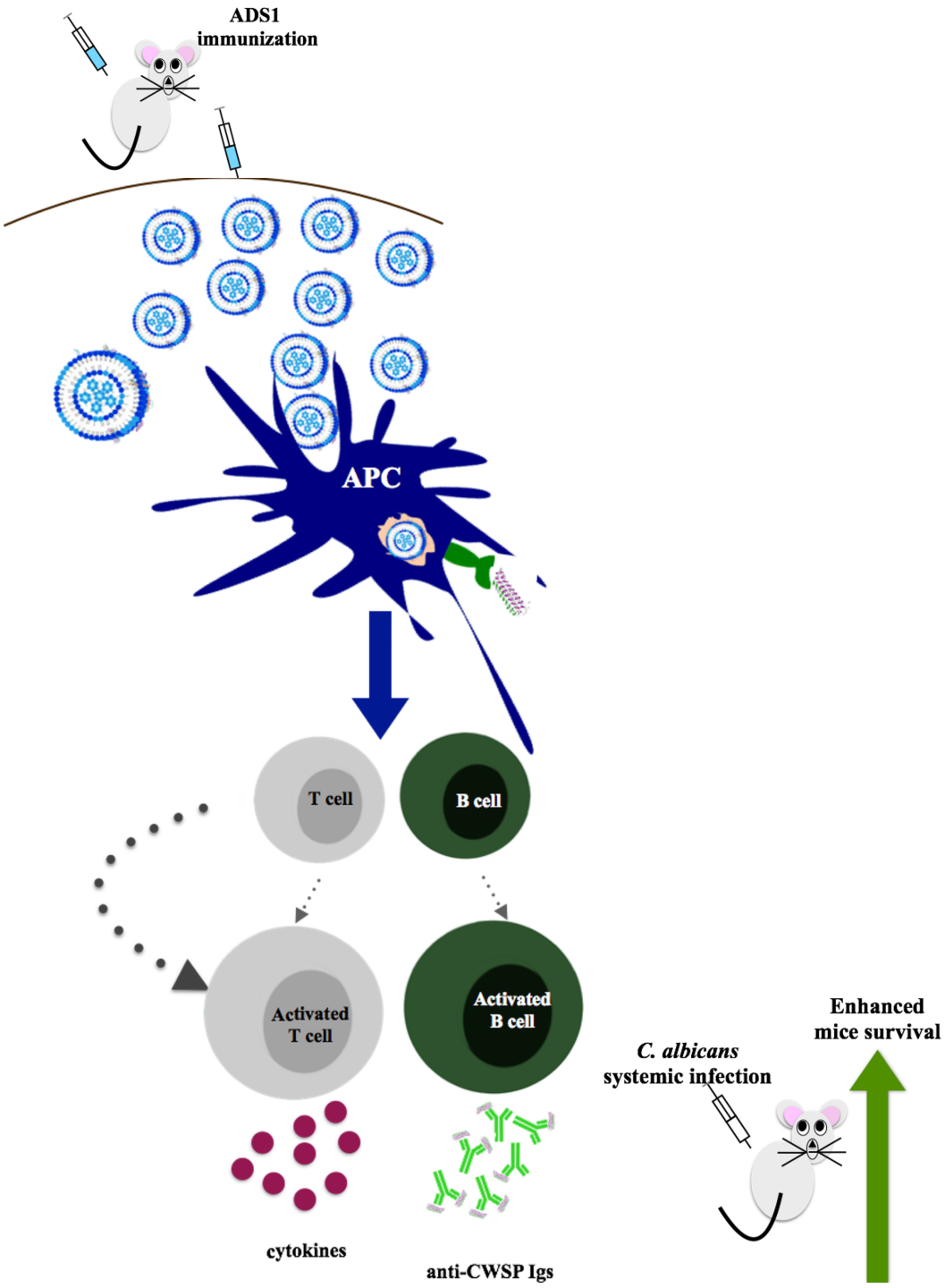

Figure 1: Schematic representation of the main conclusion of this work.

2. FUTURE PERSPECTIVES

For the efficient design of liposomal-based adjuvant delivery systems, several parameters should be further considered, such as shelf-life of the delivery system, batch-to-batch reproducibility and possibility of large-scale production of safe and efficient liposomal products.

One of the main concerns regarding the previous study was the use of a bulk of *C. albicans* cell wall proteins (CWSP) as antigens, making the large-scale production and the batch-to-batch protein extractions laborious and difficult. In this study, immunoblotting assays showed that more than 90% of the CWSP-specific antibodies present in mice immunized with ADS1 were reactive to the Cht3p cell wall protein. These results led us to consider this protein as an antigen candidate to be loaded in DODAB:MO liposomes, replacing the CWSP.

In order to fulfill these objectives, the following studies are being designed in our group:

(1) Optimize and establish a protocol for the preparation of DODAB:MO liposomes with recombinant *C. albicans* chitinase rCht3p as antigen.

(2) Characterize and explore the assembled LNPs assessing their physicochemical properties.

(3) Evaluate the humoral and cellular response of the LNPs towards the rCht3p antigen in order to assess their immunomodulatory effects;

(4) Achieve an effective immune protection against systemic candidiasis and characterize the immunological mechanisms responsible for that protective effect;

(5) Validate these LNPs as candidates for an experimental vaccine against systemic candidiasis.

Recent perspectives forecast a new paradigm for future “third generation” vaccines based on similarities found in diverse pathogens or convergent immune defenses to such pathogens. These perspectives include what is known as *convergent immunity*, where antigens from non-target organisms that contain epitope homologs found in the target organism are applied in vaccines. Convergent immunity has a potential to promote protective efficacy not usually elicited by native antigens from a target pathogen. In fact, a *C. albicans* antigen was already described to confer convergent immunity in *Staphylococcus aureus* and *C. albicans* systemic infections. In this sense it would be interesting to explore CWSP/rCht3p loaded DODAB:MO liposomes efficiency in protecting mice infected with a non-target pathogen such as *S. aureus.*